PROCESSING OF DISSOLVING PULP IN IONIC LIQUIDS

Submitted in fulfilment of the requirements

of the degree of

Doctor of Technology: Chemistry

in the Faculty of Applied Sciences at

Durban University of Technology

Zikhona Tywabi

January 2015

Supervisor: . . . . . Date: . . . . . .

Co-supervisor: . . . . . Date: . . . . . .

PREFACE

The work described herein was performed at:

- The Centre for Green Manufacturing Centre at the University of Alabama, Tuscaloosa, United States of America under the supervision of Professor Robin Rogers;
- The Council for Scientific and Industrial Research at the Forestry and Forest Products Research Centre, Durban, South Africa, under the supervision of Doctor Bruce Sithole and
- The Durban University of Technology, Durban, South Africa under the supervision of Professor Nirmala Deendayalu.

The work is original unless stated in the text and has not been previously submitted for any other degree at any other university.

Signed Date
Zikhona Tywabi

Signed Date
Dr B. Sithole

Signed Date
Prof N. Deenadayalu

ABSTRACT

This thesis forms part of the Council for Scientific and Industrial Research, Forestry and Forest Products Research Centre (CSIR-FFP) biorefinery project which aims at developing and implementing novel industrial processes production of cellulose textile fibres.

The focus of this study is to investigate the dissolution of South African *Eucalyptus* raw (unbleached) and final (bleached) dissolving pulp and saw dust wood in an ionic liquid (IL) 1-ethyl-3-methylimidazolium acetate [Emim][OAc] and the co-solvents [dimethylsulfoxide (DMSO)] or [dimethylformamide (DMF)] mixtures, to obtain regenerated cellulose by the further addition of water and acetone.

The IL/co-solvent mixtures were able to dissolve the raw and final pulp samples at 120 ˚C for 6 hours whereas the sawdust wood dissolved in 10 hours. The IL/DMF mixture gave higher cellulose recoveries of 41.88 % for the raw pulp, 49.89 % for the final pulp sample and 32.50 % for sawdust wood while the IL/DMSO mixture gave a recovery of 15.25 % for the raw pulp sample, 36.25 % for the final pulp sample and 17.83 % for the sawdust wood sample.

The regenerated cellulose materials were characterized by Fourier Transformer Infrared Spectroscopy (FTIR), Nuclear Magnetic Resonance (NMR), Scanning Electron Microscopy (SEM), Thermo gravimetric Analysis (TGA) and Powder X-Ray Diffraction (pXRD), and compared with a standard microcrystalline of cellulose. It was observed that the FTIR and NMR spectra of the regenerated cellulose and MCC were similar which then indicates that no chemical reaction occurred during the dissolution and regeneration process of cellulose. SEM and X-ray diffraction (XRD) patterns of the results showed that after dissolution the cellulose I (native form), the crystalline structure was completely converted into cellulose II (amorphous) structure, and this was due to the removal of lignin and decrease in cellulose crystallinity. TGA results showed that the regenerated cellulose samples have higher char yields compared to the MCC which is due to the IL remaining in the regenerated cellulose.

It was also observed that the addition of the co-solvents decreased the viscosity of the IL mixture, facilitating dissolution of the cellulose that led to additional swelling and reduction of the recalcitrant nature of the cellulose crystalline structure and intermolecular interactions. This led to increased accessibility and dissolution of the cellulose.

The findings in this study have the potential to bring ILs closer to applications for biomass technology in particular for an economically viable dissolution method for biomass because ILs have a benefit of being easily separated from the anti-solvent, which provides a simple solution for IL recycle ability and re-use.

The novel aspect of this study is:

- This is the first study in the South African context to examine the influence of the lignin on the dissolution and regeneration of Eucalyptus sawdust wood and dissolving pulp.

Keywords: sawdust wood, regenerated cellulose, dissolving pulp, crystallinity, dissolution, ionic liquids, co-solvents

DECLARATION 1- PLAGIARISM

I, **Zikhona Tywabi**, declare that:

1. The research reported in this thesis, except where otherwise indicated, is my original research.
2. This thesis has not been submitted for any degree or examination at any other university.
3. This thesis does not contain other person's data, graphs, pictures, text, tables or any other information, unless specifically acknowledged, and the source being detailed in the thesis and in the reference section

Zikhona Tywabi

Signed :…….

Date :…….

DECLARATION 2 - PUBLICATIONS

Publication 1: *submitted* –Journal of Carbohydrate Polymers (still under review)

Z. Tywabi*, N. Deenadayalu , B. Sithole, H. Wang, O. A. Cojocaru, and R. D. Rogers (2014). **Structural changes in South African Eucalyptus wood dissolving pulp after dissolution in [Emim][OAc]/Co-solvent mixtures**

Publication 2: *manuscript revisions submitted* –Journal of Cellulose

Z. Tywabi*, N. Deenadayalu and B. Sithole (2014). **Dissolution of South African Eucalyptus Sawdust Wood in [Emim][OAc]/Co-solvent Mixtures**

CONFERENCE ATTENDANCE

* **Oral presentation:**10th International Conference on Renewable Resources and Biorefineries, 3-6th JUNE 2014, Palacio Conde Ansúrez conference centre of Valladolid University

***Oral Presentation**: 41st SACI Convention: Chemistry for Africa, 1-6 December 2013, Riverpark conference centre, East London

* **Oral Presentation**: Durban University of Technology Institutional Research Day, 27 November 2013, Steve Biko campus, Durban

*** Poster presentation**: TAPPSA National conference and exhibition, 22-23 October 2013, Elangeni Hotel, Durban

Zikhona Tywabi was responsible for the experimental work, analysis of data, and writing of publications 1-2, and presentations. The authors contributed by providing comments as well as editing of the manuscripts.

Zikhona Tywabi

Signed :…….

Date :…….

TABLE OF CONTENTS

CHAPTER 1: INTRODUCTION

CHAPTER 2: LITERATURE REVIEW

CHAPTER 3: EXPERIMENTAL

CHAPTER 4: RESULTS & DISCUSSIONS

ACKNOWLEDGEMENTS

I would like to thank my parents, husband, my daughter, my siblings and my friends for their constant love, encouragement, support, and for always believing in me.

I would also like to thank my supervisors Prof N. Deenadayalu, Dr Sithole and Dr Rogers for their advice and assistance throughout the studies.

I would also like to thank Dr Hui, Dr Andreea and the rest of the Green Manufacturing research team at the University of Alabama for all their hard work, proof reading my papers, encouragement throughout my project.

A special thanks goes to the CSIR FFP staff, lab technicians, and students for their support and assistance during the project.

I would also like to thank the National Research Foundation, Department of Agriculture and Durban University of Technology for the financial support.

This thesis is dedicated to my daughter, Alu.

ABBREVIATIONS

[Admim][Br]	1-Allyl-2, 3-dimethylimidaolium Bromide
[Admim][Br]	1-N-Allyl-2, 3-dimethylimadazolium Bromide
[Ahim][Cl]	1-Allyl-3-hexylimidaolium Bhloride
[Amim][Cl]	1-Allyl-3-methylimidazolium Chloride
[Bmim][Ace]	1-Butyl-3-methylimadazolium Acesulfanate
[Bmim][Br]	1-Butyl-3-methylimadazolium Bromide
[Bmim][Cl]	1-Butyl-3-methylimadazolium Chloride
[BNimim][Cl]	1-Benzyl-3-methylimadazolium Chloride
[Bmim][FmO]	1-Butyl-3-methylimadazolium Formate
[Bmim][OAc]	1-Butyl-3-methylimadazolium Acetate
[ClC_2mim][Cl]	1-2-Chloroethyl-3-methylimadazolium Chloride
[C_2mim][Cl]	1-Ethyl-3-methylimadazolium Chloride
[C_2mim][$MeOPO_2$]	1-Ethyl-3-methylimadazolium methyl Phosphate
[C_4mim][Cl]	1-Butyl-3-methylimadazolium Chloride
[DiMim][$MeSO_4$]	1, 3-Methylimidazolium Dimethylsulfate

[Emim][BA]	1-Ethyl-3-methylimadazolium Benzoate
[Emim][Cl]	1-Ethyl-3-methylimadazolium Chloride
[Emim][OAc]	1-Ethyl-3-methylimadazolium Acetate
[Emim][DEP]	1-Ethyl-3-methylimadazolium diethyl Phosphate
α	Alpha
β	Beta
^{13}C NMR	Carbon Nuclear Magnetic Resonance
CEL	Cotton Linters
CMP	Chemi-mechanical Pulp
CS_2	Carbon Disulphide
DP	Degree of Polymerization
DS	Degree of Substitution
DSC	Differential Scanning
FTIR	Fourier Transform Infrared Spectroscopy
^{1}H NMR	Proton Nuclear Magnetic Resonance
IL	Ionic Liquid

K	Kappa Number
MCC	Microcyrstalline Cellulose
NMMO	N-methylmorpholine-N-oxide
NMR	Nuclear Magnetic Resonance
PIL's	Protic Ionic Liquids
PW	Ball-milled Popular Wood
SEC	Size Exclusion Chromatography
SEM	Scanning Electron Microscopy
TGA	Thermo Gravimetric Analysis
WA	Water Absorption
XRD	X-Ray Diffraction

LIST OF FIGURES

LIST OF TABLES

GLOSSARY

Cellulose: is an organic compound with the formula $(C_6H_{10}O_5)n$, a polysaccharide consisting of a linear chain of several hundred to over ten thousand β(1→4) linked D-glucose units.

Ionic liquid: is a salt in the liquid state, and is largely made of ions and short-lived ion pairs.

Degree of crystallinity: is the fractional amount of crystallinity in the material sample.

Dissolving pulp: is the bleached wood pulp that has high cellulose content, low amounts of hemicellulose and lignin.

Hemicellulose: group of heterogeneous polymers that play a supporting role in the fibre wall

Lignin: branched heterogeneous aromatic polymer former of phenylpropane units linked together mainly by β-O-4 arylether linkages

Regenerated cellulose: cellulose which has been treated with chemicals and regenerated by anti-solvents. It has lower molecular weight as compared to the native cellulose. Also known as cellulose II

CHAPTER 1: INTRODUCTION

1.1 BACKGROUND

New technologies for processing biomass into valuable products are being developed continuously to cater for the world population which is increasing, and the large amount of natural resources needs to be used to meet the shortage of raw materials. The depletion of non-renewable resources, which contribute to greenhouse gas emissions, has led to the use of renewable natural materials that are sustainable and reusable (Muhammad 2004:18).

The concept of converting biomass processes and equipment to produce fules, power of valuable chemicals from biomass is known as biorefinery (BRF). In BRF, biomass such as wood, corn, wheat, sugar cane, barley and agricultural residue are used. The wide availability of wood makes it a good raw material for the production of dissolving pulp and biofuels. Wood biorefinery includes its fractionation into hemicellulose, cellulose, lignin and extractives for production of high value added products (Muhammad 2004:18).

In this work the *Eucalyptus dunni* (hardwood tree) was used because it is the main wood pulp species in South Africa, it has low production costs, and is widely available.

1.2 WOOD SOURCE

Wood is a heterogeneous organic composite of elongated fibres (Kraäsig 1993:978). It is a renewable source for cellulose, lignin, hemicelluloses and extractives (Abdulkhani *et.al.* 2013:57; Mäki-Arvela *et.al.* 2010:176; Muhammad *et.al.* 2011:125). The structure of a typical wood fibre cell wall is shown in Figure 1.1. The structure of the cell wall consists of several layers. The lumen which is situated on top of the inner layer (S3) (white in color) is the central cavity that is surrounded by the inner S3 layer, middle S2 layer and outer S1 layer that makes up the secondary wall. The primary P wall and the middle lamella, holds the fibers together, as illustrated in Figure 1.1. The secondary wall consists mainly of lignin while the primary P wall is composed of mostly of hemicelluloses and cellulose (Kraäsig 1993:978; Kihlman 2012:2).

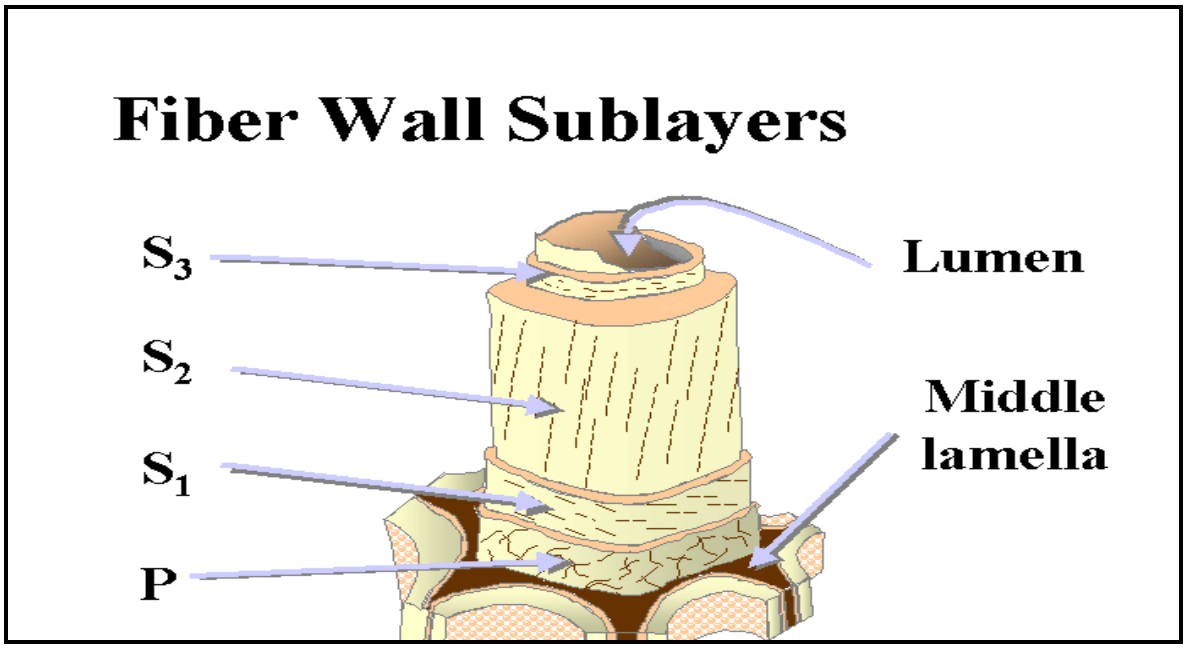

Figure 1.1 The structure of a wood fibre cell wall as reproduced from Kraäsig (1993:978)

The spatial arrangement of the three major components present in the cell walls of the lignocellulose is shown in Figure 1.2.

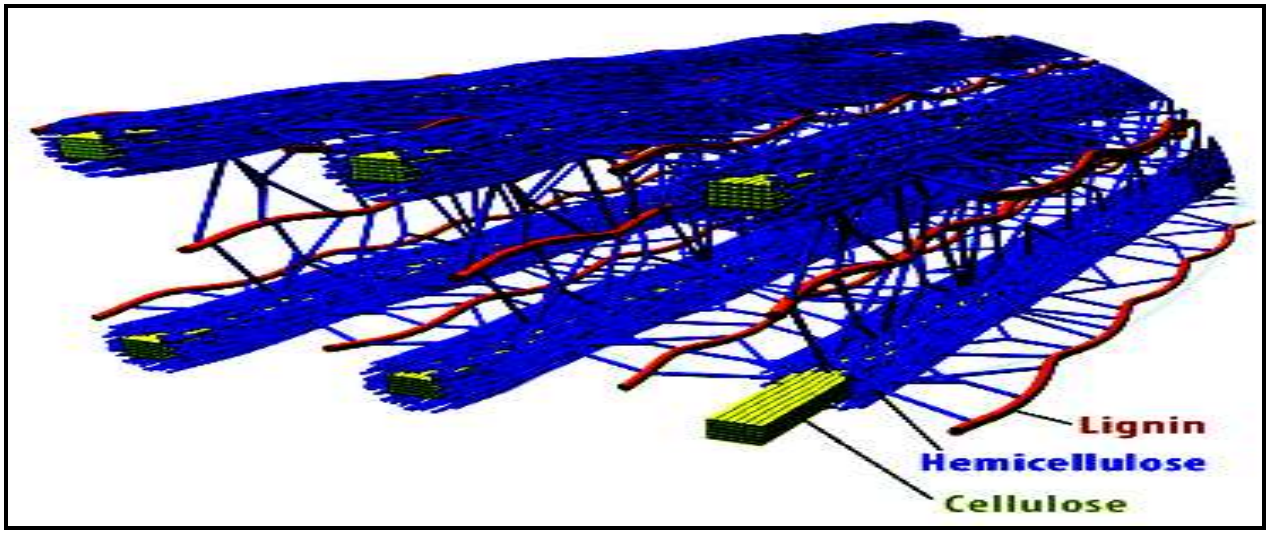

Figure 1.2 Three-dimensional arrangements of cellulose, hemicelluloses and lignin in the cell walls of lignocellulosic biomass as reproduced from Brandt *et.al.* (2013:552)

The density of wood and the shape of the fibers relate to the mechanical properties of the wood, which vary depending on the species. Trees bearing needle leaves, e.g., spruce or pine, are usually referred to as softwoods whilst those with broad leaves, e.g., eucalyptus or acacias, are known as hardwoods. The wood fibres in these two types of trees vary: softwoods have long fibers and hardwoods have shorter and thus densely packed fibres. The longer fibres of softwoods make them stronger than hardwood in papermaking (Kraäsig 1993:978; Kihlman 2012:2).

Wood is the most abundant lignocellulose resource in the world (Muhammad *et.al.* 2013:144). The use of the lignocellulosic based materials in forestry sector has received increased attention due to the growing global environmental awareness and concepts of sustainability and industrial ecology (Muhammad *et.al.* 2013:144; Cheng *et.al.* 2010:4659). The wood lignocellulosic material contains approximately 35-50 % cellulose, 35 % hemicelluloses, 5-30 % lignin as well as a few % of extractives and ash (Abdulkhani *et.al.* 2013:57; Espinoza-Acosta *et.al.* 2014:3661).

The components present in the lignocellulose biomass are discussed in detail below.

1.2.1 Wood composition

1.2.1.1 *Cellulose*

Cellulose is the largest single component of woody lignocellulose (Brandt *et.al.* 2013:552; Muhammad *et.al.* 2013:144). It is a natural, biodegradable polymer is present in a number of renewable sources (Casas *et.al.* 2012:155; Mahadeva *et.al.* 2012:289; Swatloski *et.al.* 2002:4974). Cellulose is the most abundant biopolymer on this planet that exists in the cell wall of all green plants to ensure that their structure is mechanically stable, and thus is a valuable renewable resource (Mäki-Arvela *et.al.* 2010:176; Kubisa 2009:1333).

Cellulose is a highly crystalline homopolysaccharide composed of the anhydroglucopyranose (AGU) monomers formed via 1,4-β-D-glucose linkage of carbohydroglucose units and contains several intra and inter molecular hydrogen bonds (Abdulkhani *et.al.* 2013:57; Zhao *et.al.* 2012:1490). Its molecular formula is $C_6H_{10}O_5$ and it has a degree of polymerization (DP) of up to 10 000 or higher because of its high molecular weight, while the regenerated cellulose fibres have a DP of from 250-600 (Kihlman 2012:2). Cellulose molecule can be considered as being linear, unbranched, polymer with repeating units (Kraäsig 1993:978) and the supramolecular structure consists of cellulose organized into crystalline regions that have well organized inter-molecular hydrogen bonds that can be arranged in different polymorphs (the ability of a solid material to exist in more than one form or crystal structure) named cellulose I (I_α and I_β), II, III and IV (Kihlman 2012:2).

The native cellulose, cellulose I, has a parallel crystalline structure composed of phases I_α and I_β (composition varies with the origin of the raw materials) where the latter is thermodynamically more stable than the former. Cellulose I can be converted into cellulose II either by regeneration or mercerization (Espinoza-Acosta *et.al.* 2014:3612). Cellulose II appears to have a more complex network of hydrogen bond (intra- and intermolecular) and results in a more dense and stable structure. The amorphous region (has fewer and less organized hydrogen bonds) and is more reactive because the hydroxyl groups are more accessible (Espinoza-Acosta *et.al.* 2014:3612). From the X-ray diffractions and NMR measurements, each AGU in the cellulose chain is assumed to have $4C_1$ chair conformation.

The hydroxyl groups (OH) and the hydrogen atoms are positioned at the equatorial and axial plane, respectively (Lindman *et.al.* 2010:77).

Each AGU possesses a hydroxyl group on the carbon atoms C_2, C_3 and C_6. These carbon atoms provide the opportunity for the modification and derivation of cellulose, in different manners, with reactions which are commonly used in primary and secondary alcohols. The hydroxyl groups on each end of the cellulose molecule also give the molecule a chemical polarity (Kihlman 2012:2); the reducing end of the cellulose molecule group (C_1) has an AGU with a free carbon atom whilst the non-reducing end group (C_4) has an AGU that is involved in the glycosidic linkage. Different analyses have proved the existence of intra and inter molecular hydrogen bonds between the hydroxyl groups of the C_3 to the O_5 and between C_2 and the C_6 (Kraäsig 1993:978-982) and these hydrogen bonds are reported to be the cause of cellulose insolubility in water and most solvents (Brandt *et.al.* 2013:552).

The cellulose polymer chain is shown in Figure 1.3.

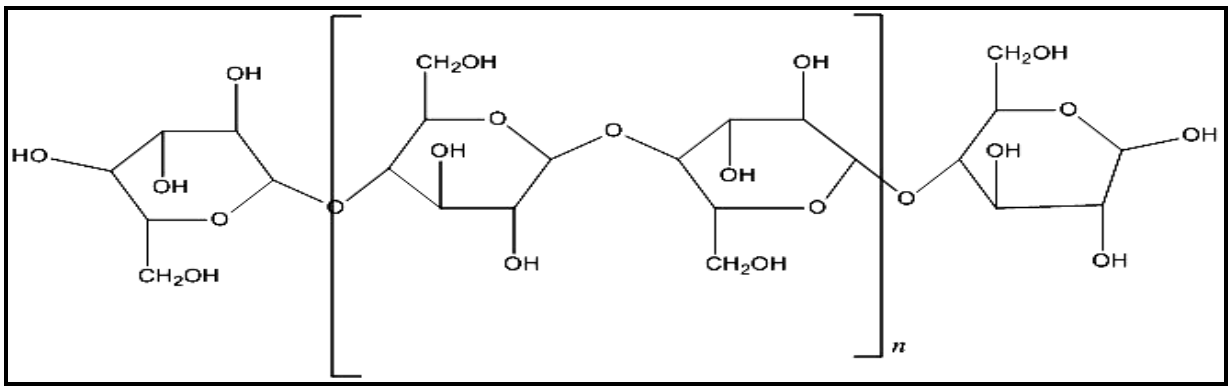

Figure 1.3 A cellulose polymer chain as reproduced from Swatloski *et.al.* (2002:4974)

Cellulose is used either in its native or derivate form in a wide range of industrial applications of which the pharmaceuticals and textile industries are the largest. The native cellulose molecule has only the ability of generating intramolecular hydrogen bonds (i.e. within a molecule) but also intermolecular bonds (i.e., between molecules) from C_6 in one chain to C_3 on the neighbouring molecules and both types of hydrogen bonds are shown in Figure 1.4.

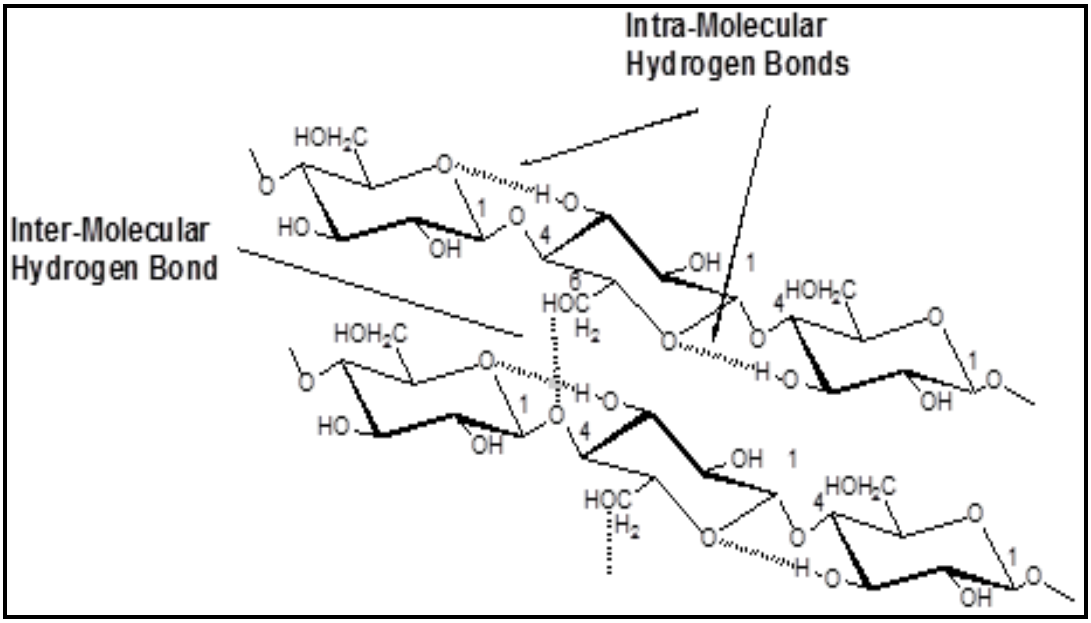

Figure 1.4 The intra- and intermolecular bonds within cellulose molecules as reproduced from Kihlman (2012:5)

Cellulose is biodegradable, renewable and environmentally friendly as a biomaterial, and this has resulted in many other industries showing interest in its use (Hermanutz *et.al.* 2008:23; Mahmoudian *et.al.* 2012:1251; Zhao *et.al.* 2012:1490). Cellulose is therefore gaining attention as new methods are discovered for processing it into products to replace those from non-renewable sources.

1.2.1.2 *Hemicelluloses*

Hemicelluloses is a group of heterogeneous complex polysaccharides (Cheng *et.al.* 2010:4659) and makes up around 35 % wt of the biomass. These carbohydrate polymers are of lower molecular weight than cellulose (DP around 100-200). Hemicelluloses is composed of both hexoses and pentoses sugars i.e., C_5 and C_6 sugars

- glucose, mannose and galactose and the C_5 sugars
- xylose and arabinose

The structure of hemicelluloses random and amorphous with short side branches of various saccharides that can be easily hydrolyzed (Espinoza-Acosta *et.al.* 2014:3612). The hemicelluloses are thought to bind to the surface of the cellulose fibrils non-covalently and also acts as an amorphous matrix material, holding the stiff cellulose fibrils in place.

The most predominant hemicelluloses sugar in hardwood is xylose and in softwood it is mannose. Due to its non-crystalline nature, hemicelluloses is more susceptible to depolymerization (especially in acidic conditions) than cellulose, this aspect of its behaviour is exploited to find uses for the hemicellulloses (Brandt *et.al.* 2013:15).

The structures of the different sugars are shown in Figure 1.5 (Brandt *et.al.* 2013:553).

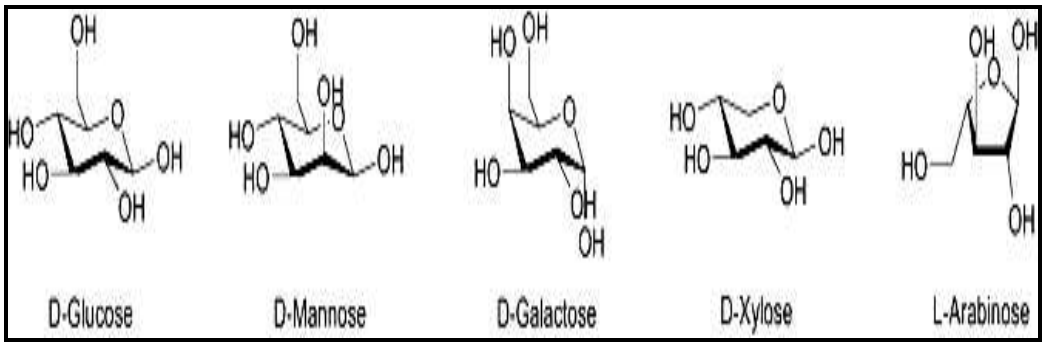

Figure 1.5 The structure of hemicelluloses as reproduced from Brandt *et. al.* (2013:553)

1.2.1.3 *Lignin*

Lignin is an aromatic, water-insoluble complex network polymer that provides water-proofing, structural reinforcement and resistance to biological and physical attack compared on the carbohydrate cell walls of immature plant tissues. It is biosynthesised from up to three monomers: coniferyl, sinapyl and *p*-courmarly alcohols (Cheng *et.al.* 2010:4659), in order of abundance and the structures are shown in Figure 1.6.

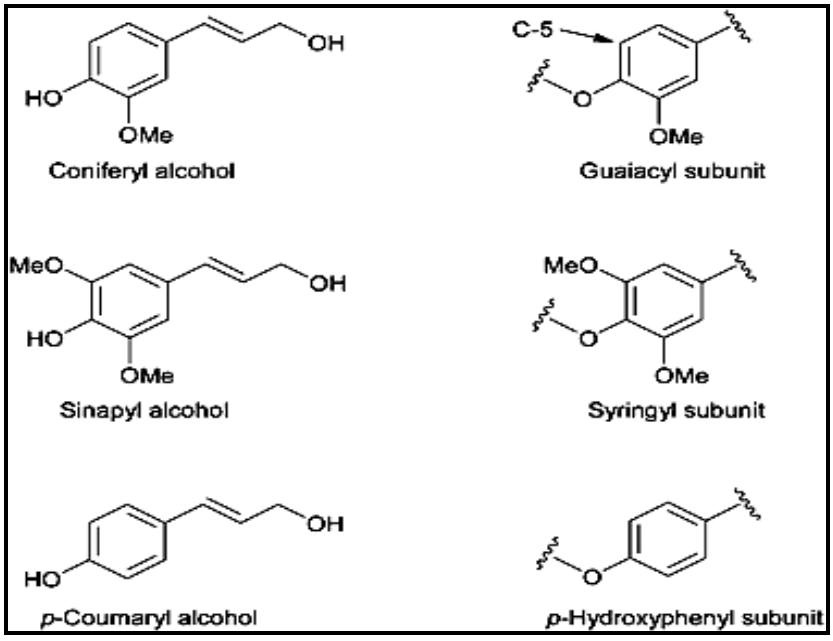

Figure 1.6 The three monolignols from which lignin is synthesised. The monomers vary in substitution at the C-3 and the C-5 ring positions as reproduced from Brandt *et.al.* (2013:554)

The composition of lignin differs between softwoods and hardwoods with softwoods consisting almost completely of guaicyl units while hardwood also contains a large number of syringly units. The lignin component is mainly used through direct combustion. However, it can be a promising source for chemicals such as phenols and aromatics (Cheng *et.al.* 2010:4659). Most chemical deconstruction methods change lignin by modifying its ether bonds, but some remove it from the pulp (e.g. Organoslov pulping and Kraft pulping). The removal of lignin is a combination of chemical fragmentation and the ability of the liquor to solvate the modified lignin fragments (Brandt *et.al.* 2013:554).

1.2.2 Extractives

Wood extractives are a heteregeneous group of organic compounds obtained from wood by either organic solvent or water extraction (Kilulya *et.al.* 2011:3272). They constitute a small fraction of compounds in wood that can range from 1 to 20 % depending upon species and position within the tree. Extractives can cause serious problems in the process of chemical cellulose production and in the quality of the final products (Kilulya *et.al.* 2011:3272). The extractives are low molecular weight constituents and can be grouped into two main classes,

i.e., lipophilic (fatty), eg., resin acids, fatty acids, triglycerides, free sterols and hydrophilic extractives, e.g., phenols, lignans, flavanoids, tannins (Sjoström, 1981:169-189).

All wood components such as hemicelluloses, lignin and extractives except for cellulose, are regarded as interferences in the pulp and papermaking process and efforts are made to remove them from the production processes. A bleached wood pulp that has high cellulose content (> 90 %) is called dissolving pulp, and is used in the production of regenerated cellulose.

Dissolving pulp is discussed in detail in the next section/ paragraph.

1.3 DISSOLVING PULP

Dissolving pulp also known as cellulose pulp or chemical cellulose, is a special grade of bleached pulp of high quality and purity. It has a high α-cellulose content (cellulose with high DP), high brightness, low hemicelluloses, and low lignin. Dissolving pulp is used as raw material for producing various cellulosic derivatives such as cellophane, rayon, acetates, nitrates, carboxymethyl cellulose and several types of regenerated cellulose such as viscose and microcrystalline cellulose (Sjoström 1981:169-189).

Dissolving pulps should have distinct characteristics such as (Kraäsig 1993:978; Dafchahi *et.al.* 2012:3283):

- High purity,
- Uniform molecular weight distribution,
- Suitable reactivity (degree of ability of reactants to access the free hydroxyl groups in a cellulose chain and to form covalent bonds), and
- Accessibility (physical ability of reactants to reach hydroxyl groups) of the cellulose to chemicals

Most chemical cellulose (dissolving pulp) is obtained from wood using the prehydrolysis Kraft or acid sulphite processes (Biermaan *et.al.* 1993:482; Hinck *et.al.* 2006:213). *Eucalyptus* species is a predominant source of dissolving pulp in South Africa and globally (Sixta 2006:1). *Eucalyptus* pulp was first introduced as a market pulp during the early 1960's. South African Eucalyptus species shows a seven year growth cycle; this is the shortest of all trees worldwide and this translates into very high forest productivity (Sixta 2006:1350).The acid sulphite and pre-hydrolysis Kraft processes are the most globally used methods for dissolving pulp production from wood (Biermaan *et.al.* 1993:482; Hinck *et.al.* 2006:213; Kihlman 2012:3) and the two methods are discussed in detail below.

Sappi Chemical Cellulose in South Africa manufactures different grades of dissolving pulp, which are predominantly made from *Eucalyptus* wood source and are used primarily for the production of viscose and acetate. Dissolving pulp is a high purity cellulose pulp, and that is achieved by the removal of the hemicelluloses, lignin and extractives by chemical pulping using sulphite or Kraft process.

Sappi Chemical Cellulose in South Africa uses an acid bi-sulphite and pre-hydrolysis Kraft process to produce dissolving pulp.

1.3.1 Acid sulphite process

This is a chemical pulping process that removes hemicelluloses, lignin and extractives under acidic conditions. Typically, a calcium, magnesium or ammonia process is used.

The acid sulphite process can be varied by the use of different cations, pulping pH and cooking temperature. Initially a calcium sulphite process (Ca $(HSO_3)_2$ and SO_2) was used which had cooking times of up to 10 hours at the temperature of 145 ˚C, which was replaced by more soluble cations such as magnesium, sodium and ammonia due to the regeneration of insoluble calcium sulphate (Sixta 2006:1350; Sjoström 1981:169-189).

The acidity in the pulping sequence ranges from pH 1-2 in the conventional calcium process, up to pH 5 for the magnesium process and a wide pH range for the sodium process.

Later, a sulphite process with two or three cooking stages was introduced to alter between different pH levels in order to improve the amount of hemicellulose and lignin removed. The major drawbacks associated with the sulphite process are:

a) the limited use of wood material and

b) the environmental concerns associated with it, particularly difficulty in chemical recovery during the process (Lekha 2012:8).

In the 2 step stage, the first step consists of a neutral to slightly acid cooking solution, during which lignin is sulfonated (treating lignin with concentrated sulphuric acid to form a sulphonate) but remains in a solid phase where the most reactive groups are protected by sulfonation and can thus condensate with pinosylvine in the second stage to form a severe lignin condensation “black cook” (Sixta 2006:1350; Sjoström 1981:169-189).

The acid conditions in the sulphite process result in the cleavage of glycosidic bonds in the cellulose and hemicelluloses. Due to their low DP, together with their amorphous state, as well as glyosidic bonds, depolymerisation of the hemicelluloses is easier than the cellulose. The cellulose chains are also affected by the acid hydrolysis during the entire cooking

process, but the major depolymerisation of cellulose only occurs at the end of the delignification (Sixta 2006:1350; Sjoström 1981:169-189).

A flow diagram for a typical acid sulphite process is shown in Figure 1.7.

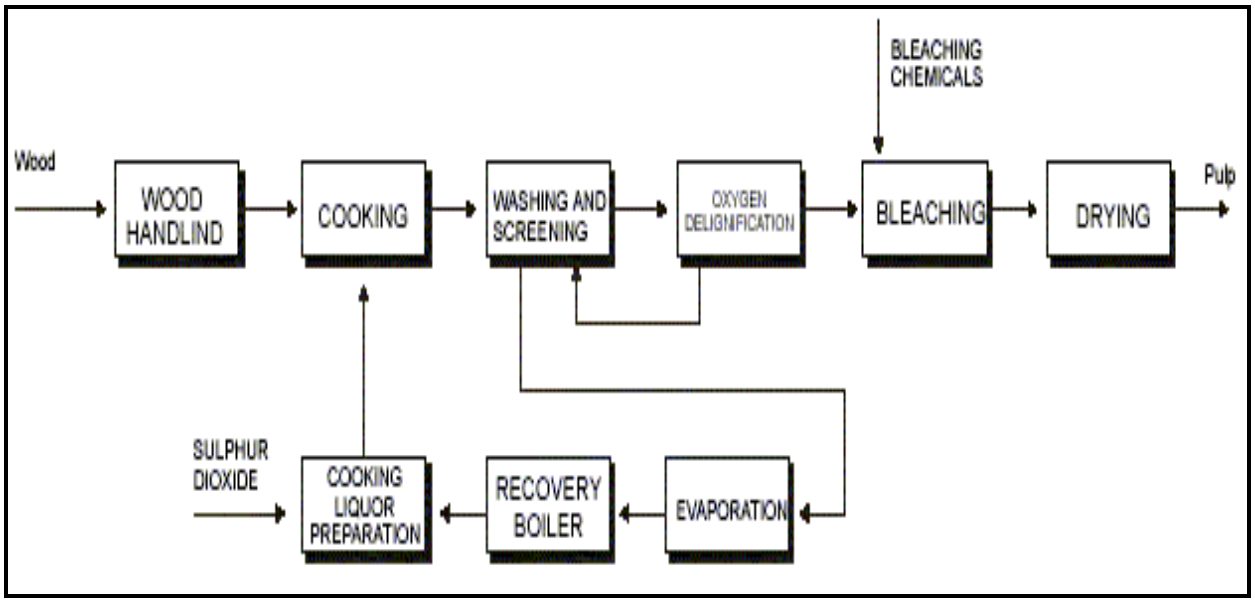

Figure 1.7 The flow diagram of an acid sulphite pulping process as reproduced from Jesus *et.al.* (2011:249)

Cellulose is not a thermoplastic polymer (type of plastic that changes properties when heated and cooled) and it degrades before melting. Thus cellulose is dissolved before conversion into variety of products such as MCC, cellulose acetate and viscose. Dissolution is a process that is necessary to transform the solid cellulose into a liquid phase. However, due to its strong inter- and intra-molecular hydrogen-bonded cellulose is insoluble in water, and in many inorganic and organic solvents (Spiridon *et.al.* 2011:400).

The solvent systems available for cellulose dissolution can be classified into two basic groups:

- Derivatizing and
- Non- derivatizing

Derivatizing solvents modify the cellulose prior to dissolution, e.g., in the viscose process discussed in detail below, these solvents react with one or several of the three reactive hydroxyl groups in the cellulose, thus making it more soluble in common organic solvents such as dimethylformamide (DMF) or dimethylsulfoxide (DMSO). Formic acid, trifluoroacetic acid, dichloroacetic acid and paraformaldehyde/ DMSO have all been investigated as derivatizing solvents. Derivatizing solvents suffer from side reactions leading to unknown products, which reduces reproducibility and may hinder downstream processing (Brown, 2012:8; Ding *et.al.* 2012:7; Sjoström 1981:169-189).

Non-derivatizing solvents do not modify the cellulose prior to dissolution but dissolve instead by disturbing the forces keeping it together without any chemical modification (Brown, 2012: 8; Ding *et. al.* 2012:7; Sjoström 1981:169-189).

1.3.2 Pre-hydrolysis Kraft process

Only a brief description of the cooking steps and their impact on the cellulose production will be mentioned here since both the processes and their possible variations have been described elsewhere (Sixta 2006:1350; Sjoström, 1981:169-189).

The Kraft process is an alkaline delignification process using sodium hydroxide (NaOH) and sodium sulphide (Na_2S). One main advantage of the Kraft process is the ability to process all wood types, while the sulphite process in most cases cannot process pine wood due to the presence of phenolic compounds in lignin and a strong concentration of pinosylvine (1,3-Benzenediol, 5-(2-phenylethenyl)) in pine wood, a lignin condensation at low pH or low concentrations of sulphur dioxide can occur, hence pine wood is not used in the sulphite pulping process.

In general, for hardwoods the pre hydrolysis stage is used to treat the wood chips before the actual Kraft pulping stage. The wood chips are steamed or cooked in water in a temperature range of 140-170 ˚C for 30-60 minutes, where acetyl and formyl groups are cleaved from the wood forming acetic and formic acid, thus lowering the pH to 3-4. The acids formed in this pre-hydrolysis step promote acid hydrolysis, reaction in depolymerisation of wood components and reducing the wood mass. During this step in softwoods, half the amount of hemicelluloses can dissolve while in hardwoods only small amounts of lignin can be

removed. Prolonging the pre hydrolysis step depolymerizes hemicelluloses to achieve higher purity in the final product, but cellulose yield decreases.

The cellulose molecules do not remain stable under these strong alkali conditions and Kraft pulping thus results in considerable carbohydrate losses. The degradation of carbohydrates in the alkali process consists of three reactions (Sixta 2006:1350; Sjoström, 1981:169-189):

a) Peeling at the end of a carbohydrate chain,

b) Oxidative peeling randomly in the chain at temperatures over 80 ˚C and,

c) Alkaline hydrolysis at temperatures over 140 ˚C

These reactions result in the yield of cellulose being reduced in Kraft pulping. However, hemicelluloses are degraded more rapidly due to their lower DP, branched chains and amorphous state. The remaining hemicelluloses then becomes less branched in their structure after degradation, increasing the tendency for crystallization and tendency to associate to the cellulose molecules which in turn can increase the caustic resistance of hemicelluloses in the viscose process.

Degradation of cellulose occurs mostly in the final phase of cooking even though the DP is decreased, the total yield loss at higher temperatures is fairly small (Sixta 2006:1350; Sjoström, 1981:169-189). A flow diagram for a typical Kraft process is shown in Figure 1.8.

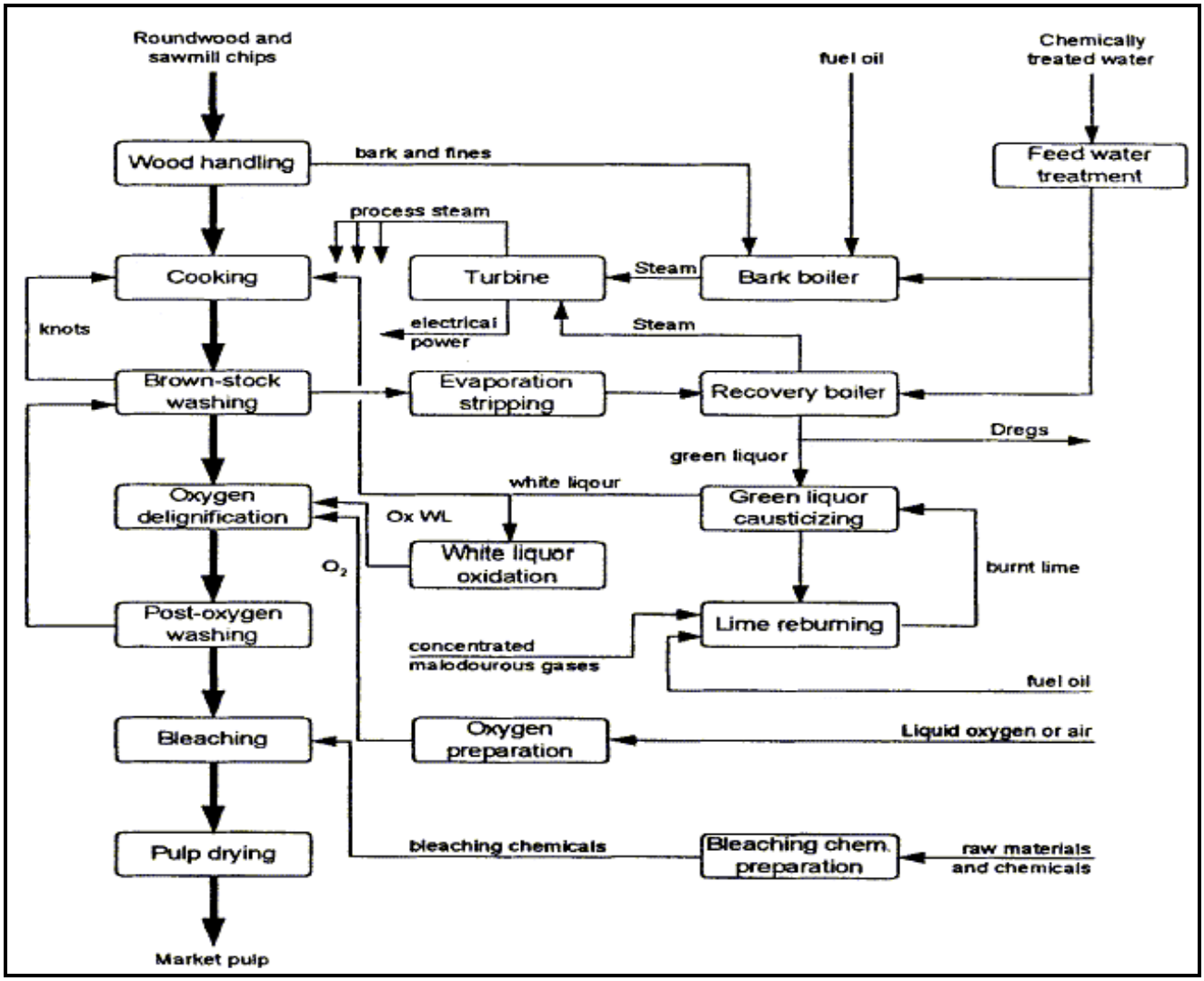

Figure 1.8 The flow diagram of Kraft pulping process as reproduced from Speak *et.al.* (2002:10)

1.4 CONVENTIONAL SOLVENTS FOR CELLULOSE DISSOLUTION

1.4.1 Viscose process

The viscose process developed in the 19th century by Cross, Bevan and Beadle has been the most widely used cellulose solvation method used commercially for the manufacture of cellophane and rayon fibres from wood cellulose (Liebert 2010b:6). Through this process, the cellulose fibres from cellulosic materials are soaked in sodium hydroxide (NaOH) solution to swell the polymer for a few hours and create alkali cellulose (Brown, 2012:8).

Most of the hemicelluloses and some low molecular weight cellulose are dissolved in the NaOH solution. This alkali cellulose is then reacted with carbon disulphide (CS_2) to form cellulose xanthate, a cellulose derivative that is soluble in a dilute NaOH solution. Side reactions in this step lead to the formation of by-products such as sodium trithiocarbonate (Na_2CS_3), giving the yellow to orange colour in the xanthate and viscose fibres (Sixta 2006:1350).
After the cellulose xanthate crumbs have been formed, water and caustic soda (NaOH) are added under vigorous agitation to facilitate the dissolution of the cellulose and the formation of the viscose dope in the dissolving step.

For textile viscose, the composition of dope is about 10 % wt. cellulose and 5 % wt. caustic. After filtration, the viscose dope is pressed through spinnerets (see Figure 1.9) into an acid spin bath consisting of mainly sulphuric acid (H_2SO_4), and sodium sulphate (Na_2SO_4), releasing both carbon disulphide (CS_2) and hydrogen sulphide (H_2S) (Strunk 2012:11).

Figure 1.9 A typical shape of a pinneret with 0.5 inch diameter as reproduced from Strunk (2012:12)

The disadvantages of the viscose process are listed below (Liu *et.al.* 2011a: 220; Liu *et.al.* 2011b: 2381; Phillip *et.al.* 2009:4; Sun *et.al.* 2008:283):

- Environmental problems caused by the release of the volatile CS_2 and H_2S solvents which are known to be toxic and are human reproductive hazards
- Process is complex and is labour intensive
- Recovery of these solvents in most viscose factories is around 50%, and the other 50% contaminates the environment
- process also uses hazardous chemicals such as sodium hydroxide and sulphuric acid

The advantages of the viscose process are listed below (Cao *et.al.* 2009:13):

- The regenerated cellulose fibres produced by the well-known viscose process last for about 100 years
- The regenerated cellulose fibres have excellent properties for a wide range of products from wet-strength cotton like textile fibres to technical fibres as the cord found in high performance tires

1.4.2 The Lyocell process

In response to the environmental concerns over the viscose process, the lyocell process was implemented and commercially used since 1984 to produce synthetic cellulose fibres.

In this process N-methylmorpholine-N-oxide (NMMO) is a direct solvent for cellulose, in that it dissolves cellulose without prior derivatization or activation. Unlike the viscose process, the lyocell process is a physical process using non-derivatizing solvent system that is based on regenerating cellulose from NMMO monohydrate solution by using a spinneret (picture of spinneret shown in Figure 1.7) whereby the solution is drawn through an air-gap and coagulated in water or an aqueous NMMO solution (Jiang *et.al.* 2011:922). NMMO is an

oxidizing agent, and it dissolves cellulose because of its strong N-O dipole. The advantages of the lyocell process are listed below (Cao *et.al.* 2009:13):

- Dissolution of cellulose is simpler than that of the viscose process
- Solvent is recycled (>99%) reducing the environmental impact and cost, while still producing high- value synthetic fabric for a variety of applications.

Dissolution of cellulose with NMMO is used commercially for manufacturing of regenerated cellulose. However, it has some disadvantages (Cao *et.al.* 2009:13; Heinze *et.al.* 2005:521; Hermanutz *et.al.* 2008:24; Zhang *et.al.* 2005:8272) such as:

- Demand for high temperatures to dissolve cellulose that may result in explosions
- High cost due to complexity of the system as there are multiple reaction pathways that take place in the system
- The regenerated fibres produced exhibit a high fibrillation trend in wet state, although indicating high strength and good stability
- The recycling of NMMO also faces a challenge with regard to solvent stability and recovery efficiency
- Degradation of cellulose

Because of the environmental concerns relating to conventional solvents such as volatility, generation of toxic gas and difficulty in recovery for recycle use (Fukaya *et.al*. 2008:44), therefore better/new cellulose solvents needed to be investigated. The new solvents should be easy to recycle, steady, non-toxic and non-derivative.

1.5 NON-CONVENTIONAL SOLVENTS FOR CELLULOSE DISSOLUTION

1.5.1 NaOH/ Thiourea solvent system method

It was reported by (Jiang 2011:1) that cellulose could be dissolved in 9.5 % wt. NaOH and 4.5 % wt. thiourea pre-cooled between -8 to -5 ˚C. This method uses a multi-roller set to draw coagulated fibres and is the first process to successfully use wet spinning to produce multi-filament fibres. The process includes two steps: coagulation and post treatment.

The regenerated fibres obtained from this process showed higher degree of crystallinity but a lower degree of crystal orientation when compared to rayon fibre obtained from the viscose process. Scanning electron microscopy (SEM) data showed that the fibres inhibited cellulose II character and had a circular cross-section and smooth surface. The mechanical properties of the pulps are improved with this process, making them better suited for the production of pure cellulose fibres, functional cellulose fibres and nano materials on an industrial scale (Jiang 2011: 1).

In order to reduce pollution and mass energy consumption caused by traditional methods of regenerating cellulose, a new NaOH/Urea system was developed by Liebert (2010b:20) and is discussed in details below.

1.5.2 NaOH/Urea aqueous solution method

This process is used for the regeneration of cellulose fibres using low cost chemical reagents and produces non-toxic by-products. In this process, cellulose is dissolved in a NaOH/Urea solution, and then rapidly pre-cooled to -12 ˚C rapidly. The presence of urea and the low temperatures plays an important role in the improvement of cellulose solubility. This solvent system formed a non-derivative aqueous cellulose solution system. The structures of the regenerated fibres wet-spun from a cotton pulp and NaOH/Urea solution under different conditions were investigated by wide angle x-ray diffraction (WAXD). The WAXD results showed that an increase in flow rate during spinning produced a higher degree of crystal orientation and higher degree of crystallinity. The solution was coagulated in a H_2SO_4/Na_2SO_4 solution at 15 ˚C, and the obtained regenerated fibres exhibited a high degree of crystallinity and high crystal orientation, which were comparable to those of rayon fibres

obtained from the viscose method. The physical properties of the fibres produced by the NaOH/Urea method were similar to those of the fibres produced by the NMMO process, because of the similar dissolution and regeneration conditions in spinning. However, according to Liebert (2010b:20), this wet spinning process has some drawbacks such as:

- Process being complex
- High cost of the process due to the solvent requiring special temperatures to operate under and the presence of urea

1.5.3 Ionic Liquids

Recently, ionic liquids (ILs) were found to be good solvents for cellulose dissolution and ILs are considered to be "green" solvents. ILs are a class of organic salts that exist as liquids at temperatures below 100 ˚C (FitzPatrick *et.al.* 2012:1124; Hermanutz *et.al.* 2008:24). ILs consists of positive and negatively charged ions.

1.5.3.1 *The structure of ILs*

The structure of ILs is similar to other salts such as sodium chloride, however the key difference in ILs is that ILs remain liquid at temperatures below 100 ˚C. ILs are typically composed of bulky asymmetric organic cations like 1-alkylpyridinium, 1-alkyl-3-methylimidazolium, 1-methylpyrrolidinium, ammonium ions (a selection of the common cations are shown in Figure.1.10), and a wide range of anions: halides tetrafluoroborate, hexafluorophosphate, bis (trifluorosulfonyl) amide, triflate or tosylate, (some common anions are shown in Figure 1.11) (Bentivoglio *et.al.* 2006:154). Both ionic species influence the final properties of ILs. Usually, the anion controls the water miscibility but the cation also has an influence on the hydrophobicity or hydrogen bonding ability (Kuzmina 2012:1).

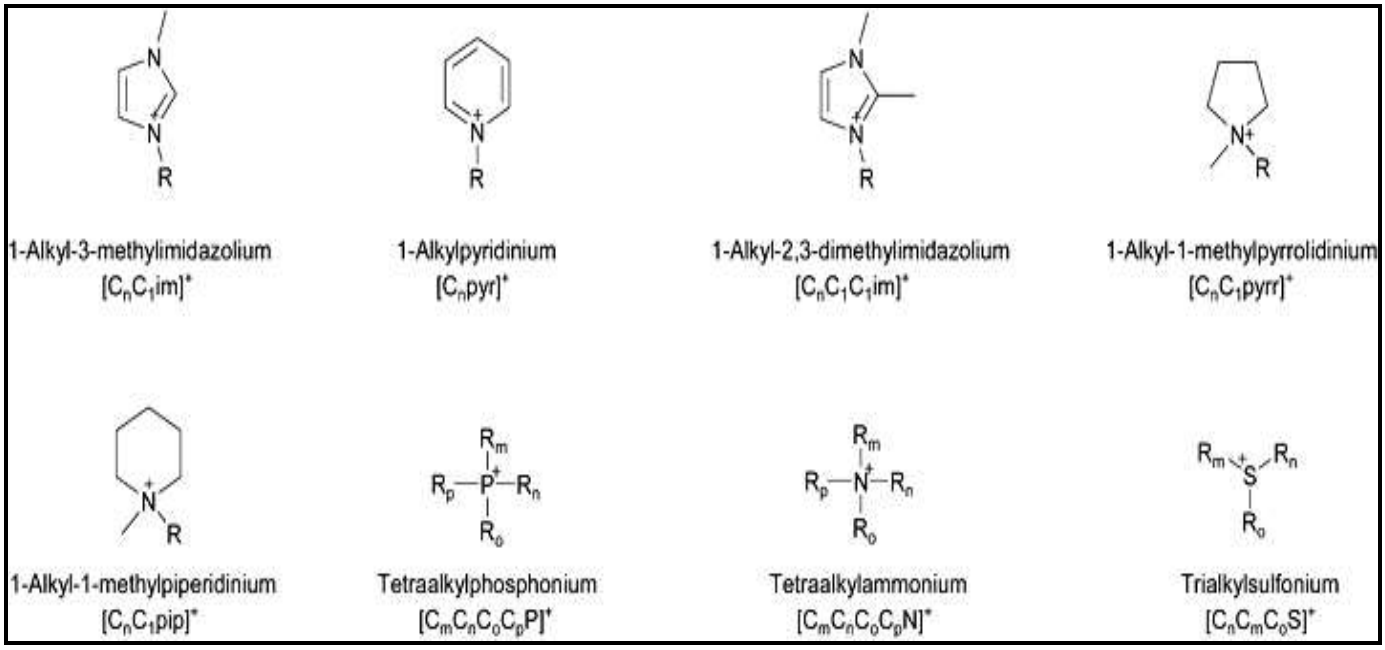

Figure 1.10 Common cations used in ionic liquids as reproduced from Bentivoglio *et.al.* (2006:154)

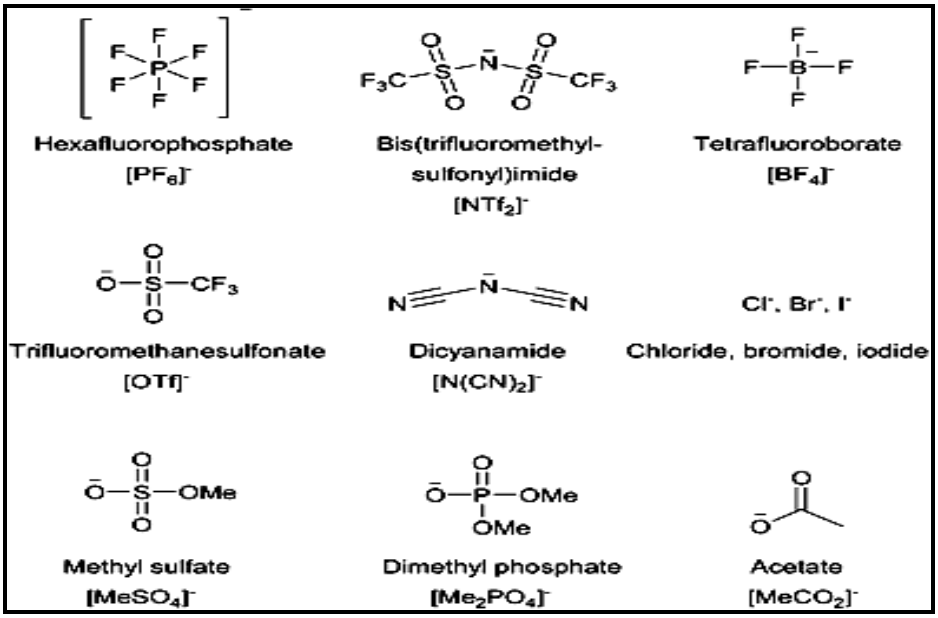

Figure 1.11 Common anions used in ionic liquids as reproduced from Bentivoglio *et.al.* (2006:154)

1.5.3.2 *Notable characteristics of ILs*

The properties of ILs can be defined mainly by the presence of both organic cations and inorganic anions. As solvents, ILs possess several advantages over traditional organic solvents, which makes them environmentally compatible (Bentivoglio *et.al.* 2006:154; FitzPatrick *et.al.* 2010:8915; Fort *et.al.* 2007:63; Seddon 1997:351):

- ILs, unlike organic solvents, have non-measurable vapour pressures because. Thus, they cannot be easily evaporated into gases. Their use therefore reduces harmful effects on the environment. This property also enhances their recycling and this is one of the reasons they are referred to as "green solvents".
- ILs have good thermal stability. The decomposition temperatures of many ILs can be more than 300 ˚C
- ILs have good electric conductivity,
- ILs have wide liquidus range from -200 to 300 ˚C
- ILs have excellent dissolution performance for organic, inorganic compounds and polymer materials
- ILs can be easily recycled
- ILs are non-flammable
- ILs have unique solubility properties for diverse kinds of materials

Another important feature of ILs is their design ability where their properties can be adjusted through side chain lengths on the cation and the choice of anion to satisfy specific application requirements (Feng *et.al.* 2008:1). Furthermore, their properties can be varied by introduction of functional groups. Because of their specific properties, ILs have been found to be useful in many fields, such as reaction media in organic synthesis or electrolytes for electrochemical applications (Bentivoglio *et.al.* 2006:154).

The diversity of ILs makes them applicable to many industries that include biocatalysis and separation processes, polymer and catalytic chemistry, electrolytes, biosensors, analytic devices, lubricants and solvent replacement applications (Pinkert *et.al.* 2009:6715).

Recently, the IL 1-ethyl-3-methylimidazolium acetate [Emim][OAc] has been in the limelight of biomass processing research because of its ability to dissolve cellulose. This IL is an attractive solvent for biomass because it has low melting point, low toxicity, non-volatility and high cellulose and lignocellulosic biomass dissolution capacity. It has been reported that IL to date is the solvent that have the greatest potential for industrial scale biomass processing (Karatzos *et. al.* 2012a:307).

1.6 SCOPE OF THIS STUDY

For decades, the forestry industry has been mainly focused on the production of paper and board. However, a small but appreciable market has been directed towards the production of cellulose derivatives and regenerated cellulose. To produce cellulose derivatives and regenerated cellulose, good cellulose accessibility and reactivity are desired. However, cellulose presents a compact structure that makes accessibility difficult and thereby results in low-quality products.

Many studies have attempted to overcome this problem. However, due to the complexity of the cellulose structure, there are still many aspects that must be considered altogether such as the type of wood species used, morphology of the regenerated cellulose, and the pulping process employed.

The aim of this work was to study the behavior of cellulose from three biomass samples viz., sawdust, fully bleached dissolving pulp and unbleached dissolving pulp in 1-ethyl-3-methylimidazolium acetate ionic liquid and dimethylsulfoxide (DMSO) /dimethylformamide (DMF) mixtures.

The development of environmentally friendly processes for dissolving and/extracting cellulose and other components from the lignocellulosic materials will be very useful in the context of the biorefinery philosophy. To this end, one promising alternative for the dissolution of cellulose is the use of the green solvents (ILs). These aprotic solvents are used as the co-solvents together with ILs due to their ability to solubilize biomass materials as well as low viscosity (Fort *et.al.* 2007:63; Gao *et.al.* 2013:1536).

The focus of working on biomass and pulp dissolution processes is to gain access to the cellulose and this can be achieved by breaking down the hydrogen bond structure within the cellulose, and also break up the lignin-hemicellulose shield to make the cellulose more accessible, as shown in Figure 1.12.

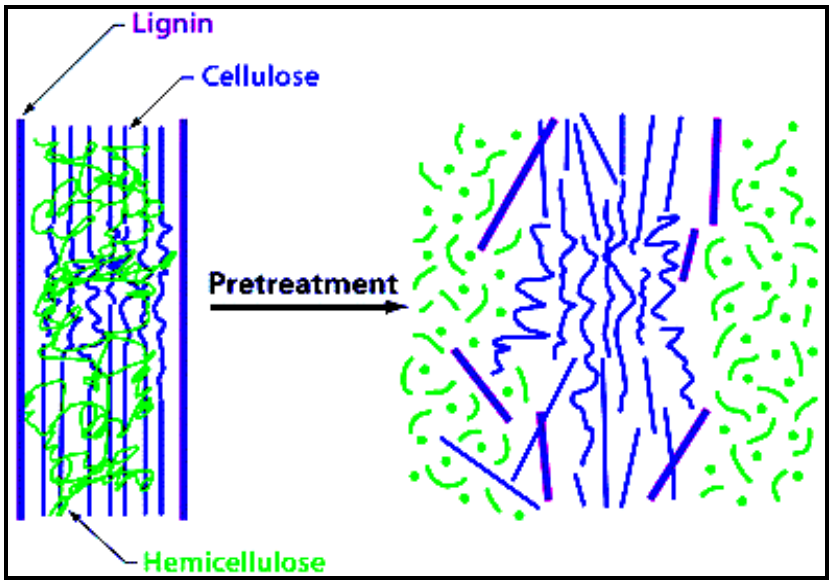

Figure 1.12 Chemical deconstruction that disrupts the lignocellulose structure to make cellulose accessible as reproduced from Brandt *et.al.* (2013:555)

Various techniques were used in this study including NMR, FTIR, XRD, SEM and TGA to assess the effect on the solid yield (wt. %) after dissolution in IL/co-solvents and on cellulose crystallinity of IL/co-solvent treatment on the lignocellulose deconstruction on a laboratory scale. Cellulose crystallinity, often measured in connection with IL/co-solvent dissolution process, is of particular interest in this study which aims to alter the structure of the native cellulose.

1.7 AIMS AND OBJECTIVES

As a fundamental step towards creating a new class of green cellulose materials, the proposed research will investigate dissolution and fibre properties of regenerated cellulose of biomass from [Emim][OAc] + co-solvent systems.

The aims of the present study were to:

i. To study the dissolution and regeneration of South African *Eucalyptus dunnii* sawdust wood, unbleached dissolving pulp and bleached dissolving pulp in [Emim][OAc] + DMF /DMSO mixtures and calculate the percentage cellulose recoveries after the dissolution and regeneration process

ii. Characterize the regenerated cellulose fibres to see changes in morphology, crystallinity, structural changes and bond breakages.

iii. Recover the IL by using the rotary evaporator and characterize the recovered IL by ^{1}H NMR and FTIR

iv. Study the influence of the lignin on the regenerated cellulose and characterization by FTIR

CHAPTER 2: LITERATURE REVIEW

2.1 INTRODUCTION

Ionic Liquids appear have an ionic character, resulting in their enhanced biopolymer dissolving capacity. Table 2.1 gives an overview of the cellulose-dissolving capacity of ILs reported in literature. A number of factors influence the cellulose dissolution (Fort *et.al.* 2007:63; Kilpelainen *et.al.* 2007:9142):

- Low viscosity ILs promote the dissolution process (mainly due to the higher mobility of the ions)
- Longer dissolution times (> 12 hours) do not always lead to better results, especially at higher temperatures

It is important to note that Table 2.1 only deals with the dissolution capacity of these solvents, and not with the kinetics.

It was first discovered by Graenacher in the 1930's that cellulose could be dissolved in molten N-ethylpyridinium chloride salt (Graenacher, 1934:1-9). However, little attention was paid to this finding at the time most probably due to the high melting points of these salts, until 2002.

A study by Rogers and co-workers in year 2002 first showed that some imidazolium-based ILs could dissolve cellulose efficiently at low temperatures (<100˚C) (Swatloski *et.al.* 2002:4974). Since, Swatloski *et.al.* (2002:4974) reported that cellulose could be dissolved in ILs without formation of any derivative, great progress in cellulose dissolution and cellulose modification was established and interesting results were reported in literature by various pioneers in the applications of ILs for cellulose, lignin and complete biomass dissolution (Ang *et.al.* 2011:4790; Brandt *et.al.* 2013:550; Cao*et. al.* 2009:13; Casas *et.al.* 2012:115; Han *et.al.* 2009:825; Heinze *et.al.* 2005:520; Heinze *et.al.* 2008:8; Karatoz *et.al.* 2012:2; Kohler *et.al.* 2007:2311; Kim *et.al.* 2011:9020; Sun *et.al.* 2009:646; Wei *et.al.* 2012:227; Zhao *et.al.* 2012:1490).

It was speculated by Olivier-Bourbigou *et.al.* (2010:1-2), that the ionic liquid cations enhance the attack in the oxygen atom of cellulose's hydroxyl group. According to Fukaya *et.al.* (2010:44), when the critical temperature is exceeded, IL dissociate to cations and anions, and the free cation-complex of the solvent associates with hydroxyl oxygen of cellulose and the free anions associate with the hydroxyl proton in cellulose.
ILs also show disadvantages like high melting points, high hygroscopicity and sometimes even degradation of cellulose (Heinze *et.al.* 2005:521).

2.2 DISSOLUTION METHODS OF CELLULOSE

2.2.1 Introduction

The dissolution of compounds in a solvent and the formation of a homogeneous solution take place only if the mixed state corresponds to a lower free energy than two separate phases. However, dissolution may not be achieved even if favourable free energy conditions prevail. The process may be too slow on the time scale of the observation. Standard techniques to enhance the rate of dissolution involve heating and stirring, as this speeds up and increases contacts between solvent and solute (Lindman *et.al.* 2010:77).

Placement of polymer samples in a solvent results in fast contact of the polymer with solvent molecules and penetrate into the surface, often resulting in a gel like consistency of the outermost part. Polymer molecule diffusion is intrinsically much slower than solvent diffusion and for concentrated polymer solutions severely delayed by entanglement and association. Therefore, polymer dissolution is slow in general and further slowed down for semi-crystalline polymers (Körner 2006:1).

The information is summarized from the preceding literature review shown in Table 2.1 summarizes the dissolution of cellulose under various parameters in different types of ILs.

Table 2.1 Summary of the dissolution of cellulose in different types of ILs

Cellulose	Ionic Liquids	Conditions		Solubility % wt.	References
		Time mins	Temp ° C		
MCC Pulp cotton (linter)	[Amim][Cl]	40-240	100-130	5-14.5	(Zhang *et.al.* 2005:7)
MCC (Avicel)	[Amim][Cl]	720	90	5	(Zavrel *et.al.* 2009:7)
Pulp(DP=1000)	[Bmim][Cl]		100	10	(Heinze *et.al.* 2005:7)
Pulp (DP=286)	[Bmim][Cl]	720	83	18	(Erdmenger *et.al.* 2007:7)
MCC (Avicel)	[Bmim][Cl]	120	100	20	(Vitz *et.al.* 2012:7)
MCC (Avicel)	[Bmim][Cl]	60	100	20	(Vitz *et.al.* 2012:7)
Pulp	[Bmim][Cl]	-	85	13.6	(Kosan *et. al.* 2008: 7)
Pulp	[Emim][Cl]	-	85	15.8	(Kosan *et.al.* 2008:7)
MCC (Avicel)	[Emim][Cl]	60	100	10-14	(Vitz *et.al.* 2009:7)
MCC (Avicel)	[Emim][Cl]	-	90	5	(Zavrel *et.al.* 2009:7)
Pulp	[Emim][OAc]	-	85	13.5	(Kosan *et.al.* 2008:7)
MCC (Avicel)	[Emim][OAc]	-	110	15	(Zhao *et.al.* 2005:7)
MCC (Avicel)	[Emim][EtO_2PO_2]	60	100	12-14	(Kosan *et.al.* 2008:7)
MCC	[Bmim][HCOO]	-	110	8	(Erdmenger *et.al.* 2007:7)
MCC (Avicel)	[Hexmim][Cl]	120	100	7	(Erdmenger *et.al.* 2007:7)
MCC	[C_2mim][(MeO)(HPO_2)]	60	60	6-10	(Fukaya *et.al.* 2008:7)

2.2.2 Different methods for dissolution

2.2.2.1 *Microwave heating*

Microwave heating, as an alternative to conventional heating technique, has been successfully applied in organic synthesis and carbohydrate degradation due to its thermal effects and non-thermal effects, raised from the heating rate, acceleration of ions and molecules collision, and rapid rotation of dipoles. In addition, microwave energy can easily penetrate to particles inside hence all particles can be heated simultaneously, which resolves the heat transfer resistance problem and make particles to be more uniform and efficient than conventional heating methods (Lan *et.al*. 2013: DOI: 10.5772/52517).
Rogers and co-workers studied the cellulose dissolving ability of several imidazolium-based ILs, using pulp and microwave irradiation, and obtained solutions with 25 % cellulose content. They suggested that this high solubility under microwave irradiation was due to decompositions that took place (Bentivoglio *et.al.* 2006:155).

2.2.2.2 *Oil bath*

Dissolution of cellulose in ILs is usually achieved by heating in an oil bath under an atmosphere of nitrogen preventing the moisture absorption (Kuzmina *et.al*. 2012b:40). Turbidity is usually used to assess the degree of dissolution and it is observed with a microscope or with a nephelometer (Mazza *et.al*. 2009:210).

(Kilpenäinen *et.al.* 2007:9144) studied the dissolution of wood in [Amim][Cl] and [Bmim][Cl] stirred the mixture mechanically at 80–120 °C :the reported solubility was 8 %. They also discovered that it took several weeks for wood chips (size in excess of 5 mm × 5 mm × 1mm) to completely dissolve at elevated temperatures, and that wood dissolution into ILs is possible under microwave irradiation, which enhances the rate
of dissolution. However, this also leads to delignification and to partial degradation of the wood components.

2.2.2.3 *Sonication*

Ultrasonic treatment is a well-established method used in the separation of plant materials, particularly for extraction of low molecular weight substances. The mechanical and chemical effects of ultrasound are believed to accelerate the extraction of organic compounds from plant materials due to disruption of cell walls and enhanced mass transfer of the cell wall contents (Lan *et. al.* 2011:672). In their studies Lan *et.al.* (2011:672) reported that ultrasonic irradiation had a beneficial effect on cellulose dissolution, because the increment of ultrasound irradiation from 0-20 minutes led to a decrease in cellulose dissolution time from 190-60 minutes, which was probably due to the fact that ultrasound irradiation provided a greater penetration of IL into cellulose and improved mass transfer.

2.3 FACTORS AFFECTING CELLULOSE DISSOLUTION

2.3.1 Presence of water in the dissolution process

The presence of water reduces the ability of ILs to dissolve cellulose due to the solvation of the ionic species and solute by the water. There is a variety of sources where potential contamination from water may come from (Mazza *et.al.* 2009: 207; Kuzmina *et.al.* 2012: 16), e.g.

a) Water content in the sawdust wood and dissolving pulp samples
b) Water content in the ionic liquid
c) Water from the environment (air/glassware)

Almost all the reports on dissolution of cellulose in ILs clearly indicate the negative influence of water on dissolution. (Swatloski *et.al.* 2002:4946) observed that the solubility of cellulose decreased with the presence of water in ILs. It was related to the competition between hydrogen bonds of water and cellulose for the anion part of IL, the strong interaction of cellulosic hydroxyl group with water molecule inhibit interaction of IL with cellulose and result in non-dissolution of cellulose in IL (Su *et.al.* 2012:1). It was observed that when the concentration of water was more than 1 w/w % in IL, the solvation ability of IL was reduced and it could not dissolve cellulose further (Muhammad *et.al.* 2012:125).

2.3.2 Number of factors that enhance cellulose dissolution in ILs

a) Low viscosities of the ILs promote the dissolution process, mainly due to the higher mobility of the ions in solution.
b) Short dissolution times (>12 hours) lead to better results preferably in lower temperatures (Kilpeläinen *et.al.* 2007: 9145).
c) The degree of polymerization (DP) of the biopolymer, as well as the structure of the IL also has additional influence on cellulose dissolution (Kilpeläinen *et.al.* 2007:9145).
d) Contamination in the solvent can also influence the dissolution capacity of an IL (Swatloski *et.al.* 2002:4946).

2.3.3 Impurities in ionic liquids

Ionic liquids may contain several impurities, such as halides, water and volatiles. Volatile impurities, primary originating from starting materials or solvents used in synthesis, can easily be removed from the non-volatile ionic liquid by evaporation (Holm *et.al.* 2011:550).

2.3.4 Effect of the anion on the dissolution

It was reported in literature that good dissolution of cellulose may be obtained using halide based ionic liquids. The higher the anion concentration, the better the solubilisation (Holm *et.al.* 2011:550). The halogen anions that are mostly used in cellulose dissolution are chloride based anions, because they have a strong electronegativity of the chloride anion and its small size (Dadi *et.al.* 2006:908). This was reported to be important since the chloride anion, being a small hydrogen-bond acceptor, is a good selection in cellulose dissolution (Swatloski *et.al.* 2002:4975).

2.3.5 Effect of the cation on the dissolution

Studies have shown the existence of weak interaction between cation of ionic liquids and cellulose. Dadi et.al. (2006:908) suggested that the cations do interact in the dissolution process and their role should not be neglected. When the length of the alkyl chain on the dialkyl imidazolium cation was increased, Olivier-Bourdigou et.al. (2010:25) reported that this led to the decrease in cellulose solubilisation.

2.4 CELLULOSE DISSOLUTION IN ILS

It was found that imidazolium–based ILs display high efficiency for dissolution of cellulose. Ang *et.al.* (2011:4790) studied the application of three ILs: [Emim][OAc], [Bmim][Cl], [Emim][DEP] in pre-treating rice husk and also investigated the ILs ability to dissolve rice husk cellulose. It was found that all three ILs were capable of dissolving rice husk. After 10 hours of dissolution, the performance of IL in rice husk dissolution in descending order was [Emim][OAc] > [Bmim][Cl] > [Emim][DEP]. All the regenerated cellulose was found to be more amorphous as compared to the untreated rice husk. Both [Emim][OAc] and [Bmim][Cl] were reported to be potential ILs the pre-treatment of rice husk as they dissolved rice husk equally well under the same conditions and required lower energy in dissolution process compared to [Emim][DEP].

Cai *et.al.* (2012:1708) investigated the two-step dissolving process and this was developed to prepare the cellulose/ IL spinning dope with high quality where cellulose was first swelled to its maximum in aqueous [Bmim][Cl] solution and then dissolved by stirring under vacuum to remove excessive water. It was found that initial water contents in [Bmim][Cl] solution have great influence on the swelling and dissolution of cellulose. With the increase of the swelling time, the swelling ratio of cellulose increased first and then stabilised. The higher the water content in [Bmim][Cl], the more time would be taken for cellulose to reach the maximum swelling ratio. It was found that cellulose dopes prepared by this method had lower viscosity and better homogeneity compared with the direct dissolving process. In addition, tensile strength of the cellulose fibres regenerated from cellulose spinning dope prepared by the new method, were better than those prepared by direct dissolving.

Casas *et.al.* (2012:115) analysed and compared the solubilities of cellulose and lignin in ILs. The excess enthalpy was successfully employed as a reference property to study the solubilities using the COSMO-RS. They reported the anions: acetate, formate and chloride, to play the main role in the dissolution process. The experimental validation and FTIR results showed that COSMO-RS can be used as a useful tool to select potential ILs to dissolve and regenerate cellulose and lignin.

Cuissinat *et.al.* (2008:7) investigated the swelling and dissolution mechanisms of native and enzymatically treated cellulose fibres (cotton and wood fibres) in three different ILs: [Bmim][Cl]/DMSO, [Amim][Br] and [Bmim][Br]. Their results showed that [Bmim][Cl]/ DMSO showed no dissolution but homogeneous swelling. The complex swelling and dissolution mechanisms that were observed, do not seem to be linked to the nature of the solvent, but are fully controlled by the physical and chemical organization of cellulose fibers. Untreated and enzymatically treated cotton and wood fibres behaves in the same way in these ILs and aqueous solvents.

Ding *et.al.* (2012:7) applied density functional theory calculations and atoms in molecules theory to investigate the mechanism of cellulose dissolution and regeneration in [Emim][OAc] and 1, 4-dimethoxy-β-D-glucose (Glc). The theoretical results showed that [Emim][OAc] forms strong H-bonds with hydroxyl groups of the cellulose system which showed that the interaction of IL + Glc is stronger than the Glc with Glc interaction. Further research suggested that the H-bonds between cellulose and IL were weakened or destroyed by the addition of water. The experimental results prove that cellulose can be readily reconstituted from the [Emim][OAc]-based cellulose solution by the addition of water, and the crystalline structure of cellulose is converted from cellulose I to cellulose II.

Duan *et.al.* (2011:4640) prepared cellulose/chitin homogeneous solutions in [Emim][OAc]. They studied the steady and oscillatory dynamic rheological properties with a Haake Mars-III rotational rheometer. Their results showed that the viscosity of the solutions decreased with increase of chitosan content. The structural viscosity index of the solution was similar to that of a NMMO solution, which indicates potential spin ability in the fibres.

Du *et.al.* (2011:1985) carried out quantum mechanical calculations to determine the mechanism for the superiority of imidazolium acetate based ILs to the corresponding chloride based ILs. Their results indicated that imidazolium cation can react with acetate anion to generate a carbine, which is a highly reactive intermediate. The carbine then reacts with cellulose to facilitate its dissolution in IL solvents in addition to the stronger hydrogen bonds formed between the acetate anion and hydroxyl groups on cellulose. The dissolution mechanism for acetate anion and imidazolium cation was reported to involve the initial ion pairing of cation via hydrogen bonding and electrostatic interactions. The hydrogen bond that

is formed between the C_2-H on the imidazolium cation and COO- of the anion facilitates the transfer of the H+ to the anion to form a carbine intermediate.

Erdmenger *et.al.* (2007:440), studied the effect of the alkyl chain length in 3-alkyl-1-methyl-imidazolium cation that is combined with chloride anion on the dissolution of cellulose. They found that there is no regular regulation for solubility of 3-alkyl-1-methyl-imidazolium chloride with its alkyl chain length. They also reported that alkyl chain with less than six carbon units and odd-numbered alkyl chain length is more efficient in cellulose dissolution than even numbered alkyl chain length.

Haykir *et.al.* (2013:430) studied the pre-treatment of cotton stalk with several ionic liquids: 2-hydroxy ethyl ammonium formate [HEAF], [Amim][Cl], [Bmim][Cl], [Emim][Cl] and [Emim][OAc] in order to enhance the enzymatic accessibility of the lignocellulosic feedstock. [Emim][OAc] was found to have demonstrated the most recognized effects among several ILs, regarding digestibility and structural changes in cotton stalk samples. Digestibility was 65% for [Emim][OAc] pre-treated cotton stalk after 72hours of enzymatic hydrolysis, which was 9-fold higher compared to untreated cotton stalk. HEAF pre-treatment resulted in enzymatic digestibility of 26%, which was similar to the digestibilities attained by [Amim][Cl] and [Emim][Cl] pre-treatments. [Emim][OAc] was reported to have maintained its effectiveness as a pre-treatment agent upon recycling. It was recycled 3 times and showed no change in terms of hydrolysis of pre-treated samples.

Heinze *et.al.* (2005:520) tested the dissolving capability of different ILs such as [Bmim][Cl], benzyldimethyl (tetradecyl) ammonium chloride [BDTAC] for cellulose. Their study showed [Bmim][Cl] was the most appropriate cellulose dissolving solvent for two primary points:
a) Its strong ability to dissolve cellulose with DP in the range from 290-1200 up to very high concentrations,
b) Almost no degradation of cellulose after dissolution. In their experiments, it was reported that [Bmim][Cl] can dissolve the cotton linter (DP =1198) with the concentration of 10 wt %, and DP is only slightly degraded to 812, which might be caused by mechanical shearing during the stirring.

Kilpeläinen *et.al.* (2007:9142) used IL [Amim][Cl] to dissolve cellulose at 60 ˚C for 2 hours under argon atmosphere with stirring, using two reagents for activation of carboxylic acids.

Acetylation was completed by adding acetic acid and pyridine to the cellulose solution at room temperature with stirring for two days. Cellulose acetate with DS up to 2.99 was obtained.

Kosan *et.al.* (2008:59) investigated a wide range of different ILs: [Bmim][Cl], [Emim][Cl], [Bdmim][Cl], [Bmim][OAc] and [Emim][OAc], for the dissolution of cellulose which was used to prepare regenerated fibres. The cellulose solutions were characterized by means of light microscopy, cone plate rheometry and particle analysis. Dopes at higher cellulose concentrations were reported for the ILs containing the acetate anion than the chloride anion. Acetate based ILs were reported to be more efficient in cellulose dissolution and shaping processes.

Lan *et.al.* (2011:672) performed ultrasonic-assisted dissolution of cellulose in [Bmim][Cl] and the dissolution was monitored with a polarizing microscope. The effects of the parameters including ultrasonic power and irradiation time on cellulose dissolution were investigated and found to have decreased from 190 minutes without assistance to 60 minutes irradiated with 30W ultrasound for 20 minutes. FTIR, NMR, XRD, TGA and CP/MAS results showed that most crystalline structure of cellulose was destroyed to amorphous structure and the remaining crystalline structure of cellulose was converted to cellulose II from cellulose I. Thermal stability after dissolution and regeneration in IL decreased and the pyrolysis residues increased.

Li *et.al.* (2012:935) studied the chemical interaction of softwood dissolving pulp with ionic liquids: 1-butyl-3-methyl-imidazolium acetate [Bmim][CH_3COO], and 1-butyl-3-methyl-imidazolium chloride [Bmim][Cl]. They found that the dissolution of cellulosic material in IL was a temperature-dependence process and the viscosity of the ILs affected the efficiency of dissolution at a given temperature. They also reported that water was a more efficient anti-solvent than ethanol for the regeneration of the cellulose when performed at elevated temperatures. They concluded that the pre-treatment decreased the crystallinity of the cellulosic material, which then leads to increased accessibility and reactivity of the cellulose.

Mahmoudian *et.al.* (2012:1251) successfully prepared regenerated cellulose/ montmorillonite (RC/MMT) nanocomposite films in [Bmim][Cl] using solution casting method. The results

revealed improved thermal stability, mechanical and gas barrier properties. X-ray diffraction analysis revealed a cellulose II crystalline structure and well dispersed MMT in RC/MMT nanocomposite films. The presence of MMT was reported to have enhanced the thermal and thermal-oxidative stability and char yield of RC. The results demonstrated that there is a possible interface interaction between cellulose and MMT which yielded better thermal and mechanical properties of the nanocomposite films as compared to pure cellulose.

Mikkola *et.al.* (2007:1229) studied dissolution of different natural cellulose biopolymers (microcrystalline cellulose, cotton linters and Kraft cellulose) in [Amim][Cl] and [Bmim][Cl] under high-intensity acoustic irradiation by means of an ultrasonic horn (10 W nominal power; 10% of max. power) to enhance the dissolution process. It was seen from their results that [Amim][Cl] displayed better dissolving abilities than [Bmim][Cl], but the two ILs demonstrated relatively small differences: 13 wt. % and 10 wt. % solution of cotton linter in [Amim][Cl] and [Bmim][Cl] in 22 and 17 minutes, respectively. TGA, DSC, SEM and NMR were applied to investigate the structure and morphology of both the cellulose samples and ILs before and after processing and it was reported that recovered samples suggested that the crystallinity has been lost during the dissolution and regeneration process. The TGA and NMR analysis revealed no degradation of the samples during the process.

Olsson *et.al.* (2012:1) prepared a series of 10 wt % cellulose solutions in [Emim][OAc], from microcrystalline cellulose and/or pulp. To obtain less crystalline cellulose the viscoelastic properties of the spin dopes were characterized by controlled stress rheometry. Fibres were characterized by means of wet and dry tensile testing and SEM. The characterization showed compact and homogeneous fibres. It was reported that fibres that are composed of polymers with the highest degree of polymerization were strongest and stiffest.

In their study, Pang *et.al.* (2013:1270) prepared regenerated cellulose films with enhanced mechanical properties by incorporating different plasticizers using the IL [Amim][Cl] as a solvent. They investigated the characteristics of the cellulose films by SEM, AFM, TG, XRD, solid state cross-polarization/magic angle spinning (CP/MAS) NMR and tensile testing. Their results showed that cellulose films exhibited a homogeneous and smooth surface structure. The thermal stability of the regenerated cellulose film plasticized with glycerol was higher when compared with other regenerated films. The incorporation of a plasticizer dramatically

strengthened the tensile strength and improved the hydrophobicity of the cellulose films when compared to the control sample.

Parviainen *et.al.* (2014:67) investigated the dissolution mechanisms of two cellulose samples with different pre-treatment or origin or crystallinity. Two softwood dissolving pulps:

- Pulp1 which had undergone mechanical treatment only.
- Pulp2 which had undergone a mechanical treatment followed by enzyme treatment using different ionic liquids as solvents: 1, 5 –Diazabicyclo [4.3.0] non-5-enium propionate) and *N*-methyl-1, 5-diazabicyclo [4.3.0] non-5-enium dimethyl phosphate and [Emim][OAc]-water mixtures by carolimetry and optical microscopy.

Their results showed that Pulp1 and Pulp2 had nearly the same crystallinity, but dissolved differently in some of the solvents used, confirming that crystallinity was not the only factor affecting cellulose dissolution. Furthermore, when dissolution of the cellulose in ILs was monitored using DSC, exothermic transition was found prior to dissolution. There was no correlation between dissolution mechanisms (swelling/ballooning) and thermal transitions. Appearance of a peak in DSC scan was not seen as the indication of whether the sample dissolved completely into a homogeneous solution, but rather that the solvent was able to interact with cellulose in such a way that dissolution/swelling was possible. DSC analysis of dissolution did not allow for quantifying the complete dissolution but gave quantitative information of the complicated dissolution phenomena of cellulose.

Swatloski *et.al.* (2002:4974) studied the dissolution of cellulose with ionic liquid [Bmim][Cl], and they found that some hydrophilic ILs are effective solvents for the dissolution of cellulose. Dissolution experiments were carried out using (cellulose acetate, lyocell and rayon fibres), fibrous cellulose and Whatman cellulose fibres. ILs containing 1-butyl-3-methylimidazolium cations were screened with a range of anions, from small hydrogen bond acceptors (Cl^-) to large, non-coordinating anions ($[PF6]^-$) also including SCN^-, Br^-, and $[BF4]^-$ were investigated. The found that out of all the ILs studied, 1-butyl-3-methylimidazolium chloride [Bmim][Cl] showed excellent dissolution capability for cellulose. The solubility of cellulose in [Bmim][Cl] was found to be as high as 10% (w/w) at 100 ˚C, and then increased to 25% under microwave heating. They also discovered that cellulose can be easily regenerated from the IL + cellulose solutions by the addition of 1% water. Some ILs can also be recycled and reused after purification. They reported that, the

presence of water in the IL resulted in significant decrease in the solubility of cellulose. However, the disadvantages associated with using [Bmim][Cl] IL (Vitz *et.al.* 2009:417). includes:

- The melting point above 70 ˚C,
- The high viscosity of the IL solution and
- The high hygroscopicity, in general valid for all imidazolium based ILs with a chloride counter anion, makes their handling difficult

Tian *et.al.* (2014:83) demonstrated the use of an acidic ionic liquid 1-vinyl-3-(3-sulfopropyl) imidazolium hydrogen sulphate [PSMIM][HSO_4] as a "quasi-homogeneous" catalyst for efficient acetylation of cellulose. Unlike existing techniques that use large amount of ILs as solvent to dissolve and acetylate cellulose, a small amount of the acidic IL was used as a catalyst to overcome the low efficiency associated with the relatively high viscosity and costs of ILs. Fully substituted cellulose acetate with a conversion of 88.8 % was obtained by using only 9 mol % of IL as a catalyst, which is much higher than that of common commercialized solid acid catalysts. The degree of substitution and solubility of the obtained cellulose acetate can be facilely controlled by varying the concentration of the IL and the reaction time. The dual function of swelling and catalysing by the acidic ILs for the acetylation of cellulose is reported to be responsible the excellent catalytic performance.

Vitz *et.al.* (2009:417) screened a wide range of potentially suitable ionic liquids to efficiently dissolve cellulose. They found that there was an alternating side chain length for the different alkyl side-chain lengths of the imidazolium chlorides which was not observed for the bromides. They also found that only ILs with chlorides (which has shorter side chains), acetate and phosphate anions showed good dissolving properties for cellulose. Furthermore, they found that 1-ethyl-3-methylimidazolium diethyl phosphate, [Emim][$(CH_3)_2PO_2$] was best suitable for dissolution of cellulose and dissolution under microwave irradiation and resulted in no colour change and no degradation of the cellulose.
[Emim][$(CH_3)_2PO_2$] was found to have low melting point which resulted in the viscosity of cellulose to be lower, and therefore easier to handle.

Zhang *et.al.* (2005:8272) investigated the use of a non derivatizing solvent 1-ally-3-methylimidazolium chloride [Amim][Cl], for the dissolution process of cellulose and the formation of the regenerated materials. [Amim][Cl] was synthesized successfully and the cellulose samples (cotton and dissolved pulp) without any pre-treatment were found to have dissolved readily in [Amim][Cl] at 60 ˚C with stirring, but they also found that at room temperature [Amim][Cl] did not dissolve the cellulose but only caused it to swell. They reported that with increasing temperature, cellulose dissolved more rapidly. It was also observed in the same study that [Amim][Cl] could dissolve cellulose with a DP of 650 and it was found that untreated or inactivated cellulose could be dissolved in this IL rapidly.
They also reported that the cellulose materials regenerated by coagulation exhibited good mechanical property and that [Amim][Cl] to be easily recycled because of its thermo stability and non-volatility.

(Zhu *et.al.* 2006:325) and his group studied the dissolution of cellulose without derivatization in some hydrophilic ILs, such as [Bmim][Cl] and [Amim][Cl], using microwave heating. This study demonstrated that solutions up to 25 wt. % can be prepared in [Bmim][Cl] under microwave heating. The high chloride concentration and activity in the IL, which was assumed highly effective in breaking the extensive hydrogen bonding network present in cellulose, was reported to play an important role in cellulose dissolution. However, the presence of water in the chloride ILs was reported to have greatly decreased the dissolution of cellulose through competitively hydrogen-bonding the chloride to water molecules (Swatloski *et.al.* 2002:4974).

2.5BIOMASS DISSOLUTION IN ILS

Abdulkhani *et.al.* (2013:57) studied the dissolution of ball-milled poplar wood (PW), chemi-mechanical pulp (CMP) and cotton linters (CEL) in the ILs: 1-butyl-3-methylimidazolium chloride [Bmim][Cl] and 1,3-methylimidazolium dimethyl sulphate [DiMim][$MeSO_4$] after heating for 2-3 hours at 90 ˚C. The solubility efficiency of the lignocellulosic materials was found to be in the order of CEL> CMP> PW for both ILs, this is probably due to the high crystallinity of cellulose and aromatic character of lignin in the PW sample. [DiMim][$MeSO_4$] indicated the inability to completely dissolve the lignocellulosic materials and sample treatment with this IL did not lead to water soluble degradation products. However, [Bmim][Cl] was able to dissolve all lignocellulosic materials by destroying the intramolecular hydrogen bonds between lignocellulose.

Ang *et.al.* (2011:4790) studied the application of three ILs: [Emim][OAc], [Bmim][Cl], [Emim][DEP] in pre-treating rice husk and also investigated the ILs ability to dissolve rice husk cellulose. It was found that all three ILs were capable of dissolving rice husk. After 10 hours of dissolution, the performance of the ILs in rice husk dissolution in descending order was [Emim][OAc] > [Bmim][Cl] > [Emim][DEP]. All the regenerated cellulose was found to be more amorphous as compared to the untreated rice husk. Both [Emim][OAc] and [Bmim][Cl] are potential ILs to be used in the pre-treatment of rice husk as they dissolved rice husk equally well under the same conditions and required lower energy in dissolution process compared to [Emim][DEP].

Casas *et.al.* (2012a:115) studied the dissolution of *Pinus radiata* and *Eucalyptus globulus* hardwoods in the imidazolium-based ILs: [Bmim][OAc], [Emim][OAc], [Emim][Cl], [Bmim][Cl] and [Amim][Cl] using microwave radiation. All ILs were reported to be able to dissolve the two types of wood. Lignin was also regenerated successfully from the wood solutions in the ILs with chloride anions. FTIR and NMR analysis of regenerated lignins were reported to have shown the absence of residual sugars.

Karatoz *et.al.* (2012b:2) studied three ILs: [Bmim][Cl], [Emim][Cl] and [Emim][OAc] for the dissolution/ pre-treatment and fractionation of 5 % sugarcane bagasse at a temperature of 150 ˚C for 90 minutes. They reported the biomass to be completely dissolved and the highest lignin removal of 60 % was achieved with [Emim][OAc], 50 % for [Emim][Cl] and the lowest lignin removal with [Bmim][Cl]. High cellulose mass recovery of 83 % was achieved with [Emim][OAc]. They also reported that ILs were fully recovered (100 %) after recycling and quantified by ion chromatography. The three studied ILs, [Emim][OAc] gave the best saccharification yield, material recovery and delignification. It was also noted that the use of the imidazolium cations with shorter alkyl side chains resulted in accelerated dissolution.

Keskar *et.al.* (2012:175) presented an analysis of Attenuated Total Reflectance (ATR)-FTIR data obtained from dissolution of sugarcane bagasse in two phosphonium ILs, i.e. tetradecyl (trihexyl) phosphonium chloride [P66614][Cl] and tributyl(methyl)phosphonium methylsulphate [P4441][$MeSO_4$]. Absorption bands related to cellulose, lignin, and hemicellulose dissolution monitored in situ in biomass-IL mixtures that indicated that lignin dissolution in both ILs. The quantitative measurement of lignin dissolution in phosphonium ILs based on absorbance at 1510 cm^{-1} which demonstrated utility in understanding the chemical reactions taking place in biomass-IL mixture.

Liu *et.al.* (2014:1) studied the pre-treatment of *Z. japonica* (grass species) with alumina-doped magnesium oxide to disrupt the lignocellulose structure and significantly reduce the lignin content of the *Z. japonica*. It was reported that after pre-treatment, *Z. japonica* showed significant solubility in 1-allyl-3-methylimidazolium chloride [Amim][Cl]. The high solubility of pre-treated *Z. japonica* samples by original alumina-doped MgO was similar to the solubility of pre-treated *Z. japonica* samples with the use of the used alumina-doped MgO. This also proved that alumina-doped MgO has a strong stability, which can be recycled and used repeatedly. The regenerated cellulose was similar to microcrystalline cellulose according to FTIR and NMR results. The crystallinity of the regenerated cellulose was reported to have decreased compared to microcrystalline cellulose.

Montalbo-Lombo *et.al.* (2014:588) evaluated the utilization of ultrasound to rapidly dissolve switch grass in IL [Bmim][Cl]. In the dissolution method, they dried and ground the switch grass, then added it to [Bmim][Cl] and sonicated at a frequency of 20 kHz. The experiments were conducted using a catenoidal horn at varying amplitudes of 96, 128, and 160 µm and sonicated times of 2, 3 and 4 minutes. Similarly, ground switch grass was dissolved in [Bmim][Cl] by conventional heat treatment at 130 ˚C for 12 and 24 hours. Their results showed good delignification results of 53 % for the 24 hour heat pre-treat samples and 50.8 % for ultrasonicated assisted samples at 160 µm amplitude at 4 minutes. SEM images displayed significant changes in biomass structure from intact and crystalline for the untreated biomass to disintegrated and amorphous for the treated biomass. With increasing ultrasonic amplitude the carbohydrate recovery decreased. Also, more than 50 % of the hemicellulose fraction was lost during biomass recovery.
It was concluded that ultrasonication was a promising technology to enhance dissolution of lignocellulose in ionic liquid.

Muhammad *et.al.* (2011: 998) studied the dissolution of bamboo biomass using a number of ILs namely: 1-ethyl-3-methylimidazoilum glycinate [Emim][Gly], 1-ethyl-3-methylimidazolium trifluoroacetate [Emim][TFA] and choline propionate synthesized in their laboratory. They observed that one of the synthesized amino-based IL [Emim][Gly] was capable of dissolving the biomass completely. They regenerated the dissolved biomass using an acetone/water mixed solvent and characterized it with FTIR spectroscopy, XRD and SEM, and they compared the results to preconditioned bamboo biomass. They found the regenerated biomass to have a macrostructure and the structure of its cellulose changed from a type1 to type 2 during the dissolution and regeneration process. The separation procedure developed for the biomass components presented by (Muhammad *et. al.* 2011: 998) showed a possible greener alternative to extract useful biomass components for various applications

Qiu *et.al.* (2012:1) evaluated the effect of [Emim][OAc] for the pre-treatment of energy cane bagasse (ECB) in terms of biomass composition, structural changes and enzymatic digestibility. ECB was pre-treated with [Emim][OAc](5% w/w) at 120 ˚C for 30 mins followed by hydrolysis with the enzymes Spezyme CP and Novozyme 188. IL-treated ECB resulted in significant lignin removal (32.0%) with slight glucan and xylan losses (8.8% and

14% respectively). They reported that the IL-treated ECB exhibited a much higher enzymatic digestibility than untreated ECB or water treated in terms of both cellulose and hemicellulose yields. SEM images revealed a loose and disordered structure of biomass post treatment. FTIR analysis indicated that IL treated biomass exhibited a significant loss of native cellulose crystalline structure. XRD analysis also confirmed that IL pre-treatment resulted in a decrease of the crystallinity index.

Rayne *et.al.* (2007:1075) studied the rapid dissolution of a range of coniferous and deciduous woods and grassy lignocellulosic plant materials (oak, ponder osa, pine, smooth sumac, grape stem, flax shives and triticale straw**)** in the IL [Bmim][Cl]. They found the dissolution behaviour for all the materials studied to be similar, with rapid initial size reduction of the biomass over the first 15-30s of irradiation. The dissolution limits for the different types of biomass studied were found to be approximately 5 %. They reported that the analysis of the liquefied solution by liquid chromatography with refractive index and diode array/fluorescence detection indicated varying degrees of structural decomposition. Large polymeric peaks were easily seen by liquid chromatography diode array fluorescence detector, indicating the partial degradation of the original lignin biopolymers. They also found the polyphenolic lignin materials were not decomposed to their constituents monomers (<10 %) and that the cellulosic and hemicellulosic degradation to be similar. Gas chromatography mass spectrometer as well as hexane extraction of biomass-IL mixture did not reveal any significant compounds.

Shill *et.al.* (2010:1075) described the use of aqueous ammonium sulfate and ILs solutions to form a two-phase system that precipitates the *Miscanthus* biomass, forming IL-rich and salt-rich phases. This is a two-component system consisting of [Emim][OAc], water and cellulose. The process was reported to partially separate the lignin from the cellulose in *Miscanthus*, and enhanced the rate of hydrolysis of the precipitated cellulose. They then concluded that this process was more rapid and gave higher yields of cellulose conversion to glucose when compared to the cellulose obtained from biomass pre-treated with only IL and precipitated with water. Addition of a kosmotropic salt during the precipitation resulted in partial delignification of the biomass, which makes the substrate more accessible, enhancing the enzymatic hydrolysis.Sun *et.al.* (2009:646) studied the complete dissolution and

delignification of softwood (southern yellow pine) and hardwood (red oak) in the IL [Emim][OAc] after mild grinding. Red oak showed higher and faster dissolution than southern yellow pine. The regenerated cellulose-rich materials and lignin fractions were characterized and compared with the original wood samples and biopolymer standards. For pine, 59% holocellulose (cellulose + hemicellulose) could be recovered in the reconstituted material, whereas 31% and 38% of the original lignin respectively was recovered. Thus, partial separation of wood components is possible with [Emim][OAc].

Vo *et.al.* (2014:89) tested the dissolution of poplar wood using [Bmim][Cl] and [Bmim][OAc]. Poplar sawdust dissolved in [Bmim][OAc] stirred at 130 ˚C gave a cellulose yield of 96 wt. % whereas poplar sawdust dissolved in [Bmim][Cl] gave a yield of 25.3 wt. % at the same reaction conditions. The higher solubility in [Bmim][OAc] could be ascribed to the higher basicity of the acetate anion in the IL.
FTIR and lignin content analysis results revealed that poplar was partially delignified during the dissolution and regeneration processes. Results from the FTIR, SEM and XRD were reported to show no serious chemical changes, and the regenerated poplar materials from ILs seemed to have lost their original crystallinity and partially delignified during dissolution and regeneration process.

Wang *et.al.* (2014:1) characterized the solutions of switch grass and the constituent biopolymer cellulose, hemicellulose and lignin, as well as a physical mixture of them mimicking the composition of switch grass, dissolved in the IL 1-ethyl-3-methylimidazolium acetate. Their results demonstrated that the IL dissolved the cellulose fibrils of switch grass and the persistence of a network-like structure indicates that dissolving switch grass in IL does not disrupt all the physical entanglements and covalent linkages between the biopolymers created during plant growth. Their results after reconstitution of the IL dissolved in switch grass showed the yields of carbohydrate-rich material to contain cellulose with low degree of crystallinity as determined by powder X-ray diffraction which would greatly impact downstream uses of the biopolymers produced by the process.

Zavrel *et.al.* (2009:2580) have carried out a high-throughput screening to find the most suitable ionic liquid for dissolving lignocellulosics. In their study 1-ethyl-3-methylimidazolium acetate [Emim][OAc] was found to be the most efficient IL for

dissolution of pure cellulose, while 1-allyl-3-methylimidazolium chloride [Amim][Cl] was the most efficient IL for dissolution of wood. [Emim][OAc] was found to be more efficient IL because it does not lead to corrosion problems which comes from the [Amim][Cl] IL and the acetate has a higher basicity than chloride including increased breaking of hydrogen bonds in cellulose.

Production of 5-hydroxymethylfurfural (HMF) and furfural from lignocellulosic biomass was studied in [Bmim][Cl] and [Bmim][Br] in the presence of $CrCl_3$ under microwave irradiation by Zhang *et.al.* (2010:1111). Corn stalk, rice straw and pine wood treated under typical reaction conditions were reported to have produced HMF and furfural in yields of (45-52%) and (23-31%) respectively within 3 mins. This method was reported to be valuable to facilitate energy-efficient and cost-effective conversion of biomass into biofuels and platform chemicals.

The information is summarized from the preceding literature review shown in Table 2.2 summarizes the dissolution of different wood samples under various parameters in different types of ILs.

Table 2.2 The dissolution of different wood samples in different ILs

Wood sample	IL	Dissolution conditions	Solubility (w/w %)	References
Maple wood	[Emim][OAc]	130 °C for 1.5 hrs	10	(Lee *et.al.* 2009:1368)
Norway spruce sawdust	[Amim][Cl] [Bmim][Cl]	110 °C for 8 hrs 110 °C for 8 hrs	8 8	(Kilpeläinen *et. al.* 2007:9142)
Ball-milled southern pine	[Amim][Cl]	80 °C for 8 hrs	8	(Kilpeläinen *et. al.* 2007:9142)
Sugar cane bagasse	[Emim][OAc]	120 °C for 30 minutes	12	(Qiu *et.al.* 2012:251)
Oak	[Emim][OAc]	100 °C for 16 hrs	10	(Sun *et.al.* 2009:646)
Spruce, beech	[Bmim][Cl]	90 °C for 16 hrs	5	(Zavrel *et.al.* 2007:2580)

2.6 CELLULOSE DISSOLUTION IN IONIC LIQUIDS AND CO-SOLVENT MIXTURES

Kuzmina *et.al.* (2012b:1) studied the production of cellulose/chitosan blends in alkyl imidazolium ILs. They also studied the effect of using DMSO (dimethylsulfoxide), EAc (ethyl acetate), and DEE (diethyl ether) as co-solvents to facilitate the dissolution process. They reported that addition of co-solvents decreased the viscosity of cellulose/chitosan in ILs and it facilitated the dissolution of the polysaccharides thereby decreasing the polymer aggregates sizes in the solutions. The decrease in viscosity of the pure solvents was of the order: DMSO> EAc> DEE> DMSO and DEE. Co-solvents improved the characteristics of the blended films, because using the co-solvents facilitated the dissolution of the polysaccharides in the ILs. This led to additional swelling and deep destruction within the fibres and the addition of co-solvents in cellulose solutions causes the solution to be more homogeneous.

Lv *et.al.* (2012:2524) studied the rheological properties of cellulose dissolved in two ILs, [Emim][Cl] and [Bmim][Cl], with the co-solvent DMSO in the concentration range of cellulose from 0.07 to 6.0 wt. %. They observed an exponential decrease in the viscosities of ILs with the addition of DMSO in the concentration of 0-100 wt. %. Reduced solution viscosity and shortened relaxation times were also observed because of the decreased monomer friction coefficient in cellulose solutions.

Xu *et.al.* (2013:540) studied the dissolution of cellulose at ambient temperature by adding a polar solvent to the IL [Bmim][OAc]. They used the aprotic solvents, DMSO, DMF and DMA as co-solvents to see if the co-solvents could enhance solubility of the cellulose. They found that the solubility can be improved in these aprotic solvents without even heating. The dissolution of cellulose was reported to have been increased due to the increased concentration of $[OAc]^-$ anions from the dissociated IL owing to the preferential solvation of $[Bmim]^+$ by the aprotic polar solvents. The DMSO co-solvent with the IL [Bmim][OAc] gave

the highest cellulose solubility and the lowest cellulose solubility was observed for [Bmim][OAc] and DMA mixture.

Zhao *et.al.* (2012b:31) synthesized the IL N-allylpyridinium chloride [APy][Cl] using a one-step process and investigated its dissolution property on a cotton linter cellulose sample. Their results showed that the solubility of the cellulose (DP=556) was 19.71% at 120 ˚C, and thermal stability results were reported to have decreased the DP to 223. They believe that the performance of the cellulose sample could be enhanced by addition of co solvents to the IL. They compared three co-solvents (DMSO, DMAc and Pyridine), and found the [APy][Cl] + DMAc to give better dissolution of the cotton linter cellulose. The solubility was 15.03 % and the DP of the regenerated cellulose was 403 at 100 ˚C. Solubility of [APy][Cl] + pyridine was 1.36 % at 70 ˚C but there were reported results on [APy][Cl] + DMSO solvent systems. Their FTIR, XRD and TGA data showed that [APy][Cl] + DMAc solvent systems have the potential to be used as non-derivatizing solvents since cellulose was changed from cellulose I to cellulose II during dissolution and regeneration and the thermal stability of the regenerated cellulose also decreased. The use of the co-solvents have been reported to enhance the dissolution of cotton linter cellulose in N-allylpyridinium chloride IL [APy][Cl] at a temperature of 100 ˚C, with an increased DP up to 403 at a lower cost.

Zhao *et.al.* (2013:1) reported on the addition of solvents (DMSO), (DMF), methanol (CH_3OH) and water (H_2O) in [Bmim][OAc]. They reported that the dissolution of cellulose in IL/co-solvent system is determined mainly by the hydrogen bond interactions between the acetate anion and hydroxyl protons of cellulose and therefore the effect of co-solvents in cellulose is achieved by influencing such hydrogen bond interactions. It was reported that protic solvents such as CH_3OH and H_2O compete with the acetate anions interactions in the cellulose dissolution process which then decrease the cellulose solubility. The aprotic solvents (DMSO and DMF) partially broke down the ionic association of [Bmim][OAc] by solvation of cation and anion. [Bmim][OAc]/ DMSO systems were reported to be better co-solvents that the other three studied and they proposed a possible mechanism. The mechanism proposed provided insight into how the DMSO affects the dissolution of cellulose in IL and may motivate further experimental studies in the field. No conclusion was drawn as to whether the DMSO facilitates the dissolution in cellulose.

2.7 SUMMARY OF THE LITERATURE REVIEW

The most successful cations for cellulose dissolution are based on the methylimidazolium and methylpyridinium cores, with ally-, ethyl-, or butyl-side chains. Even numbers of carbon atoms in the side chain show high cellulose dissolution in the series C_2 to C_{20} compared with odd numbers. The most promising anions are chloride, acetate, and formate (Erdmenger *et.al.* 2007:440). NMR relaxation studies indicate that there is a stoichiometric interaction between the chloride anions and cellulose hydroxyl groups (Pinkert *et.al.* 2009:6712). However, it is thought that both anions and cations are involved in the dissolution process.

Imidazolium-based ILs containing halide anions, especially chloride anions, seem to be more effective for dissolving cellulose. In addition, these ILs are cheaper than most well-known ILs. However, the relatively high melting points and viscosities of ILs containing chloride anion possibly limit their practical application in cellulose processing or homogeneous cellulose derivatization (Cao *et.al.* 2009:13; Wu *et.al.* 2009b:2569).

Relatively high dissolution temperatures (often above 80 ˚C) are often required for dissolving cellulose, which possibly results in thermal decomposition of ILs and produce some organohalogens which have uncertain toxicity and hazardousness to zoology and ecosystem after ineluctable release into the environment. The corrosion of imidazolium chloride ILs was also thought as a potential limitation to their future industrial applications. The halogen anion containing ILs, such as [Bmim][Br] and [Bmim][I], are found not good solvents for cellulose (Zavrel *et.al.* 2009:2580). In general, high viscosity of [Bmim][Cl] and the high hygroscopicity of halide in ILs make their handling more difficult (Vitz *et.al.* 2009:417).

Formate, acetate or phosphate based imidazolium ILs have been studied and have shown potential to dissolve cellulose under mild conditions (Olivier-Bourbigou *et.al.* 2010:1). Formate ILs generally exhibit low thermal stability due to decarboxylation (Fukaya *et. al.* 2008:44) and they are known to be basic and unsuitable for enzymes (Zhao *et.al.* 2009:217).

The dissolution capacity of chemical cellulose in different ILs was investigated by (Kilulya *et.al.* 2011:3272) at different temperatures, ranging from 50 -90 ˚C. Cellulose was found to be soluble in imidazolium-based ILs with acetate and chloride anions due to their ability to

disrupt the extensive hydrogen bonding network of cellulose and leads to its dissolution (Feng *et.al.* 2008:1; Swatloski *et.al.* 2002:4974).

Acetate-based ILs were found to be interesting due to their low melting point, lower viscosity and have less toxic and corrosive character compared with chloride-based ILs (Feng *et.al.* 2008:1). Phosphate-based ILs provide high thermal stability in the 260-290 °C range and low viscosities (Olivier-Bourbigou *et.al.* 2010:1).

In general, acetate-based ILs are less viscous than chloride based ILs and are thermally more stable than formate-based ILs (Fukaya *et.al.* 2008:44).
[Emim][OAc] has been identified as the most promising cellulose solvent, for the following reasons:

- [Emim][OAc] is in liquid state at room temperature, and
- Shows much higher capability for cellulose dissolution (Kohler *et.al.* 2007:2311).

Dissolution of cellulose with ionic liquids will allow the comprehensive utilization of cellulose by combining two major green chemistry principles: using environmentally preferable solvents and bio-renewable feed-stocks (Zhu *et.al.* 2006:325).
ILs such as [Amim][Cl], [Emim/Bmim][Cl] and [BNimim][Cl] have superior ability to dissolve cellulose, lignin, and even wood (Du *et.al.* 2011:1985; Fukaya *et.al.* 2008:44; Kosan *et.al.* 2008:59; Ohno *et.al.* 2009:2; Swatolski *et.al.* 2002:4974; Zhao *et.al.* 2009:217).

CHAPTER 3: EXPERIMENTAL

3.1MATERIALS

The effect of dissolution was ascertained by studying three samples of South African *Eucalyptus dunnii* (ED5CW) that contained varying amounts of lignin. These samples were the sawdust wood, unbleached dissolving pulp and bleached dissolving pulp supplied by SAPPI Saiccor mill from the South Coast of Durban, South Africa.
The photograph of the samples is shown in Figure 3.1.

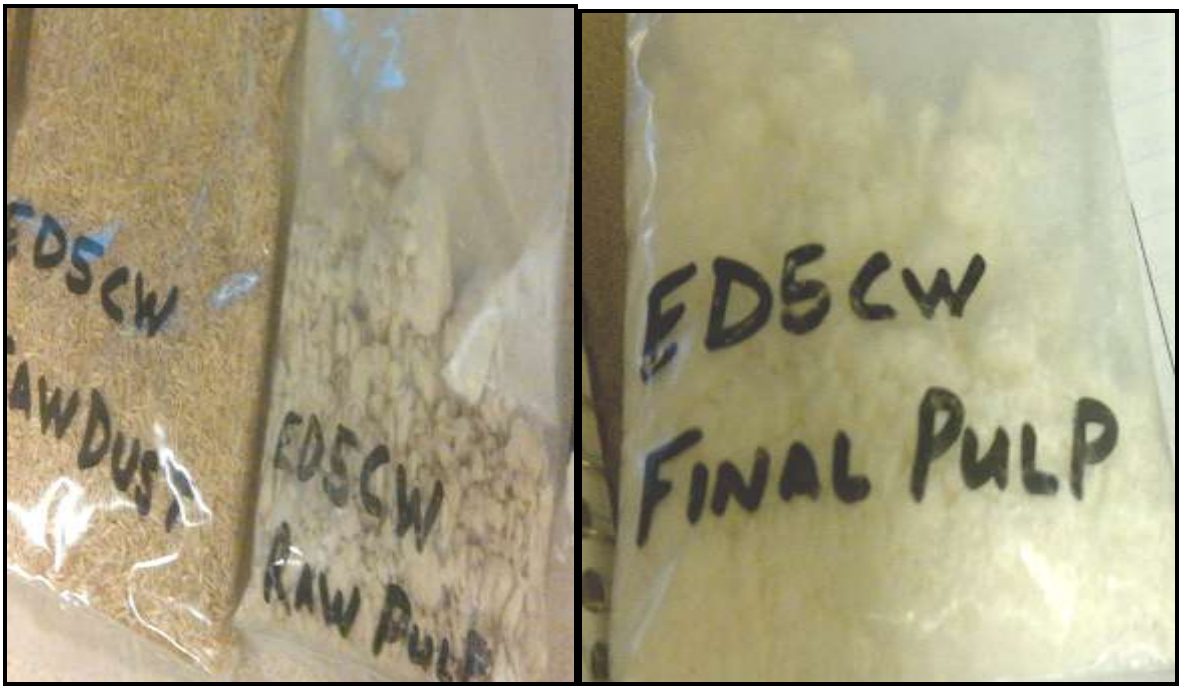

Figure 3.1 Photographs of the ED5CW samples used in this work

The samples were dried under vacuum at 50 °C for 12 hours, and thereafter ground into small particles using a mortar and pestle before use. The IL that was used in this work was the 1-ethyl-3-methylimidazolium acetate [Emim][OAc] with a purity of > 95 wt.% purchased from IOLITEC USA and its structure is shown in Figure 3.2.

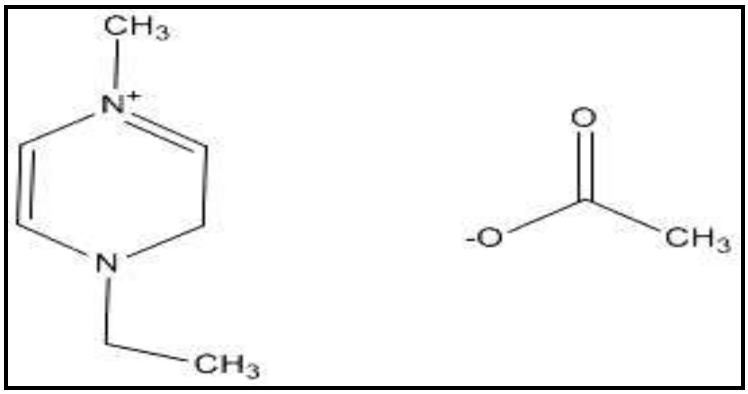

Figure 3.2 Structure of 1-ethyl-3-methylimidazolium acetate [Emim][OAc]

Prior to use, the [Emim][OAc] was dried under vacuum at 50 °C for 12 hours. Figure 3.3 shows the photograph of the vacuum pump setup for drying the IL.

Figure 3.3 Photograph of the vacuum pump setup for drying [Emim][OAc]

The aprotic (accepts H^+) co-solvents that were used in this study were DMSO and DMF. Water and organic protic solvents are reported in literature to compete for hydrogen bonding interactions with the solutes (Kuzmina *et.al.* 2012b:1). However dimethylformamide has also been reported to have the ability to swell the cellulose more efficiently than aprotic co-solvents and it has been reported to have less toxicity. DMSO has been reported in literature

to increase the speed of cellulose dissolution in ILs and it remains in solution thereby decreasing the IL viscosity (Kuzmina *et.al.* 2012b:1).

Dimethylsulfoxide (DMSO) and dimethylformamide (DMF) with a stated purity of 99.9 % were purchased from Sigma Aldrich and were used as received. Table 3.1 lists the molecular formula, molar mass and physical properties of the DMSO and DMF co-solvents used in this study. Nylon membrane filter papers with a porosity of 10 µm and 0.8 µm were purchased from Sterlitech Corporation, USA. Microcystalline cellulose (MCC) standard, with depolymerization degree of 270 and purity of 99.9 %, was purchased from Sigma Aldrich.

Table 3.1 The chemical and physical properties of DMSO and DMF

Characteristic	**DMF**	**DMSO**
Molecular formula	C_3H_7NO	C_2H_6OS
Molar mass, g/mol	73.09	78.13
Melting point	-61.0 ˚**C**	18.5
Boiling point	153 ˚**C**	189

3.2 WET CHEMICAL ANALYSIS OF SAWDUST, UNBLEACHED AND BLEACHED DISSOLVING PULP SAMPLES

The samples were analysed for sugar content (glucose, arabinose, galactose, xylan, mannose) and the total lignin content. The procedures followed in the determination of the components mentioned above are discussed below.

3.2.1 Determination of carbohydrate composition by High Performance Liquid Chromatography

The method used was adopted from TAPPI test methods (1996-1997) test method no. T249 om-85, to determine the five principal monosaccharides that constitute the carbohydrate in wood and wood pulp.

The constituents are determined quantitatively and they are: glucose, mannose, arabinose, xylose, and galactose.

3.2.2 Determination of acid insoluble lignin in the sawdust wood and dissolving pulp samples

The method which describes a procedure to determine the acid insoluble lignin in wood and unbleached dissolving pulp was adopted from TAPPI test methods (1996-1997) test method no. T222 om-88.

Determination of lignin content in the wood and dissolving pulp provides information for evaluation and application of the processes. Properties such as hardness, bleach ability, other pulp properties such as colour, are associated with the lignin content.

3.2.3 Determination of acid soluble lignin by Ultraviolet visible spectroscopy

The method which describes a procedure to determine the acid soluble lignin in wood and bleached dissolving pulp was adopted from TAPPI test methods (UMS-250) test method no. TAPPI 1985b.

This method uses acid hydrolysis of wood and pulp which then give rise to carbohydrate degradation products such as hydroxymethylfurfural which absorbs strongly at 280 nm, the wavelength commonly used to monitor lignin in solution. The acid - soluble lignin can be determined in a solution, after filtering off the insoluble lignin, by a spectrophotometry. HMF concentrations in the Klason lignin filtrates were determined by high-performance liquid chromatography (HPLC) with UV diode array detector (DAD).

3.3 THERMOPHYSICAL PROPERTIES

In this study, the thermophysical properties (speed of velocity, density and refractive index) of [Emim][OAc], DMF and DMSO were measured as a function of temperature using the Anton Paar DSA 5000M densitometer (photograph of the instrument is shown in Figure 3.4) equipped with an automatic sampler X452, and a refractive index RXA 156/170.

This device simultaneously determines three independent physical properties using one sample. The three in-one instrument is equipped with a density cell, a sound velocity cell and RXA 156/170 refractive index modules are equipped with a micro flow cell and an integrated Peltier thermostat ensuring accurate and automatic temperature control combining the Anton Paar oscillating U-tube method with a highly accurate instrument for the measurement of sound velocity.The temperature is controlled to ± 0.02 K. The sample is introduced into a U-shaped borosilicate glass tube that is excited to vibrate at its characteristic frequency electronically. The characteristic frequency changes depending on the density of the sample. Through a precise determination of the characteristic frequency and a mathematical conversion, the density of the sample can be measured.

Figure 3.4 Photograph of the Anton Paar DSA 5000M densitometer that has an automatic sampler X452, and equipped with a refractive index RXA 156/170

3.3.1 Preparation of the pure compounds

[Emim][OAc], DMF and DMSO were transferred into their respective 10 ml stoppered flasks and measured in triplicate. Acetone and ethanol were used for cleaning the instrument. The densities and refractive index equipment temperature was at 298.15 K.
Table 4.2-4.4 (shown in the results section) presents the measured and literature densities, speed of sound and refractive indexes of the pure compounds: [Emim][OAc], DMF and DMSO at 298.15 K.

3.4 KARL FISCHER MEASUREMENTS

After the measurements of the thermophysical properties of [Emim][OAc], DMF and DMSO, the water content was determined to ascertain the water uptake by IL during the experimental procedure.

The water content was measured by Karl Fischer titration method. This is a chemical analysis procedure which is based on the oxidation of sulphur dioxide by iodine in a methanolic hydroxide solution. The titration can be performed volumetrically or coulometrically. In the volumetric method a Karl Fischer solution containing iodine is added until the first trace of excess iodine is present.
The amount of iodine converted is determined from the burette volume of the iodine-containingKarlFischersolution.
In the coulometric procedure, the iodine participating in the reaction is generated directly in the titration cell by electrochemical oxidation of iodide until again a trace of unreacted iodine is detected. Faraday's law can be used to calculate the amount of iodine generated from the quantity of electricity required.

A Mettler- Toledo C20 Karl-Fischer coulometer which is shown in Figure 3.5 was used to check the water content of [Emim][OAc] after drying. Minimal water content is desired in the IL as it is an impurity which significantly affects the IL's physical properties and performance in the dissolution of cellulose as noted by Mazza *et.al.* (2009:207). The water content of the IL as reported by the supplier Sigma Aldrich was 5000ppm. After purification the proportion of the water content of the IL was found to be 1045 ppm. Water can be readily

absorbed in IL from atmosphere during storage or experiments. Therefore, the dryness of IL is essential for optimum dissolution of cellulose (Su *et.al.* 2012:1).

Figure 3.5 Photograph of Mettler-Toledo C20 Karl-Fischer coulometer

3.5 DISSOLUTION AND REGENERATION OF CELLULOSE

3.5.1 Optimization stage

Optimisation of the dissolution process is an essential step in determining the most suitable and economical condition to enhance the yield of products (Yoon *et.al.* 2012:1).

The effect of dissolution temperature and mass loading of the IL on the proportion of cellulose recovery for a dissolving pulp sample were investigated. The cellulose yield from the dissolution process would be used as a parameter to evaluate the effectiveness of [Emim][OAc] in treating pulp under different operating conditions.

Bleached dissolving pulp was used in these experiments. Five solutions with pulp mass loadings of 2.5; 5; 7.5; 10; and 12.5 wt. % were prepared in [Emim][OAc], in accordance with reported literature reports (Geng *et.al.* 2012:84).

3.5.2 Dissolution of dissolving pulp in 1-ethyl-3-methylimidazolium acetate

The dissolution was carried out at each solid loading by heating a pre-weighed amount of pulp and IL contained in 20ml glass vial with a cap, in an oil bath for 12 hours. The parameters for the experiment are listed in Table 3.2

Table 3.2 List of the different pulp loadings (%) that were prepared at different temperatures

% Pulp loading	Mass of pulp (g)	Mass of IL (g)	Temperature (˚C)
2	0.10	4.90	60; 80; 100; 120 and Microwave
5	0.20	3.80	60; 80; 100; 120 and Microwave
7.5	0.30	3.70	60; 80; 100; 120 and Microwave
10	0.40	3.60	60; 80; 100; 120 Microwave
12.5	0.50	3.50	60; 80; 100; 120 Microwave

On completion of the dissolution, the samples were cooled to room temperature.

The cooled solution was then washed with 50 ml of (water and acetone) 1:1 v/v. The washings were repeated three times to remove the IL from the cellulose. The solution was then centrifuged in a Clays Adams centrifuge at 700 rpm for 10 minutes (photograph of the centrifuge is shown in Figure 3.6). It was observed that a white cellulosic material settled at the bottom of the centrifuge tube (photograph shown in Figure 3.7).

Figure 3.6 Photograph of Clays Adams centrifuge

Figure 3.7 Photograph of white cellulosic material observed at the bottom of centrifuge tube

The mixture was then filtered using a 10 µm Nylon membrane filter paper and then dried in an oven at 80 ˚C for one hour. The dry weight was recorded. The cellulose recovery was calculated by using the equation 1, as proposed by Brown (2012:1):

$$\text{Cellulosic material recovery (\%)} = \frac{\text{mass of regenerated cellulosic material (g)}}{\text{mass of pulp for dissolution (g)}} \times 100\% \qquad (1)$$

The above procedure was reported for all the other pulp loadings. The pulp loadings (5 %) gave higher cellulose recoveries than other pulp loadings, so this pulp loading was used for preparing the pulp and sawdust wood samples in IL/ co-solvents mixtures at 120 ˚C for 12 hours.

The cellulose recovery yield obtained after the dissolution experiments was used as a parameter to evaluate the effectiveness of [Emim][OAc] in treating dissolving pulp under different operating conditions.

3.6 CHARACTERIZATION OF THE REGENERATED CELLULOSE

3.6.1 Fourier Transform Infrared Spectroscopy (FTIR)

The aim of using FTIR analysis in the present study was to determine the changes in the chemical structure of the regenerated cellulose samples in [Emim][OAc]/co-solvent mixtures. The regenerated cellulose samples obtained after dissolution of the sawdust wood, unbleached pulp and bleached pulp samples in [Emim][OAc]/DMF or DMSO mixtures and MCC samples, were ground into very small particles and characterized by Bruker Alpha FTIR ATR spectrometer shown in Figure 3.8, and spectra were recorded in the range of ν_{max} = 400–4000 cm^{-1}.

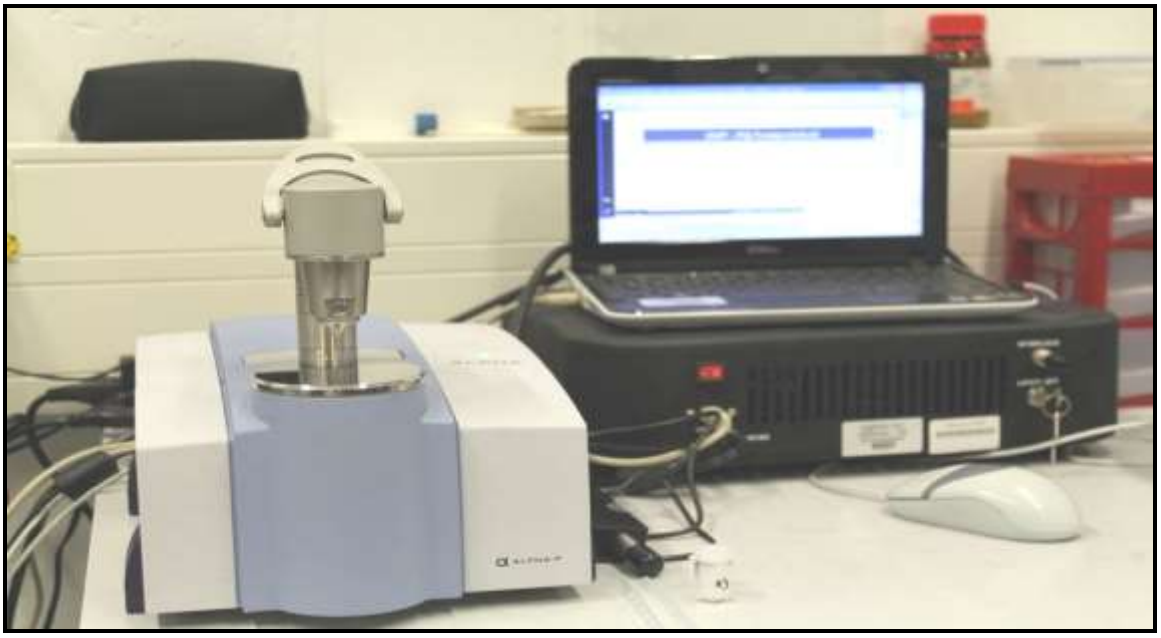

Figure 3.8 Photograph of a Bruker Alpha FTIR spectrometer

3.6.1.1 *FTIR Protocol*

According to Willard *et.al.* (1986:179-178) infrared spectroscopy involves the twisting, bending, rotating, and vibrational motions of atoms in a molecule. Upon interaction with infrared radiation, portions of the incident radiation are absorbed at particular wavelengths. The multiplicity of vibrations occurring simultaneously produces a highly complex absorption spectrum, which is uniquely characteristic of the functional groups comprising the molecule and of the overall configuration of atoms as well.

The infrared spectrum of a compound is essentially the superposition of absorption bands of specific functional groups, yet subtle interactions with the surrounding atoms of the molecule impose the stamp of individuality on the spectrum of each compound. For qualitative analysis, one of the best features of an infrared spectrum is that the absorption or the lack of absorption in specific frequency regions can be correlated with specific stretching and bending motions and, in some cases, with the relationship of these groups to the remainder of the molecule. Thus, by interpretation of the spectrum, it is possible to state that certain functional groups are present in the material and that certain others are absent. With this one datum, the possibilities for the unknown can be sometimes narrowed so sharply that comparison with a library of pure spectra permits identification (Willard *et.al.* 1986:179-178).

3.6.2 Nuclear magnetic resonance (NMR)

^{13}C solid state NMR spectroscopy is a well-established method used for analysing the regenerated cellulose morphology such as crystallinity or the presence of cellulose I and II (Krässig 1993:101). Theoretically, crystalline and less-ordered (paracrystalline) cellulose is indicated by the $C\text{-}_4$ and $C\text{-}_6$ signals in the spectrum (Horii *et.al.* 1982:168;Li *et.al.* 2012:941). ^{1}H NMR spectroscopy was used to analyse the influence of the co-solvents (DMSO or DMF) on the chemical shifts of [Emim][OAc] and the regenerated cellulose.

In order to enhance the spectral resolution, all the regenerated cellulose samples were dissolved in DMSO-d_6 and analysed using the Bruker Avance III 400MHz NMR instrument. The untreated sawdust wood, unbleached dissolving pulp and bleached dissolving pulp samples were analysed using the Bruker Avance III 400MHz NMR spectrometer. In all the cases, the chemical shift for the solvent peak DMSO-d6 were seen at 2.6 ppm for ^{1}H and 41 ppm for ^{13}C (Grasvik *et.al.* 2014:9).
All samples were packed in a 4 mm diameter rotar and a Bruker Avance III 400MHz (Figure 3.9) was used for analysing the samples.

Figure 3.9 Photograph of a Bruker 400 III Ultrashield NMR spectrometer

3.6.2.1 *NMR Protocol*

According to Willard *et.al.* (1986:316), nuclear magnetic resonance spectroscopy is an important characterization tool to verify the structure and quality of chemicals. NMR spectroscopy is used to determine the content of sample and structures of atoms and molecules, due to their magnetic nuclei in a magnetic field that can absorb or re-emit electromagnetic radiation under the application of an applied magnetic field. NMR spectroscopy also can provide the detailed state and chemical shift of molecules which help scientists to confirm physical and chemical properties of their products.

In NMR spectroscopy, the characteristic absorption of energy by certain spinning nuclei in a strong magnetic field, when irradiated by a second and weaker field perpendicular to it, permits identification of atomic configurations in molecules. Absorption occurs when these nuclei undergo transitions from one alignment in the applied field to the opposite one. The amount of energy required to cause a particular nucleus to realign depends upon such factors as field strength, electronic configuration around the particular nucleus, type of molecule, and intermolecular interactions (Willard *et.al.* 1986:316).

Proton NMR is used for determination of proton skeleton of products. Normally, protons are spinning in randomly. Once an external magnetic field is applied, the protons will spin either parallel or anti-parallel it, protons with parallel spin has lower energy than one with anti-parallel spin. Hence, an energy difference (ΔE) between the parallel and anti-parallel states will be created. The signal in NMR spectroscopy results from the energy difference and is proportional to the population difference between the two states (Su 2012:18).

3.6.3 X-Ray diffraction (XRD)

The diffraction patterns of the regenerated cellulose samples that were previously dissolved in [Emim][OAc]/co-solvent mixtures were obtained using a Bruker D2 Phaser Powder XRD instrument (shown in Figure 3.10) and were compared with the diffractogram of the MCC standard of cellulose. The patterns were recorded using Cu-K_{α} radiation at 40kV and the range for angle of diffraction was 2θ =5-40º.

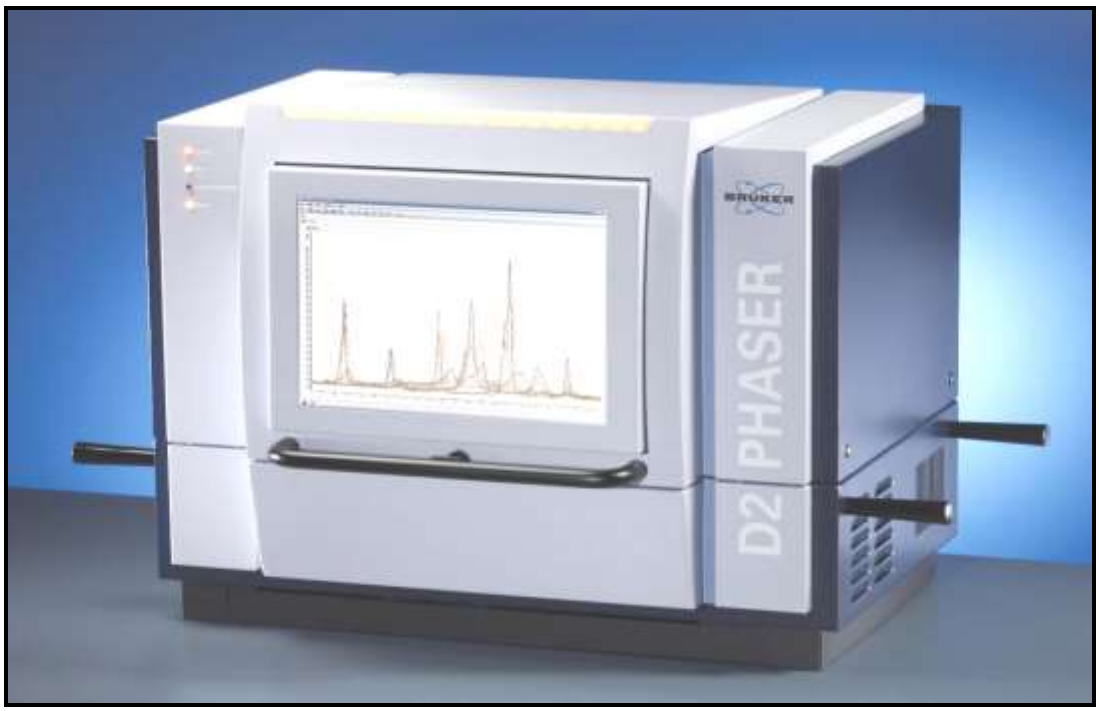

Figure 3.10 Photograph of a Bruker D2 Phaser Powder XRD

3.6.3.1 *XRD Protocol*

Powder diffraction is one of the primary techniques used to characterize materials, providing structural information even when the crystallite size is too small for single crystal x-ray diffraction methods. X-ray diffraction is based on constructive interference of monochromatic X-rays and crystalline sample. These X-rays are generated by a cathode ray tube, filtered to produce monochromatic radiation, collimated to concentrate, and directed toward the sample. The interaction of the incident rays with the sample produces constructive interference (and a diffracted ray) when conditions satisfy Bragg's Law ($n\lambda = 2d \sin \theta$). This

law relates the wavelength of electromagnetic radiation to the diffraction angle and the lattice spacing in a crystalline sample. These diffracted X-rays are then detected, processed and counted. By scanning the sample through a range of 2θ angles, all possible diffraction directions of the lattice should be attained due to the random orientation of the powdered material. Conversion of the diffraction peaks to the d-spacings allows identification of the sample, because each sample has a set of unique d-spacings. Typically, this is achieved by comparison of d-spacings with standard reference patterns. All diffraction methods are based on generation of X-rays in an X-ray tube, these X-rays are directed at the sample, and the diffracted rays are collected. A key component of all diffraction is the angle between the incident and diffracted rays. Powder and single crystal diffraction vary in instrumentation (Ewald 1962:82-101).

3.6.4 Scanning electron microscopy (SEM)

SEM images of the regenerated cellulose samples that were previously dissolved in [Emim][OAc]/co-solvent mixtures were taken at 300 x magnification using a Jeol 6310 Electron Probe analyser SEM instrument (shown in Figure 3.11) which was operated at 5-10 kV accelerating voltage. Prior to imaging, the samples were sputter-coated with gold to make the fibres electrical conductive, avoiding degradation and build up of charge on them.

The regenerated cellulose samples were first dipped in liquid nitrogen to dry the samples. The samples were then mounted onto the SEM aluminium stub with a carbon tape and then Au (gold) coated. They were then cooked for 10 minutes with a Gold Polaron SC 5000 sputter coater to make the samples more electric conducting.

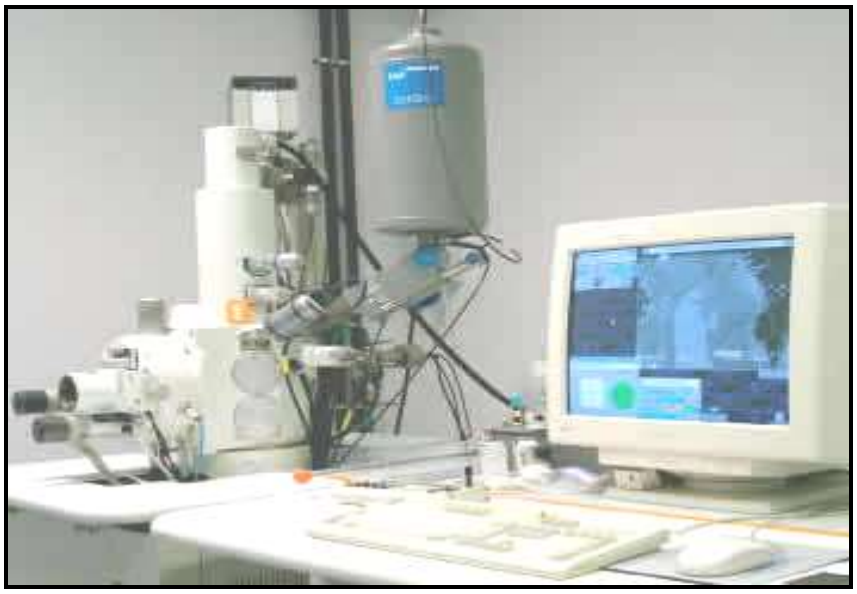

Figure 3.11 Photograph of a Jeol 6310 Electron Probe analyser SEM instrument

3.6.4.1 *SEM Protocol*

The basic principle of SEM is that a beam of electrons is generated by a suitable source, typically a tungsten filament or a field emission gun. The electron beam is accelerated through a high voltage and passed through a system of apertures and electromagnetic lenses to produce a thin beam of electrons, and then the beam scans the surface of the specimen by means of scan coils. Electrons are emitted from the specimen by the action of the scanning beam and collected by a suitably-positioned detector. The beam scanning the specimen surface is exactly synchronized with the spot in the screen that the operator watches. The electron detector controls the brightness of the spot on the screen. The magnification of the image is the ratio of the size of the screen to the size of the area scanned on the specimen. There are different types of electron images and the two most common types are:

- The secondary electron image (SEI) used mainly to image fracture surfaces and gives high resolution images, and
- The backscattered electron image (BEI) used typically to image a polished section; brightness of BEI is dependent on the atomic number of the specimen or the average atomic number for compounds. All SEM images are in black and white (Willard *et.al.* 1986:316).

3.6.5 Thermogravimetric analysis (TGA)

Thermal analysis was recorded with a Perkin Elmer TGA 4000 analyser (shown in Figure 3.12). Approximately 10 mg of the regenerated cellulose samples that were previously dissolved in [Emim][OAc]/co-solvent mixtures were analysed by the Thermo Analyzer at a heating rate of 5 °C /min under continuous nitrogen flow in a temperature range from 25 °C to 600 °C, with an isotherm process at 75 °C for 30 min to remove any absorbed water.

Figure 3.12 Photograph of a Perklin Elmer TGA analyser

3.6.5.1 *TGA Protocol*

Thermal analysis includes a group of techniques in which a physical property of a substance is measured as a function of temperature while the substance is subjected to a controlled temperature program. A complete modern thermal analysis instrument measures temperatures of transitions, weight losses in materials, energies of transitions, dimensional changes, and viscoelastic properties.

TGA provides the analyst with a quantitative measurement of any weight change associated with a transition. TG curves are characteristic for a given compound or system because of the unique sequence of physicochemical reactions which occur over definite temperature ranges and at rates that are a function of the molecular structure. Changes in weight are a result of

the rupture and/or formation of various physical and chemical bonds at elevated temperatures that lead to the evolution of volatile products or the formation of heavier reaction products. From the thermograms, data obtained is usually concerning the thermodynamics and kinetics of the various chemical reactions, reaction mechanisms, and the intermediate and final reaction products.

The usual temperature range is from ambient to 1200 ˚C with inert or reactive atmospheres. The derivative in the TG is often used to pinpoint completion of the weight-loss steps or to increase resolution of overlapping weight-loss occurrences (Willard *et.al.* 1986:316).

3.7 DISSOLUTION OF UNBLEACHED, BLEACHED DISSOLVING PULP AND SAWDUST WOOD SAMPLES IN [Emim][OAc]/DMSO or DMF MIXTURES

In this work aprotic dimethylformamide (DMF) and dimethylsulfoxide (DMSO) were used as co-solvents for dissolving pulp solutions in 1-ethyl-3-methylimidazolium acetate [Emim][OAc]. It was assumed that the co-solvents enhanced the pulp swelling to make its dissolution in IL easier. It has been reported in literature (Kuzmina 2012:1) that swelling of cellulose pulp with water or co-solvent and its evaporation under vacuum during the dissolution procedure facilitates the preparations of cellulose solutions with up to 20 wt. % of cellulose in [Emim][OAc]. Further, it has been concluded that swollen cellulose dissolves easily in ILs.

3.7.1 Dissolution and regeneration process

The aim throughout the project was to increase the cellulose yield proportion after dissolution and regeneration. Five replicates of different pulp loadings (5 wt. %) using two dissolutions methods was studied, to examine which method could improve the degree of dissolution and give highest cellulose recovery yield. In method A, the pulp samples were first soaked in a co-solvent to which the IL was then added. In method B, there was no prior soaking of pulp samples. A discussion of the two dissolution methods A and B is given below:

A) 0.5 g of the previously dried and grounded bleached and unbleached pulp samples were placed in 10ml capped glass vials, to which 2ml of DMSO or DMF, and dried 9.5 g [Emim][OAc] were added. The mixture was heated in an oil bath and stirred for 12 hours.

B) 0.5 g of the previously dried and grounded bleached and unbleached pulp samples were placed in a 10ml capped glass vials to which 2ml of DMSO or DMF and 9.5 g dried [Emim][OAc] were added simultaneously, respectively. The mixture was heated in an oil bath and stirred for 6 hours.

Once dissolution was completed, the samples were cooled to room temperature. The cooled solutions were then washed 3 times with 50 mL mixture of water/acetone (1:1, v/v). The

solution was then centrifuged in a Clays Adams centrifuge at 700 rpm for 10 minutes. It was observed that a white cellulosic material settled at the bottom of the centrifuge tube.

The top liquid phase was taken out and the cellulosic material was further washed with 50 mL of the mixture of water/acetone twice more. The cellulosic material was finally obtained by filtration using a 10 μm Nylon membrane filter paper, and then dried in an oven at 80 °C for one hour. The dried weight of the precipitate was recorded and the percentage recovery of the cellulose was calculated by using the equation (1).

3.7.2 Lignin recovery

The filtrate which contained acetone, water and [Emim][OAc], was stirred in open air for an hour to precipitate the lignin while evaporating the acetone in the air. Unfortunately there was no precipitate observed in the final pulp sample, but just a few small black particles were observed at the bottom of the beaker after stirring for 3 hours. The small precipitate lignin material from all the samples could not be weighed, but FTIR spectra of the small precipitate was collected and compared with an Indulin lignin from Westvaco.

3.8 RECYCLING OF THE IONIC LIQUID

The ionic liquid liquor (filtrate) obtained after washing was transferred into a round bottom flask attached to a rotary evaporator (Figure 3.13) and distilled to remove any water and acetone remained in the mixture. The [Emim][OAc] recovered was then dried under vacuum at 50 °C for 12 hours and characterized by FTIR and ^{1}H NMR and compared with the neat IL spectrum before the dissolution process.

Figure 3.13 Photograph of the rotary evaporator for recycling of [Emim][OAc]

CHAPTER 4: RESULTS AND DISCUSSIONS

4.1 OPTIMIZATION STAGE

4.1.1 Wet chemical analysis of sawdust wood, unbleached and bleached dissolving pulp samples

The amount of carbohydrate constituents, i.e., glucose, arabinose, galactose, xylose and mannose, and the total lignin of the sawdust wood, unbleached and bleached dissolving pulp samples were carried out according to the TAPPI methods (see Chapter 3 page 54-55) and the results are shown in Table 4.1 below. The other components that are present in dissolving pulp and sawdust wood samples are extractives and ash.

Table 4.1 Chemical composition of the biomass samples

Sample name	Glucose (%)	Arabinose (%)	Galactose (%)	Xylan (%)	Mannose (%)	Total lignin (acid soluble and insoluble) (%)
ED5CW Sawdust wood	40.95	0.44	1.40	14.55	2.57	27.45
ED5CW unbleached pulp	91.60	-	-	4.70	2.00	3.60
ED5CW bleached pulp	92.40	-	-	5.30	0.90	1.40

4.1.2 Thermophysical properties of [Emim][OAc], DMF and DMSO

The measured and literature densities, speed of sound and refractive indexes of the pure compounds: [Emim][OAc], DMF and DMSO are presented in Table 4.2 -4.4 at T = 298.15 K.

Table 4.2 Densities, speed of sound and refractive index values of [Emim][OAc] measured and compared to literature at 298.15 K

Experimental	Density (g/cm^3)	Speed of sound (m/s)	Refractive Index (n_D)
	1.1062	1825.02	1.4887
	1.1063	1824.51	1.4887
	1.1063	1825.60	1.4886
Literature	1.0978[1]	1329.10[1]	1.4290[1]

[*1] Quijada-Maldonado *et.al.* (2012:55)

Table 4.3 Densities, speed of sound and refractive index values of DMF measured and compared to literature at 298.15 K

Experimental	Density (g/cm^3)	Speed of sound (m/s)	Refractive Index (n_D)
	0.9442	1456.89	1.4282
	0.9438	1457.02	1.4286
	0.9441	1456.98	1.4283
Literature	0.9439[2]	1457.30[2]	1.4288[2]

Table 4.4 Densities, speed of sound and refractive index values of DMSO measured and compared to literature at 298.15 K

Experimental	Density (g/cm^3)	Speed of sound (m/s)	Refractive Index (n_D)
	1.0953	1483.69	1.4765
	1.0956	1484.83	1.4766
	1.0954	1483.25	1.4768
Literature	1.0954[2]	1484.51[2]	1.4768[2]

[*2]Miyai *et.al.* (1997:973)

4.1.3 Effectiveness of [Emim][OAc] in treating dissolving pulp under different operation conditions

The cellulose recovery yield (%) obtained after the dissolution experiments, was used as a parameter to evaluate the effectiveness of [Emim][OAc] in treating dissolving pulp under different operating conditions.

Figure 4.1-4.5 shows the plots of different pulp mass loadings (%w/%w) vs. cellulose recovery yield (%) at different temperatures T = (333.15, 353.5, 373.15 and 393.15) K and under microwave conditions (900W, 60 Hz).

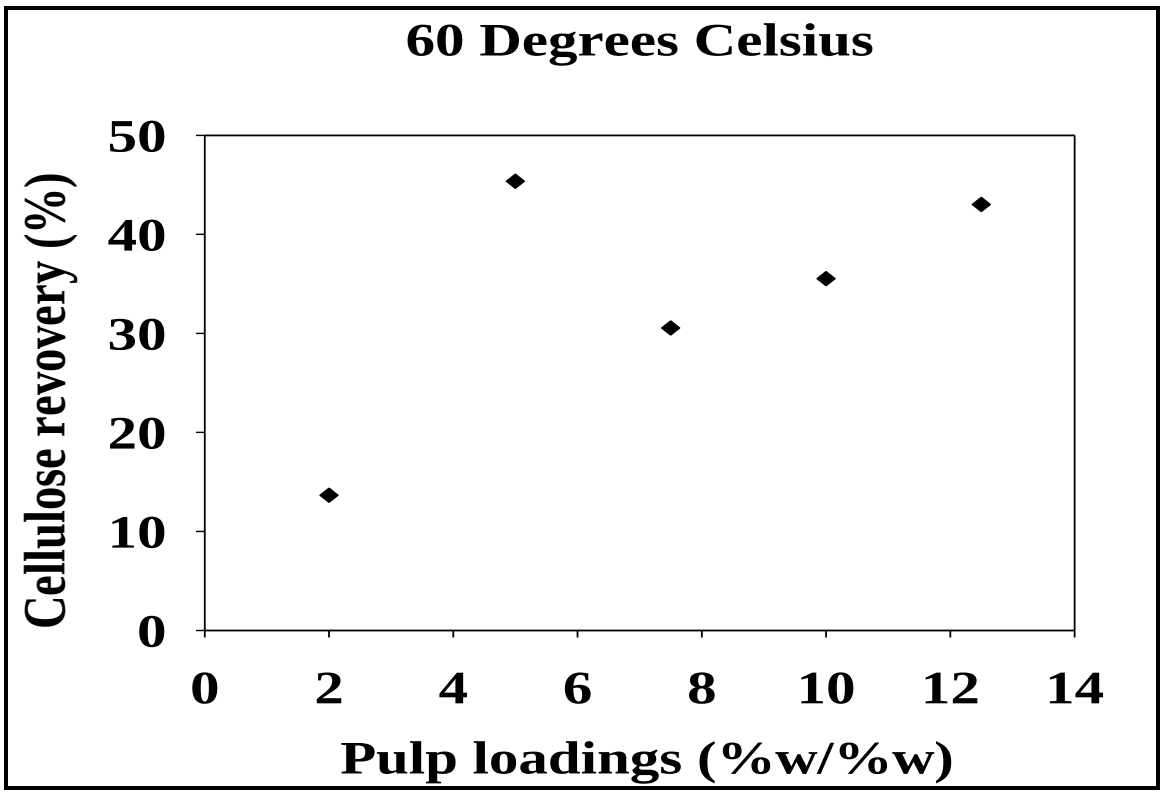

Figure 4.1 The effect of pulp mass loadings (%w/%w) on cellulose recovery (%) at *T* = 60°C

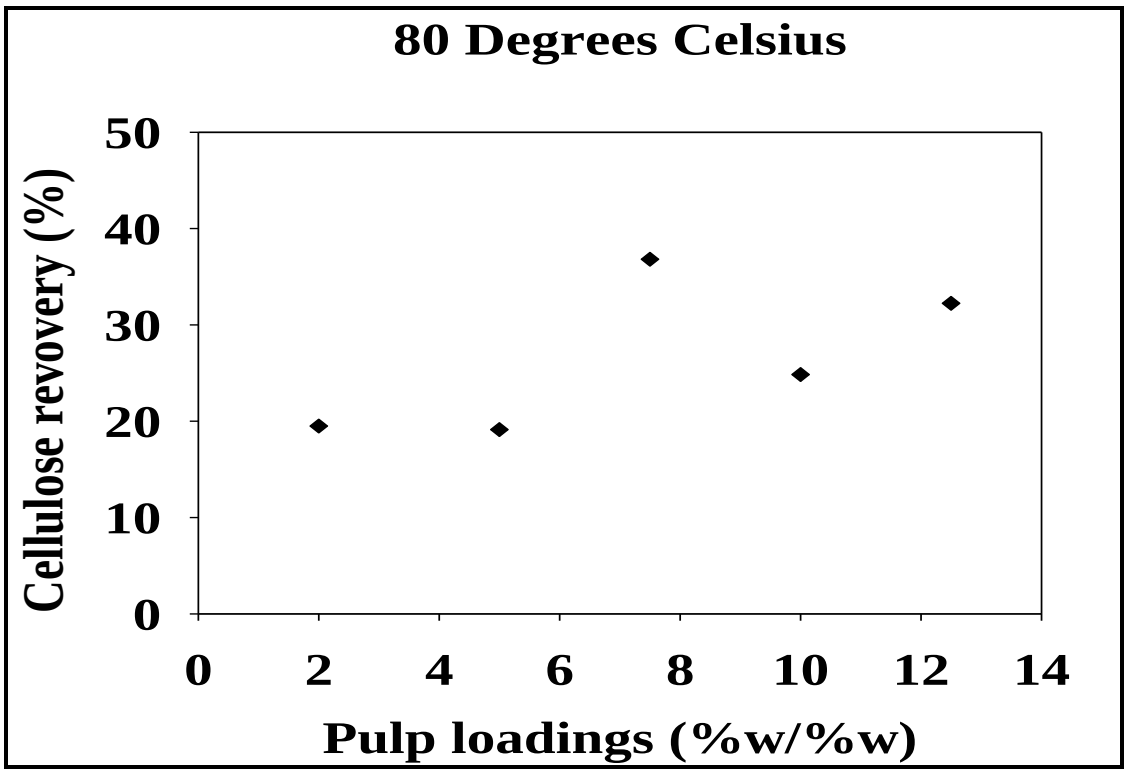

Figure 4.2 The effect of pulp mass loadings (%w/%w) on cellulose recovery (%) at T = 80°C

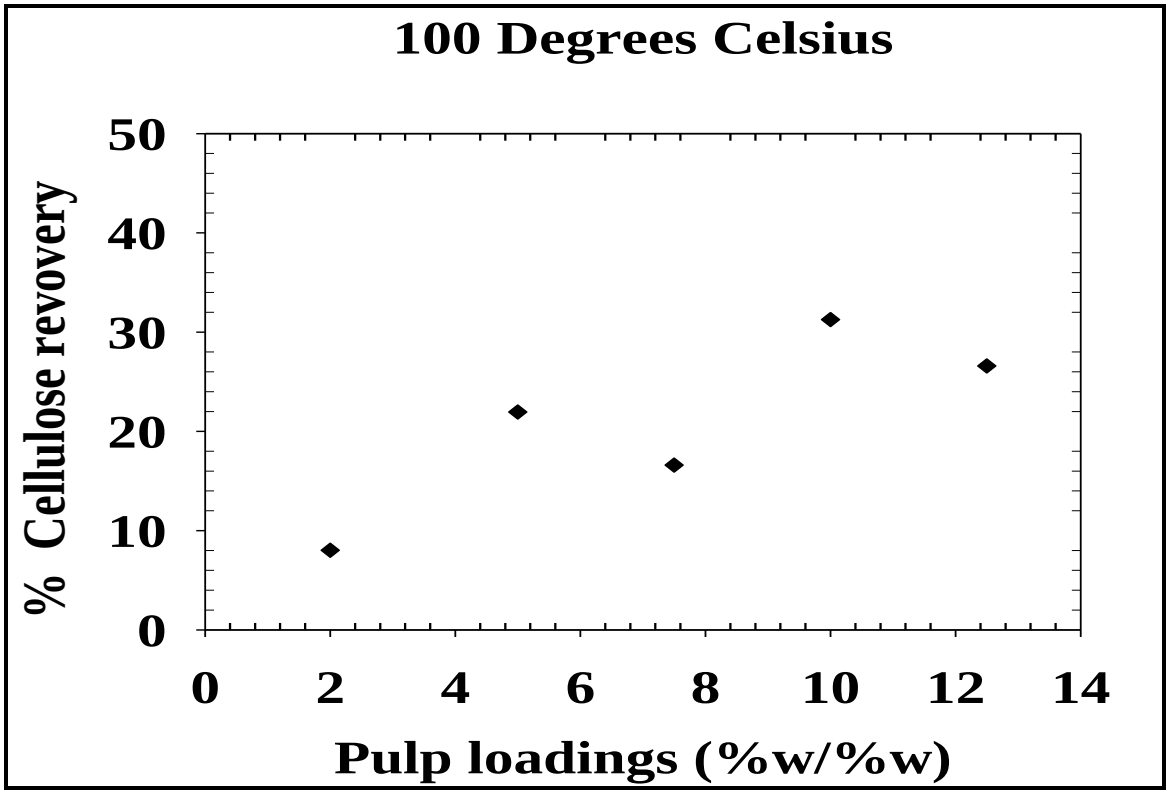

Figure 4.3 The effect of pulp mass loadings (%w/%w) on% cellulose recovery at T = 100°C

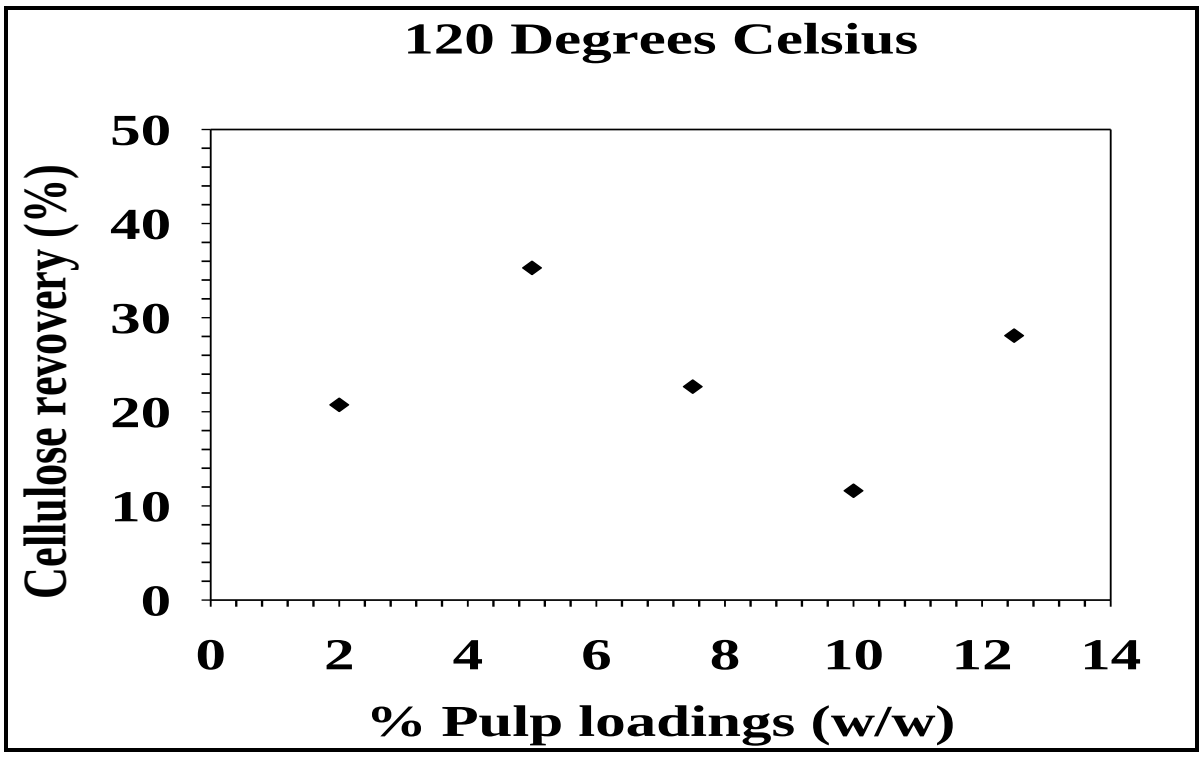

Figure 4.4 The effect of pulp mass loadings (%w/%w) on cellulose recovery (%) at T = 120°C

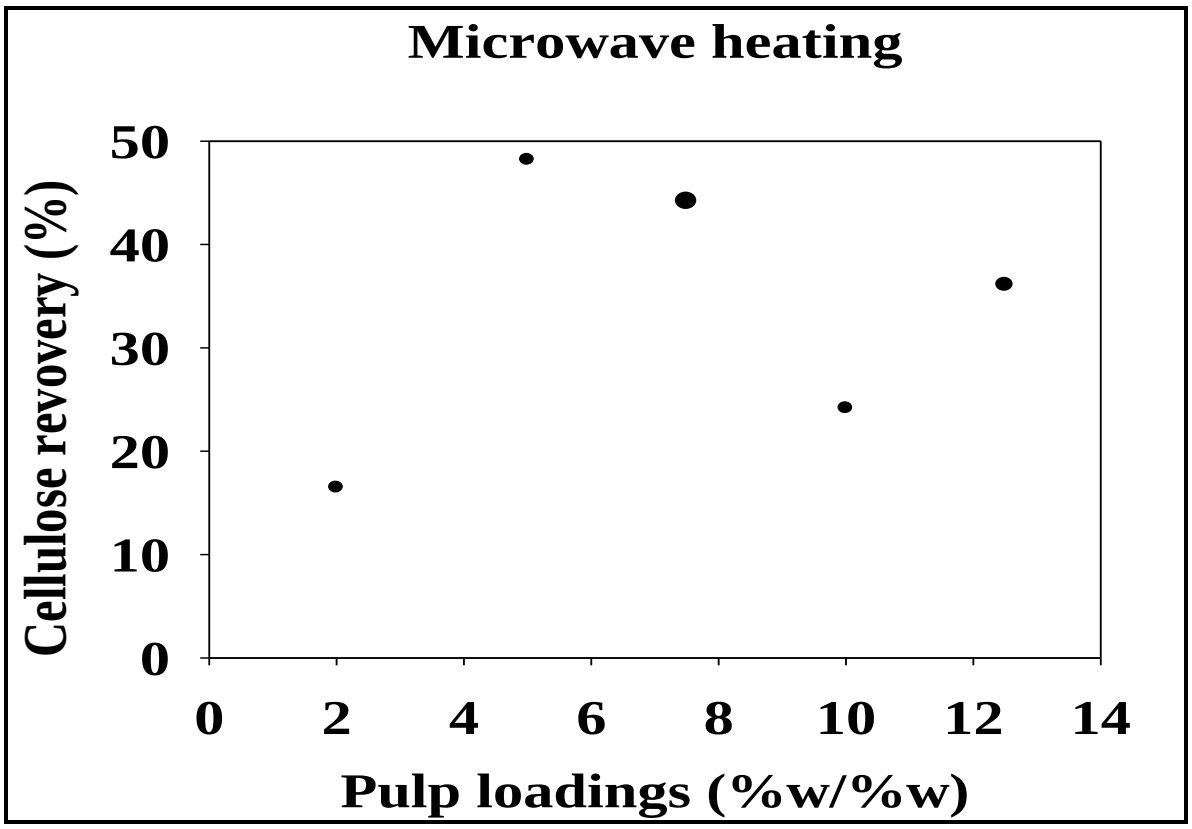

Figure 4.5 The effect of pulp mass loadings (%w/%w) on cellulose recovery (%) using microwave oven

In all the experiments, it was observed that the regenerated cellulose at lower temperatures i.e., 60 and 80 ˚C had very high viscosities which caused difficulty in stirring and dissolution of the dissolving pulp in IL solution.

10 and 12.5(%w/%w) pulp loadings gave higher cellulose recovery yields than 7.5 and 2 % (%w/%w) pulp loadings, whereas one would expect limitations in mass and heat transfer when it comes to higher solid loading, but in this study it was different at lower temperatures. This could be due to the lack of solvent penetration because at 10 and 12.5 (%w/%w) pulp loadings, the solution was highly viscous and very hard to stir.

At 120 ˚C, the pulp could be dissolved at 4-6 hours of continuous stirring whereas at 100 ˚C, it took 10-12 hours to completely dissolve all the pulp in the IL. Even though the microwave irradiation dissolved the pulp quicker than with traditional heating, the results of cellulose recovery (%) using microwave were higher compared to conventional heating, however, the regenerated cellulose samples and IL solution were observed to have a very dark brown color

which may impact on the brightness of the regenerated cellulose fibres, as well as damage the IL original structure. It has been reported in literature that ILs are good microwave absorbers and heating occurs rapidly which can easily lead to degradation of the ILs and biopolymers or even lead to explosion of the system (Wang *et.al.* 2012:1521).

In all the experiments, it was observed that 5 (%w/%w) loading gave higher cellulose recoveries than other pulp loadings, so therefore pulp loadings (5 %w/%w) was used in this work for preparing the biomass samples in IL/ co-solvents mixtures at 120 ˚C for 12 hours. Temperature is also an important variable to be considered, temperatures from 80 ˚C to 130 ˚C have been used in literature (Ning 2010:116). Higher temperatures help dissolution, but at the same time result in more degradation of the cellulose, and indeed, the ILs. It has also been pointed out by Lindman *et.al.* (2010:79) that higher cellulose concentrations are reached using microwave heating, which clearly indicates that kinetic rather than thermodynamic control is decisive.
For this study, we chose a temperature of 120 ˚C as a compromise between enhanced dissolution and higher energy demand.

Acetate has higher hydrogen bond basicity and thus has the ability to disrupt hydrogen bonds and dissolve cellulose. This positive correlation between the hydrogen bond basicity of the IL anion and the IL's ability to dissolve cellulose or lignocellulose has been reported in literature (Sun *et.al.* 2009:648). Dissolution of cellulose in ILs is attributed to the latter's ability to break the extensive network of hydrogen bonds existing in the cellulose. [Emim][OAc] disrupts the hydrogen bonding interactions present in the cellulose allowing it to diffuse into the interior of the cellulose, which then results in the complete dissolution of cellulose (Kilpeläinen *et.al.* 2007: 9145).

In their investigations, Heinze *et.al.* (2008:10) suggest that [Emim][OAc] forms a covalent bond between the $C\text{-}_1$ carbon of glucose unit and the $C\text{-}_2$ of the imidazolium core. This suggestion was based on the fact that the $C\text{-}_1$ carbon signal of the glucose unit disappeared after dissolution in [Emim][OAc] (Heinze *et.al.* 2008:10). According to the electron-donor-acceptor (EDA) mechanism, imidazolium cation with positive charge acting as electron acceptor and acetate anion with a negative charge acting as an electron donor, interact with oxygen and hydrogen of OH bonding of cellulose, respectively and promote the dissolution of cellulose in ionic liquid (Muhammad *et.al.* 2012:127). The ILs exhibiting relatively low

viscosities such as [Emim][OAc], facilitate dissolution of cellulose at lower temperatures thus giving less thermal degradation of cellulose (Mäki-Arvela *et.al.* 2010:177).

Figure 4.6-4.7 shows the plots of the cellulose yields against the unbleached and bleached dissolving pulp initially soaked in DMSO (right) and then after soaking, dissolved in [Emim][OAc] + DMSO mixture (left). Figure 4.8-4.9 shows the plots of the cellulose yields against the unbleached and bleached dissolving pulp initially soaked in DMF (right) and then after soaking, dissolved in [Emim][OAc] + DMF mixture (left).

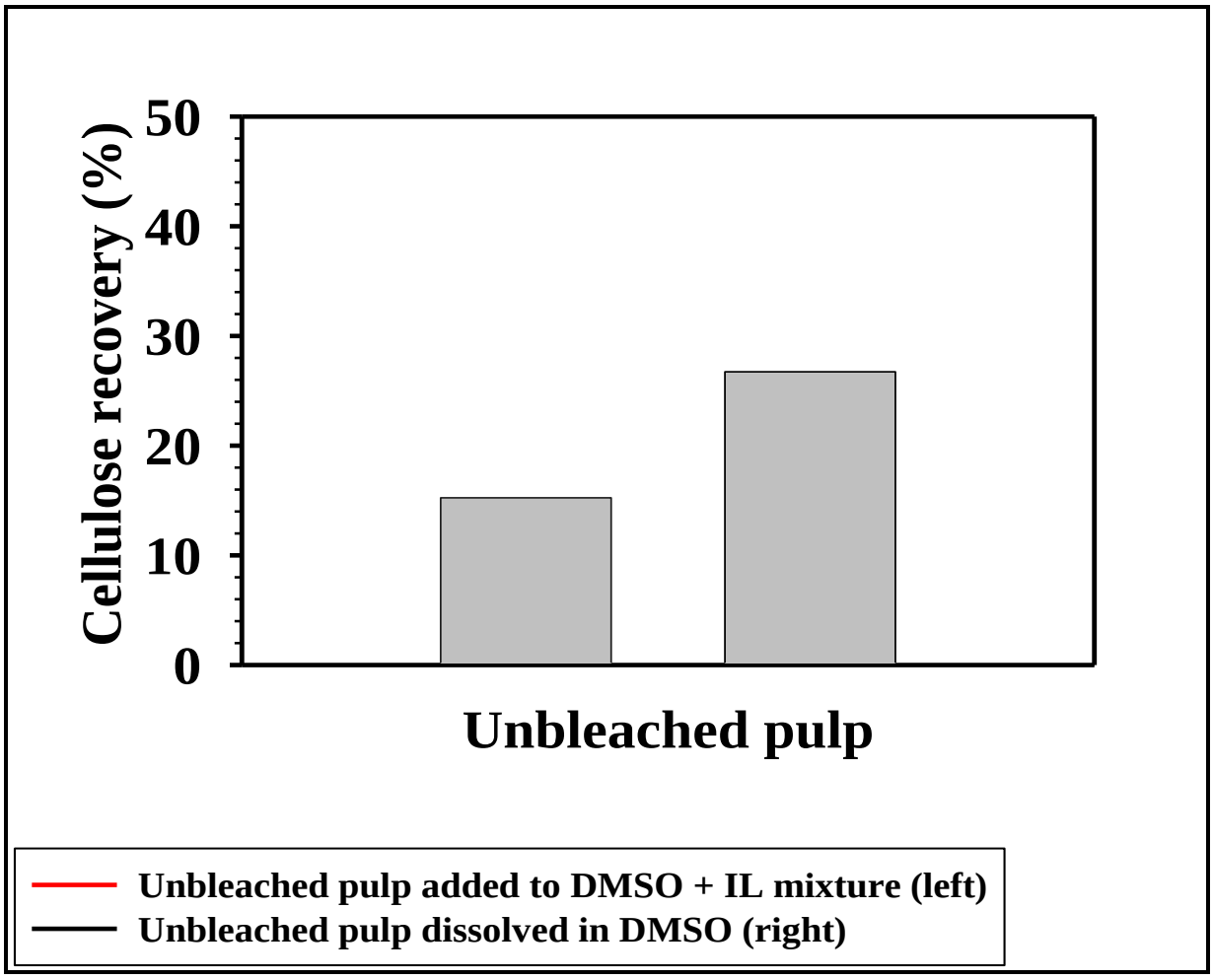

Figure 4.6 Effect of unbleached dissolving pulp initially soaked in DMSO (left) and then after soaking, dissolved in [Emim][OAc] + DMSO mixture (right) on cellulose recovery

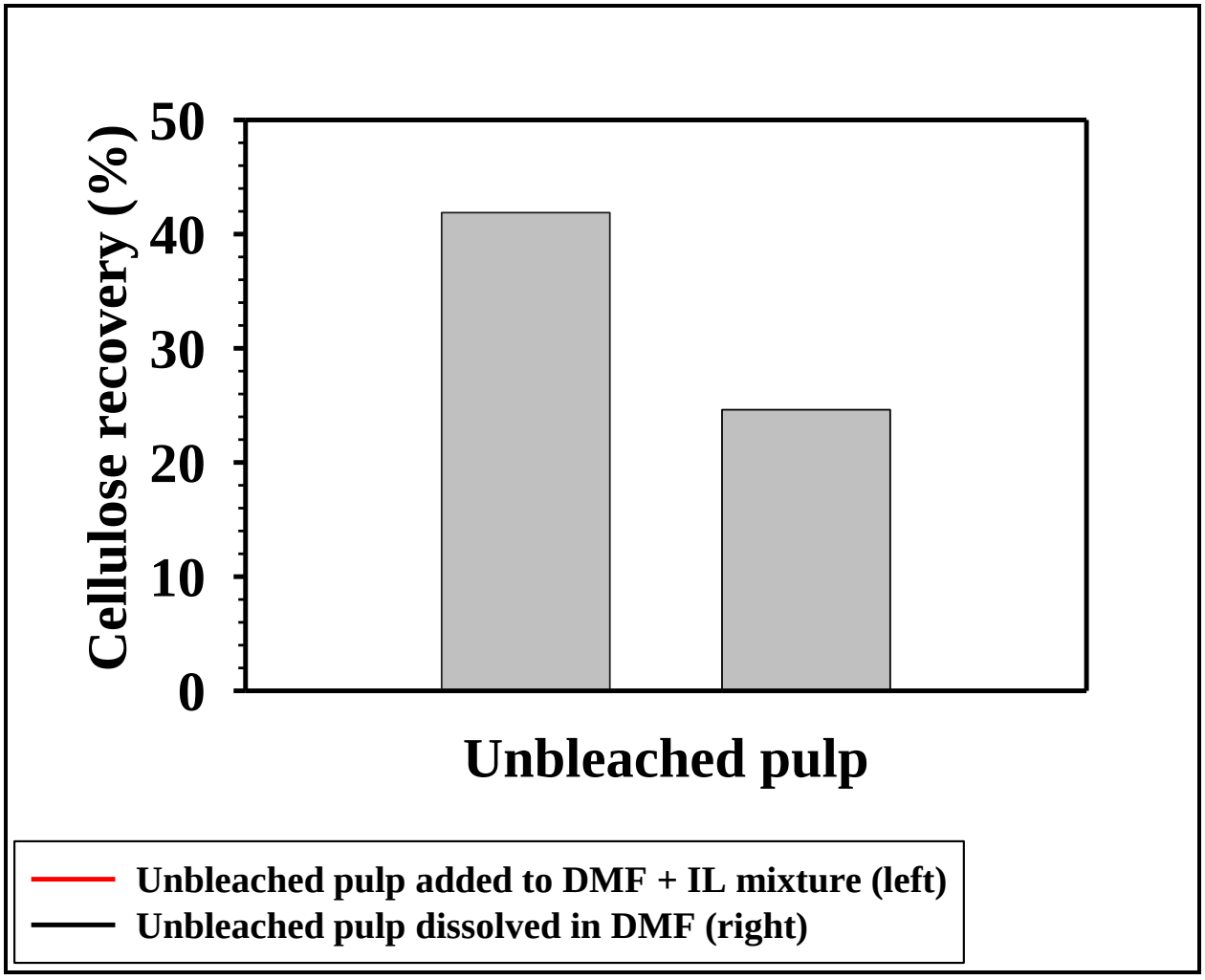

Figure 4.7 Effect of the soaked unbleached dissolving pulp initially soaked in DMF (left) and then after soaking, dissolved [Emim][OAc] + DMF mixture (right) on cellulose recovery (right)

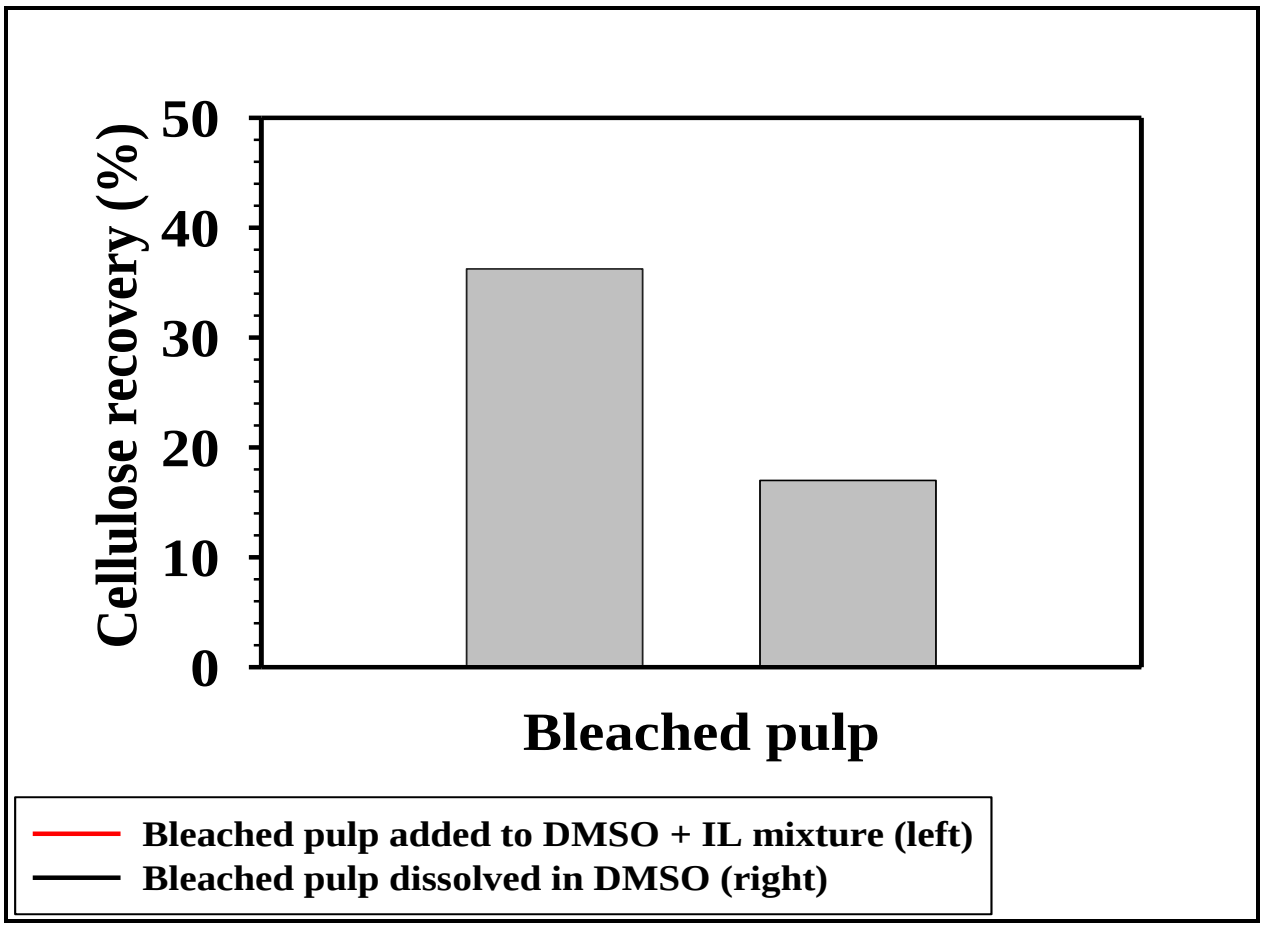

Figure 4.8 Effect of the soaked bleached dissolving pulp initially soaked in DMSO (right) and then after soaking, dissolved in [Emim][OAc] + DMSO mixture (left) on cellulose recovery

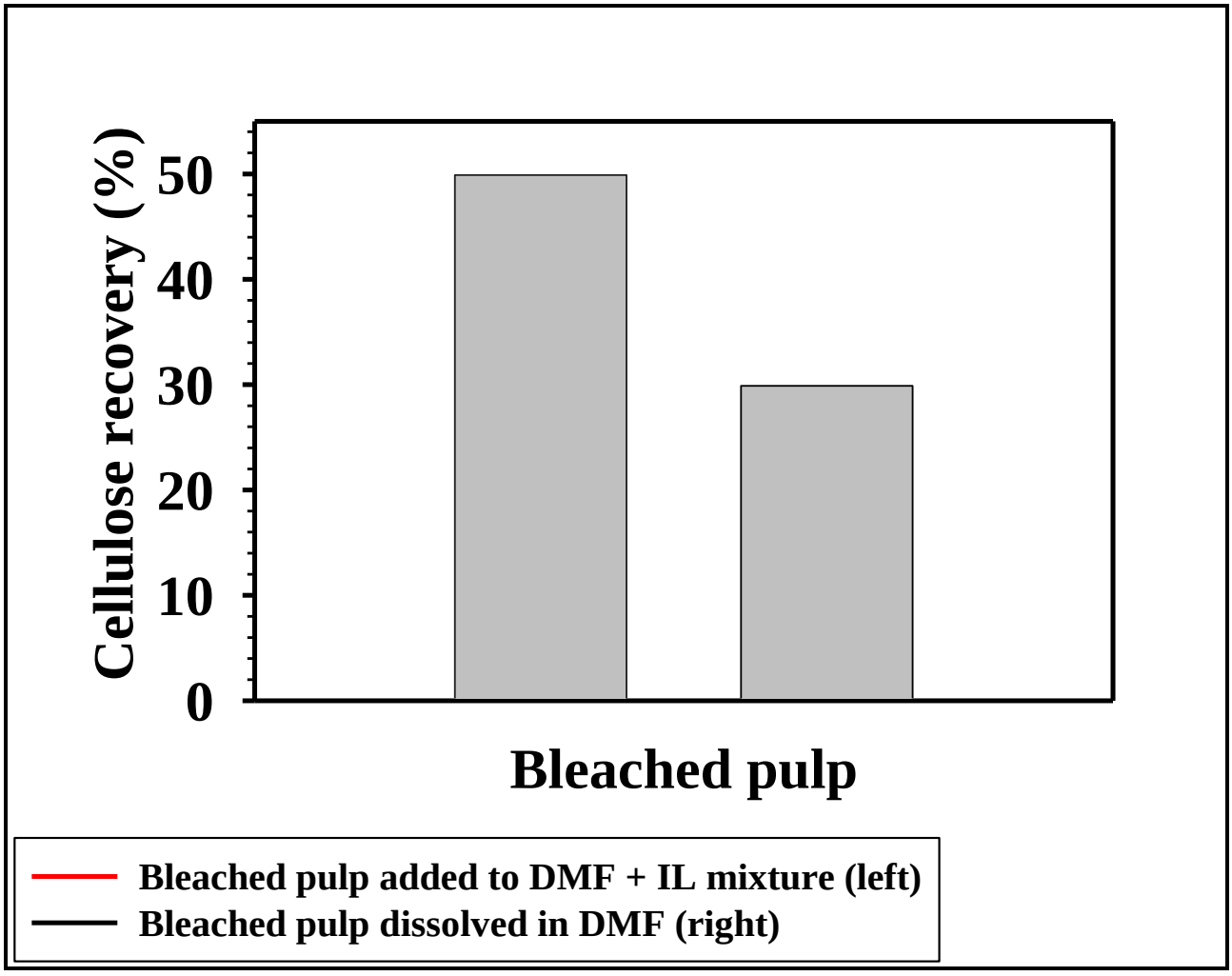

Figure 4.9 Effect of the soaked bleached dissolving pulp initially soaked in DMF (right) and then after soaking, dissolved in [Emim][OAc] + DMF mixture (left) on cellulose recovery

Method B, was adopted as the method of choice because it gave high cellulose yields (%) when the bleached dissolving pulp was dissolved in IL and co-solvent mixtures simultaneously, rather than when dissolving pulp is soaked in co-solvent before IL is added (method A).

Initially, 5(%w/%w) of the previously dried and ground bleached dissolving pulp was dissolved in neat [Emim][OAc] only without the addition of co-solvents. The 5 (%w/%w) of the previously dried and ground unbleached dissolving pulp, bleached dissolving pulp and sawdust wood samples were dissolved in [Emim][OAc]/DMSO and [Emim][OAc]/DMF mixtures, the concentration of co-solvents used in the mixtures was 25 %, with stirring at 120 °C for 12 hours for the sawdust and 6 hours for the pulp samples in an oil bath (see Figure

4.10 for dissolution setup in an oil bath). The samples were dried using the method described in Chapter 3.

The addition of co-solvents decreased the viscosity of the cellulose solutions in ILs. This is due to the destruction of the cellulose structure and intermolecular interactions.
Solutions of pulp treated with DMF/IL mixture have shown higher cellulose recoveries than in DMSO because

- DMF has the ability to swell the cellulose more efficiently than aprotic solvents. Swelling helps to break the bonds in the cellulose and make it more accessible to solvents for dissolution as reported by Kuzmina (2012:1).
- DMSO increase the speed of dissolution in ILs and it remains in solution thereby decreasing the IL viscosity which will improve the dissolution of cellulose in ILs and this has been reported by Zhao *et.al.* (2013:1).

Figure 4.10 Photograph of the dissolution setup in an oil bath

4.2 DISSOLUTION AND REGENERATION OF CELLULOSE

4.2.1 Dissolution of unbleached dissolving pulp and bleached dissolving pulp samples in neat [Emim][OAc]and [Emim][OAc]/ DMSO or DMF mixtures

The dissolution of the neat IL [Emim][OAc] and [Emim][OAc] with a co-solvent DMF or DMSO in unbleached dissolving pulp and bleached dissolving pulp was investigated. Regenerated cellulose was precipitated from the different mixtures by addition of water and acetone.

The dissolution of the unbleached dissolving pulp and bleached dissolving pulp samples in neat [Emim][OAc] and in [Emim][OAc]/DMSO and [Emim][OAc]/DMF mixtures was already described in Chapter 3- experimental section. The cellulose yield (%) for the regenerated cellulose using three types of solvents i.e. neat [Emim][OAc], [Emim][OAc]/DMSO and [Emim][OAc]/DMSO was calculated from equation 1 (refer to chapter 3) and is shown in Table 4.5.

After regeneration of cellulose the unbleached as well as the bleached dissolving pulp and IL/co-solvent solutions became viscous, almost gel like substance (shown in Figure 4.11). This gel is believed to be caused by the formation of hydrogen bonds between the IL and the dissolving pulp (Zavrel *et.al.* 2009:2584).

Figure 4.11 A photograph of the unbleached dissolving pulp (left) and bleached dissolving pulp (right) after dissolution in [Emim][OAc]/co-solvent mixtures

The regenerated cellulose material appeared to be “fluffy” and more open, which would make it more susceptible for solvents to penetrate in it. Figure 4.12 shows a visual representation of the recovered cellulosic material.

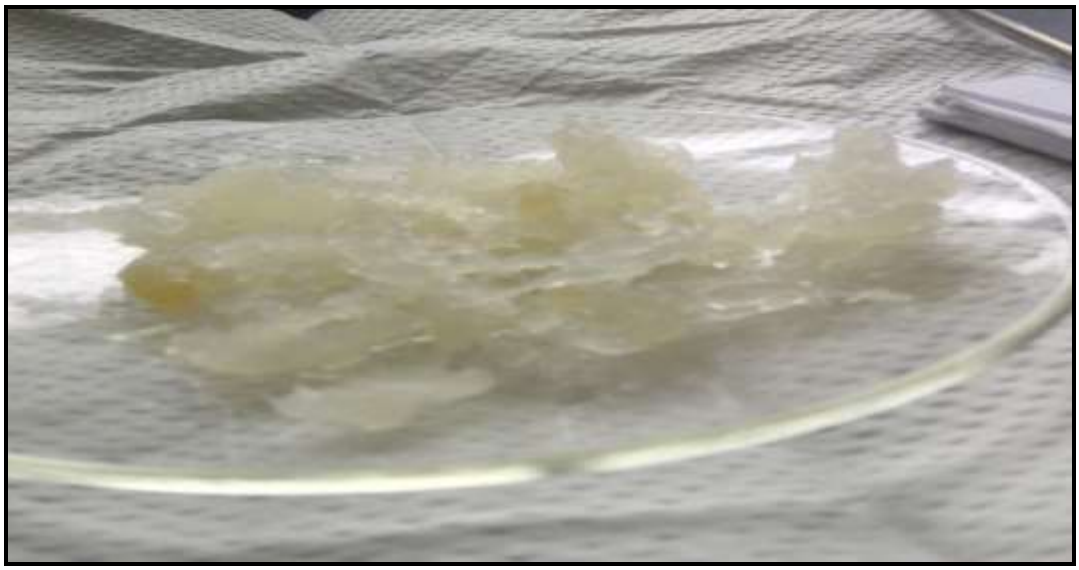

Figure 4.12 A photograph of the recovered cellulosic material after dissolution of sawdust wood/ dissolving in IL/co-solvent mixtures

Table 4.5 The yield of regenerated cellulose after dissolution of unbleached dissolving pulp and bleached dissolving pulp samples in neat [Emim][OAc], [Emim][OAc]/DMSO or DMF mixtures

Type of Solvent	**Regenerated cellulose from unbleached pulp**	**Regenerated cellulose from bleached pulp**
[Emim][OAc]	10.54 %	35.29 %
[Emim][OAc]/DMSO	15.25 %	41.88 %
[Emim][OAc]/DMF	36.25 %	49.89

As shown in Table 4.5, the yield of the regenerated cellulosic samples from unbleached dissolving pulp was between 10 % and 37%, whereas for the cellulose samples regenerated from bleached dissolving pulp, the yield was between 35% and 50%. From these results, it was expected that the bleached pulp would give higher cellulose recoveries compared to the unbleached pulp due to the low amount of lignin and hemicelluloses present in the bleached dissolving pulp.

The [Emim][OAc]/DMF mixture gave the highest percentage cellulose recoveries for the unbleached dissolving pulp and bleached dissolving pulp than [Emim][OAc]/DMSO mixture and pure [Emim][OAc] (refer to Table 4.1 for the values of the percentage cellulose recoveries). The low percentage cellulose recoveries may be due to the weight loss of cellulose during cellulose regeneration processes, including washing and transferring, similar results were reported by Lan et al (2011:674) where they reported a weight loss after dissolving cotton pulp in [Bmim][Cl]. The cellulose recoveries (%) for the regenerated cellulosic materials from [Emim][OAc]/DMF mixtures are higher than cellulose recoveries for regenerated cellulosic materials from [Emim][OAc]/DMSO. DMSO has a higher dielectric constant than DMF which makes DMSO more polar than DMF, and affects the dissolution process. DMSO has a stronger ion-dipole interaction resulting in the force of attraction becoming stronger between ions in the solution and the dipole-dipole interaction (hydrogen bonding) between solvent molecules ILs and co-solvents and this has also been reported by Gao *et.al.* (2013:1535). This effect results in a decrease in the solubility of cellulose in DMSO because the latter forms strong inter- and intramolecular hydrogen bonds which cannot break the hydrogen bonds in the macromolecular chains of cellulose (Cao *et.al.* 2009:13). Similar reports in the literature show that solvents with higher dielectric constants provide stronger ion-solvent interactions with ILs, which can strongly reduce the viscosity of IL solutions (Lv *et.al.* 2012: 2524). DMF is reported to be more hydrophobic than DMSO or IL by Gao *et.al.* (2013:1535).

The anion-cellulose interactions increase when DMF is added to IL which leads to increased solubility, but decrease when DMSO is added to the IL anion-cellulose interaction which leads to decreased cellulose solubility. This conclusion is in good agreement with the results reported in the literature (Xu *et.al.* 2013:540; Zhao *et.al.* 2013:1).

Aprotic solvents DMSO and DMF form weak C-H---O hydrogen bonds with $[Emim]^+$ and $[OAc]^-$. The strong preferential solvation of anions of the IL results in the reduced interaction between anions and cellulose and thus decreased solubility of cellulose. The solvation of [Emim]+ and [OAc]- by the aprotic solvents makes it possible to produce more "free" [OAc]- from the anion-cation pairs, which would readily interact with cellulose, leading to the increase in cellulose solubility (Zhao *et.al.* 2013:1).
The dissolution of cellulose in IL/co-solvent systems is still mainly determined by the hydrogen bond interaction between the $[OAc]^-$ and the hydroxyl protons of cellulose.

In ILs there are ionic interactions, π-π interactions and hydrogen bonds present. Therefore, ILs can compete with the lignocellulose components for their intramolecular hydrogen bonding, thus disrupting the three-dimensional network and this is attributed to the anions (Dadi *et. al.* 2007:410; Kilpelainen *et.al.* 2007:9145; Zavrel *et.al.* 2009:2584).

Past studies have shown that the dissolution ability of ILs is influenced by the interaction between anions and hydroxyl groups of the cellulose molecules (Ang *et.al.* 2011:4794; Zhao *et.al.* 2009:49). However, it was later proposed that the cations can also interact with cellulose, especially with the hydroxyl oxygen atoms (Dadi *et.al.* 2007:410; Zhang *et. al.* 2005:8275). The anions of the IL are believed to attack the hydroxyl group of cellulose and unfold the intra- and inter- molecular bonds in cellulose, leading to dissolution, whereas the cationic imidazolium moieties of the ILs do not get involved in the dissolution due to steric hindrance between the cation and hydroxyl group of cellulose (Ang *et.al.* 2011:4794).

The cation is reported to show efficient dissolution if it is an imidazolium cation with a C2-C6 side chain (Swatolski *et.al.* 2002:4974), which was a case in this study.
It is stated in the literature (Lindman *et.al.* 2010:79) that cellulose dissolution depends on the following:

a) way of handling,
b) temperature and time of heating,
c) as well as the molecular weight of the sample.

4.2.2 Mechanism for the cellulose dissolution process in [Emim][OAc]

In this work, the possible mechanism of dissolving pulp cellulose in [Emim][OAc] is shown in Figure 4.13 as follows:

- Above the critical temperature, the ion pairs in [Emim][OAc] dissociated to individual OAc^- and $Emim^+$ ions. Then free OAc^- ions associated with cellulose hydroxyl oxygen, which disrupted hydrogen bonding in cellulose and led to the dissolution of cellulose (Cao *et. al.* 2009: 15).
- Although some simulation studies reported in literature (Cao *et.al.* 2009: 15) suggest that little or weak interactions between cations of ILs and the glucose of cellulose existed, the authors believed that the cations of the ILs were involved in the dissolution process and their role in the dissolution mechanism should not be neglected.

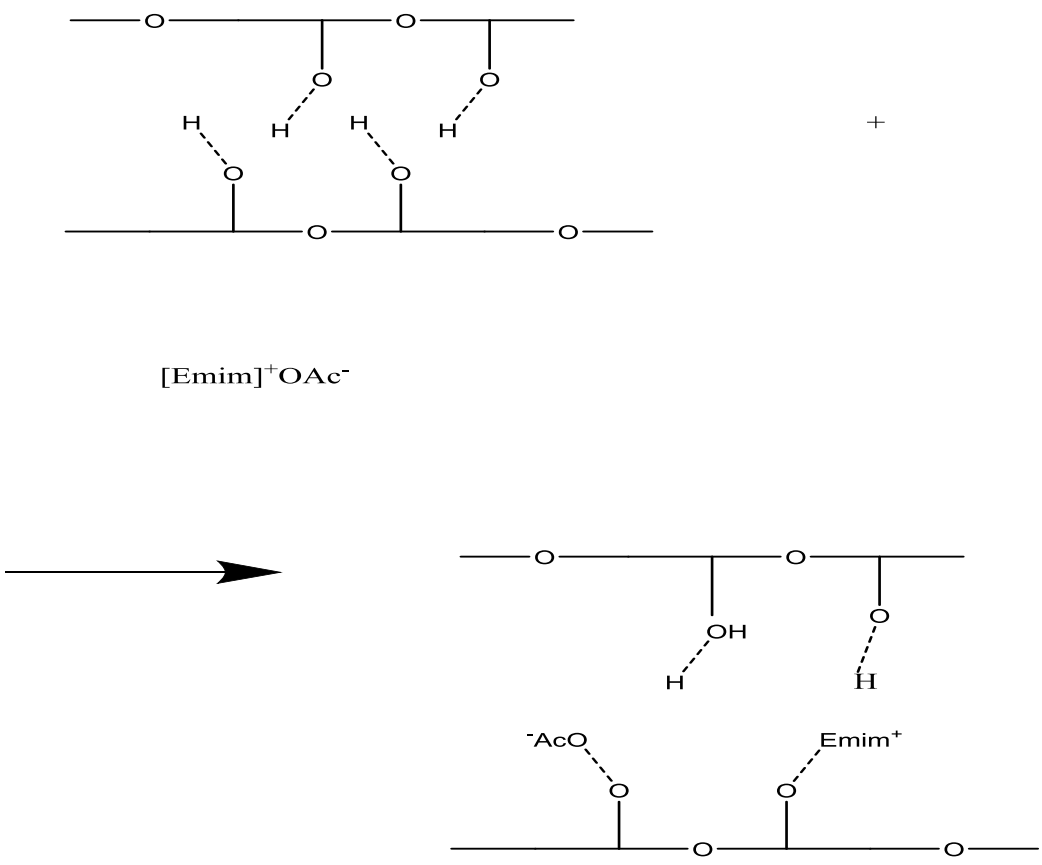

Figure 4.13 Possible dissolution mechanism of dissolving pulp cellulose in [Emim][OAc] as reproduced by Cao *et.al.* (2009: 15) and Zhang *et.al.* (2005: 8275)

The excellent capability of ILs for cellulose dissolution inspires many researchers to explore the possible mechanisms. In the early studies, it was widely believed that the ions, especially the anions of the ILs, could effectively break the extensive intra- and inter-molecular hydrogen bonding network in cellulose (Fukaya *et.al.* 2008: 44: Zhang *et.al.* 2005: 8272).

Based on this hypothesis, the interaction between ILs and cellulose was investigated by ^{13}C and $^{35/37}$ Cl NMR relaxation measurements (Remsing *et.al.* 2006: 1271). They found that the carbons C_4 and C_1 of $[Bmim]^+$ cation showed a slight variation in the relaxation times as the concentration of cellobiose in [Bmim][Cl] increased. Their study proves the presence of 1:1 hydrogen bonding between Cl^- and carbohydrate hydroxyl proton. Similar conclusions have also been obtained by computer modelling as reported by (Novoselov *et.al.* 2007:153).

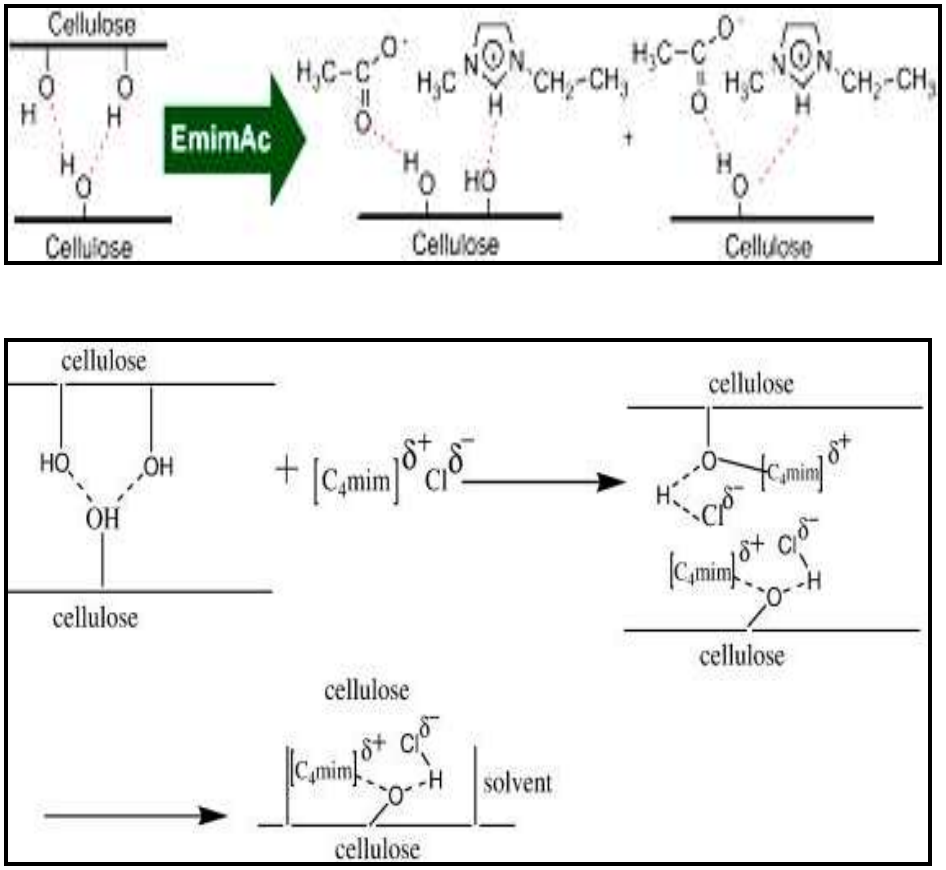

Figure 4.14 Dissolution mechanism of cellulose by ionic liquids as reproduced by Feng and Chen (2008:2).

The mechanism for the dissolution of cellulose in ILs is shown in Figure 4.14, Feng and Cheng (2008:2) indicated that interactions between the oxygen and hydrogen atoms of cellulose-OH and the cation and anion of IL results in the dissolution of cellulose.

The cellulose atoms served as electron pair donors and hydrogen atoms act as electron acceptors. Upon interaction, the oxygen and hydrogen atoms from the hydroxyl groups are separated, which leads to the opening of hydrogen bonds between molecular chains of the cellulose and, as a result, the cellulose dissolves (Qiu 2012:18).

4.2.3 Dissolution of sawdust wood samples in neat [Emim][OAc]and [Emim][OAc]/ DMSO or DMF mixtures

The cellulose yield (%) for the regenerated cellulose from sawdust that was previously dissolved in three types of solvents, i.e., neat [Emim][OAc], [Emim][OAc]/DMSO and [Emim][OAc]/DMF was calculated from equation 1) and is shown in Table 4.6.

Table 4.6 Percentage yield and losses of regenerated cellulose after dissolution of sawdust wood samples in neat [Emim][OAc], [Emim][OAc]/DMSO or DMF mixtures

Type of Solvent	**Regenerated cellulose in Sawdust wood**	**Losses in solids (%)**
[Emim][OAc]	7.21 %	33.74 %
[Emim][OAc]/DMSO	17.83 %	23.12 %
[Emim][OAc]/DMF	32.50 %	8.45 %

There were higher cellulose recoveries for the bleached pulp *vs.* the unbleached pulp and sawdust wood which may be due to the fewer amount of hemicelluloses and lignin content of 1.40% present in the bleached pulp compared to 3.60 % in the unbleached pulp (refer to chapter 4 Table 4.1). Compared with the pulp, wood has a much more complex structure composed of cellulose, hemicellulose and lignin hence the difficulty in breaking the hydrogen bonds within the cell wall of wood. This would thus result in low % cellulose yield. The losses in solids may be associated with the filtration step. The losses in sawdust are 33.74 % for cellulose regenerated from neat [Emim][OAc], 23.12 % for cellulose regenerated in [Emim][OAc]/DMSO mixture and 8.45 % for cellulose regenerated from [Emim][OAc]/DMF. More work needs to be done in this study, to fully understand, and account for the losses that happen during the dissolution and regeneration process.

The low percent 7.21 of cellulose recoveries of sawdust wood regenerated from neat [Emim][OAc]; 17.83% for the [Emim][OAc]/DMSO and 32.50% [Emim][OAc]/DMF mixtures may be due to the fact that the highly crystalline character of cellulose in wood is

due to regular intermolecular and intramolecular hydrogen-bonding (SEM micrograph shown in Figure 4.15) interactions together with the three-dimensional network character of lignin and its possible covalent linkages with the carbohydrates are primarily responsible for the complex and compact structure of wood.

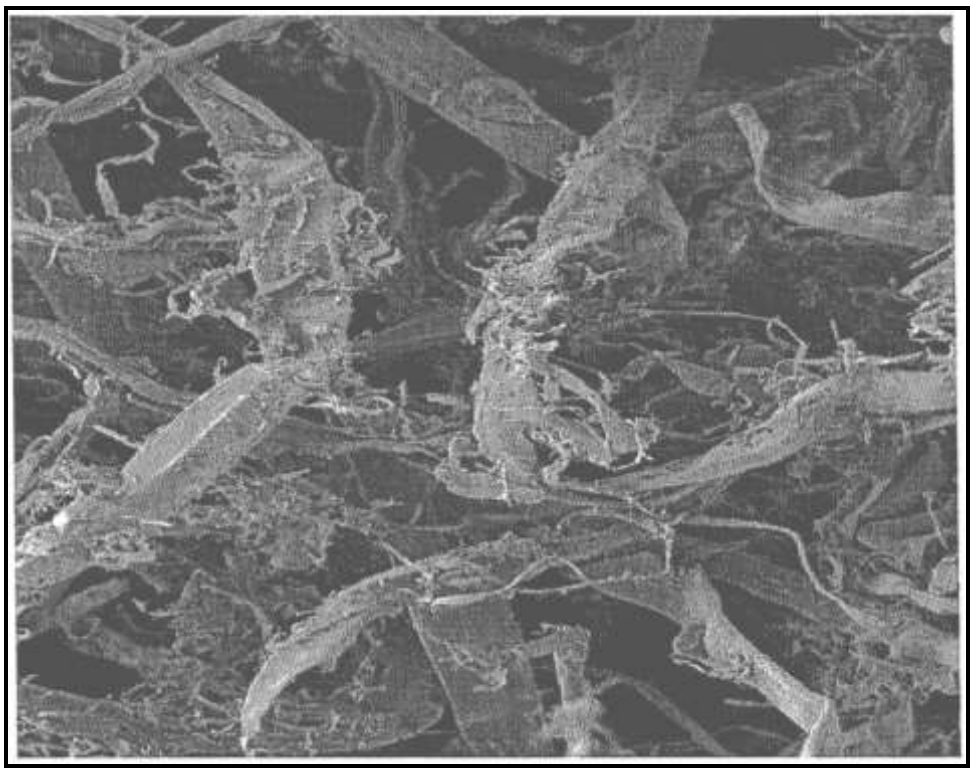

Figure 4.15 SEM image of inter- and intramolecular hydrogen bonding interactions in wood as reproduced from Argyropoulos (2012:2)

Furthermore, the kinetics and the time of wood dissolution in ionic liquids are dependent on the applied temperature, which is consistent with the results in previous publications related to the dissolution of wool keratin fibres (Xie *et.al.* 2005:607). In this work a temperature of 120 ˚C was used for the dissolution of sawdust in [Emim][OAc]/DMF or DMSO mixtures.

In another study, using woody lignocellulose (southern yellow pine sawdust), the biomass was completely dissolved in the acetate-based IL only when heated to 110 ˚C for 46 hours (Sun *et.al.* 2009:646). However, another similar study showed that air-dried pine wood chips were not completely dissolved in acetate-based ILs, even though the reaction mixture was heated at 120 ˚C for 48 hours (Brandt *et.al.* 2010:673). On the contrary, Li *et.al.* (2009:3570)

claimed that complete dissolution of wheat straw in acetate-based IL [Emim][OAc] was achieved by heating the reaction mixtures at 100 ˚C for only 1 hour.
The findings from various researchers also suggested that the difference in solvating ability of the ILs could be attributed to their degree of saturation with solute (Brandt *et.al.* 2010:673; Sun *et.al.* 2009:646).
The type of wood biomass also plays an important role in the dissolution process when using ILs (Sun *et.al.* 2009:646).

The acetate-based IL was reported to show better dissolution of wood (Sun *et. al.* 2009:646) and cellulose (Ang *et. al.* 2011:4794). One possible reason for this is that the acetate anion seems to favour dissolution because acetate has higher hydrogen bond basicity (a property of the anion that is influenced primarily by the size and charge localization on the anion) than other anions (Brandt *et.al.* 2010:673; Karatoz *et.al.* 2012:2). Thus it has the ability to disrupt hydrogen bonds in cellulose and thereby have a potential to dissolve cellulose is higher. This positive correlation between the hydrogen bond basicity of the IL anion and the IL's ability to dissolve cellulose or lignocellulose is discussed more in literature (Brandt *et.al.* 2010:673).

However, Swatolski *et.al.* (2002:4974) claimed that [Bmim][Cl] is the most effective IL in dissolving pure cellulose, such as cellulose-dissolving pulps, fibrous cellulose, and Whatman cellulose filter papers. This indicates that IL dissolution is selective on the type of substrate, and the selectivity of ILs could be attributed to their ionic functional groups.
The lignin content after dissolution of sawdust wood in [Emim][OAc]/DMF and DMSO mixtures could not be weighed because only a few precipitated black particles were observed, more time is needed for the evaporation of lignin.
This lignin content is not in agreement with literature findings that report lignin content to be approximately 20 % in hardwoods (Casas *et.al.* 2012:472).

The decrease of lignin content was probably due to more hemicelluloses/cellulose remaining dissolved in the regeneration step. This probably indicates that lignin is harder to degrade than hemicelluloses and cellulose components. More research is needed to settle this.
In the regenerated cellulose, according to Dadi *et.al.* (2006:904), it was reported that in dissolving the maple wood powder by [Emim][OAc], the crystalline structure of cellulose in wood powder was disrupted when the experiment was performed at higher temperatures, i.e., about 130 ˚C. At the same time, lignin extraction also took place.

The dissolution rate of wood is highly dependent on the particle size of the wood sample. This is because the complex and compact structure of wood cell walls would inhibit the diffusion of the ionic liquid into its interior, resulting in only a partial dissolution of wood (Kilpeläinen *et.al.* 2007:9144).

Kilpeläinen *et.al.* (2007:9144) discovered that the solubilisation efficiency of lignocellulose materials in ILs is in the order of: ball-milled wood powder > sawdust > thermo mechanical pulp fibres > wood chips.

4.3 CHARACTERIZATION OF THE REGENERATED CELLULOSE

The regenerated cellulose samples were characterized by FTIR, NMR, SEM, P'XRD and TGA and compared with data for standard microcrystalline cellulose (MCC).

4.3.1 Fourier transformer infrared spectroscopy (FTIR) of the regenerated cellulose

FTIR analysis was conducted to examine the structural changes in chemical bonds of cellulose after regeneration and compared with the FTIR of microcrystalline standard of cellulose.

4.3.1.1 *FTIR of regenerated cellulose from unbleached and bleached dissolving pulp samples previously dissolved in [Emim][OAc]/DMSO or DMF mixtures*

Figure 4.16 is the spectra of cellulose regenerated from the unbleached pulp dissolved in [Emim][OAc]/DMSO (**1**) and [Emim][OAc]/DMF (**2**) mixtures compared to the MCC standard of cellulose (**3**), while Figure 4.8 is the spectra of cellulose regenerated from the bleached pulp dissolved in [Emim][OAc]/DMSO (**1**) and [Emim][OAc]/DMF (**2**) compared to the MCC standard of cellulose (**3**). The FTIR analysis for neat [Emim][OAc] was not done in this study, due to time constraints.

The bands in the 6 spectra shown in (Figures 4.16-4.17) are rather similar, indicating the structure of MCC and the two regenerated cellulose spectra are similar, which thus suggests that [Emim][OAc] dissolved cellulose and no new peaks appear in the regenerated samples. This indicates that no chemical reactions occurred during the dissolution and regenerating processes of the cellulose (Lan *et al.* 2011:675; Zhang *et.al.* 2005:8272).

From Figures 4.16-4.17, it can be seen that there is no significant difference between the FTIR spectra of the regenerated cellulosic materials from unbleached pulp and bleached pulp that were previously dissolved in [Emim][OAc]/DMSO and [Emim][OAc]/DMF mixtures and the spectras are all in excellent agreement with the MCC standard with all the relevant bond vibrations.

In the spectra A, the absorption at ~3400-3200 cm^{-1} is attributed to the O-H stretching and vibrations which is due to the free hydroxyls groups and association of cellulose chains via hydrogen bonds. It is a strong broad absorption indicating a hydrogen bonding which indeed takes place between repeating units within the cellulose matrix (Lan *et.al.* 2011: 675; Lateef *et.al.* 2009: 1818; Mahadeva *et.al.* 2012:1) and that of at ~3100-2900 cm^{-1} attributed to the C-H and CH_2 stretching which is unaffected by changes in crystallinity (Qiu *et.al.* 2012: 1). The band at ~1654.00 cm^{-1} is due to the bending mode of the absorbed water (Lan *et.al.* 2011:675).

A small peak at ~1400 cm^{-1} in both of the spectra relates to the CH_2 symmetric bending, and is viewed as typical of crystalline regions of cellulose and the absorption band at 893 cm^{-1} typical of amorphous regions (Karatzos *et.al.* 2012:307). It can also be noted that the absorption peak referred to CH_2 scissoring motion was shifted from higher intensity to lower intensity upon regeneration which indicates the destruction of the intermolecular hydrogen bond involving O at C_6 (Mahadeva *et.al.* 2012:1).

Since there is no absorption band for aromatic skeletal vibration (in lignin found and observed at around 1550-1640 cm^{-1}) in the regenerated cellulose pulp samples, this confirms the absence of residual lignin in the regenerated cellulose samples. [Emim][OAc]/DMSO or DMF mixtures removed the lignin in the regenerated cellulose material.
The absorbances at ~1315 cm-1 originate from the O-H bending, C-H bending, and C-O symmetric stretching (Lan *et.al.* 2011: 675; Liu *et.al.* 2011:220). A shoulder band at
~1100 cm^{-1} C belongs to the C-OH skeletal vibration. The C-O-C pyranose ring skeletal vibration gives a prominent band at ~1030 cm^{-1}. A small sharp peak at ~900 cm^{-1} corresponds to the glycosidic C_1-H deformation with ring vibration contribution, which is characteristic of β-glycosidic linkages between glucose in cellulose (Lan *et.al.*2011:675; Lateef *et.al.* 2009:1818).

The results indicate that the highly crystalline cellulose structure in unbleached and bleached dissolving pulp samples was transformed to amorphous form after treating with [Emim][OAc] and co-solvents. Decrease in crystallinity of Avicel pulp (Zhao *et.al.* 2009:217) was also reported after pretreatment with ILs. Decrystallisation of cellulose is a known and unique effect of IL pretreatments (Karatzos *et.al.* 2012:307).

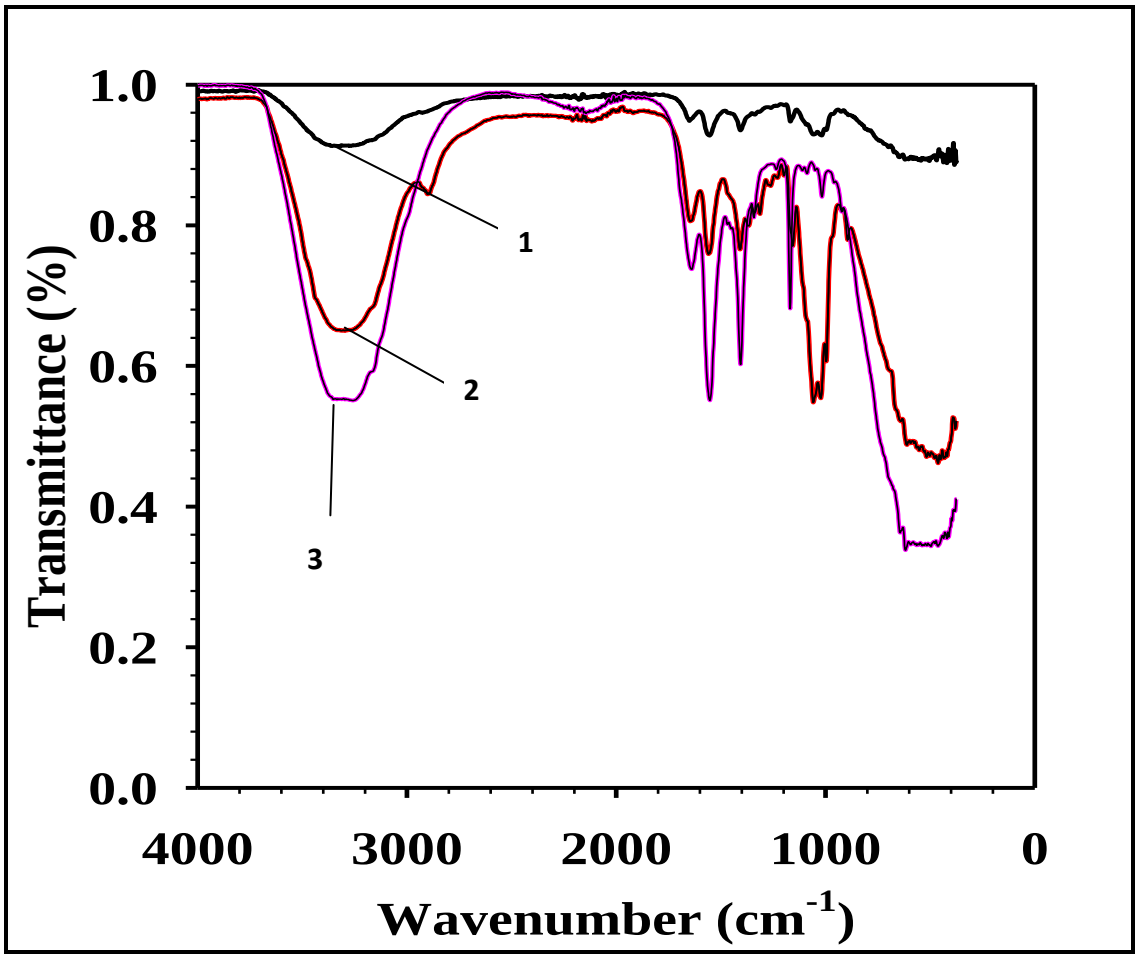

Figure 4.16 FTIR spectra A of cellulose regenerated from the unbleached pulp dissolved in [Emim][OAc]/DMSO (**1**) and [Emim][OAc]/DMF (**2**) mixtures compared to the MCC standard of cellulose (**3**)

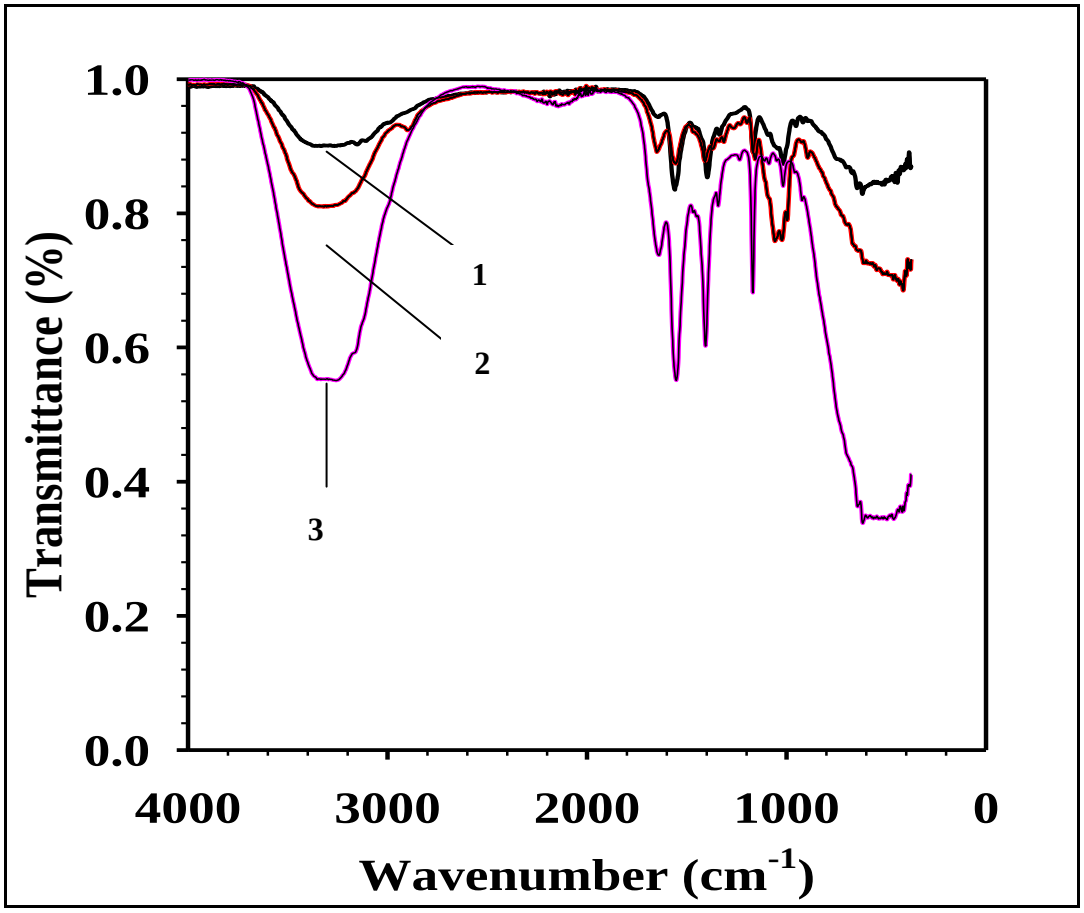

Figure 4.17 FTIR spectra B of cellulose regenerated from the bleached pulp previously dissolved in [Emim][OAc]/DMSO (**1**) and [Emim][OAc]/DMF (**2**) mixtures compared to the MCC standard of cellulose (**3**)

4.3.1.2 *FTIR of cellulose regenerated from sawdust wood samples previously dissolved in [Emim][OAc]/DMSO or DMF mixtures*

The FTIR spectrum shown in Figure 4.18 of the regenerated cellulose from sawdust wood that was previously dissolved in [Emim][OAc]/DMF or DMSO is similar to that of the MCC, indicating that no other chemical reaction occurred besides the breakage of hydrogen bonds during the process of dissolution and regeneration, similar results were reported in literature (Liu et.al. 2011:223; Sun et.al. 2011:647; Zhang et.al. 2005:8273). This is similar to the results for the dissolving pulp samples.

The broad absorption band in the spectrum at ~3400-3200 cm-1 corresponds to the stretching vibration of OH- groups; the band at ~2700-2900 cm-1 attributes to the vibration of CH2 groups, similar results were reported in literature (Lateef et.al. 2009:1822; Liu et.al. 2011:223). The appearance of an absorption band at ~ 1700 cm-1 corresponds to the C-O stretching vibration of C-O-H and it became stronger after regeneration. The intensity peak of CH2 bending shifted from highest to low in transmittance, which is a hint of the cleavage of hydrogen bond in C6-OH to some extent (Zhang et.al. 2005:8274).

The peaks at ~ 1400 cm-1 is attributed to the O-H bending vibration and is also viewed as typical crystalline regions of cellulose (Karatzos et.al. 2012:307). The characteristic peaks appearing at ~ 1300 cm-1 are attributed to the C-O bond stretching vibration. The peaks at ~ 1100 cm-1 attributes to the C-O bond stretching vibration of C-O-C group in the anhydroglucose ring (Liu et.al. 2011:223).

The small sharp peak around ~ 900 cm-1 corresponds to the glycosidic C-H deformation with vibration contribution and O-H bending and is viewed as typical of the amorphous region (Karatzos et.al. 2012:307), which is characteristic of β-glycosidic linkages between glucose in cellulose. It is observed only in the regenerated cellulose spectrums and this might indicate that the crystal structure of sawdust wood was transformed from cellulose I to cellulose II (Liu et.al. 2011:223).

All the regenerated cellulose for the unbleached dissolving pulp, bleached dissolving pulp and sawdust wood in [Emim][OAc]/DMF and DMSO mixtures were more amorphous compared to the microcrystalline standard of cellulose, which was interpreted from the band

broadening at approximately 800 cm-1 (Ang et.al. 2011:4976; Brandt et.al. 2010:673; Sun et.al. 2009:646). The precipitation of regenerated cellulose with deionized water prevents the restructuring of dissolved cellulose back into its crystalline form (Dadi et.al. 2009:904).

Figure 4.18 illustrates the spectra of cellulose regenerated from the sawdust wood dissolved in [Emim][OAc]/DMSO (**1**) and [Emim][OAc]/DMF (**2**) compared to MCC standard of cellulose (**3**).

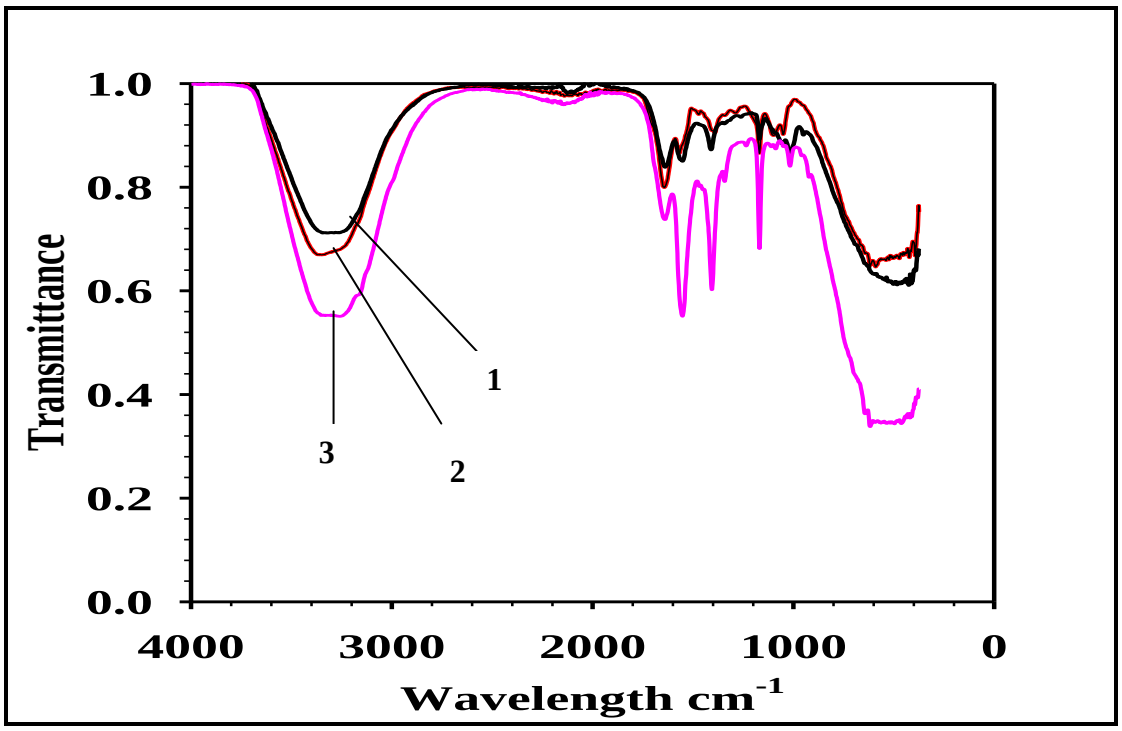

Figure 4.18 FTIR spectra of cellulose regenerated from the sawdust wood previously dissolved in [Emim][OAc]/DMSO (**1**) and [Emim][OAc]/DMF (**2**) mixtures compared to the MCC standard of cellulose (**3**)

Table 4.7 Summary of some FTIR-ATR absorption bands for bagasse as reported in literature (Karatzos *et.al.* 2012:307).

Table 4.7 Summary of some FTIR-ATR absorption bands for bagasse

Band position cm^{-1}	**Assignment**
1730	C=O stretching vibration in acetyl groups of hemicelluloses
1600	C=C stretching vibration in aromatic ring of lignin
1510	C=C stretching vibration in aromatic ring of lignin
1421	CH_2 scissoring at C_6 in cellulose
1368	Symmetric C-H bending in cellulose
1236	C-O stretching vibration in lignin, xylan, and ester groups
1100	O-H association band in cellulose and hemicelluloses (associated with crystalline cellulose)
1030	C-O stretching vibration in cellulose and hemicellulose
974	C-O stretching vibration in arabinosyl side chains in hemicellulose
895	Glucose ring stretch, C_1-H deformation

4.3.2 FTIR of lignin precipitated from sawdust wood samples and [Emim][OAc]/DMF mixtures

The FTIR spectra of Indulin AT a lignin standard was taken from literature (Sun *et. al.* 2009: 653) and is shown in Figure 4.19. The FTIR standard Indulin was analysed on its own, but when tried to open the file, we found that it was corrupted, hence we opted for the literature spectra of FTIR lignin standard.

Figure 4.20 shows the FTIR spectra of lignin precipitate regenerated from the sawdust wood previously dissolved in [Emim][OAc]/DMF (**1**) mixtures compared to the lignin sample obtained after Kraft pulping (**2**) and to the Indulin AT standard of lignin (**3**).

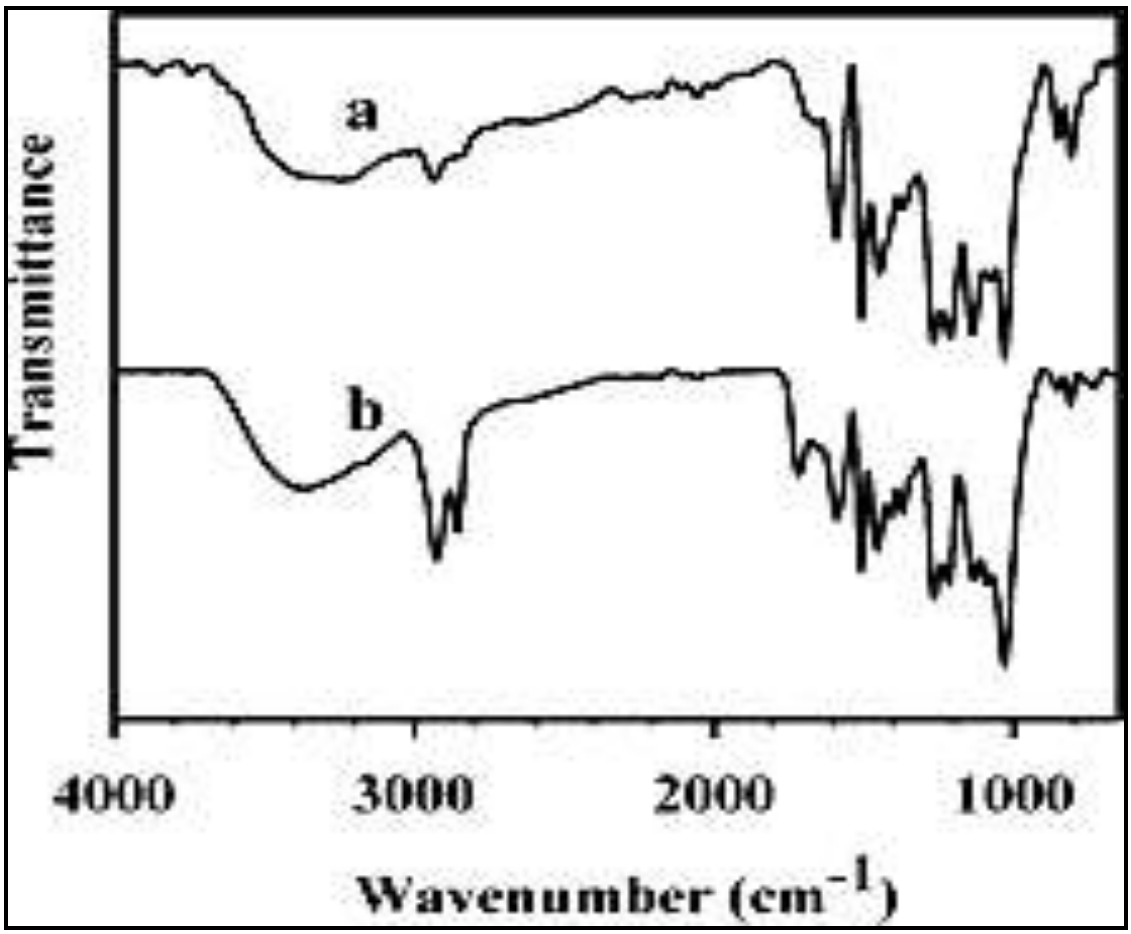

Figure 4.19 FTIR spectra of Indulin AT standard of lignin (spectrum **a**) taken from literature (Sun *et.al.* 2009:653)

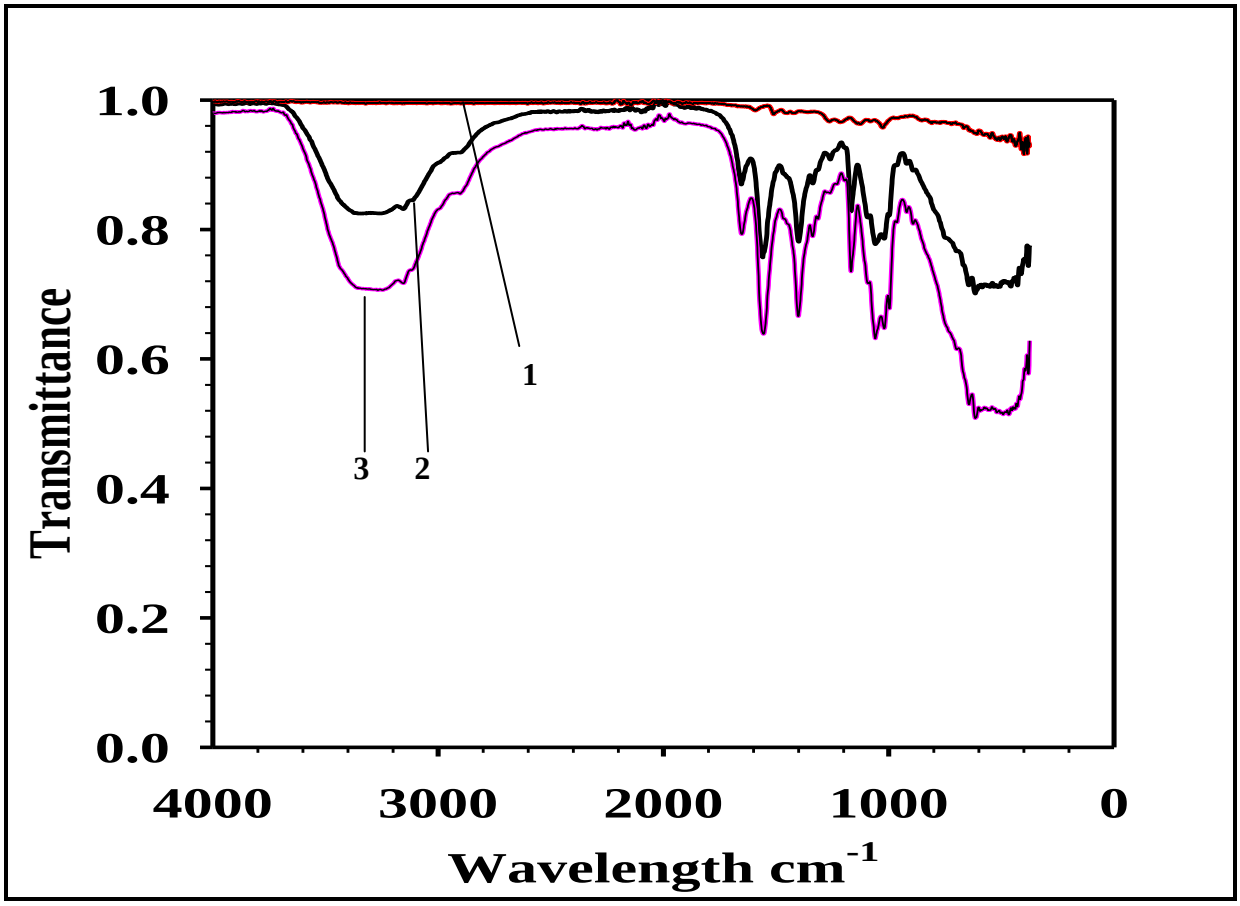

Figure 4.20 FTIR spectra of lignin precipitate regenerated from the sawdust wood previously dissolved in [Emim][OAc]/DMF (**1**) mixtures, lignin sample obtained after Kraft pulping supplied by Sappi (**2**) compared to the Indulin AT standard of lignin (**3**)

The FTIR spectra of Indulin AT lignin standard shown in Figure 4.19 showed not much difference compared with the Indulin FTIR spectra shown in Figure 4.20. It was observed that there is a close similarity of Lignin standard (**3**) to the lignin recovered after pulping (**2**) where the typical peaks of lignin were observed and the spectrum of lignin precipitate shows large differences of absorbance's in the spectrum.

The absorption from O-H stretching was observed at ~3200-3400 cm^{-1} indicating the content of free hydroxyl group. The FTIR spectra shown in (Figure 4.20 spectrum (**1**)) shows the characteristic vibration of lignin, at ~1510 cm^{-1} which appears as the aromatic skeletal vibration of lignin and is similar to Indulin standard of lignin (Figure 4.20 spectrum (**2**)), and similar results have been reported in literature (Casas *et.al.* 2012a:161; Casas *et.al.* 2012b:117). A decrease in the aromatic skeletal vibrations may be due to the transformation

of the aromatic ring into the quinonoid structures during the dissolution and regeneration process (Casas *et.al.* 2012a:161).

The band at ~1200 cm^{-1} corresponds to the vibration of the guaicyl ring in lignin and the characteristic vibration of the syringly ring appears at ~1300 cm^{-1} (Casas *et.al.* 2012b:117).

All the spectra have absorbance at the hemicellulose characteristic bands between ~1200 cm^{-1} and 1000 cm^{-1} and are more intense in the Indulin spectra than in the lignin recovered from the bleached and unbleached pulp samples. The low intensity of these bands in the lignin recovered from the bleached and unbleached pulp samples may be due to the oxidation of the secondary and primary alcohols to form carbonyl groups, as consequence of dissolution and regeneration process (Casas *et.al.* 2012a:161). This indicates that the majority of the non-lignin components are comprised of hemicellulose and this is in agreement with results reported in literature (Karatzos *et.al.* 2012:307).

The spectra of lignin recovered after evaporation of acetone (Figure 4.11 spectra (**1**)) did not compare very well with the lignin standard (shown in Figure 4.11 spectra (**2**)), but small peaks can be seen around the 600-1300 cm^{-1} which compare with the lignin standard, so one can conclude that indeed the spectra refers to a lignin. The precipitated lignin after dissolution also shows a strong absorbance ~980 cm^{-1} indicative of arabinosyl groups. This is in agreement with a previous discussion supporting preservation of covalent bonds to arabinosyl groups during [Emim][OAc] dissolution (Karatzos *et al.* 2012:307).

The bands at ~ 800 cm^{-1} corresponds to the C-H out of plane vibrations in guaiacyl rings in lignin (Casas *et.al.* 2012a:161) and the vibration of the glucose ring in cellulose.

The characteristic bands of lignin taken from literature (Casas *et.al.* 2012b:116) are shown in Table 4.8.

Table 4.8 FTIR absorption bands for hardwood lignin

Band position cm^{-1}	Assignment
1735	C=O stretching (unconjugated)
1658	C=O stretching (conjugated)
1603	Aromatic skeletal vibration breathing with C=O stretching
1510	Aromatic skeletal vibration
1462	C-H deformations asymmetric
1425	Aromatic skeletal vibration combined with C-H in plane deformation
1375	Phenolic OH and aliphatic C-H in methyl groups
1328	S unit breathing with C=O stretching and condensed G rings
1269	G ring breathing with carbonyl stretching
1220	C-C plus C-O plus C=O stretch
1140	C-H in plane deformation of G ring + secondary alcohols and C=O stretch
1116	Aromatic C-H deformation in S ring
1086	C-O deformation in secondary alcohols and aliphatic ethers
1033	Aromatic C-H in plane deformation
835	C-H out of plane deformation

Therefore, according to these results, lignin mixed with cellulose, could not be regenerated from solutions of eucalyptus sawdust wood in [Emim][OAc]/co-solvent mixtures, and this may be probably due to the limitations in the operating conditions (higher temperature leads to IL decomposition) (Casas *et.al.* 2012b:472).

Similar results were reported by Lan *et.al.* (2011:675) where they revealed that the cellulose isolated from bagasse in [Bmim][Cl] was found to be free of residual lignin and Casas *et.al.* (2012b:117) also concluded that lignin could not be precipitated from solutions of *Eucalyptus* woods in ILs with acetate anions because acetate based ILs are able to establish hydrogen bonds with wood and probably dissolve it.

The unaccounted losses maybe a result of fragmentation of lignin and changed solubilities in the washing steps (Sun *et.al.* 2011:1).

4.3.3 FTIR of recovered [Emim][OAc]

To achieve environmentally friendly biomass processing, the recovery and reuse of ILs is one of the main challenges. The [Emim][OAc] was recovered in excellent yield, > 99 % by using the rotary evaporator (shown in Figure 4.21) by evaporation and drying from aqueous solution obtained after regeneration.

Hermanutz *et.al.* (2008:23) reported that ILs used as solvents for manufacturing cellulose fibres were almost entirely recovered (99.5 %).The colorless [Emim][OAc] became reddish brown after recycling, this may be due to exposure to elevated temperatures and contaminants present in [Emim][OAc], which could be degradation from [Emim][OAc] and biomass as well as carbohydrate (Sun *et.al.* 2013: 283; Wu *et.al.* 2012:231).

Figure 4.21 Photograph the recycling apparatus of [Emim][OAc] by rotary evaporation

Figure 4.22 shows the FTIR spectra of pure IL after drying and before dissolution (**1**) and the recovered IL after dissolution (**2**).

From Figure 4.22, it can be seen that FTIR spectrum of the recovered IL (spectrum **2**) is in good agreement with the dried IL before dissolution (reference FTIR spectra **1**), with the only difference being an increase in the OH absorption at ~2900 cm^{-1}, which reflects both the use of water in the process chemistry and the hygroscopic nature of the IL.

Generally the hydrogen bonding will greatly increase the intensity of the band and move to lower frequencies and if the hydrogen bonding is especially strong, the band becomes quite broad.

The recovered IL contains water, the drying method needs to be done over longer periods of time, maybe for 24 hours instead of 12 hours. The drying should perhaps be done under a glove box, to avoid absorption of water from the environment.

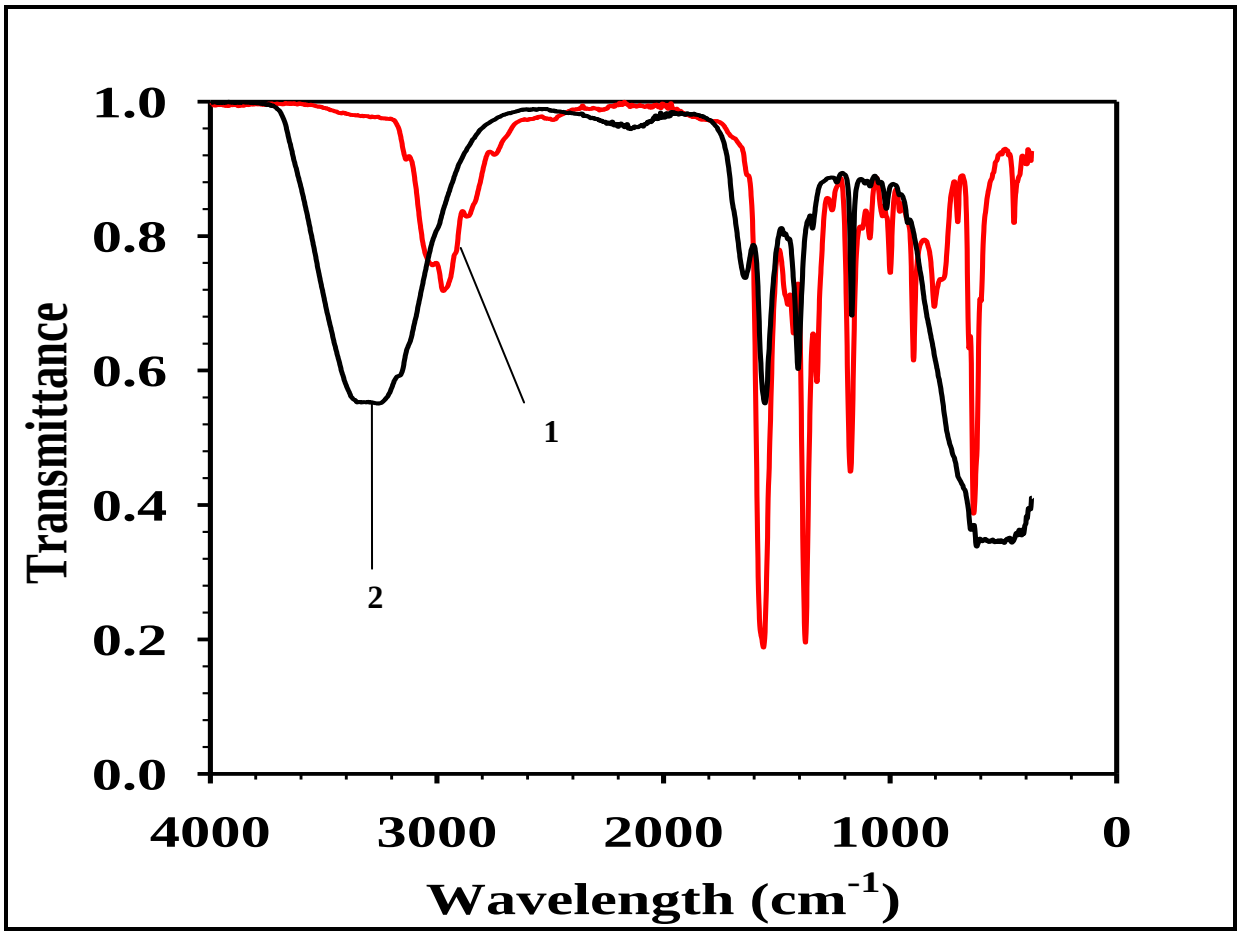

Figure 4.22 FTIR spectra of pure [Emim][OAc] after drying (**1**) with the recovered [Emim][OAc] after dissolution of pulp (**2**)

4.4NUCLEAR MAGNETIC RESONANCE SPECTROSCOPY (NMR) OF THE REGENERATED CELLULOSE

4.4.1 NMR of the regenerated cellulose of unbleached and bleached dissolving pulp samples previously dissolved in [Emim][OAc]/DMSO or DMF

Figure 4.23 illustrates the ^{13}C NMR spectra of untreated unbleached dissolving pulp, while Figure 4.24 shows the ^{13}C NMR spectra of untreated bleached dissolving pulp.

It can be seen in Figure 4.23 and 4.24 there is no difference between the ^{13}C NMR spectra of untreated bleached dissolving pulp and unbleached dissolving pulp. All the noticeable signals in the untreated unbleached dissolving pulp and untreated bleached dissolving pulp spectrums are distributed in the region between 60-110 ppm for the carbon atoms of the cellulose. The signals at 106 ppm ($C\text{-}_1$), 89 ppm ($C\text{-}_4$ of crystalline cellulose), 84 ppm ($C\text{-}_4$ of amorphous cellulose), 75 ppm ($C\text{-}_2$, $C\text{-}_3$ and $C\text{-}_5$), 66 ppm ($C\text{-}_6$ of crystalline cellulose) and 63 ppm ($C\text{-}_6$ of amorphous cellulose) have all been reported before in literature (Lan *et.al.* 2011:675). The signal at 86–92 ppm corresponds to C4 of the highly ordered cellulose of the crystallite interiors, whereas the broader upfield signal (79–86 ppm) has been assigned to the C4 of disordered cellulose as well as to the less ordered cellulose chains of the crystallite surfaces.

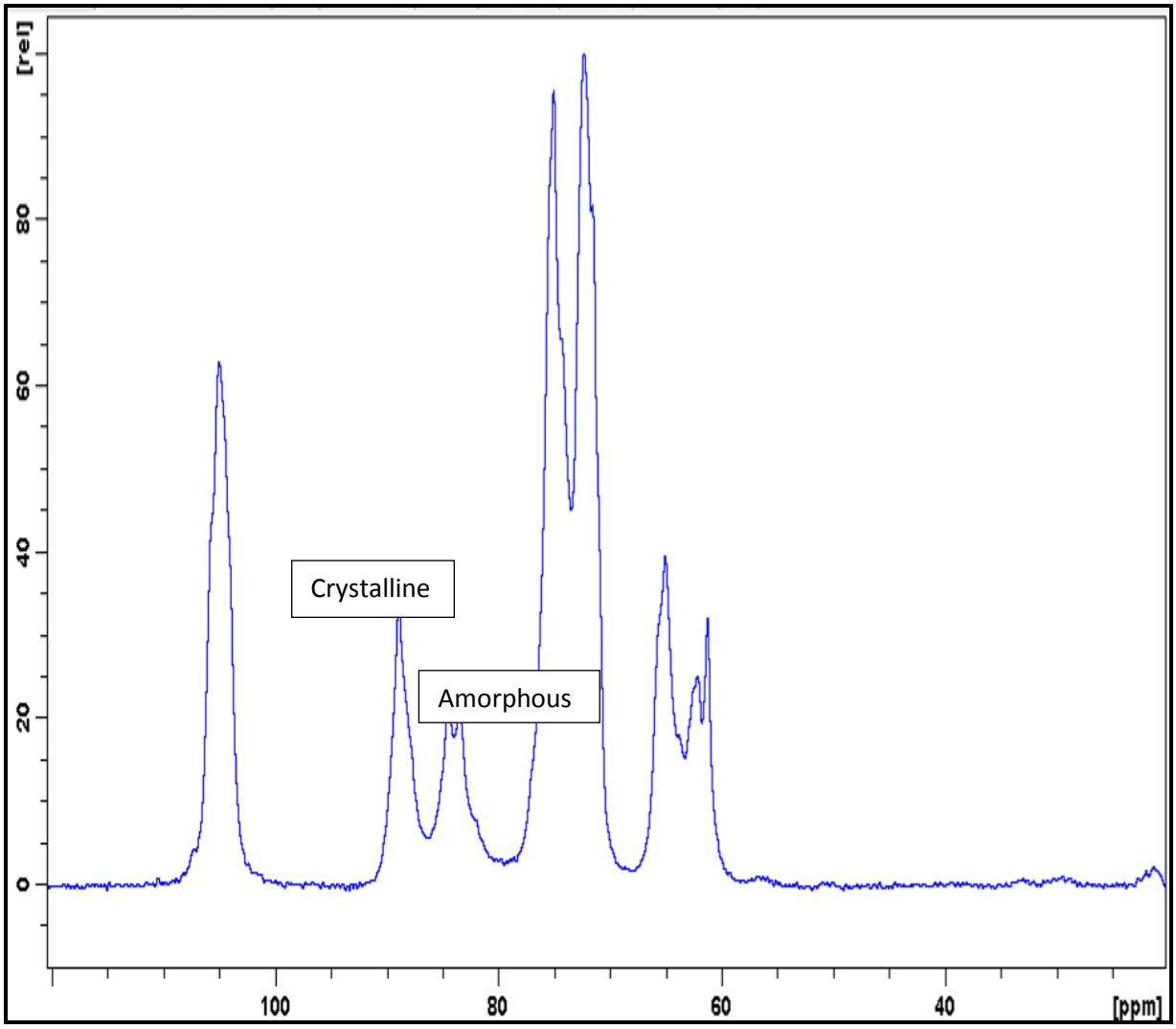

Figure 4.23 ^{13}C NMR spectra of untreated unbleached dissolving pulp

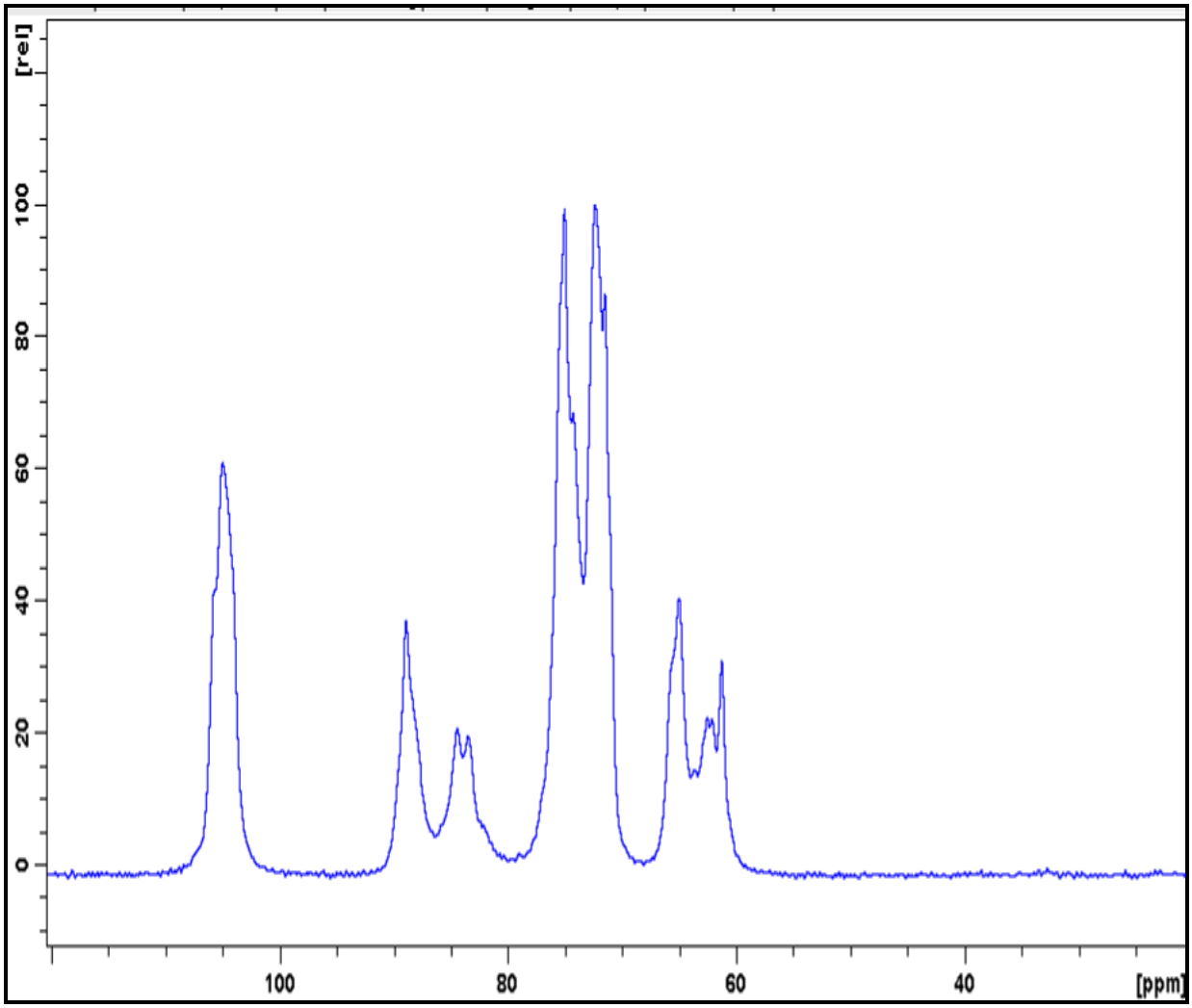

Figure 4.24 ^{13}C NMR spectra of untreated bleached dissolving pulp

Figure 4.25-4.26 illustrates the ^{1}H NMR spectra of cellulose regenerated from unbleached pulp previously dissolved in [Emim][OAc]/DMSO (spectrum **A**) and [Emim][OAc]/DMF (spectrum **B**) and cellulose regenerated from bleached pulp previously dissolved in [Emim][OAc]/DMSO (spectrum **A**) and [Emim][OAc]/DMF (spectrum **B**) while Figure 4.27 shows the ^{1}H NMR spectra of pure DMSO taken from literature.

To simplify the analysis of chemical shift changes (Δδ), H6 is then defined to have a fixed chemical shift. The choice of H6 as a reference point follows previous studies in which this spectral band was found not to be dependent on temperature and concentration of solute (Zhang 2010:1941).

The regenerated cellulose in Figure 4.25-4.26 shows a signal at 2.5 ppm corresponding to the signal of the DMSO solvent (see Figure 4.27). DMSO signals are of very low intensity,

which means that these co-solvents have almost completely evaporated upon heating during the dissolution process.

There is no difference between the ^{1}H-NMR spectrum of cellulose regenerated from unbleached dissolving pulp previously dissolved in [Emim][OAc]/DMSO and bleached pulp previously dissolved in [Emim][OAc]/DMSO.

This study has shown that [Emim][OAc]/DMSO or DMF can be used as a non-derivatizing solvent for cellulose. The OAc anion is a strong hydrogen bond acceptor which makes it more effective for the dissolution process.

One advantage of ^{1}H NMR is that the ^{1}H nucleus is the most abundant among the nuclei that can be detected by NMR, thus giving a high signal to noise (S/N) ratio in a short experimental time (typically within several minutes). The drawback of ^{1}H NMR is that it usually suffers from severe signal overlaps due to its short chemical ranges (i.e. 12-0 ppm) (Pu *et.al.* 2013:372).

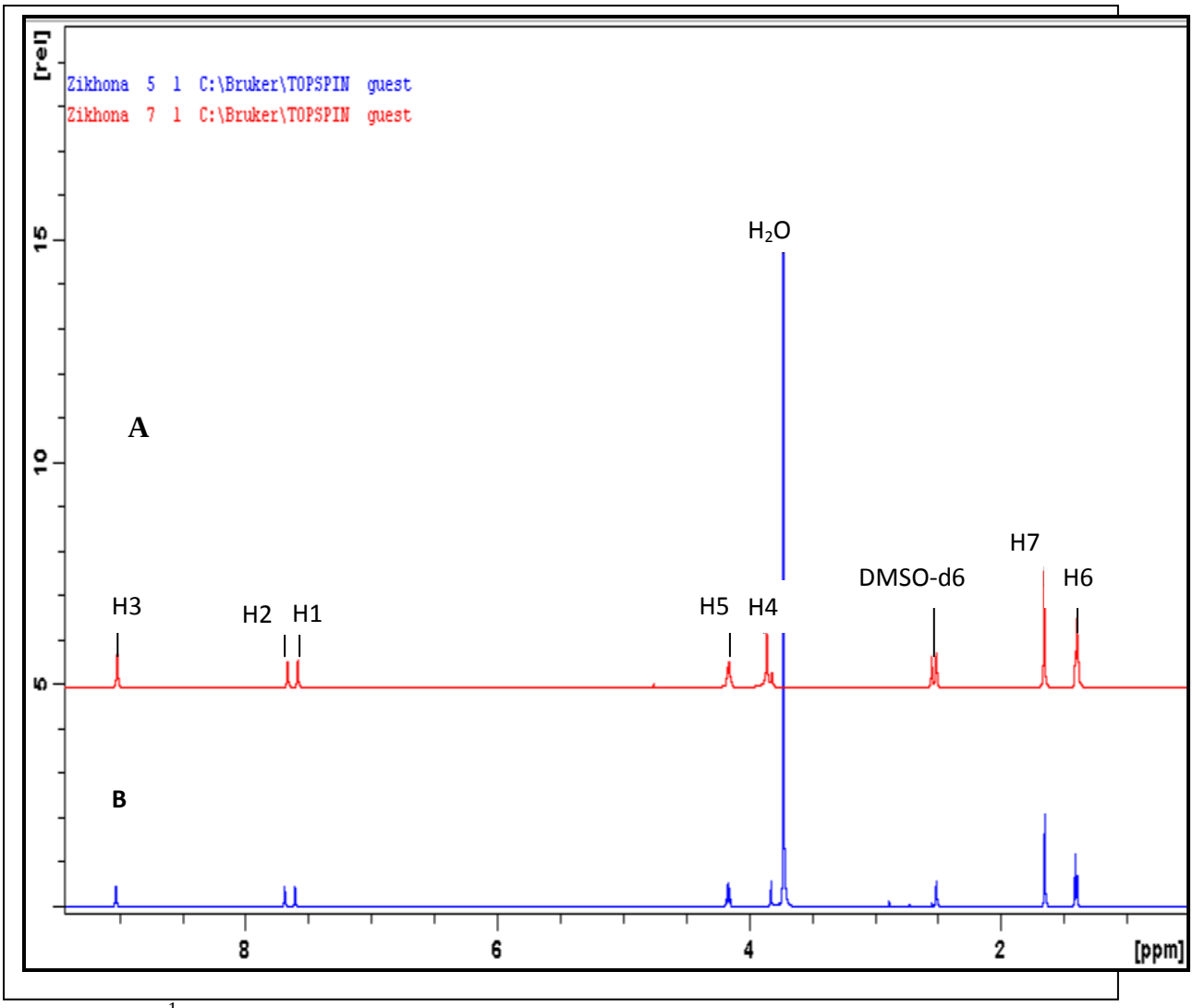

Figure 4.25 ^{1}H NMR spectra of cellulose regenerated from unbleached pulp previously dissolved in [Emim][OAc]/DMSO (spectrum **A**) and [Emim][OAc]/DMF (spectrum **B**)

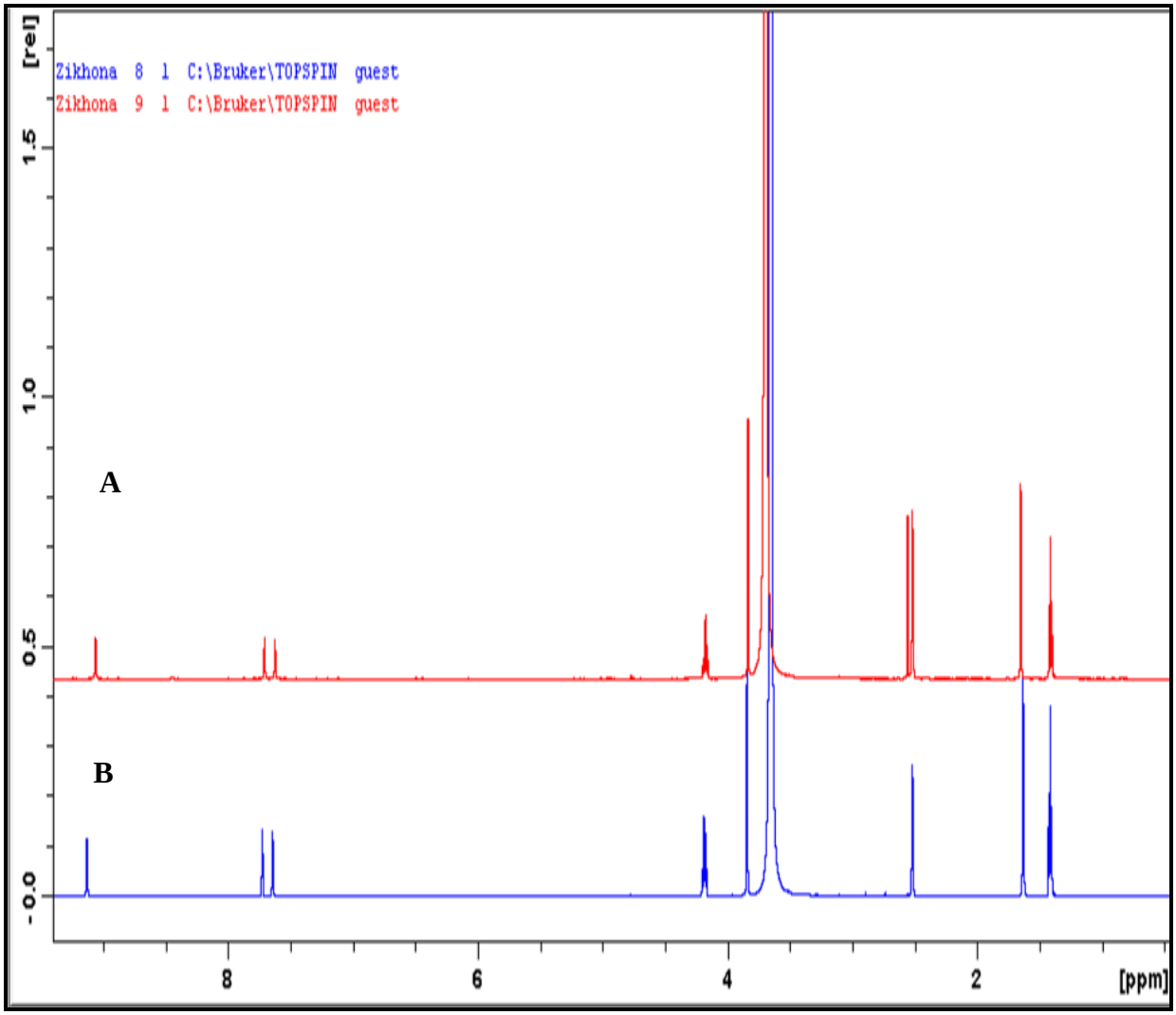

Figure 4.26 ^{1}H NMR spectra of cellulose regenerated from bleached pulp previously dissolved in [Emim][OAc]/ DMSO (spectrum **A**) and [Emim][OAc]/DMF (spectrum **B**)

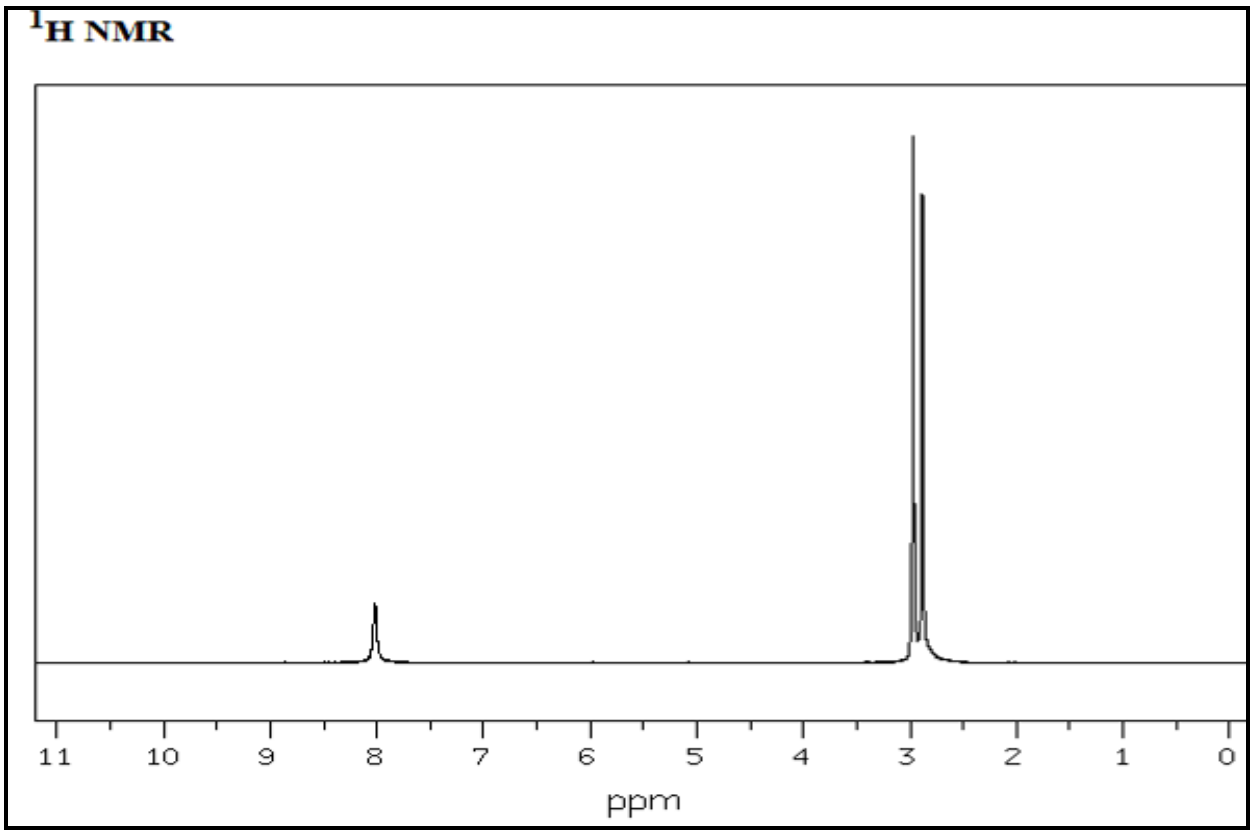

Figure 4.27 ^{1}H NMR spectra of pure DMSO

^{1}H- NMR chemical shifts of the cellulose regenerated from the mixture of unbleached dissolving pulp with [Emim][OAc]/DMSO or DMF and bleached dissolving pulp with [Emim][OAc]/DMSO or DMF were determined by ^{1}H NMR.

The regenerated cellulose/DMSO-d_6 mixtures were too viscous for ^{1}H NMR measurements at room temperatures; consequently the temperature of 70 ˚C was selected. All samples were diluted with DMSO-d_6.

In Table 4.9, the influence of co-solvents on the chemical shifts of hydrogen atoms in [Emim][OAc] are numbered according to Figure 4.28, taken from literature (Kuzmina 2012:31).

Table 4.9 ^{1}H- NMR chemical shifts of [Emim][OAc] in the presence of DMSO and DMF in DMSO-d_6

[Emim][OAc]	1	2	3	4	5	6	7	8	9
DMSO	7.68	7.77	9.27	3.80	4.19	1.40	-	-	1.58
DMF	7.68	7.77	9.30	3.80	4.19	1.40	-	-	1.58

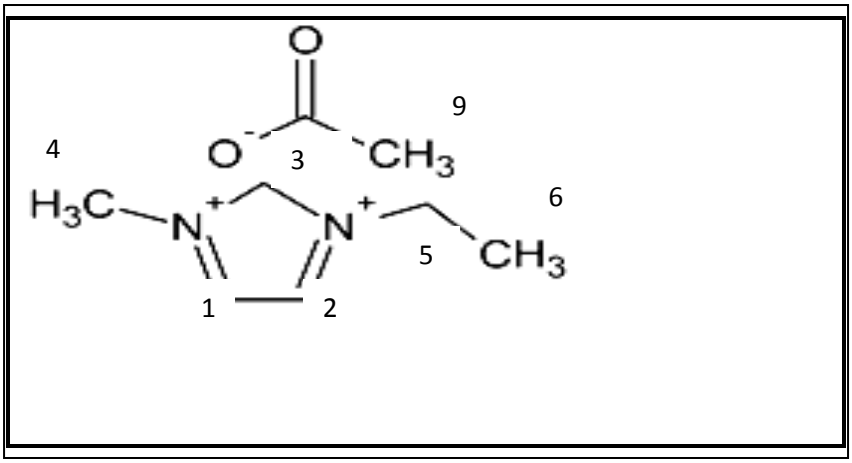

Figure 4.28 Structure of [Emim][OAc], showing the numbering of hydrogen atoms as reproduced from Kuzmina (2012:31)

Liquid-state ^{1}H NMR, has shown that imidazolium-based proton resonances H1-H3 significantly shift depending on the type of organic solvent used for the dilution (Hesse-Ertelt *et.al.* 2010:78). ^{1}H NMR chemical shift values (given in Table 4.9), the proton resonance H3 exhibited minor shifting, while the remaining proton resonances (H1-H9) were not shifted. The displacement strongly depended both, on the co- solvent and on the IL, which might be due to strong interactions of the imidazolium ring protons with the solvent during the dissolution process (Hesse-Ertelt *et.al.* 2010:78).

4.4.2 NMR spectra of cellulose regenerated from sawdust wood samples previously dissolved in [Emim][OAc]/DMSO or DMF mixtures

Figure 4.29 represents the ^{13}C NMR spectra of untreated sawdust wood. In the spectrum, most of the noticeable signals are distributed in the region between 60-110 ppm for the carbon atoms of cellulose and hemicelluloses. The signals at: 105.5 ppm corresponds to the $C\text{-}_1$ of cellulose and xylan; 89 ppm corresponds to the $C\text{-}_4$ of crystalline cellulose; 83 ppm corresponds to the $C\text{-}_4$ of amorphous cellulose; 75.5 ppm corresponds to the $C\text{-}_2$, $C\text{-}_3$ & $C\text{-}_5$ of cellulose and $C\text{-}_2$, $C\text{-}_3$ & $C\text{-}_4$ of xylan; 63.4 ppm corresponds to the $C\text{-}_6$ of cellulose which indicated that the crystalline structure of sawdust wood is typical of cellulose I (Horri *et.al.* 1987:2119;Pang *et.al.* 2013:1278) and $C\text{-}_5$ of xylan, and all these signals have been reported in literature (Yue *et.al.* 2012:2204).

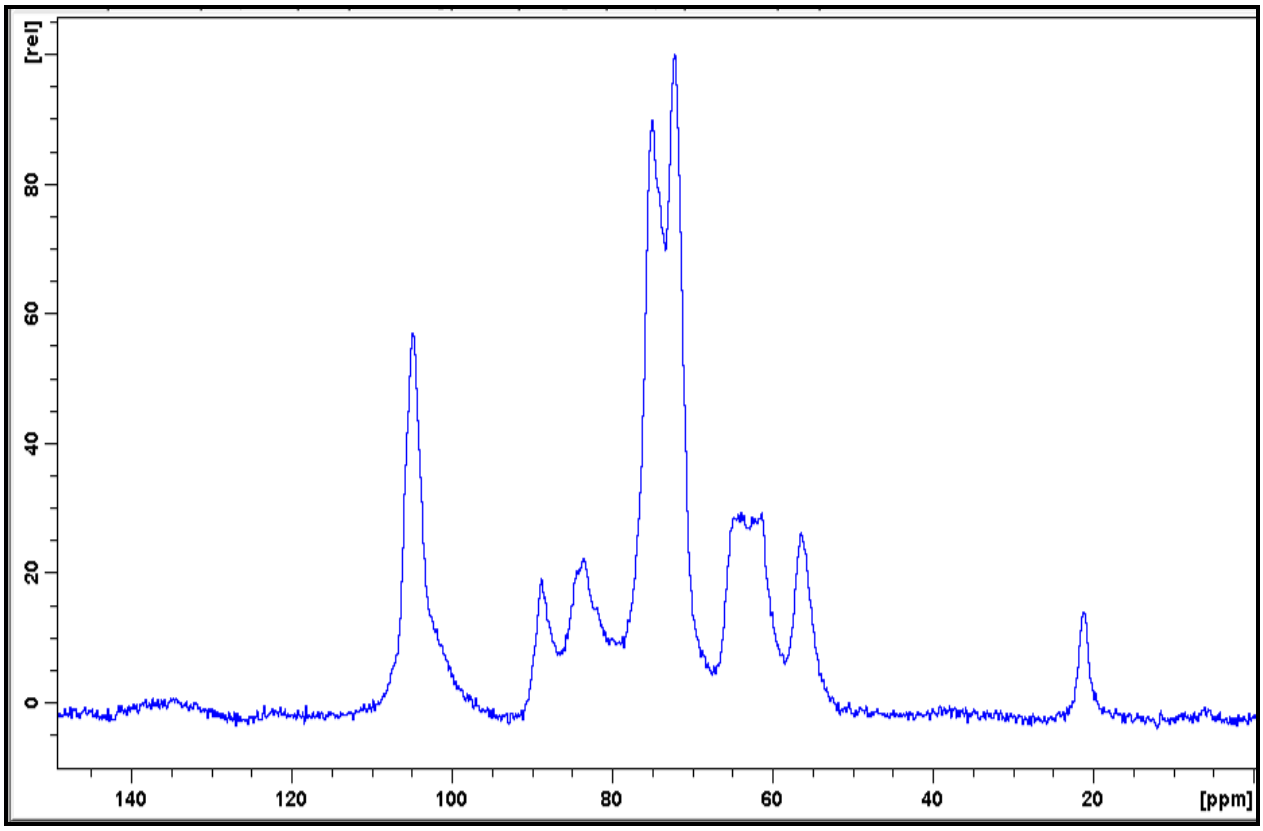

Figure 4.29 ^{13}C NMR spectra of untreated sawdust wood

Figure 4.30 shows the ^{1}H NMR spectra of cellulose regenerated from sawdust wood previously dissolved in [Emim][OAc]/DMSO (spectrum **A**) and [Emim][OAc]/DMF (spectrum **B**), which exhibits sufficient resolution to clearly identify the distinct proton signals of hydroxyls ranging from 9 ppm- 0.5 ppm.

The assignment of the peaks has been done according to the literature (Zhang *et. al.* 2010:1942).

The peaks ranging from H = 2.5 ppm - 5.5 ppm belongs to the cellulose components. The anomeric C-H correlation for 1,4-beta-D-glucosyl residues which is mostly due to cellulose and it appears at H = 4.3 ppm. Other correlation at H = 3.85 ppm is assigned to H4 and H5 in 1,4-beta-D-glucosly residues (Chen *et.al.* 2012:3484).

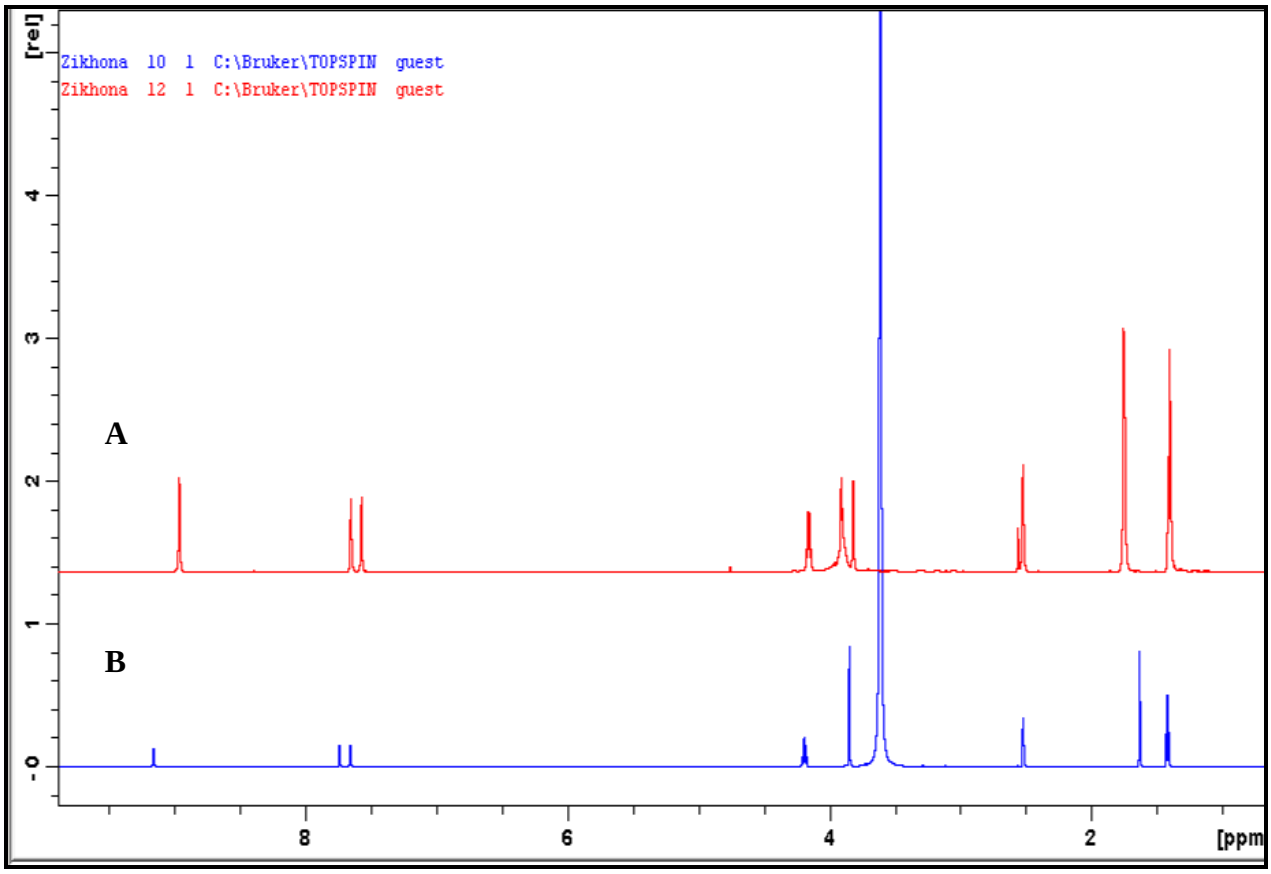

Figure 4.30 ^{1}H NMR spectra of cellulose regenerated from sawdust wood previously dissolved in [Emim][OAc]/DMSO (spectrum **A**) and [Emim][OAc]/DMF (spectrum **B**)

4.4.3 ^{1}H NMR of recovered [Emim][OAc]

In order to check for the purity of the ionic liquid [Emim][OAc], the ^{1}H NMR spectra of the fresh [Emim][OAc] and recycled [Emim][OAc] was shown in Figure 4.31 and Figure 4.32, respectively.

The recovered IL was too viscous for ^{1}H NMR measurements, so DMSO-d_6 was used to dilute the sample.

^{1}H NMR spectra in Figure 4.32 indicates that the IL recovered was relatively pure. No extra peaks were noted; therefore, it confirmed the recycling process as well as thermal stability of IL during dissolution and regenerated process. Similar results were reported in literature (Sun 2010:81).

The results reported for the NMR of recovered [Emim][OAc] complements the results of the FTIR specta of recovered [Emim][OAc].

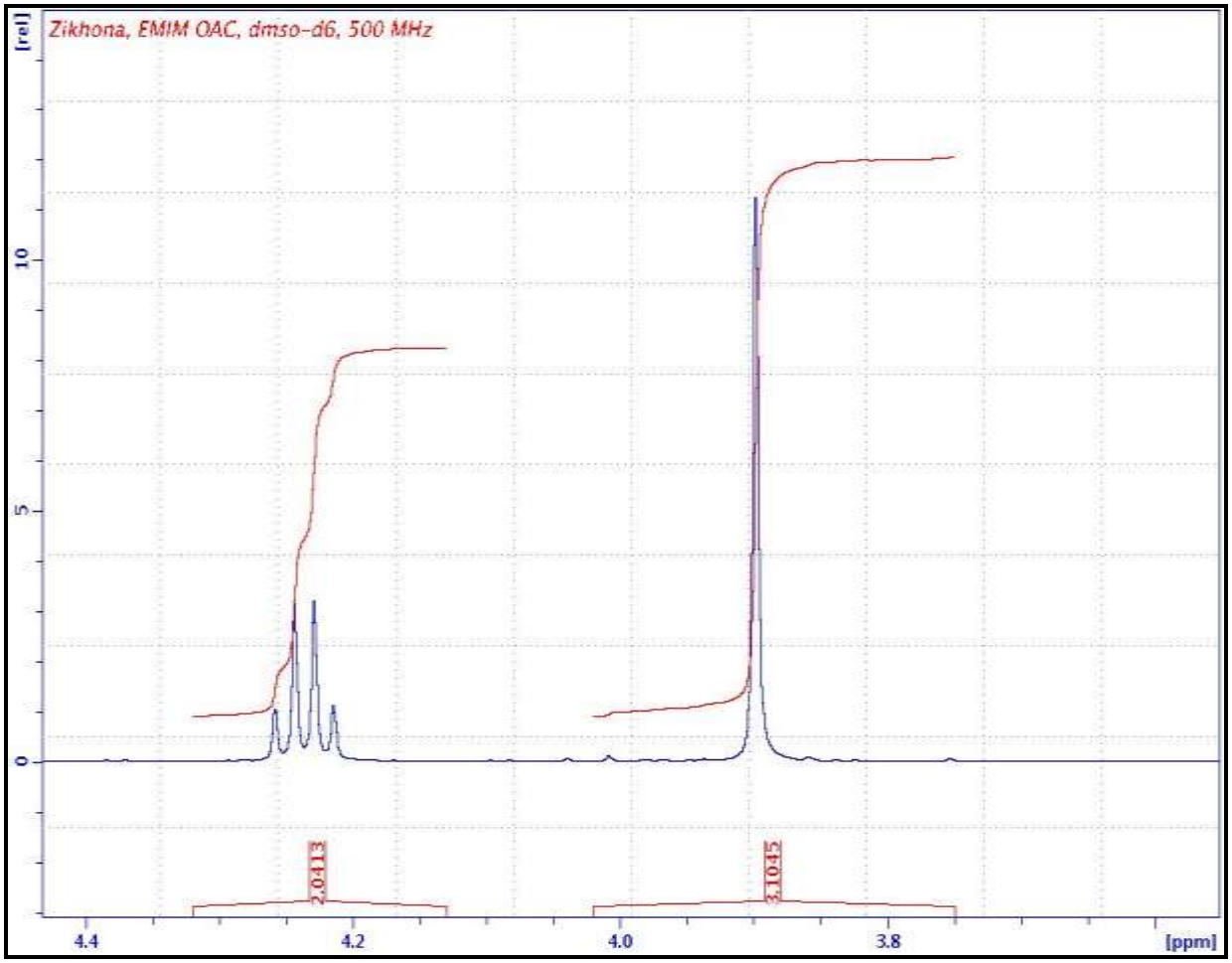

Figure 4.31 ^{1}H NMR spectra of [Emim][OAc] before dissolution

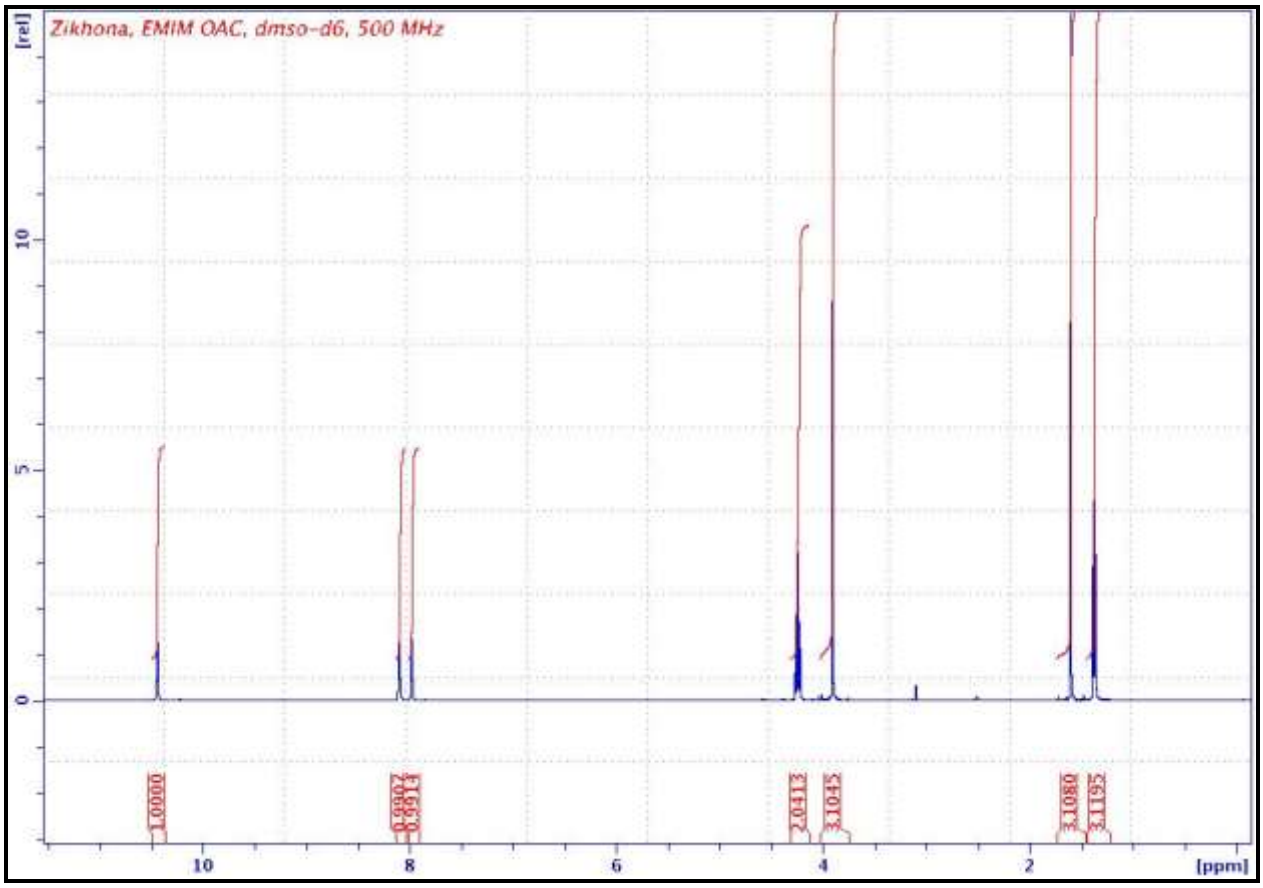

Figure 4.32 ^{1}H NMR spectra of recovered [Emim][OAc]

4.5 POWDER X-RAY DIFFRACTION (P'XRD) OF THE REGENERATED CELLULOSE

XRD measurements can provide information about the crystalline structure of cellulose components in lignocellulose. This information is important to estimate the relative amount of crystalline material present in the sample. A number of different methods exist to calculate the crystallinity index (CrI) from XRD data, and the results can vary depending on the applied method (Pinkert *et.al.* 2011:3133).

In this study, the degree of crystallinity was calculated according to the peak height method, which is the most popular and useful method to compare relative differences in the CrI of cellulose (Pinkert *et.al.* 2011:3133).

4.5.1 P'XRD of cellulose regenerated from unbleached and bleached dissolving pulp samples previously dissolved in [Emim][OAc]/DMSO or DMF mixtures

P'XRD analysis was conducted to further examine the crystallinity of the regenerated cellulose. The X-ray diffraction pattern of the MCC (native form) was taken from literature (Chen *et.al.* 2012:4) is shown in Figure 4.33 and it shows a principal peak at (002) lattice diffraction at 2θ = 22.8° for cellulose I and 2θ = 16° for cellulose II.

The crystallinity index (CrI) gives a quantitative measure of the crystallinity in powders, and can relate to the strength and stiffness of fibres (Azubuike *et.al.* 2012:3).

CrI of MCC and regenerated cellulose was calculated by using equation 2, proposed by Segal et.al (1959:10):

$$\mathbf{CrI = I_{TOT}\text{-}I_{am} / I_{TOT} \times 100\ \%} \qquad (2)$$

Where I_{TOT} is the maximum intensity of the principal peak (002) lattice diffraction at (2θ = 22.7° for cellulose I and 2θ = 21.7° for cellulose II) and I_{AM} is the intensity diffraction attributed to the amorphous cellulose at 2θ = 18° for cellulose I and 2θ = 16° for cellulose II (Azubuike *et.al.* 2012:3).

The diffraction curve of MCC (Figure 4.33 diffractogram A) is of a typical cellulose I structure as indicated by the strong crystalline peaks at 2θ = 15°, 17°and 23° corresponding to

the (110), (100), and (002) crystal planes and a weak crystalline peak at 35° corresponding to the (004) plane (Cheng *et.al.* 2012:4; Lan *et.al.* 2011:672; Zhao *et.al.* 2012:1492).

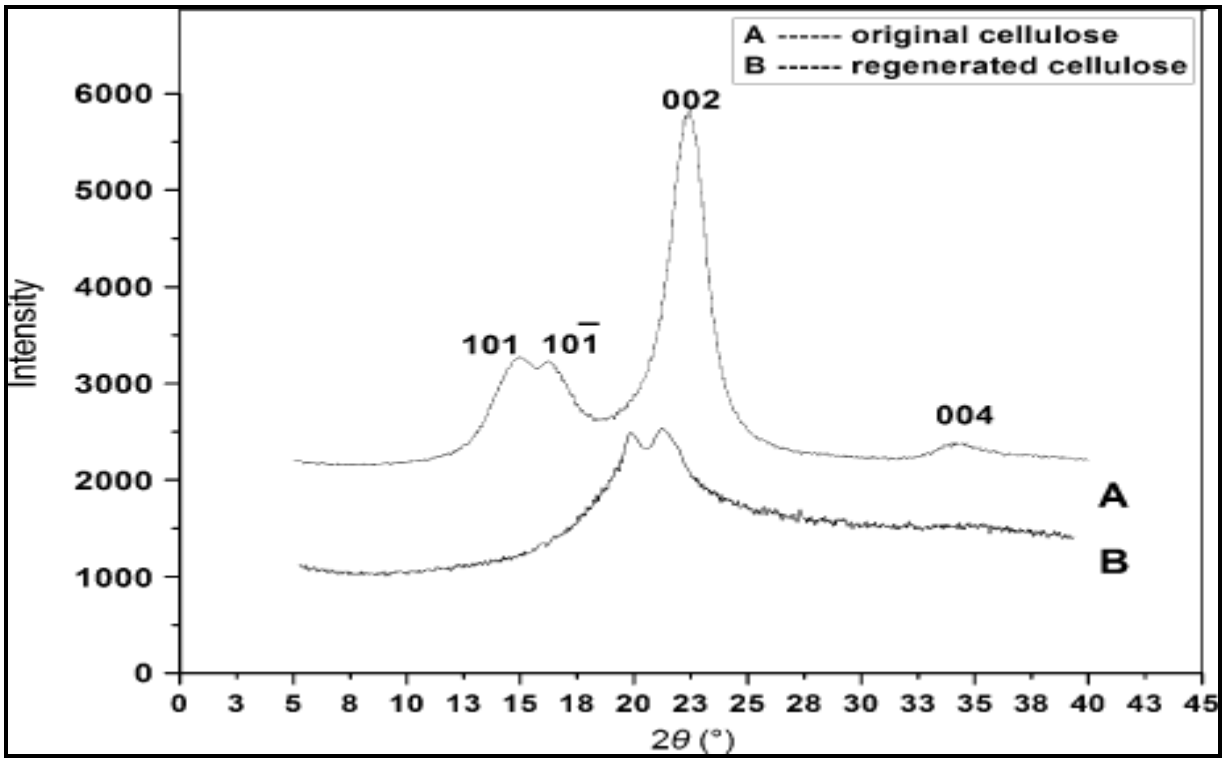

Figure 4.33 P'XRD diffractogram patterns of A) MCC standard of cellulose and B) regenerated cellulose as reproduced from Chen *et.al.* (2012:4)

Figure 4.34 illustrates the angle of X-ray diffractograms of MCC standard of cellulose (diffractogram **A**) and regenerated cellulose fibres from unbleached dissolving pulp that was dissolved in [Emim][OAc]/DMSO (diffractogram **B**) and [Emim][OAc]/ DMF mixture (diffractogram **C**), while Figure 4.35 shows the X-ray diffractograms of MCC standard native cellulose (diffractogram **A**) and regenerated cellulose fibres from bleached dissolving pulp that was dissolved in [Emim][OAc]/DMSO (diffractogram **B**) and [Emim][OAc]/DMF mixture (diffracttogram **C**).

After dissolution and regeneration, the diffraction curves of regenerated cellulose samples shown in Figures 4.34-4.35, are of typical diffraction patterns of cellulose II.

There is a presence of the broad crystalline peaks at around 12° and 21° as also found by Cheng *et.al.* (2012:4) and Zhang *et.al.* (2005:8276) and the first two peaks in all the diffractograms are well resolved and have a sharp intensive appearance for all the diffractograms, presumably due to larger crystallites formed during the dissolution process as also reported by Liu *et.al.* (2011:222) indicating the transformation of cellulose I to cellulose II as a result of the regeneration as also reported by Li *et.al.* (2012:941).
Moreover, compared to the MCC (cellulose I), the intensity of the diffraction patterns of the regenerated cellulose decreased drastically, which implies a decrease in crystallinity after dissolution and regeneration from [Emim][OAc]/DMSO or DMF mixtures, i.e., the crystallinity of the regenerated cellulose was lower than the original cellulose. The decrease in the intensity of the diffraction peaks implies the transformation of cellulose I to cellulose II after dissolution and regeneration. This happens because of the IL, which rapidly broke intermolecular and intra hydrogen bonds in the cellulose crystal structure thereby destroying the original crystalline forms.

Similar results have been reported by Luo *et.al.* (2005:233); Ding *et.al.* (2012:15); Mäki-Arvela *et.al.* (2010:175); Sun *et.al.* (2009:646) and Zhang *et.al.* (2005:8272) where they reported a decrease in the X-ray peak intensity and the shift of the peak position to the left when cellulose I transformed to cellulose II after dissolution in [Emim][OAc].
Dadi *et.al.* (2006:908); and Kilpeläinen *et.al.* (2007:9146) reported that the degree of crystallinity and thermal stability decreased in ILs, and cellulose I was irreversibly changed to cellulose II (Feng & Cheng *et.al.* 2008:3).

CrI of MCC in Figure 4.34 was calculated from the height ratio between the intensity of the crystalline peak ($I_{TOT} - I_{AM}$) and total intensity (I_{TOT}) using equation 2 and the CrI values for the MCC, regenerated cellulose from unbleached pulp samples previously dissolved in [Emim][OAc]/DMSO or DMF mixtures as well as regenerated cellulose from bleached pulp samples previously dissolved in [Emim][OAc]/DMSO or DMF mixtures are shown in Table 4.10.

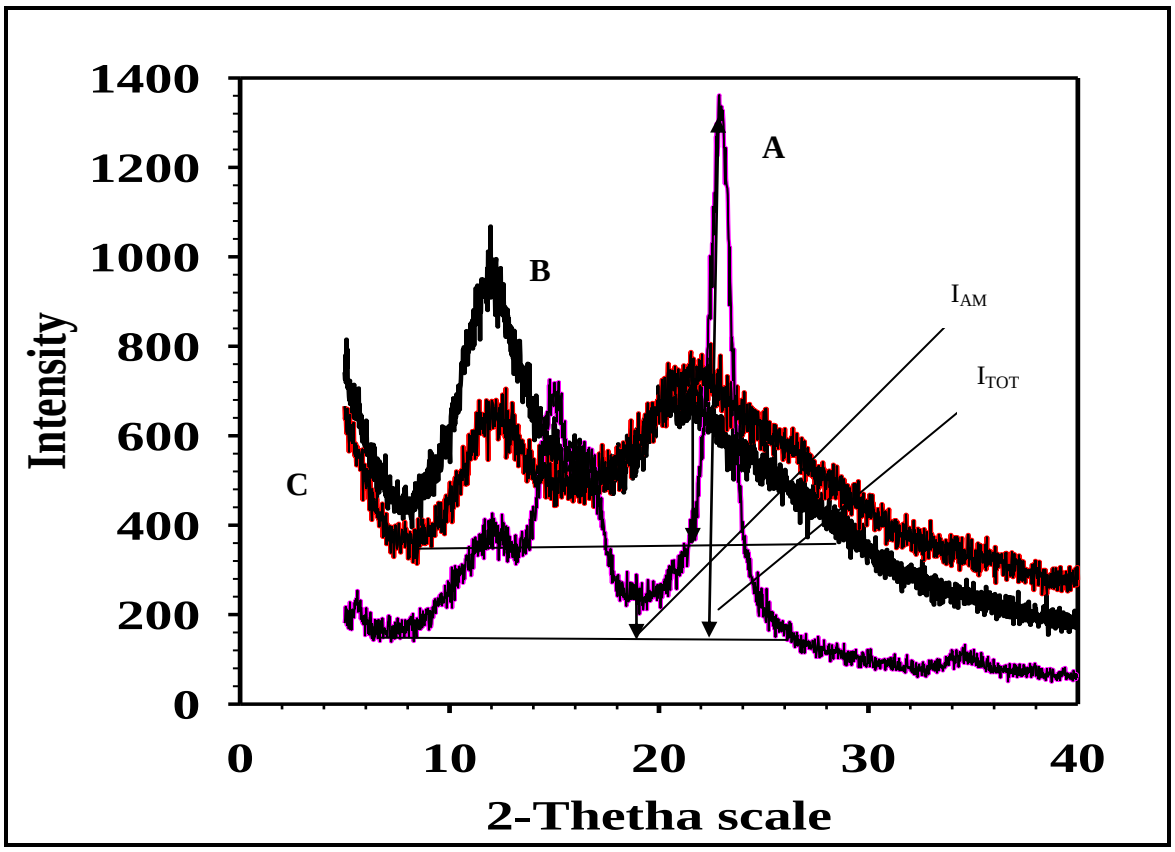

Figure 4.34 P'XRD diffractograms of cellulose regenerated from unbleached dissolving pulp previously dissolved in [Emim][OAc]/DMSO and DMF mixtures compared to MCC standard of cellulose

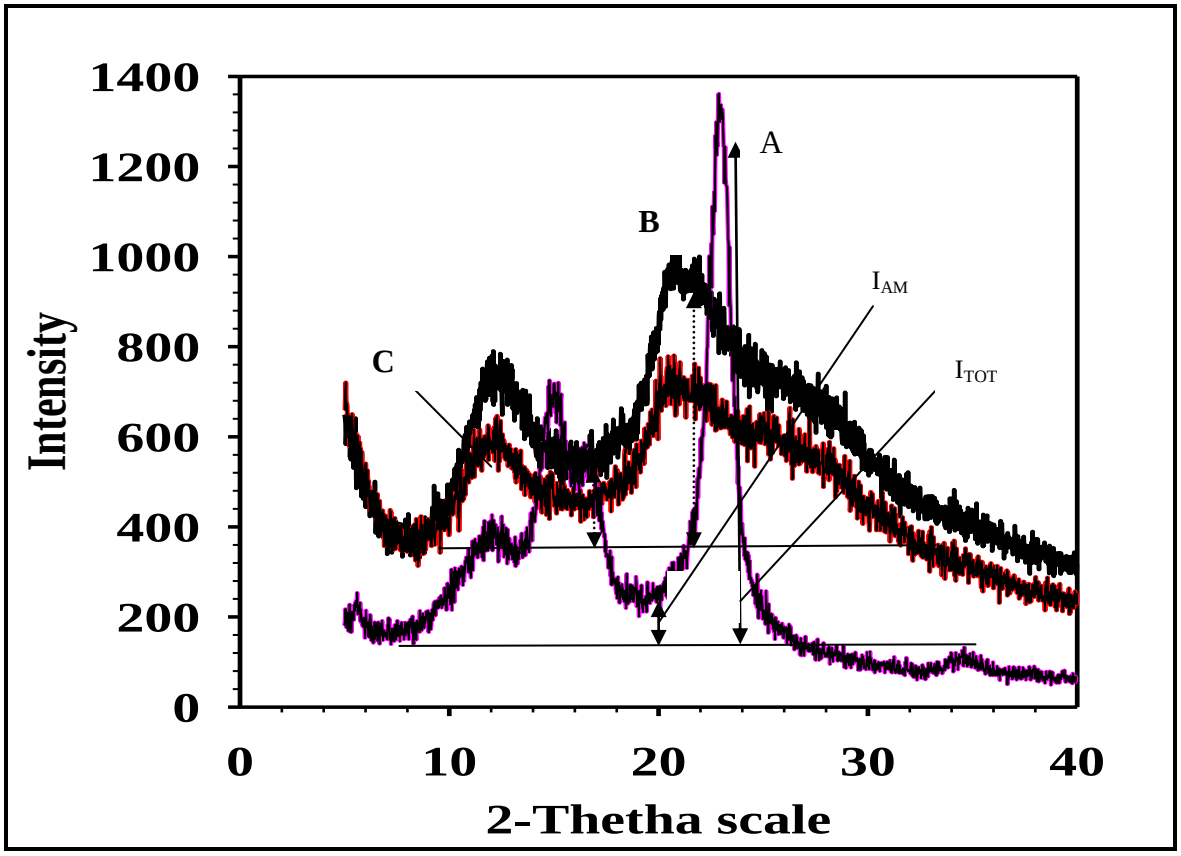

Figure 4.35 P'XRD diffractograms of cellulose regenerated from bleached dissolving pulp previously dissolved in [Emim][OAc]/DMSO and DMF mixtures compared to MCC standard of cellulose

Table 4.10 Calculated crystallinity index values of MCC and regenerated cellulose samples

Sample	Crystallinity index (%)
MCC	90.4
Cellulose regenerated from unbleached pulp in [Emim][OAc]/ DMSO	42.0
Cellulose regenerated from unbleached pulp in [Emim][OAc]/ DMF	54.0
Cellulose regenerated from bleached pulp in [Emim][OAc]/ DMSO	47.2
Cellulose regenerated from bleached pulp in [Emim][OAc]/ DMF	36.4

From the CI results presented in Table 4.10, it can be seen that MCC had the highest crystallinity index of 90.4 % as compared to the regenerated cellulose samples, which then confirms the presence of the strong crystalline peak at $2\theta = 23°$. There is a controversy as to which baseline should be used for the measurement of the intensity values in equation 2, of which this was also found to be a challenge in literature as well (Karatoz 2011: 69).

The straight baseline used in this study was drawn by hand. This approach may lead to overestimation of crystallinity (since there is no account for background scattering). However, this overestimation will be of similar magnitude for all the samples and thus should not affect the overall reliability and consistency of the conclusions.

This technique was used for all cellulose crystalline index results shown in this thesis, except where otherwise noted.

4.5.2 P'XRD of cellulose regenerated from sawdust wood samples previously dissolved in [Emim][OAc]/DMSO or DMF mixtures

The X-ray diffraction patterns of MCC standard native cellulose (diffractogram A) and regenerated cellulose fibers from sawdust wood that was dissolved in [Emim][OAc]/ DMSO (diffractogram B) and [Emim][OAc]/ DMF mixture (diffractogram C) are shown in Figure 4.36.

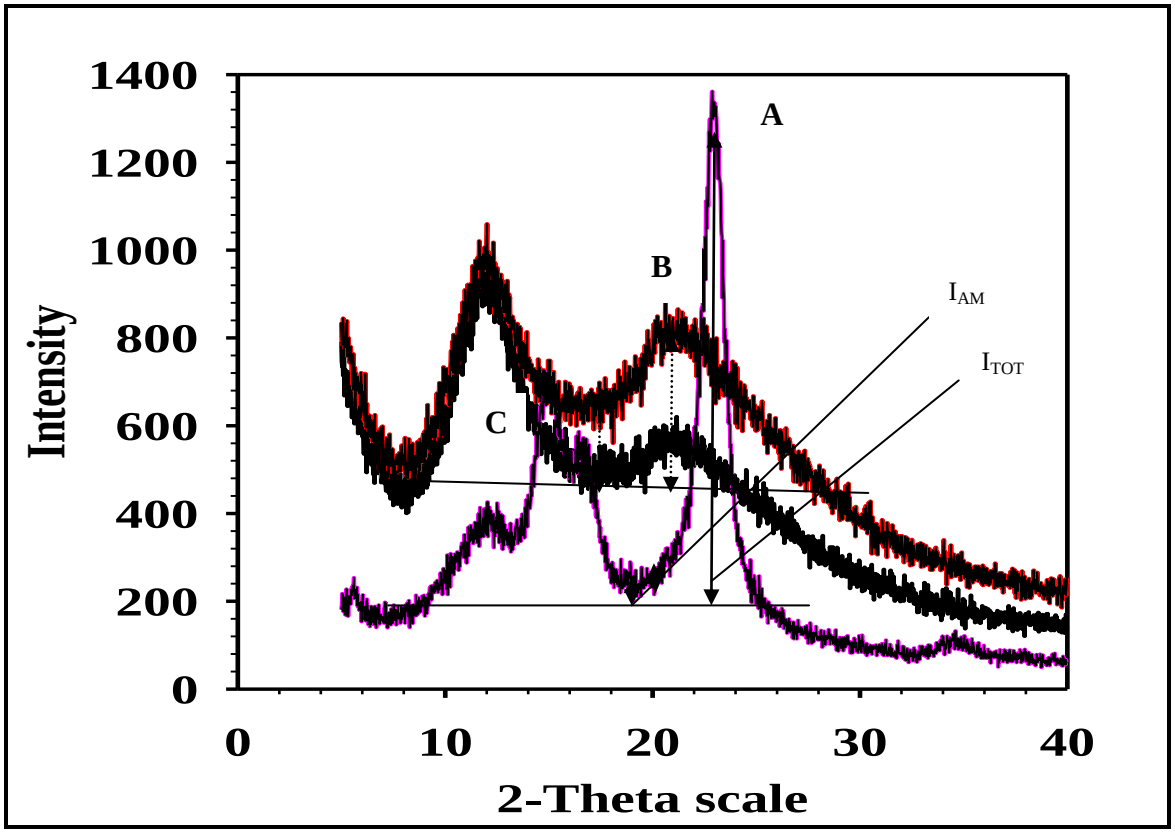

Figure 4.36 P'XRD diffractograms of cellulose regenerated from sawdust wood previously dissolved in [Emim][OAc]/DMSO and DMF mixtures compared to MCC standard of cellulose

The diffraction patterns of MCC as shown in Figure 4.36 showed typical cellulose I structure, with a sharp peak at 22.5° and a wide peak between 12° and 18° (Liu *et.al.* 2011:225; Sun *et.al.* 2009:653) and a weak band peak at 35°. After dissolution and regeneration, the regenerated cellulose samples from sawdust previously dissolved in [Emim][OAc]/DMSO or

DMF mixtures showed typical cellulose II structure with peaks at 12° and 20°, the results illustrates that after the dissolution and regeneration processes, the crystal structure of the sawdust wood was transformed from cellulose I to cellulose II. This also shows that the crystallinity of the regenerated cellulose decreased significantly, which indicated that the [Emim][OAc]/DMF or DMSO mixtures broke the intermolecular hydrogen bonds of the original cellulose during the dissolving process (Liu *et. al.* 2011: 225).

In earlier work, Wei *et.al.* (2007:140) investigated the structural differences between cellulose regenerated from [Bmim][Cl] and untreated cellulose, using FTIR, XRD and TGA. Their data showed that the crystalline form of wood pulp cellulose was transformed completely from cellulose I to cellulose II after regeneration from [Bmim][Cl] solution which was not the case in this study because the cellulose regenerated from the sawdust wood still had some crystallinity.

Results from both FTIR and XRD suggests the dissolving pulp and sawdust wood samples dissolved in [Emim][OAc]/ DMF or DMSO mixture can reduce the cellulose crystallinity in the samples. The X-ray analysis indicated that the MCC is more crystalline than the regenerated cellulosic material. The changes in diffractograms were analysed in order to determine the crystallinity index (CrI) of MCC and regenerated cellulose from sawdust wood previously dissolved in [Emim][OAc]/DMSO or DMF mixtures and the values are reported in Table 4.11.

Table 4.11 Calculated crystallinity index values of MCC and regenerated cellulose samples

Sample	**Crystallinity index (%)**
MCC	90.4
Cellulose regenerated from sawdust wood in [Emim][OAc]/ DMSO	40.0
Cellulose regenerated from sawdust wood in [Emim][OAc]/ DMF	39.3

The values of CI are in the range 39-40 % and are not in agreement with those reported by Andersson *et.al.* (2004:350) who found the crystallinity of wood to be varying from 24 % to 31% for Scots pine wood. The increase of CrI can be attributed to the degradation caused by weathering, which causes the amorphous fractions of wood, consequently, enriches the relative crystalline content, taking into account that less than one third of the wood polysaccharides are crystalline and the remaining wood constituents are hemicelluloses, amorphous and para-crystalline regions of cellulose fibrils.

If the amorphous polysaccharides are degraded more than the crystalline cellulose, the overall crystallinity content is then expected to increase (Lionetto *et.al.* 2012:1914). Compared to the MCC, the crystallinity of the regenerated cellulose was lower than that of MCC (results shown in Table 4.6). These results mean that the inter- and intramolecular hydrogen bonds between cellulose molecule were rapidly broken during the dissolution process, thus destroying the original crystalline form (Pang *et.al.* 2014:4).

For XRD methods, one important factor to consider is the preferred orientation of crystallites (also known as texture). Often the manner in which samples are synthesized, the nature of crystallites and the method of sample preparation for XRD causes the development of texture in the sample. It is well known that this will drastically influence the relative intensities of the diffraction peaks (Park *et.al.* 2010:4).

4.6 SCANNING ELECTRON MICROSCOPY (SEM) OF THE REGENERATED CELLULOSE

4.6.1 SEM images of the regenerated cellulose from unbleached and bleached dissolving pulp samples previously dissolved in [Emim][OAc]/DMSO or DMF

The surface morphologies of the MCC standard and the cellulose samples regenerated from unbleached pulp previously dissolved in [Emim][OAc]/DMSO or DMF mixtures and from bleached pulp previously dissolved [Emim][OAc]/DMSO or DMF mixtures, were observed using a SEM microscope and the images are shown in Figures 4.37-4.41.

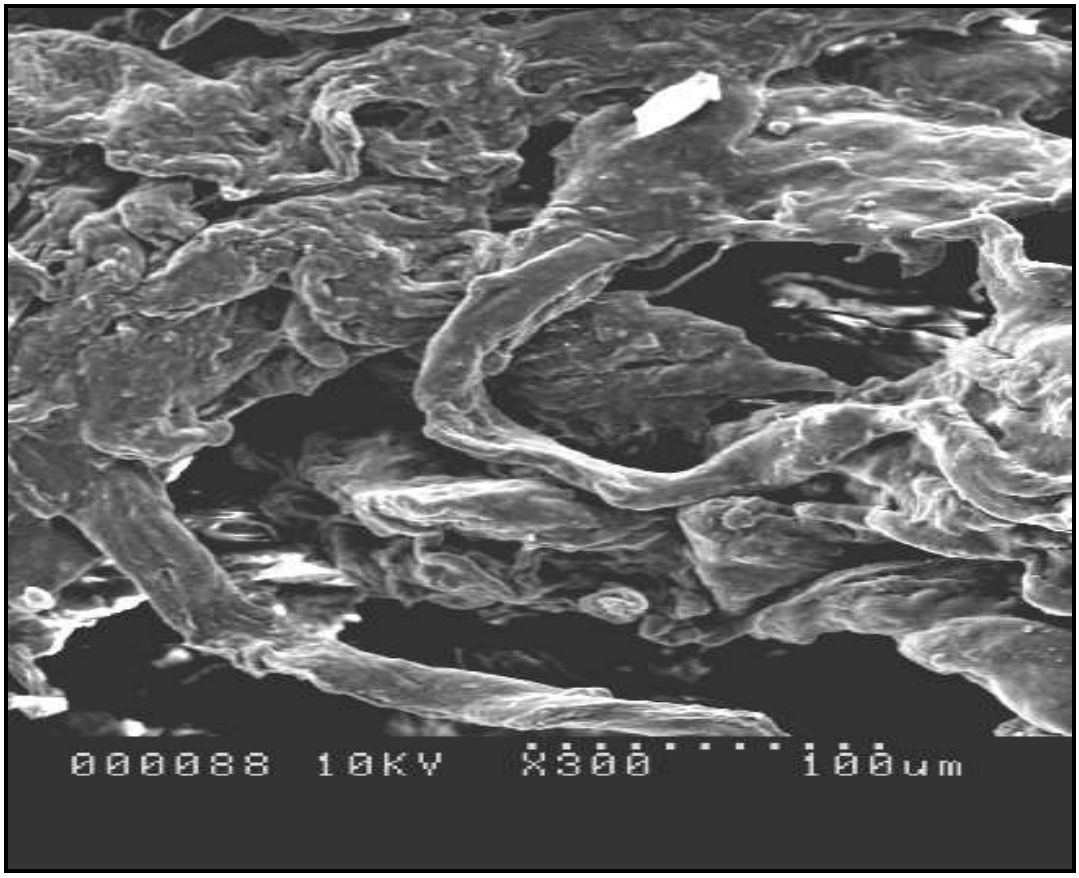

Figure 4.37 SEM photographs of MCC standard of cellulose

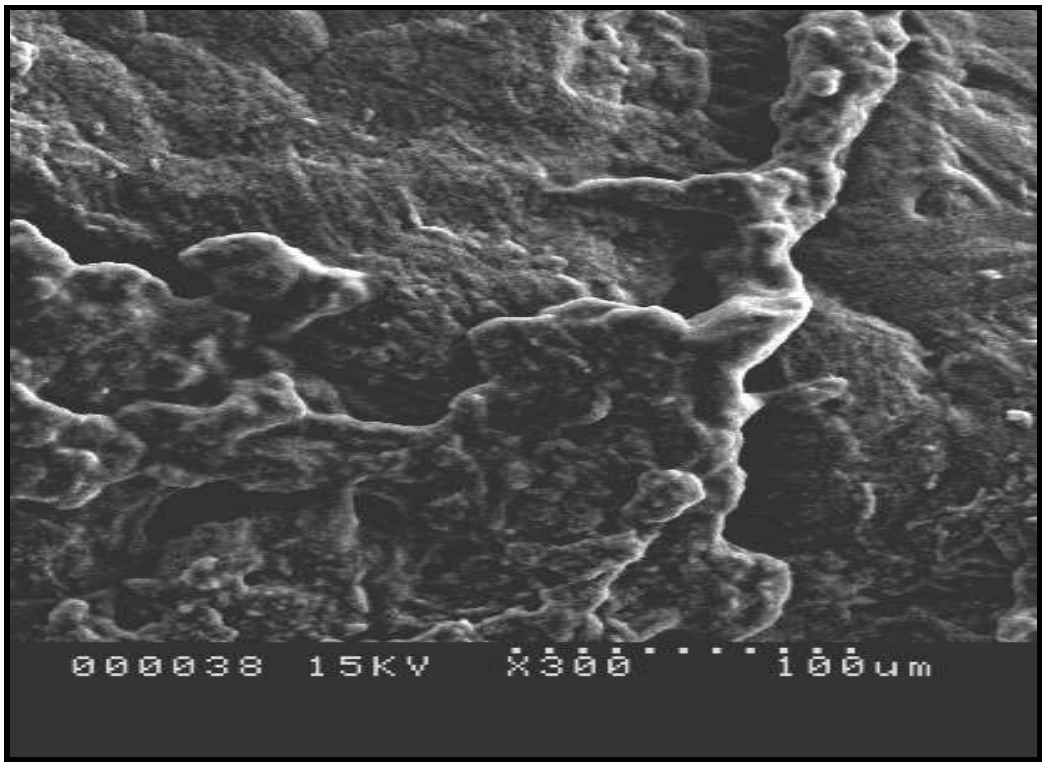

Figure 4.38 SEM photograph of regenerated cellulose from unbleached dissolving pulp in [Emim][OAc]/DMSO mixture

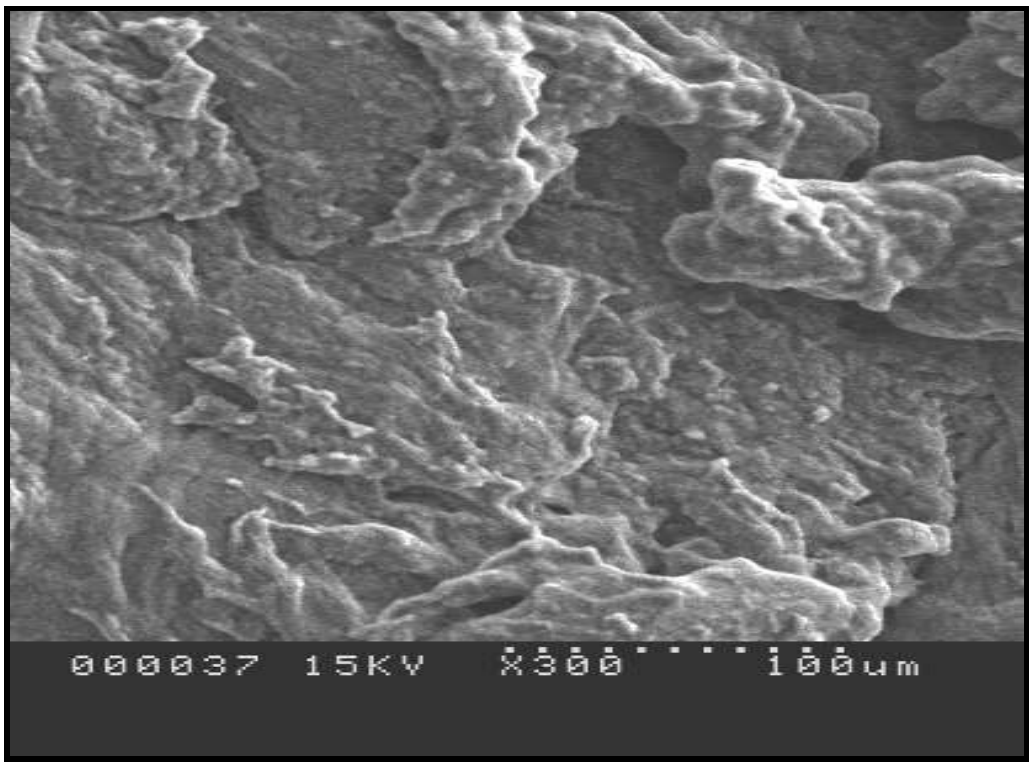

Figure 4.39 SEM photograph of regenerated cellulose from unbleached dissolving pulp in [Emim][OAc]/DMF mixture

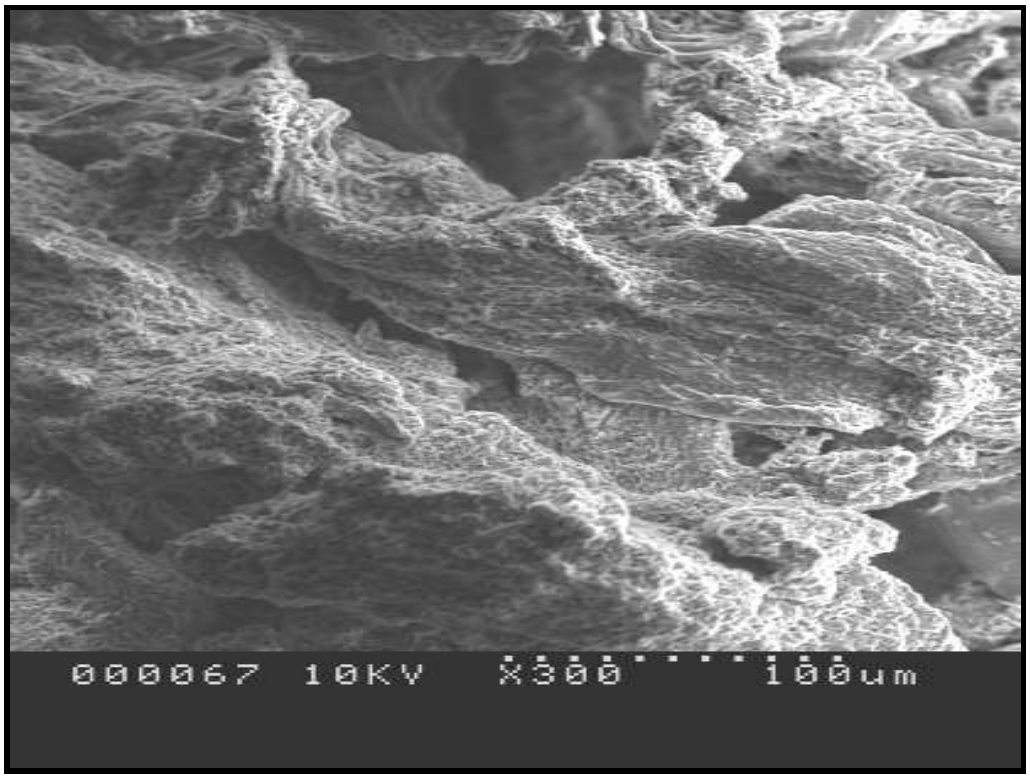

Figure 4.40 SEM photograph of regenerated cellulose from bleached dissolving pulp in [Emim][OAc]/DMSO mixture

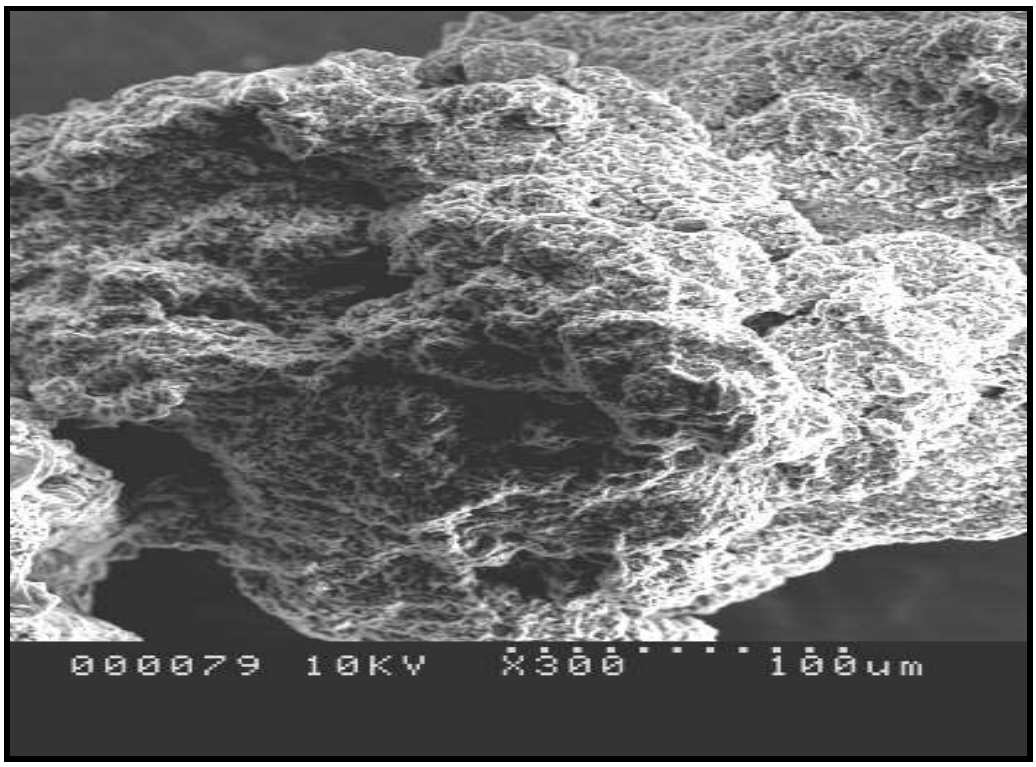

Figure 4.41 SEM photograph of regenerated cellulose from bleached dissolving pulp in [Emim][OAc]/DMF mixture

The SEM image of MCC (Figure 4.37) showed a compact, ordered and rigid fibril structures. After treatment of unbleached and bleached dissolving pulp samples with [Emim][OAc]/DMSO or DMF mixtures, the structure became loose, disordered and curly (shown in Figures 4.30- 4.33), most probably due to the lignin removed during the dissolution process and the decrease of cellulose crystallinity which have already been confirmed by FTIR and pRXD. These results are in agreement with the results reported by Li *et.al.* (2014:941) where they reported that the regenerated cellulose from [Emim][OAc] and water mixture lost its fibrous structure compared to the original dissolving pulp. In both cases, the results clearly indicate that the morphology of the fibre material was significantly changed after dissolution.

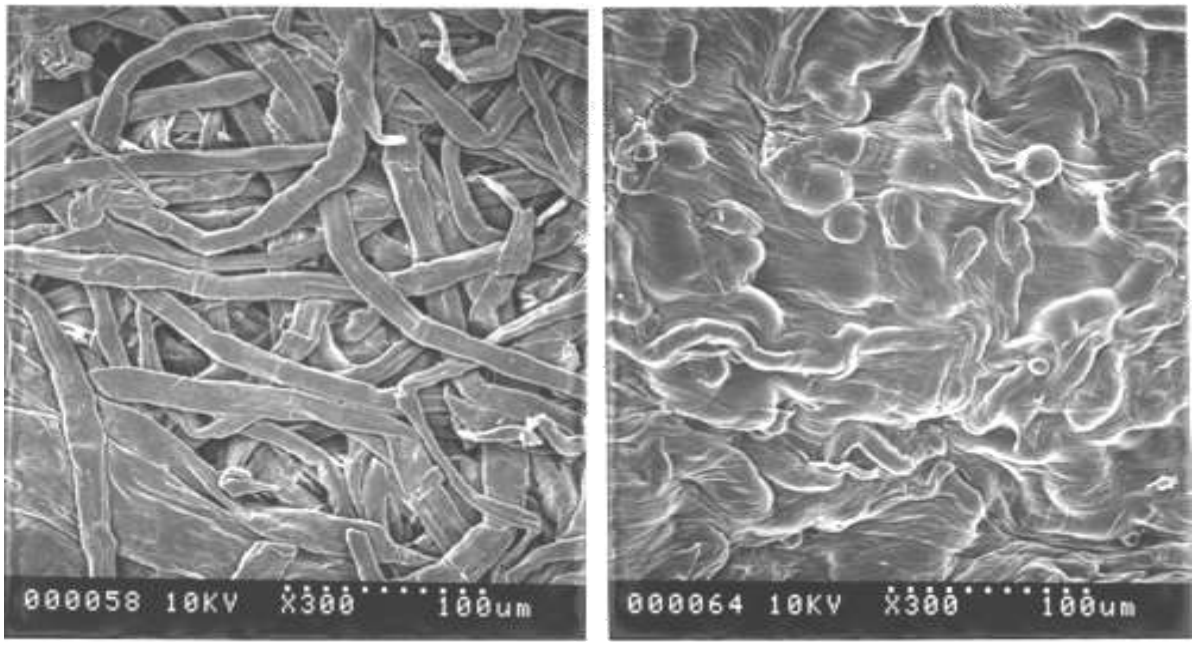

Figure 4.42 SEM photographs of the initial dissolving pulp (**left**) and after dissolution in [Bmim][Cl] and regenerated cellulose (**right**) as reproduced from Swatloski *et.al.* (2002:4975).

SEM images of the pulp before dissolution in IL is shown in Figure 4.42 to compare with the results obtained in this study. The SEM results shows a rough texture of the fibers, which then confirms that the highly crystalline cellulose structure in the dissolving pulp was transformed to amorphous form after treating with [Emim][OAc]/co-solvents.

These results are similar to the findings of (Kuzmina 2012:55; Zhao *et.al.* 2013:49) who reported a decrease in the crystallinity of cellulose and chitosan after dissolving in IL/co-solvent mixtures. Sun *et. al.* (2009:4975) demonstrated the effect of [Emim][OAc] on structural changes of switchgrass through SEM images and concluded that the regenerated sample attained a structure lacking lignin. Doherty *et.al.* (2010:1967) provided the structural changes of maple wood flour upon pretreatments via [Emim][OAc], [Bmim][OAc] and [Bmim][$MeSO_4$] through SEM analysis in which [Emim][OAc] and [Bmim][OAc] pretreated maple wood flour exhibited highly altered morphology compared to [Bmim][$MeSO_4$] pre-treat sample.

It can be implied that the primary walls of the dissolving pulp fibers were destroyed by the IL and co-solvent treatment, resulting in the linkages between the lignin and carbohydrates to be diminished. This then resulted in the regenerated cellulose structure to be loose because of the breakage of bonds which will create a favourable environment for the IL penetration (Muhammad *et.al.* 2011:1006).

After regeneration, the morphology of the material was significantly changed, displaying a rough but conglomerate texture in which the fibres are fused into a relatively homogeneous macrostructure (Swatloski *et.al.* 2002:4975).
It has been reported in previous studies (Swatloski *et.al.* 2002:4975; Zhu *et.al.* 2006:325) that the phenomenon might result from the formation of more amorphous structure. The newly found structure enables the regenerated cellulose to react with chemical or biological reagents more easily, due to the increased accessibility and reactivity after dissolution in IL/co-solvent mixtures (Zhao *et.al.* 2009:47).

4.6.2 SEM images of the regenerated cellulose from sawdust wood samples previously dissolved in [Emim][OAc]/DMSO or DMF mixtures

The SEM images of the morphology of the regenerated cellulose from sawdust wood and [Emim][OAc]/DMSO and DMF mixtures are shown in Figure 4.43 and 4.44, respectively. SEM has been useful in order to monitor the altered structure of pretreated lignocellulosic biomass via various ILs (Swatloski *et.al.* 2002:4975)

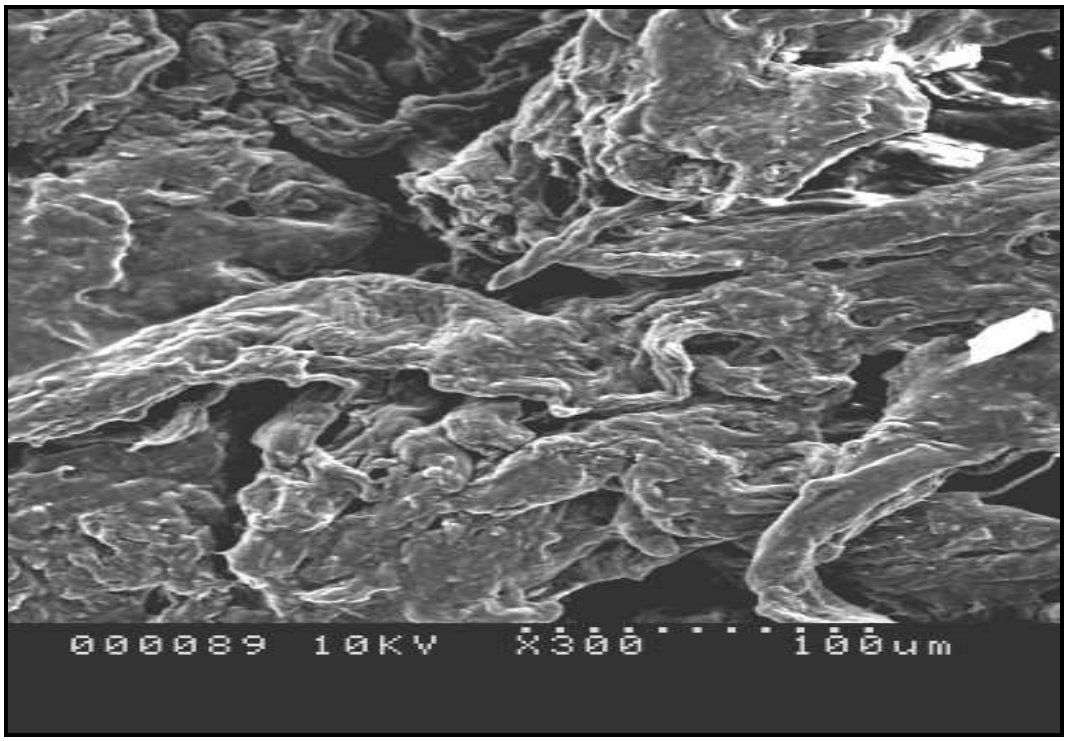

Figure 4.43 SEM photograph of regenerated cellulose from sawdust wood previously dissolved in [Emim][OAc]/DMSO mixture

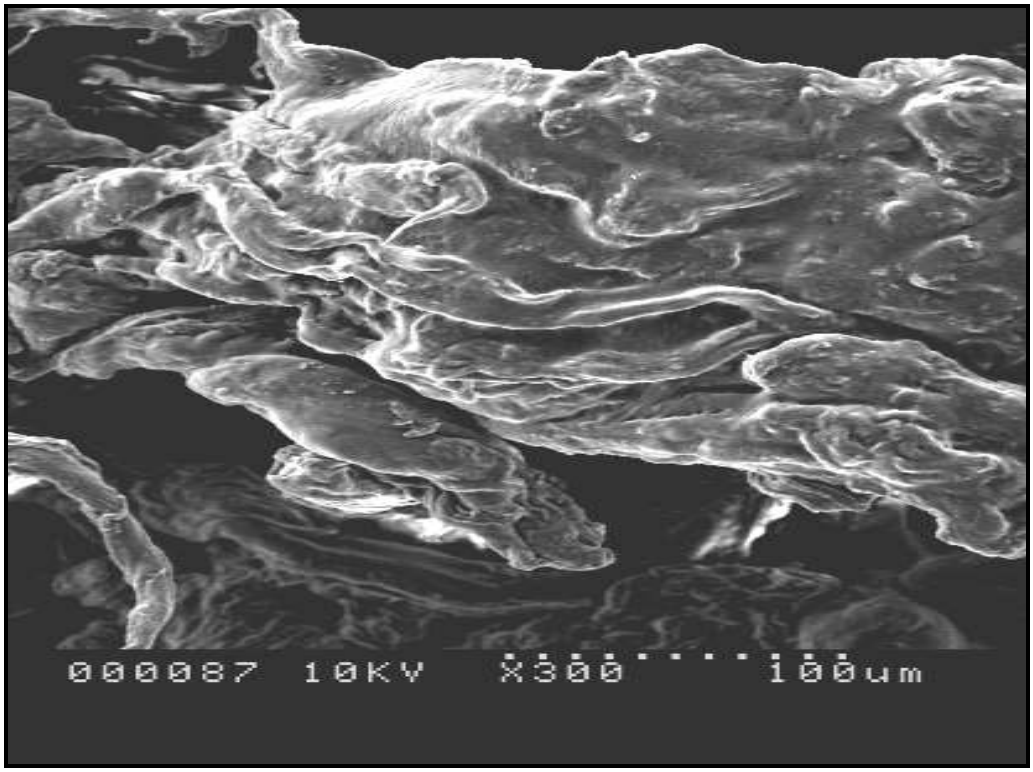

Figure 4.44 SEM photograph of regenerated cellulose from sawdust wood in [Emim][OAc]/DMF mixture

As shown in Figures 4.43-4.44, the compact framework exhibited by the MCC standard of cellulose (Figure 4.28) was highly disrupted after dissolution of sawdust wood in [Emim][OAc]/DMSO and DMF mixtures. The regenerated cellulose-rich material in Figures 4.43-4.44 shows a different morphology compared to the MCC (Figure 4.37), with a conglomerate texture in wood fibres that is fused into a relatively more homogeneous macrostructure and similar results were reported in literature (Muhammad *et.al.* 2011:1006; Sun *et.al.* 2009:653; Swatloski *et.al.* 2002:4975). Upon dissolution and regeneration, the DMF and DMSO were removed by evaporation

4.7 THERMOGRAVIMETRIC ANALYSIS (TGA) OF THE REGENERATED CELLULOSE

4.7.1 TGA curves of the regenerated cellulose from unbleached and bleached dissolving pulp previously dissolved in [Emim][OAc]/DMSO or DMF mixtures

The thermal decomposition curves of the MCC standard of cellulose and the regenerated cellulose from a unbleached dissolving pulp and bleached dissolving pulp samples previously dissolved in [Emim][OAc]/DMSO and DMF mixtures were determined using TGA. Thermal stability of cellulose depends on the crystallinity and the intermolecular bonds (Mahadeva *et.al.* 2012:292).

The TGA curves of the native cellulose (MCC standard) shown in Figure 4.45 was taken from literature (Su 2012: 15) while the regenerated cellulose from unbleached and bleached dissolving pulp in [Emim][OAc]/ DMSO and DMF mixtures are shown in Figures 4.46 and 4.47, respectively.

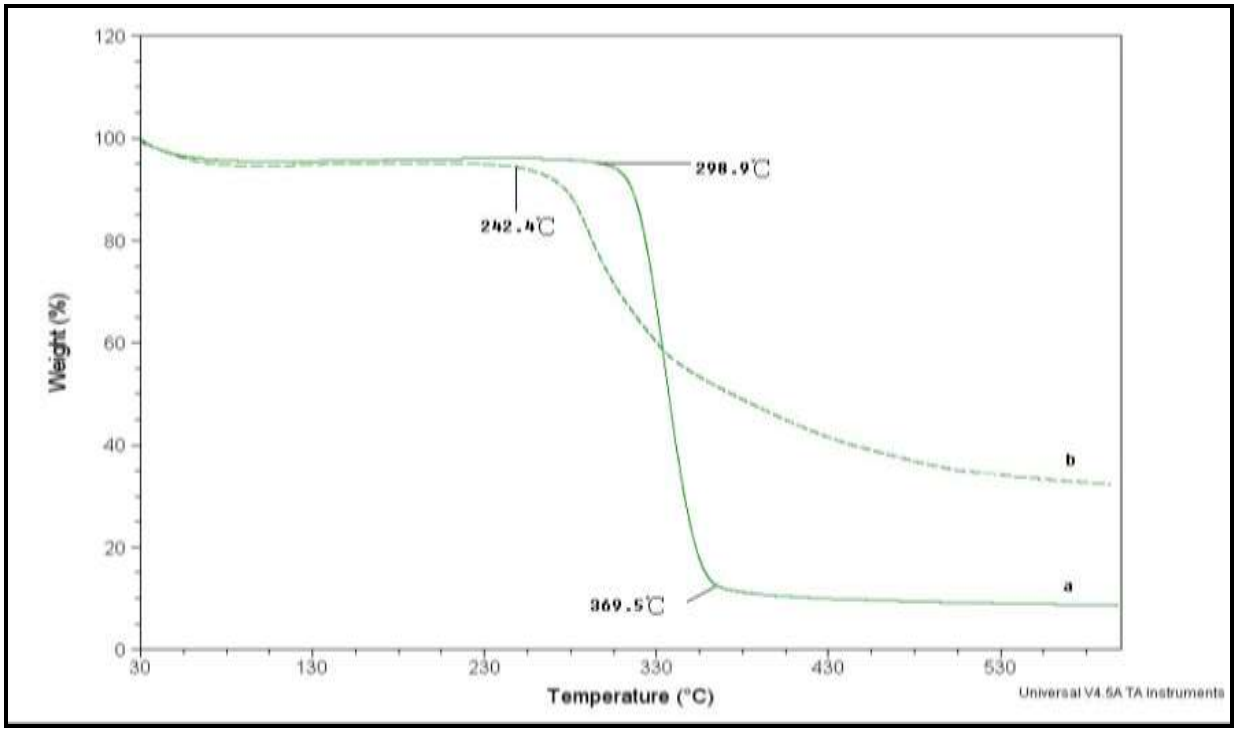

Figure 4.45 Thermal decomposition profiles of different cellulose **a**) MCC standard, **b**) regenerated cellulose as reproduced from Su (2012:15)

The small initial drop occurring near 100 ˚C is quite significant in both Figures 4.46 & 4.47, which is probably due to the evaporation of retained moisture (Lan *et.al.* 2011:672; Zhao *et.al.* 2012:1493). The thermal decomposition of the original cellulose and the regenerated cellulose is divided into three stages.

The original cellulose (Figure 4.45 **a**) had a higher thermal stability than regenerated cellulose. The pronounced decomposition onset was at 298.9 ˚C, the maximum decomposition rate temperature was 369.5 ˚C; and the decomposition was complete at 420 ˚C (Chen *et.al.* 2012:4).
For the cellulose regenerated from unbleached and bleached dissolving pulp samples previously dissolved in [Emim][OAc]/DMSO or DMF mixtures, the pronounced decomposition onset was at 230 ˚C, the maximum decomposition rate temperature was 290 ˚C, and the decomposition was complete at 340 ˚C.

The onset decomposition temperature for the cellulose regenerated from the unbleached and bleached dissolving pulp was 70 ˚C lower than that for MCC standard of cellulose, similar results were reported in literature (Chen *et.al.* 2012:4). This demonstrated that after cellulose regeneration, the thermal stability decreased; this was consistent with the decrease in molecular weight of cellulose (Chen *et.al.* 2012:4). This phenomena can be explained by noting that cellulose is attracted to OAc^- during the dissolving process in [Emim][OAc], and the most of the hydrogen bonds and part of molecular cellulose chain are degraded, resulting in a decrease in molecular weight and thermal stability.

In Figure 4.46, it can be noted that the regenerated cellulose from unbleached dissolving pulp and [Emim][OAc]/DMSO mixture retained 80 % weight after heating to 600 ºC, while regenerated cellulose from [Emim][OAc]/DMF mixture retained 2 % weight, and the similar trend is observed in Figure 4.47, where the retained weight was 50 % for the cellulose regenerated from bleached dissolving pulp in [Emim]/DMSO mixture and 10 % for cellulose regenerated from bleached dissolving pulp previously dissolved in [Emim][OAc]/DMF mixture, as compared to the original cellulose which retained 8 % weight while pulp dissolved in pure [Emim][OAc] gave a retained weight of 15 % (Su 2012:15). This can be attributed to DMSO reported to increase the speed of dissolution and remained in solution, decreasing its viscosity which makes it less efficient for dissolving the pulp in IL, and pulp material still contains large amount of water even after drying (Su 2012:15).

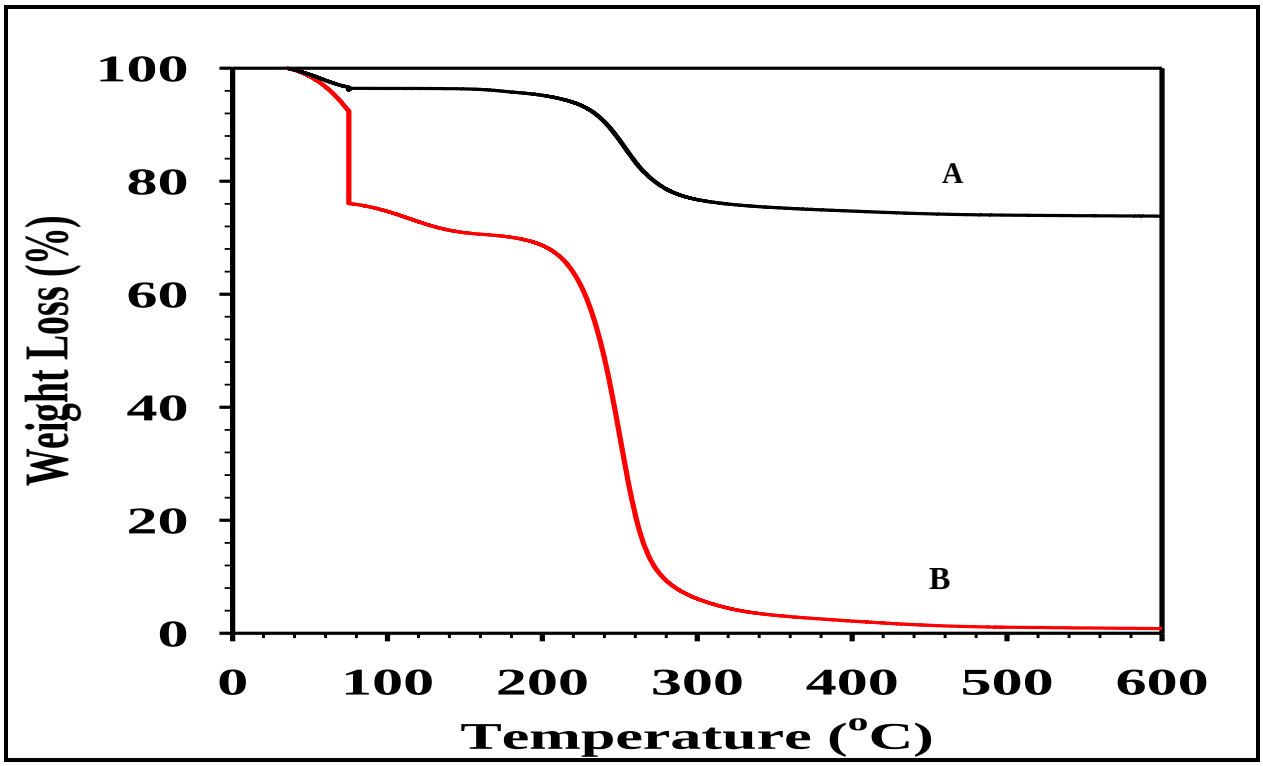

Figure 4.46 TGA curves of cellulose regenerated from unbleached pulp previously dissolved in [Emim][OAc]/DMSO mixture (curve **A**) and [Emim][OAc]/DMF mixture (curve **B**)

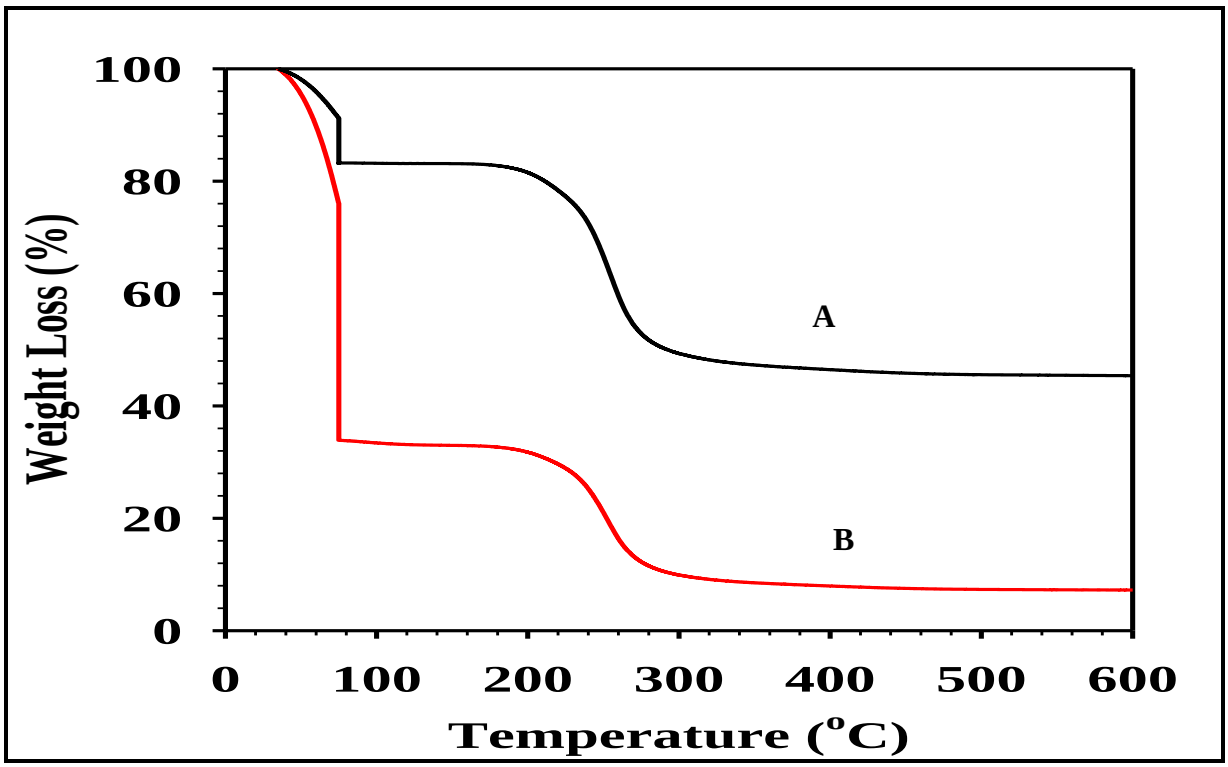

Figure 4.47 TGA curves of cellulose regenerated from bleached pulp previously dissolved in [Emim][OAc]/DMSO mixture (curve **A**) and [Emim][OAc]/DMF mixture (curve **B**)

4.7.2 TGA curves of regenerated cellulose from sawdust wood samples and IL/co-solvent mixtures

Essential information concerning the sample compositions can be obtained from TGA. All the regenerated cellulose samples demonstrated a lower decomposition temperature and lower weight loss with [Emim][OAc]/DMF mixture, in comparison to the MCC standard of cellulose shown in (Figure 4.45 **a**).

The cellulose regenerated from sawdust wood previously dissolved in [Emim][OAc]/DMSO mixture (curve **A**) and [Emim][OAc]/DMF mixture (curve **A**) regenerated cellulose has a lower decomposition temperature of 200 ˚C than the MCC which is reported in literature to have a decomposition of 250 ˚C (Kilulya *et.al.* 2011:3278). A decrease in the crystallinity and the decrease in depolymerization of the regenerated cellulose explain this finding (Dongfang *et.al.* 2012: 939; Liu *et.al.* 2011:223). TGA curves of regenerated cellulose from sawdust wood that was previously dissolved in [Emim][OAc]/DMF retained 5 wt. %, while the cellulose regenerated from sawdust previously dissolved in [Emim][OAc]/DMSO retained 75 wt.%.

It was also noted that the thermal stabilities of the regenerated cellulose samples were lower than that of MCC, which was probably caused by the lower crystallinity of the regenerated cellulose as the previous work has shown that lower crystallinity and lower cellulose crystallite size can accelerate the degradation process and reduce wood thermal stability (Pang *et.al.* 2014:5).

These regenerated cellulose samples show higher char yields (non-volatile carbonaceous materials) which is exhibited by the higher mass residual after decomposition compared to the original cellulose where MCC retained 8 wt.%, this may probably happen because of IL that remained in the regenerated cellulose as also reported by Dongfang *et.al.* (2012:939) and may also be attributed to the incomplete pyrolysis of the non-volatile carbonaceous materials, which are characteristics of regenerated cellulose as also found by Swatloski *et.al.* (2002:4975) . Similar kind of TGA results have been observed by (Mikkola *et.al.* 2007:1235; Swatloski *et.al.* 2002:4975), indicating a good accordance with our results.

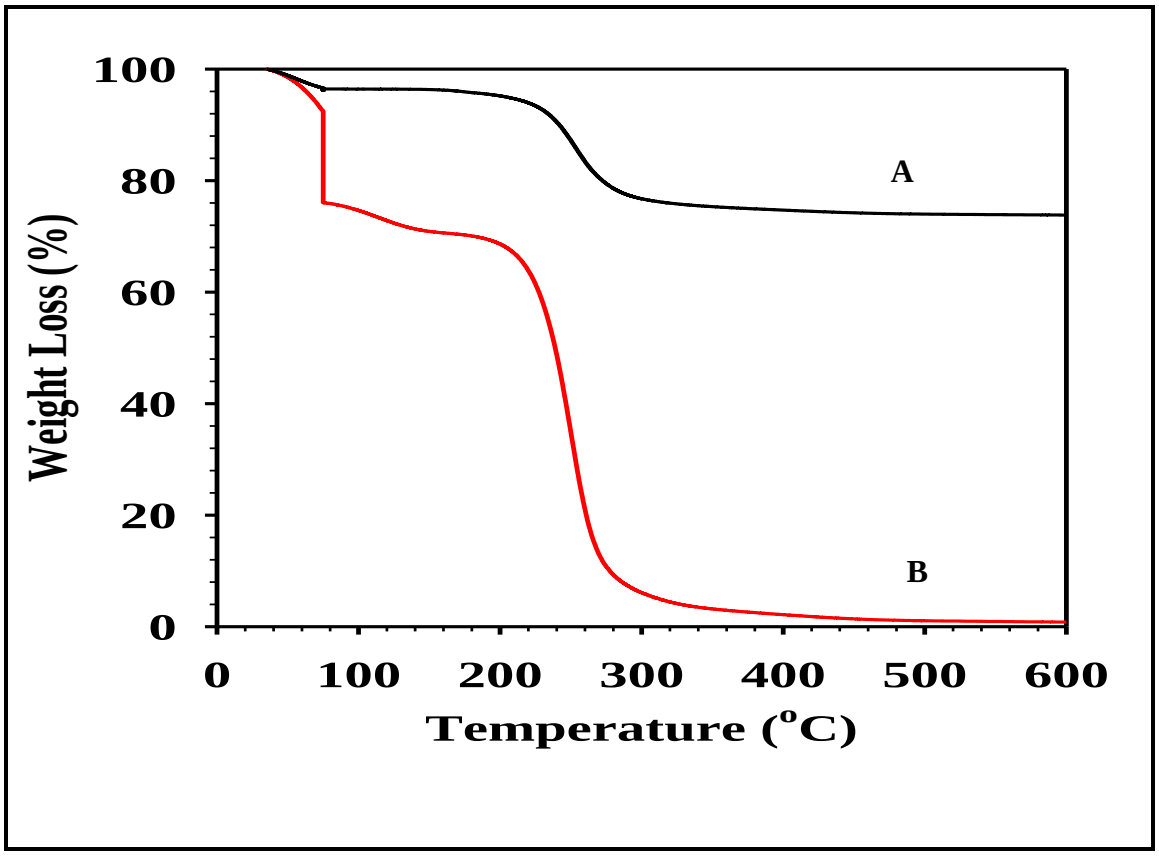

Figure 4.48 TGA curves of cellulose regenerated from sawdust wood previously dissolved in [Emim][OAc]/DMSO mixture (curve **A**) and [Emim][OAc]/DMF mixture (curve **B**)

CHAPTER 5: CONCLUSIONS

5.1 SUMMARY AND FUTURE RECOMMENDATIONS

Ionic liquids have a great promise and potential in the manufacture and processing of cellulose fibres. The results show that the use of ILs and co-solvents enhances the efficiency of processing cellulose. Due to the high polar nature, low vapour pressure, thermal stability and ease of recycling, ILs opens up a new horizon for the efficient utilization of dissolving pulp cellulose.

The dissolution of cellulose in [Emim][OAc]/DMSO or DMF mixtures effectively stimulated the escalating of active research towards the better utilization of cellulose and biomass.
Cellulose was regenerated successfully from South Africa unbleached dissolving pulp, bleached dissolving pulp and sawdust wood sample in [Emim][OAc]/DMSO or DMF mixtures with the cellulose yield recovery being greatest in cellulose regenerated from bleached pulp in [Emim][OAc]/DMF mixture due to the less amount of hemicelluloses and lignin present in the bleached pulp, which then makes it more easier for the solvents to break the hydrogen bonds in the pulp samples.
The pXRD results indicate that the crystal structure of cellulose was transformed from cellulose 1 to cellulose II. The SEM images show that the surface of the regenerated cellulose became homogeneous after dissolving in IL/co-solvent mixtures.
The regenerated cellulosic material seems to be more amorphous, and therefore might be easier for the solvent penetration.

A series of simultaneous advantages of IL processing can be highlighted.

- The simple dissolution of cellulose in ILs and co-solvent mixtures which enables the simple dissolution and regeneration strategies for the development of advanced materials
- Direct dissolution of lignocellulosic biomass, with separation of its major components (cellulose and lignin).

In summary, ILs offer tremendous possibilities as the basis for the constitution of an innovative technological platform for the development of a sustainable industry of chemicals and advanced materials. Although these technologies are in the early laboratory stages, they

are promising and offer better pathways, less energy intensive processes and significantly improved health and environmental benefits when compared to the current processes.
However, it must be noted that the industrial adoption of new methods and practices is based on cost and demonstration of both viability and improvements over the current practice. The recovery and reuse of the IL solvents, as well as the current cost, could be an obstacle to application of the ILs.
Due to their current high cost of ILs and the increasing concern for environmental and safety issues, efficient recycling of IL is one of the key issues that needs to be solved in order to apply these solvents in industrial scale processes that are profitable and sustainable. If ILs are used as solvents for dissolution of cellulosic fibres, they have to compete with the viscose and lyocell processes that are well established and commercialized. 99% of the cellulose solvent system NMMO are recovered implying that comparable rates are required for ILs in order to make them economically attractive.

Generally, ILs, as the environmentally friendly solvents, have the strong potential to be used for cellulose dissolution and derivatization. The efficiency of dissolution could be further improved by using ILs with suitable mixing approaches such as mechanical stir. However, further investigation by using X-ray and solid state NMR to evaluate the impact of ILs' treatment on the crystallinity of cellulose are needed.
In conclusion, [Emim][OAc] is promising to be a powerful, non-derivative single component solvent for cellulose.

CHAPTER 6: REFERENCES

Abdulukhani, A., Marast, E.H., Ashori, A. and Krimi, A. 2013. Effects of dissolution of some lignocellulosic materials with ionic liquids as green solvents on mechanical and physical properties of composite films. *Carbohydrate Polymers*, **95**, pp. 57-63.

Andersson, S., Wikberg, H., Pesonen, E., Maunu, S.L., and Serimaa, R. 2004. Studies of crystallinity of Scotts pine and Norway spruce cellulose. *Trees-Struct.Fund.* **18**, pp. 346-353.

Ang, T.N., Yoon, L.W., Lee, K.M., Ngoh, G.C., Chua, A.S.M. and Lee, M.G. 2011. Efficiency of ionic liquids in the dissolution of rice husk. *BioResources*, **6**(4), pp. 4790-4800.

Armand, M., Endres, F., Macfarlan, D.R., Ohno, H. and Scrosati, B. 2009. Ionic-liquid materials for the electrochemical challenges of the future. *Nature materials,* **8**(8), pp.

621-629.

Audu, I.G., Brosse, N., Desharnais, L. and Rakshit, S.K. 2013. Investigation of the Effects of ionic liquid 1-Butyl-3-Methylimidazolium Acetate Pretreatment and Enzymatic Hydrolysis of Typha capensis. *Energy & Fuels,* **27**(1), pp. 189-196.

Auxenfans, T., Buchoux, S., Djellab, K., Avondo, C., Husson, E. and Sarazin, C. 2012. Mild pretreatment and enzymatic saccharification of cellulose with recycled ionic liquids towards one-batch process. *Carbohydrate Polymers,* **90**(2), pp. 805-813.

Azubuke, P.C., Okhamafe, O.A.2012. Physiochemical, spectroscopic and thermal properties of MCC derived from corn cobs. *International Journal of recycling of organic waste in agriculture*, pp. 1-9.

Bentivoglio, G., Roder, T., Fasching, M., Buchberger, M., Schottenberger, H. and Sixta, H. 2006. Cellulose processing with chloride-based ionic liquids. *Lenzinger Berichte,* **86**, pp. 154-161.

Biermann, C.J. 1993. *Essentials of pulping and papermaking.* pp 72-100. New York: academic press.

Bose, S., Armstrong, D.W. and Petrich, J.W. 2010. Enzyme-catalyzed hydrolysis of cellulose in ionic liquids: a green approach toward the production of biofuels. *The Journal of Physical Chemistry B*, **114**(24), pp. 8221-8227.

Brandt, A., Gräsvik, J., Halletta, J.P. and Welton, T. 2013. Deconstruction of lignocellulosic biomass with ionic liquids. *Green Chem.*, **15**, pp. 550-583.

Brodeur, G., Yau, E., Badal, K., Collier, J., Ramachandran, and Ramakrishnan, S. 2011. Chemical and physiochemical pretreatment of lignocellulosic biomass: A review. USA. *Enzyme Research*, pp 1-17.

Brown, E.K. 2012. Cellulose dissolution in ionic liquids and their mixtures with solvents: linking ion/ solvent structure and efficacy of biomass pretreatment. Doctorate Thesis, North Carolina State University, USA.

Cai, T., Yang, G., Zhang, H., Shao, H. and Hu, X. 2012. A new process for dissolution of cellulose in ionic liquids. *Polymer Engineering and Science*, **52**(8), pp. 1708-1714.

Cao, Y., Wu, J., Zhang, J., Li, H., Zhang, Y. and He, J. 2009. Room temperature ionic liquids (RTILs): A new and versatile platform for cellulose processing and derivatization. *Chemical Engineering Journal*, **147**(1), pp. 13-21.

Casas, A., Alonso, M.V., Oliet, M., Rojo, E. and Rodríguez, F. 2012a. FTIR analysis of lignin regenerated from *Pinus radiata* and *Eucalyptus globulus* woods dissolved in imidazolium-based ionic liquids. *Journal of Chemical Technology and Biotechnology*, **87**(4), pp. 472-480.

Casas, A., Oliet, M., Alonso, M.V. and Rodríguez, F. 2012b. Dissolution of *Pinus radiata* and *Eucalyptus globulus* woods in ionic liquids under microwave radiation: Lignin regeneration and characterization. *Separation and Purification Technology*, **97**(0), pp. 115-122.

Casas, A., Palomar, J., Alonso, M.V., Oliet, M., Omar, S. and Rodríguez, F. 2012c. Comparison of lignin and cellulose solubilities in ionic liquids by COSMO-RS analysis and experimental validation. *Industrial Crops and Products*, **37**(1), pp. 155-163.

Chen, H.Z., Wang, N. and Liu, L.Y. 2012. Regenerated cellulose membrane prepared with ionic liquid 1-butyl-3-methylimidazolium chloride as solvent using wheat straw. *J.Chem Technol Biotechnol,* **87**(12), pp 1634-1640.

Christoffersson, E.K. 2005. Dissolving Pulp- Multivariate characterization and analysis of reactivity and spectroscopic properties, Doctorate thesis, Umea University, Sweden.

Cuissinat, C., Navard, P. and Heinze, T. 2008. Swelling and dissolution of cellulose. Part IV: Free floating cotton and wood fibres in ionic liquids. *Carbohydrate Polymers,* **72**(4), pp. 590-596.

Dadi, A.P., Varanasi, S. and Schall, C.A. 2006. Enhancement of cellulose saccharification kinetics using an ionic liquid pretreatment step. *Biotechnology and Bioengineering,* **95**(5), pp. 904.

Dafchachi, M.N. and Resalati, N. 2012. Evaluation of pre-hydrolyzed soda-AQ dissolving pulp from *Populus Deltoides* using an ODED bleaching sequence. *BioResources,* **7**(3), pp. 3283.

Ding, Z., Chi, Z., Gu, W., Gu, S., Liu, J. and Wang, H. 2012. Theoretical and experimental investigation on dissolution and regeneration of cellulose in ionic liquid. *Carbohydrate Polymers,* **89**(1), pp. 7-16.

Du, H. and Qian, X. 2011. The effects of acetate anion on cellulose dissolution and reaction in imidazolium ionic liquids. *Carbohydrate research,* **346**(13), pp. 1985-1990.

Duan, X., Xu, J., He, B., Li, J. and Sun, Y. 2011. Preparation and rheological properties of cellulose / chitosan homogeneous solution in ILs. *BioResources,* **6**(4), pp. 4640.

Ebner, G., Schiehser, S., Potthast, A. and Rosenau, T. 2008. Side reaction of cellulose with common 1-alkyl-3-methylimidazolium-based ionic liquids. *Tetrahedron letters,* **49**(51), pp. 7322-7324.

Egorov, V.M., Smirnova, S.V., Formanovysky, A.A., Pletnev, I.V. and Zolotov, Y.A. 2007. Dissolution of cellulose in ionic liquids as a way to obtain test materials for metal-ion detection. *Analytical and bioanalytical chemistry,* **387**(6), pp. 2263-2269.

Endres, F. and El Abedin, S.Z. 2006. Air and water stable ionic liquids in physical chemistry. *Phys.Chem.* **8**(18), pp. 2101-2116.

Erdmenger, T., Haensch, C., Hoogenboom, R. and Schubert, U.S. 2007. Homogeneous Tritylation of Cellulose in 1-Butyl-3-methylimidazolium Chloride. *Macromolecular bioscience,* **7**(4), pp. 440-445.

Feng, L. and Chen, Z. 2008. Research progress on dissolution and functional modification of cellulose in ionic liquids. *Journal of Molecular Liquids,* **142**(1), pp. 1-5.

Fitzpatrick, M. 2011. Characterization and Processing of Lignocellulosic Biomass in Ionic Liquids, Master's Thesis, Queen's University, Canada.

Fitzpatrick, M., Champagne, P., Cunningham, M.F. and Whitney, R.A. 2010. A biorefinery processing perspective: treatment of lignocellulosic materials for the production of value-added products. *Bioresource technology,* **101**(23), pp. 8915-8922.

Fitzpatrick, M., Champagne, P. and Cunningham, M.F. 2012. Quantitative determination of cellulose dissolved in 1-ethyl-3-methylimidazolium acetate using partial least squares regression on FTIR spectra. *Carbohydrate Polymers,* **87**(2), pp. 1124-1130.

Fort, D.A., Remsing, R.C., Swatolski, R.P., Moyna, P., Moyna, G. and Rogers, R.D. 2007. Can ionic liquids dissolve wood? Processing and analysis of lignocellulosic materials with 1-n-butyl-3-methylimidazolium chloride. *Green Chemistry*, **9**(1), pp. 63-69.

Fu, D., Mazza, G. and Tamaki, Y. 2010. Lignin extraction from straw by ionic liquids and enzymatic hydrolysis of the cellulosic residues. *Journal of Agricultural and Food Chemistry,* **58**(5), pp. 2915-2922.

Fu, D. and Mazza, G. 2011. Optimization of processing conditions for the pretreatment of wheat straw using aqueous ionic liquid. *Bioresource technology,* **102**(17), pp. 8003-8010.

Fu, L., Zhao, D., Ren, P., Li, H. and Zhang, J. 2011a. Synthesis of pyridinium-based ionic liquid and its dissolubility of cellulose. *Xiandai Huagong/Modern Chemical Industry*, **31**(9), pp. 39-42.

Fukaya, Y., Hayashi, K., Wada, M. and Ohno, H. 2008. Cellulose dissolution with polar Ionic Liquids under mild conditions: required factors for anions. *Green Chem.*, **10**, pp. 44.

Gao, J., Chen, L., Yan, Z. and Yu, S. 2013. Influence of Aprotic Solvents on the Phase Behaviour of Ionic Liquid Based Aqueous Biphasic Systems. *Journal of Chemical & Engineering Data*, **58**, pp. 1535.

Geng, X. and Henderson, W.A. 2012. Pretreatment of corn stover by combining ionic liquid dissolution with alkali extraction. *Biotechnology and Bioengineering*, **109**(1), pp. 84.

Gericke, M., Fardim, P. and Heinze, T. 2012. Ionic liquids-promising but challenging solvents for homogeneous derivatization of cellulose. *Molecules*, **17**, pp. 7458.

Gericke, M., Schulfter, K., Liebert, T., Heinze, T. and Budtova, T. 2009. Rheological properties of cellulose/ ionic liquid solution from dilute to concentrated states. *Biomacromolecules*, **10**, pp. 1188.

Gericke, M.L.T. and Heinze, T. 2011. Solvent for cellulose chemistry. *Nachrichten Aus Der Chemie*, **59**(4), pp. 405.

Graencher, C. 1934. Cellulose solution.*US Patent* 1.943.176.

Gräsvik, J., Eliasson, B. and Mikkola, J. 2012. Halogen-free ionic liquids and their utilization as cellulose solvents. *Journal of Molecular Structure*, **1028**(0), pp. 156-163.

Ha, S.H., Mai, N.L., An, G. and Koo, Y. 2011. Microwave-assisted pretreatment of cellulose in ionic liquid for accelerated enzymatic hydrolysis. *Bioresource technology*, **102**(2), pp. 1214-1219.

Han, S.Q.L., Zhu, J.L., Chen, S.D., Wu, R., Zhang, Y.X. and Yu, Z.N. 2009. Potential applications of ionic liquids in wood related industries. *BioResources*, **4**(2), pp. 825.

Hao, Y., Peng, J., Ao, Y., Li, J. and Zhai, M. 2012. Radiation effects on microcrystalline cellulose in 1-butyl-3-methylimidazolium chloride ionic liquid. *Carbohydrate Polymers*, **90**(4), pp. 1629-1633.

Härdelin, L., Thunberg, J., Perzon, E., Westman, G., Walkenström, P. and Gatenholm, P. 2012. Electrospinning of cellulose nanofibers from ionic liquids: The effect of different cosolvents. *Journal of Applied Polymer Science.*

Hauru, L.K.J., Hummel, M., King, A.W.T., Kilpäinen, I.A. and Sixtha, H. 2012. Role of solvent parameters in the regeneration of cellulose from ionic liquid solutions. *Biomacromolecules.*

Haykir, N.I., Bahcegul, E., Bicak, N. and Bakir, U. 2013. Pretreatment of cotton stalk with ionic liquids including 2-hydroxy ethyl ammonium formate to enhance biomass digestibility. *Industrial Crops and Products,* **41**, pp. 430.

Hazarika, S., Dutta, N.N. and Rao, P.G. 2012a. Dissolution of lignocellulose in ionic liquids and its recovery by nanofiltration. *Separation and Purification Technology,* pp. 1.

Hazarika, S., Dutta, N.N. and Rao, P.G. 2012b. Dissolution of lignocellulose in ionic liquids and its recovery by nanofiltration membrane. Separation and Technology, **97,** pp. 123-129.

Heinze, T., Schwikal, K. and Barthel, S. 2005. Ionic liquids as reaction medium in cellulose functionalization. *Macromolecular Bioscience,* **5**(6), pp. 520-525.

Heinze, T.D., Schoebitz, S., Libert, M., Koehler, T. and Meister, F. 2008. Interactions of ionic liquids with polysaccharides-2. *Cellulose. Macromolecular Symposia,* **262**, pp. 8.

Hermanutz, F., Gähr, F., Ueringen, E., Meister, F. and Kosan, B. 2008. New developments in dissolving and processing of cellulose in ionic liquids. *Macromolecular Symposia,* 2008, **262**, pp23-27.

Hesse-Ertelt, S., Heinze, T., Kosan, B., Schwikal, K. and Meister, F. 2010. Solvent Effects on the NMR Chemical Shifts of Imidazolium-Based Ionic Liquids and Cellulose Therein. *Macromolecular Symposia,* 2010, **294**, pp75-89.

Hinck, J.F., Casebier, R.L. and Hamilton, J.K. 2006. Pulp and paper manufacture. *TAPPI press,* **4**, pp. 213.

Hirai, A., Horii, F. and Kitamaru, R. 1980. Structure of native and regenerated cellulose as revealed by proton NMR analysis. *Journal of Polymer Science: Polymer Physics Edition,* **18**(8), pp. 1801-1809.

Holbrey, J.D., Reichert, W.M., Reddy, R. and Rogers, R. 2003. Ionic liquids as green solvents: progress and prospects. *ACS symposium series,* American Chemical Society Washington, DC pp121-133.

Holbrey, J.D., Reichert, W.M., Swatloski, R.P., Broker, G.A., Pitner, W.R., Seddon, K.R. and Rogers, R.D. 2002. Efficient, halide free synthesis of new, low cost ionic liquids: 1, 3-dialkylimidazolium salts containing methyl-and ethyl-sulfate anions. *Green Chem.,* **4**(5), pp. 407-413.

Holm, J. and Lassi, U. 2011. Ionic liquids in the pretreatment of lignocellulosic biomass chapter 24. *Ionic liquids: Applications and perspectives*. Finland: Intech pp 545-560.

Hong, F., Guo, X., Zhang, S., Han, S., Yang, G. and Jönsson, L.J. 2012. Bacterial cellulose production from cotton-based waste textiles: Enzymatic saccharification enhanced by ionic liquid pretreatment. *Bioresource technology,* **104**(0), pp. 503-508.

Horii, F., Hirai, A., Kitamaru, R. 1982. Solid state high resolution ^{13}C NMR studies of regenerated cellulose samples with different crystallinities. *Polym. Bull.,* **8**, pp. 163.

Husson, E., Buchoux, S., Avondo, C., Cailleu, D., Djellab, K., Gosselin, I., Wattraint, O. and Sarazin, C. 2011. Enzymatic hydrolysis of ionic liquid-pretreated celluloses: Contribution of CP-MAS ^{13}C NMR and SEM. *Bioresource technology*, **102**(15), pp. 7335-7342.

Iguchi, M., Aida, T.M., Watanabe, M. and Smith JR, R.L. 2012. Dissolution and recovery of cellulose from 1-butyl-3-methylimidazolium chloride in presence of water. *Carbohydrate Polymers, .*

Jahan, M.S., Ahsan, L., Noori, A. and Quaiyyum, M.A. 2008. Process for the production of dissolving pulp from *Trema Orientals* (Nalita) by prehydrolysis kraft and soda-ethylenediamine (EDA) process. *BioResources,* **3**(3), pp. 816.

Jiang, G., Huang, W., Li, L., Wang, X., Pang, F. and Zhang, Y. 2012a. Structure and properties of regenerated cellulose fibers from different technology processes. *Carbohydrate Polymers*, **87**, pp. 2012.

Jiang, G., Yuan, Y., Wang,B.,Yin,X., Mukuze, K.S., Huang, W., Zhang, Y. and Wang, H. 2012b. Analysis of regenerated cellulose fibers with ionic liquids as a solvent as spinning speed is increased. *Cellulose*, **19**, pp. 1075.

Jiang, M., Zhao, M., Zhou, Z., Huang, T., Chen, X. and Wang, Y. 2011. Isolation of cellulose with ionic liquid from steam exploded rice straw. *Industrial Crops and Products*, **33**(3), pp. 734-738.

Jung, W.G., Sung, Y.J. and Lee, W. 2013. Improvement in dissolution of cellulose with ionic liquid by the electron beam treatment. *Palpu Chongi Gisul/Journal of Korea Technical Association of the Pulp and Paper Industry*, **45**(2), pp. 56-65.

Karatzos, K.S., Allan, L. and Mark, R. 2012a. The Undesirable Acetylation of Cellulose by the Acetate Ion of 1-ethyl-3-methylimidazolium acetate. *Cellulose*, **19**(1), pp. 307.

Karatzos, K.S., Edye, L.A. and Doherty, W.O.S. 2012b. Sugarcane baggase pretreatment using three imidazolium-based ionic liquids; mass balances and enzyme kinetics. *Biotechnology for Biofuels*, **62**(5), pp. 2.

Keskar, S.S., Edye, L.A., Fellowa, C.M. and Doherty, W.O.S. 2012. ATR-FTIR measurement of biomass components in phosphonium ionic liquids. *Journal of Wood Chemistry and Technology*, **321**, pp. 175.

Kihlman, M. 2012. Dissolution of cellulose for textile fibre applications, PhD thesis. Karlstad University,Sweden.

Kilpeäinen, I., Xie, H., King, A., Granstrom, M., Heikkinen, S. and Argyropoulos, D.S. 2007. Dissolution of wood in ionic liquids. *Journal of Agricultural and Food Chemistry*, **55**(22), pp. 9142-9148.

Kilulya, K.F., Msagati, T.A.M., Mamba, B.B., Ngile, J.C. and Bush, T. 2011. Imidazolium ionic liquids as dissolving solvents for chemical grade cellulose in the determination of fatty acids using gas chromatography-mass spectrometry. *BioResources,* **6**(3), pp. 3272.

Kilulya, K.F., Msagati, T.A., Mamba, B.B., Ngila, J.C. and Bush, T. 2012a. Ionic Liquid–Liquid Extraction and Supported Liquid Membrane Analysis of Lipophilic Wood Extractives from Dissolving-Grade Pulp. *Chromatographia,* , pp. 1-8.

Kilulya, K.F., Msagati, T.A., Mamba, B.B., Ngila, J.C. and Bush, T. 2012b. Study of the Fate of Lipophilic Wood Extractives During Acid Sulphite Pulping Process by Ultrasonic Solid-Liquid Extraction and Gas Chromatography Mass Spectrometry. *Journal of Wood Chemistry and Technology,* **32**(3), pp. 253-267.

Kilulya, K.F. 2012. Profiling of organic extractives in wood and dissolving pulping process by chromatographic and spectroscopic methods. PhD thesis, University of Johannesburg.

Kim, J., Shine., Eom, I., Won, K., Kim, Y.H., Choi, D., Choi, I. and Choi, J.W. 2011. Structural features of lignin macromolecules extracted with ionic liquid from poplar wood. *Bioresource technology,* **102**(19), pp. 9020-9025.

Kim, S., Dwiatmoko, A.A., Choi, J.W., Suh, Y., Suh, D.J. and Oh, M. 2010. Cellulose pretreatment with 1-n-butyl-3-methylimidazolium chloride for solid acid-catalyzed hydrolysis. *Bioresource technology,* **101**(21), pp. 8273-8279.

Kimon, K.S., Leslie Aalan, E. and William O. S. D. 2011. Enhanced saccharification kinetics of sugarcane bagasse pretreated in 1-butyl-3-methylimidazolium chloride at high temperature and without complete dissolution. *Bioresource technology,* **102**(19), pp. 9325-9329.

Kohler, S., Liebert, T., Schobitz, M., Schaller, J., Meister, F., Gunther, W. and Heinze, T. 2007. Interactions of ionic liquids with polysaccharides. unexpected acetylation of cellulose with 1-ethyl-3-methylimidazolium acetate. *Macromol. Rapid. Commun.,* **28**, pp. 2311.

Kosan, B., MichelsI, C. and Meister, F. 2008. Dissolution and forming of cellulose with ionic liquids. *Cellulose,* **15**(1), pp. 59-66.

Krässig, H.A. 1993. *Cellulose-structure, accessibility and reactivity: Polymer Monographs.*Voume **11**. Amsterdam: Gordan and Breach science publishers.

Kubisa, P. 2009. Ionic liquids as solvents for polymerization processes—Progress and challenges. *Progress in Polymer Science,* **34**(12), pp. 1333-1347.

Kuzmina, O. 2012a. *Research of Dissolution Ability of Ionic Liquids for Polysaccharides such as Cellulose.* Msc edn. Leningrad (Sankt Petersburg), Russland: Rat der Chemisch-Geowissenschaftlichen Fakultät der Friedrich-Schiller-Universität Jena.

Kuzmina, O., Heinze, T. and Wawro, D. 2012b. Blending of Cellulose and Chitosan in Alkyl Imidazolium Ionic Liquids. *ISRN Polymer Science,* **2012**.

Labbe, N., Kline, L.M., Moens, L., Kim, K., Kim, P.C. and Hayes, D.G. 2012. Activation of lignocellulosic biomass by ionic liquid for biorefinery fractionation. *Bioresource technology,* **104**(0), pp. 701-707.

Lan, W., Liu, C., Yue, F., Sun, R. and Kennedy, J.F. 2011. Ultrasound-assisted dissolution of cellulose in ionic liquid. *Carbohydrate Polymers,* **86**(2), pp. 672-677.

Lan, W., Liu, C., Yue, F., and Sun, R. 2011. Rapid Disoolution of cellulose in ionic liquids with different methods. *Agricultural and biological sciences- cellulose fundamental aspects.* DOI: 10.5772/52517.

Lappainen, K., Kärkkäinen, J. and Lajunen, M. 2013. Dissolution and depolymerization of barley starch in selected ionic liquids. *Carbohydrate Polymers*, **93**(1), pp. 89-94.

Lateef, H., Grimess, S., Kewcharoenwong, P. and Feinberg, B. 2009. Separation and recovery of cellulose and lignin using ionic liquids: a process for recovery from paper-based waste. *Journal of Chemical Technology and Biotechnology,* **84**(12), pp. 1818-1827.

Laus, G., Bentivoglio, G., Schottenberger, H., Kahlenberg, V., Kopacka, H., Roder, T. and Sixta, H. 2005. Ionic liquids: current developments, potential and drawbacks for industrial applications. *Lezinger Berichte,* **84**, pp. 71-85.

Lee, S.H., Doherty, T.V., Lindhardt, R.J. and Dordick, J.S. 2009. Ionic liquid mediated selective extraction of lignin from wood leading to enhanced enzymatic cellulose hydrolysis. *Biotechnology and Bioengineering,* **102**(5), pp. 1368.

Lekha, P. 2012. Ultrastructural localisation of the hemicellulose, xylan and mannan, in a range of Eucalyptus wood and dissolving pulp fibres during processing, PhD thesis. University of KwaZulu Natal.

Li, D., Sevastyanova, O. and E, M. 2012. Pretreatment of softwood dissolving pulp with ionic liquids. *Holzforschung,* **66**(8), pp. 935-943.

Li, W.Y.J., Liu, C., Sun, R.C., Zhang, A.P. and Kennedy, J.F. 2009. Homogeneous modification of cellulose with sucinic aanhydride in ionic liquid using 4-dimethylaminopyridine as a catalyst. *Carbohydrate Polymers,* **78**(3), pp. 389-395.

Liebert, T. and Heinze, T. 2008. Interaction of ionic liquids with polysaccharides 5. Solvents and reaction media for the modification of cellulose. *BioResources,* **3**(2), pp. 576-601.

Liebmann, B., Fried, A. and Rodrigues, J.F.C. 2012. Lignocellulosic biomass dissolution and fractioning using ionic liquids as a solvent. *Chemical Engineering Transictions,* **29**, pp. 553-558.

Lindman, B., Karlström, G. and Stigsson, L. 2010. On the mechanism of dissolution of cellulose. *Journal of Molecular Liquids,* **156**(1), pp. 76-81.

Liu, H., Sale, K.L., Holmes, B.M., Simmons, B.A. and Singh, S. 2010. Understanding the interactions of cellulose with ionic liquids: a molecular dynamics study. *The Journal of Physical Chemistry B,* **114**(12), pp. 4293-4301.

Liu, C. and Sun, R, 2010. Chapter 5 - Cellulose. *Cereal Straw as a Resource for Sustainable Biomaterials and Biofuels.* Amsterdam: Elsevier, pp. 131-167.

Liu, D., Xia, K., Cai, W., Yang, R., Wang, L. and Wang, B. 2012. Investigations about dissolution of cellulose in the 1-allyl-3-alkylimidazolium chloride ionic liquids. *Carbohydrate Polymers,* **87**(2), pp. 1058-1064.

Liu, L., Ju, M., Li, W. and Jiang, Y. 2014. Cellulose extraction from Zoysia japonica pretreated by alumina-doped MgO in AMIMCl. *Carbohydrate Polymers,* **113**(0), pp. 1-8.

Liu, W. and Budtova, T. 2013. Dissolution of unmodified waxy starch in ionic liquid and solution rheological properties. *Carbohydrate Polymers,* **93**(1), pp. 199-206.

Liu, Z., Wang, H., Li, Z., Lu, X., Zhang, X., Zhang, S. and Zhou, K. 2011. Characterization of the regenerated cellulose films in ionic liquids and rheological properties of the solutions. *Materials Chemistry and Physics,* **128**(1–2), pp. 220-227.

Luan, Y., Zhang, J., Zhan, M., Wu, J. and Zhang, He, J. 2013. Highly efficient propionylation and butyralation of cellulose in an ionic liquid catalyzed by 4-dimethylminopyridine. *Carbohydr.Polym.,* **92**, pp. 307-311.

Lucas, M., Wagner, G.L., Nishiyama, Y., Hanson, L., Samayam, I.P., Schall, C.A., Langan, P. and Rector, K.D. 2011. Reversible swelling of the cell wall of poplar biomass by ionic liquid at room temperature. *Bioresource technology,* **102**(6), pp. 4518-4523.

Luo, J., Cai, M. and Gu, T. 2013. Pretreatment of Lignocellulosic Biomass Using Green Ionic Liquids. *Green Biomass Pretreatment for Biofuels Production.* Springer, pp. 127-153.

Lv, Y., Wu, J., Zhang, J., Niu, Y., Liu, C., He, J. and Zhang, J. 2012. Rheological properties of cellulose/ionic liquid/dimethylsulfoxide (DMSO) solutions. *Polymer,* **53**(12), pp. 2524-2531.

Ma, B., Zhang, M., He, C. and Sun, J. 2012a. New binary ionic liquid system for the preparation of chitosan/cellulose composite fibers. *Carbohydrate Polymers,* **88**(1), pp. 347-351.

Ma, J. and Hong, X. 2012b. Application of ionic liquids in organic pollutants control. *Journal of environmental management,* **99**(0), pp. 104-109.

Mahadeva, S.K. and Kim, J. 2012. Influence of residual ionic liquid on the thermal stability and electromechanical behaviour of cellulose regenerated from 1-ethyl-3-methylimidazolium acetate. *Fibres and Polymers,* **13**(3), pp. 289-294.

Mahmoudian, S., Wahit, M.A., Ismail, A.F. and Yussuf, A.A. 2012. Preparation of regenerated cellulose/ montmorillonite nanocomposite films via ionic liquids. *Carbohydrate Polymers,* **88**, pp. 1251-1257.

Mäki-Arvela, P., Anugwom, I., VirtanenI, P., Sjöholm, R. and Mikkola, J.P. 2010. Dissolution of lignocellulosic materials and its constituents using ionic liquids—A review. *Industrial Crops and Products,* **32**(3), pp. 175-201.

Mallakpour, S. and Rafiee, Z. 2011. New developments in polymer science and technology using combination of ionic liquids and microwave irradiation. *Progress in Polymer Science,* **36**(12), pp. 1754-1765.

Mazza, M., Catana, D.A., Vaca-Garcia, C. and Cecutti, C. 2009. Influence of water on the dissolution of cellulose in selected ionic liquids. *Cellulose,* **16**(2), pp. 207-215.

Mikkola, J.P., Kirilin, A., Tuuf, J.C., Pranovich, A., Holmbom, B., Kustov, L.M., Murzin, D.Y. and Salmi, T. 2007. Ultrasound enhancement of cellulose processing in ionic liquids: from dissolution towards functionalization. *Green Chemistry,* **9**(11), pp. 1229-1237.

Miyai, K., Nakamura, M., Tamura, K. and Murakani, S. 1997. Isotope effects of thermodynamic properties in four binary systems: water and DMSO or DMF. *Journal of solution chemistry,* **26**(10), pp. 973-980.

Moniruzzaman, M. and Ono, T. 2012. Ionic liquid assisted enzymatic delignification of wood biomass: A new 'green' and efficient approach for isolating of cellulose fibers. *Biochemical engineering journal,* **60**(0), pp. 156-160.

Montalbo-Lomboy, M. and Grewell, D. 2014. Rapid dissolution of switchgrass in 1-butyl-3-methylimidazolium chloride by ultrasonication. *Ultrasonics sonochemistry,* **22**, pp. 588-599.

Muhammad, A. 2004. Effect of prehydrolysis prior to kraft cooking on Swedish Spruce Wood. Master's thesis, Karlstads University, Sweden.

Muhammad, N., Man, Z., Bustam, M.A., Mutalib, M.I.A., Wilfred, C.D. and Rafiq, S. 2011. Dissolution and delignification of bamboo biomass using amino acid-based ionic liquid. *Appl. Biochem. Biotechnol.,* **165**, pp. 998-1009.

Muhammad, N., Man, Z. and Khalil, M.A.B. 2012. Ionic liquid- a future solvent for the enhances uses of wood biomass. *Eur.J.Wood.Prod.,* **70**, pp. 125-133.

Ninomiya, K., Kamide, K., Takahashi, K. and Shimizu, N. 2012. Enhanced enzymatic saccharification of kenaf powder after ultrasonic pretreatment in ionic liquids at room temperature. *Bioresource technology,* **103**(1), pp. 259-265.

Novoselov, N., Sashina, E., Petrenko, V. and Zaborsky, M. 2007. Study of dissolution of cellulose in ionic liquids by computer modeling. *Fibre Chemistry,* **39**(2), pp. 153-158.

Ohiro, K., Yashida, Y., Hayase, S., Itoh, T. 2012. Amino Acid Ionic Liquid as an Efficient Cosolvent of Dimethyl Sulfoxide to Realize Cellulose Dissolution at Room Temperature. *Chemistry Letters,* **41**(9), pp. 987-989.

Ohno, H. and Fukaya, Y. 2009. Task specific ionic liquids for cellulose technology. *Chemistry Letters,* **38**(1), pp. 2-7.

Olivier-Bourbigou, H., Magna, L. and Morvan, D. 2010. Ionic liquids and catalysis: Recent progress from knowledge to applications. *Applied Catalysis A: General,* **373**(1–2), pp. 1-56.

Olsson, C. and Westman, G. 2013. Wet spinning of cellulose from ionic liquid solutions-viscometry and mechanical perfomance. *Journal of Applied Polymer Science,***127**(6), pp. 4542-4548.

Pang, J., Liu, X., Zhang, X., Wu, Y. and Sun, R. 2013. Fabrication of cellulose film with enhanced mechanical properties in ionic liquid 1-Allyl-3-methyjiimidazolium chloride (AmimCl). *Materials,* **6**(4), pp. 1270-1284.

Parviainen, H., Parviainen, A., Virtanen, T., Kilpeläinen, I., Ahvenainen, P., Serimaa, R., Grönqvist, S., Maloney, T. and Maunu, S.L. 2014. Dissolution enthalpies of cellulose in ionic liquids. *Carbohydrate Polymers,* **113**(0), pp. 67-76.

Phillipp, B.S.W. 2009. Progress in cellulose research in the reflection of the Zellcheming Cellulose Symposia. *Macromolecular symposia,* **280**(1), pp. 4-15.

Pinkert, A., Marsh, K.N., Pang, S. and Staiger, M.P. 2009. Ionic liquids and their interaction with cellulose. *Chem.Soc.Rev.,* **109**, pp. 6712-6728.

Pu, Y., Jiang, N. and Ragauskas, A.J. 2007. Ionic liquid as a green solvent for lignin. *Journal of Wood Chemistry and Technology,* **27**(1), pp. 23-33.

Pu, Y., Hallac, B. and Ragauskas, A.J. 2013. *Plant Biomass characterization:Application of solution and solid state NMR spectroscopy.* pp 372-400. John Wiley & Sons, Ltd.

Qiu, Z., Aita, G.M. and Walker, M.S. 2012. Effect of ionic liquid pretreatment on the chemical composition, structure and enzymatic hydrolysis of energy cane bagasse. *Bioresource technology,***117**, pp. 251-256.

Quan, S., Kang, S., Chin, I. 2010. Characterization of cellulose fibers electrospun using ionic liquid. *Cellulose*, **17**, pp. 223-230.

Rayne, S. & Mazza, G. 2007. *Rapid dissolution of lignocellulosic plant materials in an ionic liquid.* volume 2 edn. Canada: Nature preceding.

Remsing, R.C., Swatloski, R.P., Rogers, R.D. and Moyna, G. 2006. Mechanism of cellulose dissolution in the ionic liquid 1-n-butyl-3-methylimidazolium chloride: a ^{13}C and $^{35/37}Cl$ NMR relaxation study on model systems. *Chemical communications,* (12), pp. 1271-1273.

Rogers, R.D. and Seddon, K.R. 2003. Ionic Liquids-solvents for the future? *Science,* **302**, pp. 792.

Rosenboom, J., Afzal, W. and Pausnitz, J.M. 2012. Solubilities of some organic solutes in 1-ethyl-3-methylimidazolium acetate. Chromatographic measurements and predictions from COSMO-RS. *The Journal of Chemical Thermodynamics,* **47**(0), pp. 320-327.

Ruan, M., Chen, J., Liu, D. and Xia, K. 2014a. Dissolution of pulp in room temperature ionic liquids: a comparative study. *wood and fiber science,* **46**(2), pp. 206-215.

Sant'ana Da Silva, A., Lee, S., Endo, T. and P.S. Bon, E. 2011. Major improvement in the rate and yield of enzymatic saccharification of sugarcane bagasse via pretreatment with the ionic liquid 1-ethyl-3-methylimidazolium acetate ([Emim] [Ac]). *Bioresource technology,* **102**(22), pp. 10505-10509.

Santos, N.M., Puls, J., Saake, B. and Navard, P. 2013. Effects of nitren extraction on a dissolving pulp and influence on cellulose dissolution in NaOH–water. *Cellulose,* pp. 1-14.

Sasaki, M., Adschiri, T. and Arai, K. 2003. Fractionation of sugarcane bagasse by hydrothermal treatment. *Bioresource technology,* **86**(3), pp. 301-304.

Sathitsuksanoh, N., George, A., Zhang, Y. and Percival, H. 2013. New lignocellulose pretreatments using cellulose solvents: a review. *Journal of Chemical Technology and Biotechnology,* **88**(2), pp. 169-180.

Sescousse, R., Gavillion, R. and Budtova, T. 2011. Aerocellulose from cellulose–ionic liquid solutions: Preparation, properties and comparison with cellulose–NaOH and cellulose–NMMO routes. *Carbohydrate Polymers,* **83**(4), pp. 1766-1774.

Shafiei, M., Zilouei, H., Zamani, A., Taherzadeh, M.J. and Karimi, K., Enhancement of ethanol production from spruce wood chips by ionic liquid pretreatment. *Applied Energy*, **102**, pp. 163-169.

Shakeri, A. and Staiger, M.P. 2010. Phase Transformations in Regenerated Microcrystalline Cellulose Following Dissolution by an Ionic Liquid. *BioResources,* pp. 979-989.

Shill, K., Padmanabhan, S., Xin, Q., Prausnitz, J.M. and Clark, D.S. 2010. Ionic liquid pretreatment of cellulosic biomass: enzymatic hydrolysis and IL recycle. *Biotechnology and Bioengineering,* **108**(3), pp. 511-520.

Singh, S., Simmons, B.A. and Vogel, K.P. 2009. Visualization of biomass solubilization and cellulose regeneration during ionic liquid pretreatment of switchgrass. *Biotechnology and Bioengineering*, **104**(1), pp. 68-75.

Sixta. H. 2006. Handbook of Pulp. 2 edn. Austria: Wiley.

Sjoström, E. 1981. Wood chemistry: fundamentals and applications. pp. 169-189.

Stark, A., Sellin, M., Ondruschka, B. and Massonne, K. 2012. The effect of hydrogen bond acceptor properties of ionic liquids on their cellulose solubility. *Science China Chemistry,* **55**(8), pp. 1663-1670.

Stefanesu, C., Daly, W.H. and Negulescu, I.I. 2012. Biocomposite films prepared from ionic liquid solutions of chitosan and cellulose. *Carbohydrate Polymers,* **87**(1), pp. 435-443.

Su, W. 2012. A study of cellulose dissolution in ionic liquid-water brines, PhD thesis, Umea University.

Sun, N. 2010. Dissolution and processing of cellulosic materials with ionic liquids: fundamentals and applications, PhD thesis, University of Alabama.

Sun, N., Rahman, M., Qin, Y., Maxim, M.L., Rodriguez, H. and Rogers, R.D. 2009. Complete dissolution and partial delignification of wood in the ionic liquid 1-ethyl-imidazolium acetate. *Green Chem.,* **11**, pp. 646-656.

Sun, N., Rodriguez, H., Rahman, M. and Rogers, R.D. 2011. Where are ionic liquid strategies most suited in the pursuit of chemicals and energy from lignocellulosic biomass? *Chem.Commun.,* **47**, pp. 1405-1421.

Swatloski, R.P., Spear, S.K., Holbrey, J.D. and Rogers, R.D. 2002. Dissolution of cellose with ionic liquids. *Journal of the American Chemical Society*, **124**(18), pp. 4974-4975.

Tang, S., Baker, G.A., Ravula, S., Jones, J.E., and Zhao, H. 2012. PEG-functionalized ionic liquids for cellulose dissolution and saccharification. *Green Chemistry*, **14**(10), pp. 2922-2932.

Tian, D., Han, Y., Lu, C., Zhang, X. and Yuang, G. 2014. Acidic ionic liquid as "quasi-homogeneous" catalyst for controllable synthesis of cellulose acetate. *Carbohydrate Polymers,* **113**(0), pp. 83-90.

Turner, M.B., Spear, S.K., Holbrey, J.D. and Rogers, R.D. 2004. Production of bioactive cellulose films reconsituted from ionic liquids. *Biomacromolecules*, **5**(4), pp. 1379-1384.

Ueki, T. and Watanabe, M. 2008. Macromolecules in ionic liquids: progress, challenges, and opportunities. *Macromolecules,* **41**(11), pp. 3739-3749.

Vancov, T., Alston, A., Brown, T. and Mcintosh, S. 2012. Use of ionic liquids in converting lignocellulosic material to biofuels. *Renewable Energy*, **45**(0), pp. 1-6.

Varanasi, P., Singh, P., Auer, M., Adams, P.D., Simons, B.A. and Singh, S. 2013. Survey of renewable chemicals produced from lignocellulose biomass during IL pretreatment. *Biotechnology for Biofuels,* **6**(14), pp. 1-9.

Vitz, J., Erdmenger, T., Haensch, C. and Schubert, U.S. 2009. Extended dissolution studies of cellulose in imidazolium based ionic liquids. *Green Chem.,* **11**(3), pp. 417-424.

Wang, H., Gurau, G., Pingali, S.V., O'Neill, H.M., Evans, B.R., Urban, V.S., Heller, W.T. and Rogers, R.D. 2014. Physical insight into switchgrass dissolution in ionic liquid 1-ethyl-3-methylimidazolium acetate. *ACS sustainable chemistry and engineering,* **2**(5), pp. 1264-1269.

Wang, H., Gurau, G. and Rogers, R.D, 2012. Ionic liquid processing of cellulose. *Chemical Society Reviews,* **41**(4), pp. 1519-1537.

Wang, X., Li, H., Cao, Y. and Tang, Q. 2011. Cellulose extraction from wood chip in an ionic liquid 1-allyl-3-methylimidazolium chloride (AmimCl). *Bioresource technology,* **102**(17), pp. 7959-7965.

Wang, Y. and Cao, X. 2012. Extracting keratin from chicken feathers by using a hydrophobic ionic liquid. *Process Biochemistry,* **47**(5), pp. 896-899.

Wei, L., Li, K., Ma, Y. and Hou, X. 2012. Dissolving lignocellulosic biomass in a 1-butyl-3-methylimidazolium chloride–water mixture. *Industrial Crops and Products,* **37**(1), pp. 227-234.

Welton, T. 1999. Room-temperature ionic liquids. Solvents for synthesis and catalysis. *Chemical Reviews,* **99**(8), pp. 2071.

Wendler, F., Todi, L. and Meister, F. 2012a. Thermostability of imidazolium ionic liquids as direct solvents for cellulose. *Thermochimica Acta,* **528**(0), pp. 76-84.

Wendler, F., Todi, L. and Meister, F. 2012b. Thermostability of imidazolium ionic liquids as direct solvents for cellulose. *Thermochimica Acta,* **528**(0), pp. 76-84.

Willard, H.H., Merritt, L.L., Dean, J.A. and Settle, F.A. 1986. *Instrumental methods of analysis.* 6 edn. India: CBS Publisher and Distributors.

Willfor, S., Sundberg, A., Hemming, J. and Holmbom, B. 2005. Polysaccharides in some industrially important hardwood species. *Wood Sci Technology,* **39**, pp. 601-617.

Wu, B., Liu, W.W., Zhang, Y.M. and Wang, H.P. 2009a. Do we understand the recyclability of ionic liquids? *Chemistry-A European Journal*, **15**(8), pp. 1804-1810.

Wu, R., Wang, X., Li, F., Li, H. and Wang, Y. 2009b. Green composite films prepared from cellulose, starch and lignin in room-temperature ionic liquid. *Bioresource technology*, **100**(9), pp. 2569-2574.

Xiao, W., Chen, Q., Wu, Y., Wu, T. and Dai, L. 2011. Dissolution and blending of chitosan using 1,3-dimethylimidazolium chloride and 1-H-3-methylimidazolium chloride binary ionic liquid solvent. *Carbohydrate Polymers*, **83**(1), pp. 233-238.

Xie, H., King, A., Kilpeläinen, I., Granstrom, M. and Argyropoulos, D.S. 2007. Thorough chemical modification of wood-based lignocellulosic materials in ionic liquids. *Biomacromolecules*, **8**(12), pp. 3740-3748.

Xie, H., Li, S. and Zhang, S. 2005. Ionic liquids as novel solvents for the dissolution and blending of wool keratin fibers. *Green Chemistry*, **7**(8), pp. 606-608.

Xing, L., Wu, Z. and Gong, G. 2013. Dissolution of cotton cellulose with ionic liquids 1-butyl-3-methylimidazolium chloride and 1-allyl-3-methylimidazolium chloride to prepare reducing sugar. *Journal of Energy Engineering*,**140**(2), pp. 1-12.

Xiong, R., Hameed, N. and Guo, Q. 2012. Cellulose/polycaprolactone blends regenerated from ionic liquid 1-butyl-3-methyl imidazolium chloride. *Carbohydrate Polymers*, **90**(1), pp.575-582.

Xu, A., Zhang, Y., Zhao, Y. and Wang, J. 2013. Cellulose dissolution at ambient temperature: Role of preferential solvation of cations of ionic liquids by a cosolvent. *Carbohydrate Polymers*, **92**(1), pp. 540-544.

Xu, F., Shi, Y. and Wang, D. 2012. Enhanced production of glucose and xylose with partial dissolution of corn stover in ionic liquid, 1-Ethyl-3-methylimidazolium acetate. *Bioresource technology*, **114**(0), pp. 720-724.

Yang, Z. and Pan, W. 2005. Ionic liquids: Green solvents for nonaqueous biocatalysis. *Enzyme and microbial technology*, **37**(1), pp. 19-28.

Yang, F., Li, L., Li, Q., Tan, W., Liu, W. and Xian, M. 2010. Enhancement of enzymatic in situ saccharification of cellulose in aqueous-ionic liquid media by ultrasonic intensification. *Carbohydrate Polymers*, **81**(2), pp. 311-316.

Yue, Z., Xin, L., Xuan, Z., Feng, L.H. and Muhuo, Y. 2012. Current status of applications of ionic liquids for cellulose dissolution and modifications: review. *International Journal of Engineering Science and Technology*, **4**(7), pp. 3556-3571.

Zavrel, M., Bross, D., Funke, M., Buchs, J. and Spiess, A.C. 2009. High-throughput screening for ionic liquids dissolving (ligno-)cellulose. *Bioresource technology*, **100**(9), pp. 2580-2587.

Zhang, H., Wang, Z., Zhang, Z., Wu, J., Zhang, J. and He, J. 2007. Regenerated cellulose/multiwalled-carbon-nanotube composite fibers with enhanced mechanical properties prepared with the ionic liquid 1-allyl-3-methylimidazolium chloride. *Adv. Mater.*, **19**(5), pp. 698-704.

Zhang, H., Wu, J., Zhang, J. and He, J. 2005. 1-Allyl-3-methylimidazolium chloride room temperature ionic liquid: A new and powerful nonderivatizing solvent for cellulose. *Macromolecules*, **38**(20), pp. 8272-8277.

Zhang, J., Zhang, H., Wu, J., Zhang, J., He, J. and Xiang, J. 2010a. NMR spectroscopic studies of cellobiose solvation in EmimAc aimed to understand the dissolution mechanism of cellulose in ionic liquids. *Physical Chemistry Chemical Physics*, **12**(8), pp. 1941-1947.

Zhang, S., Li, F.X. and Xu, J.Y. 2010b. Structure and properties of cellulose fibers produced from NaOH/PEG treated cotton linters. *Iranian Polymer*, **19**(12), pp. 949.

Zhang, Z. and Zhao, Z.K. 2010. Microwave-assisted conversion of lignocellulosic biomass into furans in ionic liquids. *Bioresource technology*, **101**(3), pp. 1111-1114.

Zhao, Q., Yam, R.C.M., Zhang, B., Yang, Y., Cheng, X. and Li, R.K.Y. 2009. Novel all-cellulose ecocomposites prepared in ionic liquids. *Cellulose*, **16**(2), pp. 217-226.

Zhao, Y., Wang, J., Liu, X., and Zhang, S. 2012a. Effects of cationic structure on cellulose dissolution in ionic liquids: A molecular dynamics study. *ChemPhysChem,* **13**(13), pp. 3126-3133.

Zhao, Y., Liu, X., Wang, J. and Zhang, S. 2013. Insight into co-solvent effect of cellulose dissolution in imidazolium-based ionic liquid systems. *Phys.Chem.B,* **117**(30), pp. 9042-9053.

Zhao, D., Fu, L., Ren, P., Li, J., and Li, H. 2012b. The dissolution of cellulose in N-allylpyridinium chloride ionic liquid/organic solvent. *Gaofenzi Cailiao Kexue Yu Gongcheng/Polymeric Materials Science and Engineering,* **28**(7), pp. 31-34.

Zhao, D., Li, H., Zhang, J., Fu, L., Liu, M., Fu, J. and Ren, P. 2012c. Dissolution of cellulose in phosphate-based ionic liquids. *Carbohydrate Polymers,* **87**(2), pp. 1490-1494.

Zhao, H., Jones, C.L., Baker, G.A., Xia, S., Olubajo, O. and Person, V.N. 2009. Regenerating cellulose from ionic liquids for an accelerated enzymatic hydrolysis. *Journal of Biotechnology,* **139**(1), pp. 47-54.

Zhong, C., Wang, C., Huang, F., Jia, H. and Wei, P, 2013. Wheat Straw Cellulose Dissolution and Isolation by tetra-n-Butylammonium Hydroxide. *Carbohydrate Polymers,* **94**(1), pp. 38-45.

Zhu, S. 2008a. Perspective use of ionic liquids for the efficient utilization of lignocellulosic materials. *Journal of Chemical Technology and Biotechnology,* **83**, pp. 777.

Zhu, S., 2008b. Use of ionic liquids for the efficient utilization of lignocellulosic materials. *Journal of Chemical Technology and Biotechnology,* **83**(6), pp. 777-779.

Zhu, S., Wu, Y., Chen, Q., Yu, Z., Wang, C., Jin, S., Ding, Y. and Wu, G. 2006. Dissolution of cellulose with ionic liquids and its application: a mini-review. *Green Chem.,* **8**(4), pp. 325-327.

Zhu, H.X., Li, J.S., Xu, R. and Yang, S.Y. 2012. An environmental friendly approach for the synthesis of the ionic liquid 1-ethyl-3-methylimidazolium acetate and its dissolubility to 1, 3, 5-triamino-2, 4, 6-trinitrobenzene. *Journal of Molecular Liquids,* **165**(0), pp. 173-176.

APPENDICES

Structural changes in South African *Eucalyptus* pulp after dissolution in [Emim][OAc]/ co-solvent mixtures.

Z. Tywabi[a,*], N. Deenadayalu [a], B. Sithole[b], H. Wang[c], O. A. Cojocaru[c], and R. D. Rogers[c]

[a]Department of Chemistry, Faculty of Applied Sciences, Durban University of Technology, KwaZulu Natal, Durban, South Africa, 4001; .[b]Council for Scientific and Industrial Research, Natural Resources and Environment, Forestry and Forest Products Research Centre, KwaZulu Natal, Durban, South Africa, 4013; [c]Centre for Green Manufacturing and Department of Chemistry, The University of Alabama, Tuscaloosa, AL 35487, United States of America.

**Corresponding author:ztywabi@gmail.com*

ABSTRACT

Mixtures of the ionic liquid (IL) 1-ethyl-3-methylimidazolium acetate ([Emim][OAc]) and dimethylsulfoxide (DMSO) and dimethylformamide (DMF) were used to dissolve the South African *Eucalyptus* raw (unbleached) and final (bleached) dissolving pulp. The IL/co-solvent mixtures were able to dissolve the raw and final pulp samples at 120 ˚C for 6 hours with continuous stirring and heating in an oil-bath. Regenerated cellulose was obtained by adding a 1:1 (v/v) water/acetone mixture followed by filtration. The IL/DMF mixture gave higher cellulose recoveries of 41.88 % for the raw pulp and 49.89 % for the final pulp sample, while IL/DMSO mixture gave a recovery of only15.25 % for the raw pulp sample and 36.25 % for the final pulp sample. The regenerated cellulose materials were characterized by SEM, FTIR, TGA and pXRD, and compared with microcrystalline standard of cellulose (MCC). It was also observed that the addition of co-solvents decreased ILs viscosity, facilitating the dissolution that led to additional swelling and destruction of cellulose structure and intermolecular interactions: SEM and pXRD results showed that after dissolution the crystalline structure of cellulose I (native form) has been transformed to cellulose II (amorphous) structure.

Keywords: dissolving pulp, cellulose, ionic liquids, co-solvent

INTRODUCTION

Cellulose is the most widely used natural organic chemical in earth, and therefore our most important biorenewable resource (Liu et al., 2010; Cao et al., 2009; Lindman et al., 2010). Industrial grade chemical cellulose (bleached sulphite/ dissolving pulp) refers to the pulp that contains more than 90% of pure cellulose. Dissolving pulp comes from wood using pre-hydrolysis kraft or acid sulphite processes (Biemann, 1993; Dafchachi&Resalati, 2012). Apart from cellulose, wood also contains other compounds such as lignin, hemicelluloses and a small fraction of organic extractives and these wood components except cellulose are regarded as troublemakers, and efforts are made to remove them from production processes (Dafchachi & Resalati , 2012; Sjostrom , 1981). The preparation of dissolving cellulose (dissolving pulp) involves the cooking of wood in a chemical solution at a temperature range

of 130-160 ˚ C to remove all non-cellulosic compounds in the fibers to obtain the raw (unbleached) pulp and to obtain the final pulp, and the raw dissolving pulp samples are then bleached at different stages *i.e.*, chlorine dioxide, oxygen and hydrogen peroxide stages to improve its brightness and purity. The end uses of dissolving pulp include cellophane, rayon, cellulose esters and cellulose ethers (Sjostrom, 1981). The main characteristics of the dissolving pulps are the higher purity in cellulose, low content of hemicelluloses, lignin, extractive and ashes. In addition they have uniform molecular weight distribution; high brightness and high reactivity towards specific chemicals, with the disadvantages such as use of harsh conditions, serious environmental problems because they cannot be recovered and reused (Swatloski et al., 2002; Hazarika et al., 2012; Zhang et al., 2005). Due to environmental concerns about the dangerous gases formed during the pulping process, it is essential to develop greener solvents for cellulose dissolution under mild conditions (Hermanutz et al., 2008; Liebert&Heinze, 2008; Liu et al., 2011). The discovery that ionic liquids (ILs) can dissolve cellulose provides new opportunities to utilize cellulose/pulp (Zhao et al., 2005; Swatloski et al., 2002; Pinkert et al., 2009). The dissolved cellulose can subsequently be precipitated from the IL solution by adding water or protic organic solvents such as ethanol.

Many kinds of ILs have been reported as cellulose solvents in literature (Liu et al., 2012; Xu et al., 2013; Xu et al., 2012; Zhao et al., 2012a; Zhao et al., 2012b). Alkyl phosphate-based and acetate-based ILs having lower viscosities is reported in literature to have the ability to dissolve cellulose under mild conditions (Zhao et al., 2005). For example, 1-ethyl-3-methylimidazolium acetate ([Emim][OAc]) was demonstrated to be able to dissolve biomass more efficiently than any other ILs (Kosan et al., 2008; Ang et al., 2011; Casas et al., 2012a; Casas et al., 2012b; Ding et al., 2012; Duan et al., 2011; Karatzos et al., 2012; Kilpeläinen et al., 2007; Phillips et al., 2004; Wu et al., 2009; Sun et al., 2009). Xu et al. (2013) reported several highly effective cellulose solvents consisting of 1-butyl-3-methylimidazolium acetate ([Bmim][OAc]) and aprotic solvents (*e.g.*, DMSO, DMA and DMF), and they suggested that the enhanced dissolution of cellulose resulted from the preferential solvation of cation of the IL by the co-solvents because the co-solvents are aprotic solvents that only solvate the (+) ions which then results in little solvation. Therefore, cellulose can be dissolved in the IL/co-solvent systems at ambient temperature with high solubility. These solvent systems are reported to show many advantages such as, non derivatization, low viscosity, and high dissolution speed (Zhao et al., 2013). Liu et al., (2010) investigated the dissolution of cellulose in [Emim][OAc] and in other solvents (*e.g.* water and methanol) and they proposed that the dissolution was promoted by the favourable interactions between the IL anions and hydroxyl protons of glucose.

(Kilulya et al., 2011) used the IL [Emim][OAc] to dissolve the South African *Eucalyptus* dissolving pulp and he obtained a percentage yield of regenerated cellulose to be 15% after dissolution in IL at 90 °C for 45 minutes. A literature search reveals that there is no published work on the dissolution effect of the IL [Emim][OAc] and the aprotic co-solvents DMSO and DMF for the South African raw and final dissolving pulp samples used in this work. In the present work, two aprotic co-solvents DMSO and DMF were chosen to study the effect of co-solvent addition to process bleached and unbleached dissolving pulp in [Emim][OAc]. Cellulose-rich materials were regenerated by adding the mixture of water/acetone (1:1, v/v), which were then characterized by SEM, TGA, FT-IR, and pXRD.

EXPERIMENTAL

Materials

The pulp sample used in this study was the South African *Eucalyptus* ED5CW raw and final pulp samples were supplied by SAPPI Saiccor mill from the South Coast of Durban, South Africa. The pulp samples were dried in the vacuum at 50 °C for 12 hours to remove the water, and then ground into small particles using a mortar and pestle before use. The IL [Emim][OAc], with a purity of > 95 %, was purchased from IOLITEC USA. Prior using, the ionic liquid was dried at 50 °C under high vacuum line for 12 hours; and its water content was determined by Coulometric Karl Fischer and found to be 10435 ppm. Dimethylsulfoxide (DMSO) and dimethylformamide (DMF) with a purity of 99.9 % were purchased from Sigma Aldrich and were used as received. Nylon membrane filter paper, 10 and 0.8 µm, was purchased from Sterlitech Corporation, USA. Microcystalline cellulose (MCC) standard, with depolymerization degree of 270 and purity of 99.9 %, was purchased from Sigma Aldrich.

Dissolution and regeneration of cellulose

Approximately 5 wt.% of the previously dried and ground bleached or unbleached dissolving pulp samples were dissolved in [Emim][OAc]/DMSO or [Emim][OAc]/DMF mixtures (the concentration of co-solvents used in the mixtures was 25 wt. %), with stirring at 120 °C for 6 hours in an oil bath. Once dissolution was completed, the samples were cooled to room temperature. The cooled solutions were then washed 3 times with 50 mL mixture of water/acetone (1:1, v/v). The solution was then centrifuged in a Clays Adams centrifuge at 700 rpm for 10 minutes. It was observed that a white cellulosic material settled at the bottom of the centrifuge tube. The top liquid phase was taken out and the cellulosic material was further washed with 50 mL of the mixture of water/acetone twice more. The cellulosic material was finally obtained by filtration using a Nylon membrane filter paper with pore size of 10 µm, then dried in an oven at 80 °C for one hour. The dried weight of the precipitate was recorded and the percentage recovery of the cellulose was calculated by using equation (1) taken from literature (Brown et al., 2012 thesis):

$$\text{Cellulosic material recovery (\%)} = \frac{\text{mass of regenerated cellulosic material (g)}}{\text{mass of pulp for dissolution (g)}} \times 100\% \quad (1)$$

Recycling of ionic liquid

The ionic liquid liquor (filtrate) obtained after washing was transferred into a round bottom flask attached to a rotary evaporator and distilled to remove any water and acetone remained in the mixture. The [Emim][OAc] recovered was then dried under vacuum at 50 °C for 12 hours, characterized by FTIR and ^{1}H NMR and compared with the IL spectrum before dissolution process.

Characterization

Infrared spectra of MCC standard and regenerated cellulose samples from [Emim][OAc]/DMF or DMSO mixtures were collected using Bruker Alpha FTIR spectrometer, and spectra were obtained in the range of ν_{max} = 400–4000 cm^{-1}. The cellulose samples for the bleached and unbleached pulp regenerated from IL/DMSO and IL/DMF mixtures were cut and ground into very small particles and characterized by FTIR.

SEM images of the regenerated cellulose samples were taken at 300 x magnifications using a Jeol 6310 Electron Probe analyser SEM instrument which was operated at 5-10 Kv accelerating voltage. Prior to imaging, the samples were sputter-coated with gold to make the fibers electrical conductive, avoiding degradation and build -up of charge on them.

The diffraction patterns of the regenerated cellulose samples and MCC standard were obtained using a Bruke D2 Phaser Powder XRD instrument. The patterns were recorded using a Cu-Ka radiation at 40kV and the range for angle of diffraction was $2\theta = 5\text{-}40^{o}$.

Thermal analysis was recorded with a Perklin Elmer TGA analyser. Approximately 10 mg of the regenerated cellulose samples were put in the pans and analysis was carried out by the Thermo Analyzer at a heating rate of 5 °C/min under continuous nitrogen flow in a temperature range from 25 °C to 600 °C, with an isotherm process at 75 °C for 30 min to remove any absorbed water.

RESULTS AND DISCUSSIONS

Dissolution and regeneration of cellulose

The dissolution of the bleached and unbleached pulp in [Emim][OAc]/DMSO and [Emim][OAc]/DMF mixtures at 120 °C was studied and the cellulose was regenerated by adding the mixture of water/acetone (1:1, v/v), and separated from the liquid phase by centrifugation followed by filtration, which was further dried in the oven. The cellulose yield was calculated and is shown in Table 1.

Table 1. Percentage yield of regenerated cellulose after dissolution of raw and final pulp samples in [Emim][OAc]/DMSO and DMF mixtures

IL or IL + co-solvent mixtures	% Raw (unbleached) pulp	% Final (bleached) pulp
[Emim][OAc]	10.54 %	35.29 %
[Emim][OAc]/DMSO	15.25 %	41.88 %
[Emim][OAc]/DMF	36.25 %	49.89 %

The [Emim][OAc]/DMF mixture gave higher cellulose yields for both the bleached and unbleached pulps than [Emim][OAc]/DMSO mixture and pure [Emim][OAc]. This can be attributed to the fact that DMSO has a higher dielectric constant than DMF which makes DMSO more polar than DMF, and this has some effect on the dissolution process because DMSO has a stronger ion-dipole interaction resulting in the force of attraction becoming stronger between ions in a solution and the dipole-dipole interaction (hydrogen bonding) between solvent molecules. This effect results in the decrease in cellulose solubility because DMSO forms competing hydrogen bond to the macromolecular chains of cellulose (Swatolski et al., 2002; Cao et al., 2009). This has been found to be consistent with the literature reports showing that solvents with higher dielectric constants provide stronger ion-solvent interactions with ILs, which can strongly affect or extremely reduce the viscosity of ILs solutions (Lv et al., 2012). The viscosity of the IL plays an important role in the dissolution speed (Fukaya et al., 2006). Addition of co-solvents results in a reduction of the viscosity of the mixture, and thus leads to an acceleration of the dissolution process due to facilitated diffusion, thereby enhancing further processing of the polymer solution (Liu et al., 2008; Froschauer et al., 2013).

Dissolution of cellulose in ILs is attributed to their ability to break the extensive network of hydrogen bonds existing in the cellulose. [Emim][OAc] disrupts the hydrogen bonding interactions present in the cellulose allowing it to diffuse into the interior of the cellulose, which then results in the complete dissolution of cellulose (Kilpainen et al., 2007).

The higher cellulose recoveries for the bleached pulp *vs.* the unbleached pulp may also be due to the fewer amounts of hemicelluloses and lignin content of 1.40% present in the bleached pulp compared to 3.60 % in the unbleached pulp.

FTIR Spectroscopy of the regenerated cellulose fibers

Figure 1. illustrates the spectra of cellulose regenerated from the raw pulp dissolved in [Emim][OAc]/DMSO (black spectrum) and [Emim][OAc]/DMF (red spectrum) mixtures compared to the MCC standard of cellulose (pink spectrum) while Figure 2 illustrates the spectra of cellulose regenerated from the final pulp dissolved in [Emim][OAc]/ DMSO and [Emim][OAc]/DMF compared to MCC standard.

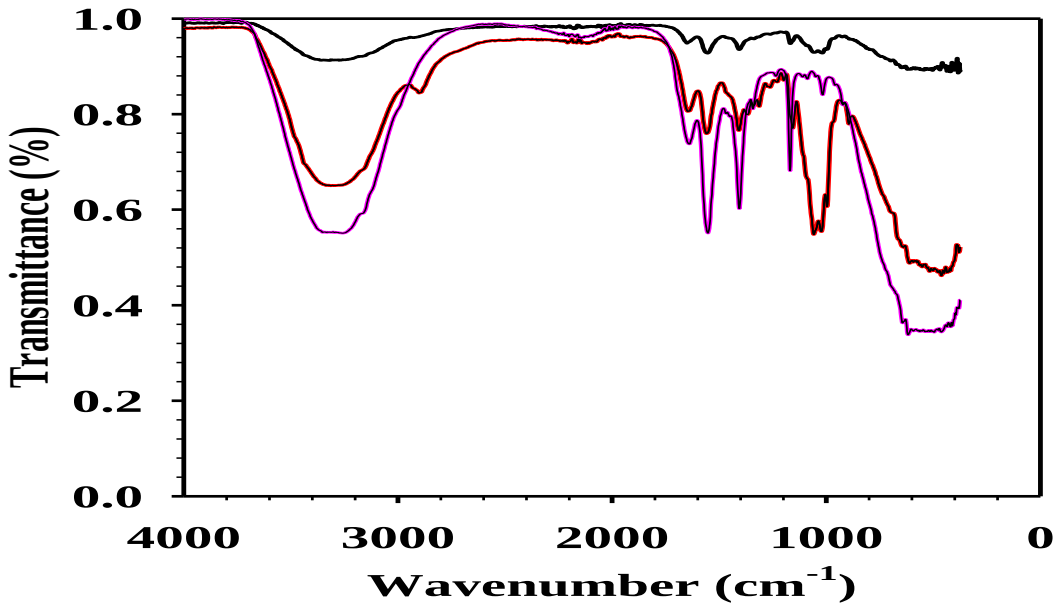

Figure 1. FTIR spectra of cellulose regenerated from the raw pulp dissolved in [Emim][OAc]/ DMSO (black) and [Emim][OAc]/ DMF (red) mixtures compared to the MCC standard of cellulose (pink).

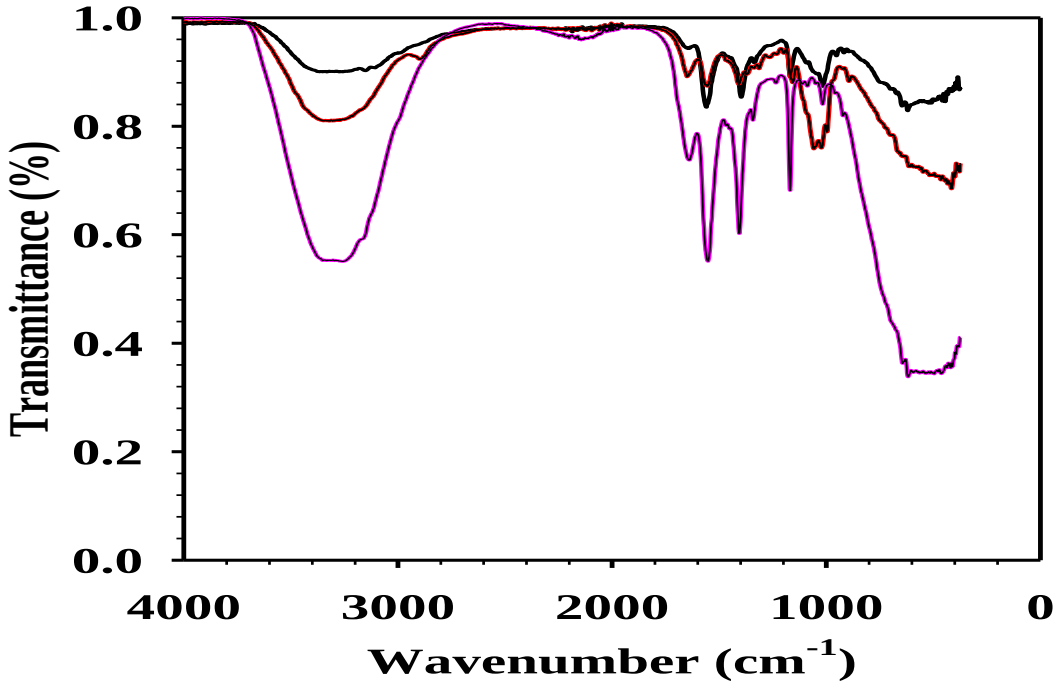

Figure 2. FTIR spectra of cellulose regenerated from the final pulp dissolved in [Emim][OAc]/DMSO (black) and [Emim][OAc]/DMF (red) mixtures compared to the MCC standard of cellulose (pink).

From Figures 1 and 2, it can be seen that there are no significant difference between the FTIR spectra of the regenerated cellulosic materials from raw pulp and final pulp dissolved in [Emim][OAc]/DMSO and [Emim][OAc]/DMF mixtures and are in excellent agreement with the MCC standard (reference spectrum of cellulose) with all the relevant bond vibrations, including OH-stretching which appears between (~3400-3200 cm^{-1}) and is a strong broad absorption indicating a hydrogen bonding which indeed takes place between repeating units within the cellulose matrix (Lateef et al., 2009; Mahadeva & Kim, 2012). C-H stretching can be seen as a sharp absorption at (~3100-2900 cm^{-1}) (Lateef et al., 2009; Mahadeva & Kim, 2012; Kuzmina, 2012) and C-O stretching (~ 1400-1300 cm^{-1}) are clearly visible in all the spectrums (Kuzmina, 2012). A small peak at ~1400 cm^{-1} in both of the spectra relates to the CH_2 symmetric bending. It can also be noted that the absorption peak referred to CH_2 scissoring motion was shifted from higher intensity to lower intensity upon regeneration which indicates the destruction of the intermolecular hydrogen bond involving O at C_6 (Mahadeva & Kim, 2012), compared with the results of Qiu et al., (2012) reported in literature. Since there is no absorption band for aromatic skeletal vibration in lignin observed at around 1550-1640 cm^{-1} which confirms the absence of lignin in the pulp samples. [Emim][OAc]/ co-solvents removed the lignin in the regenerated cellulose material.

The [Emim][OAc] was recovered in excellent yield, > 99 %. The FTIR spectrum of the recovered IL was observed to be in no good agreement with the dried IL before dissolution (reference FTIR spectra), with the only difference being an increase in the OH absorption, which reflects both the use of water in the process chemistry and the hygroscopic nature of the IL.

Powdered X-Ray diffraction

Figure 3, illustrates the angle of X-ray diffractograms of MCC standard native cellulose (pink diffractogram) and cellulose fibers of raw pulp regenerated from [Emim][OAc]/ DMSO (black diffractogram) and from [Emim][OAc]/ DMF mixture (red diffractogram).
Figure 4, shows the X-ray diffraction curves of MCC standard native cellulose (pink diffractogram) and cellulose fibers of final pulp regenerated from [Emim][OAc]/DMSO (black diffractogram) and from [Emim][OAc]/DMF mixture (red diffractogram).

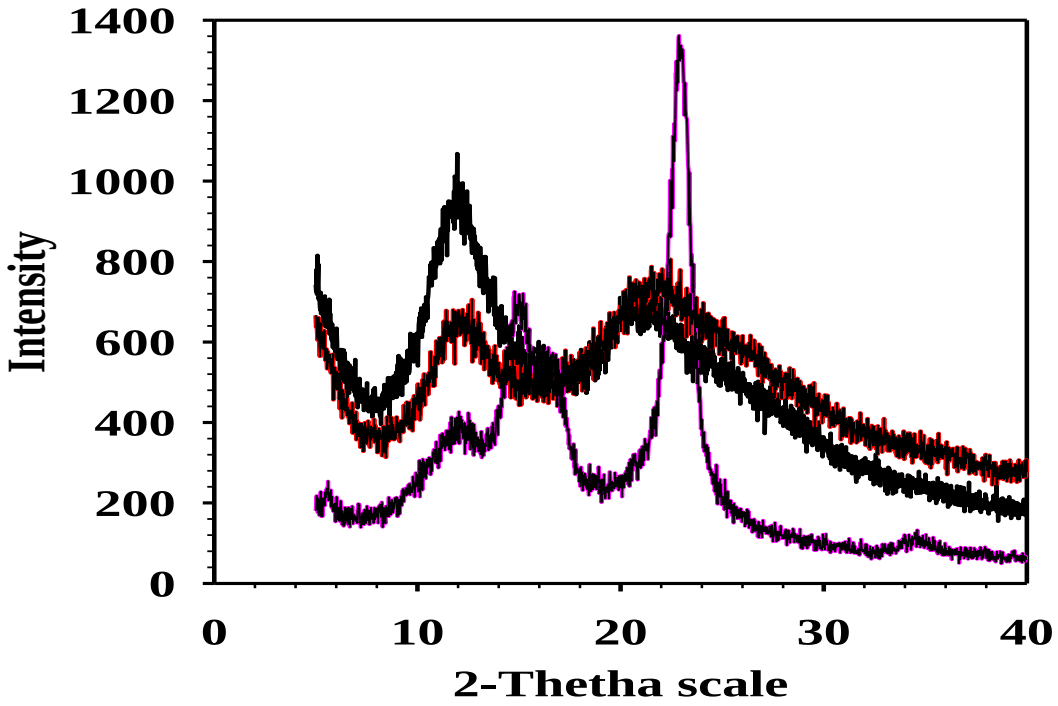

Figure 3. PXRD diffractograms of cellulose fibers regenerated from raw pulp in [Emim][OAc]/DMF and DMSO mixtures compared to MCC standard.

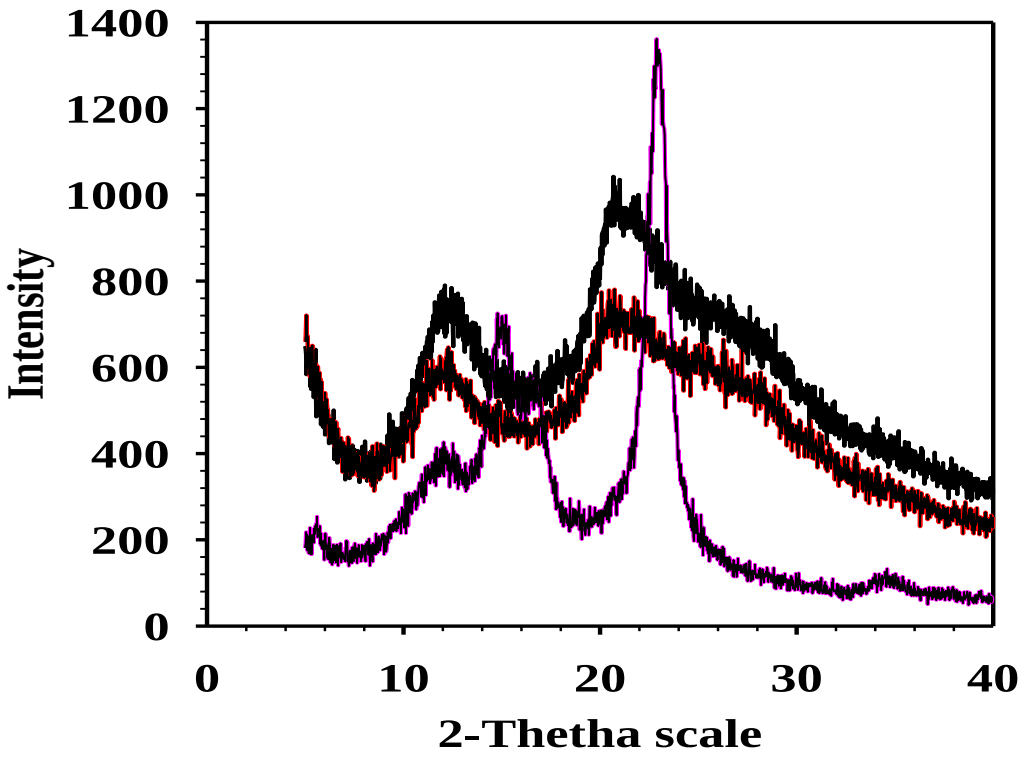

Figure 4. PXRD diffractograms of cellulose fibers regenerated from bleached pulp in [Emim][OAc]/ DMF and DMSO mixtures compared to MCC standard.

The diffraction curve of native cellulose is of typical cellulose I structure. In both Figures 3 and 4, it can be seen that it has strong crystalline peaks at 2θ = 15°, 17° and 23° and weak crystalline peak at 35° (Lan et al., 2011). After dissolution and regeneration, the diffraction curves of regenerated cellulose samples shown in figures 3 and 4, are of the typical diffraction patterns of cellulose II by the presence of the broad crystalline peaks at around 21°. The pXRD scans in Figures 3 and 4 shows only small changes in the morphology after regeneration. The degree of crystallinity for both the final and raw pulp appears to be slightly decreased after dissolution and regeneration from [Emim][OAc]/DMSO and DMF mixtures. The decrease in the intensity of the diffraction peaks implies the transformation of cellulose I to cellulose II. This happens because of the IL, which rapidly broke intermolecular and intra hydrogen bonds and destroyed the original crystalline forms. Similar results have been reported by (Sun et al., 2009; Mäki-Arvela et al., 2010) where they noticed a decrease in the X-ray peak intensity and the shift of the peak position to the left when cellulose 1 transformed to cellulose II after dissolution in [Emim][OAc].

Morphology of regenerated cellulose

The detailed morphology of the regenerated cellulose samples was observed using a SEM microscope and the images are shown in Figure 5.

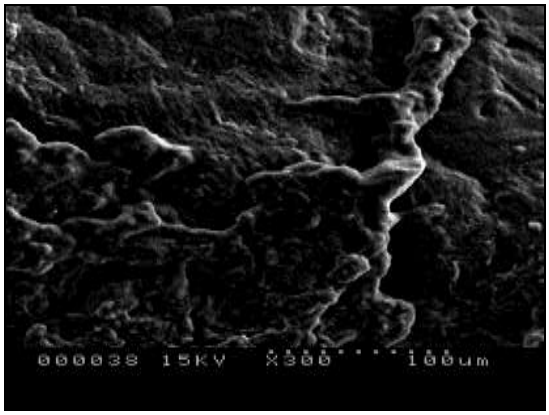

A

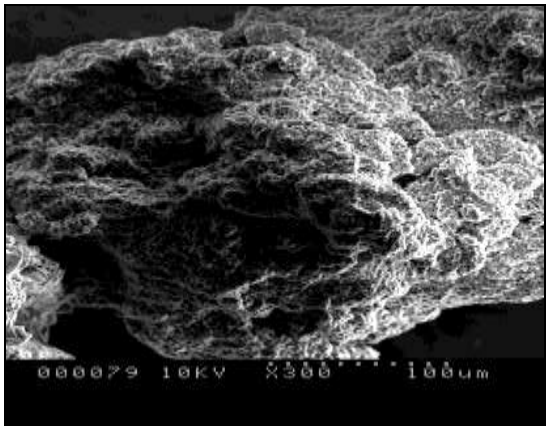

B

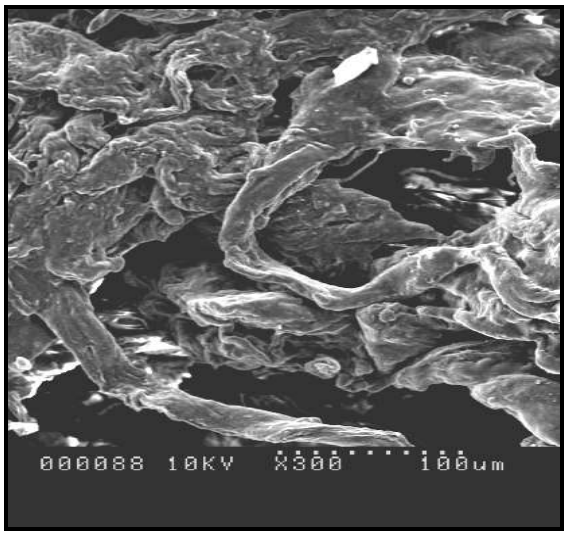

C

Figure 5. SEM photographs of the cellulose regenerated from raw pulp in A) [Emim][OAc]/DMSO mixture,and the cellulose regenerated from final pulp in B) [Emim][OAc]/DMF mixture compared to the pure cellulose sample C.

It can be seen that the fibers were disordered and curly for the fibers regenerated from [Emim][OAc]/DMF (B) and the fibers regenerated from [Emim][OAc]/DMSO (A) mixtures, most probably due to the removal of lignin and the decrease of cellulose crystallinity which have already been confirmed by FTIR and pRXD . In both cases, the results clearly indicate that the morphology of the fiber material was significantly changed after dissolution SEM images of the pulp before dissolution in IL is shown in Figure 5 (C) to compare with our results displaying a rough texture of the fibers, which then confirms that the highly crystalline cellulose structure in the dissolving pulp was transformed to amorphous form after treating with [Emim][OAc]/co-solvents, which is similar to the findings of (Zhao et al., 2013; Kuzmina et al., 2012) who reported a decrease in the crystallinity of cellulose and chitosan after dissolving in IL/co-solvent mixtures. It can be implied that the primary walls of the dissolving pulp fibers was destroyed by the IL and co-solvent treatment, resulting in the linkages between the lignin and carbohydrates to be diminished. This then resulted in the regenerated cellulose structure to be loose because of the breakage of bonds which will create a favourable environment for the IL penetration.

Thermal analysis

TGA curves for cellulose regenerated from raw and final pulp in [Emim][OAc]/ DMSO and DMF mixtures are shown in Figures 6. The TGA curve of the native cellulose (MCC standard) is shown in literature (Kilulya et al., 2011; Sun, 2010) and is not shown in this paper.

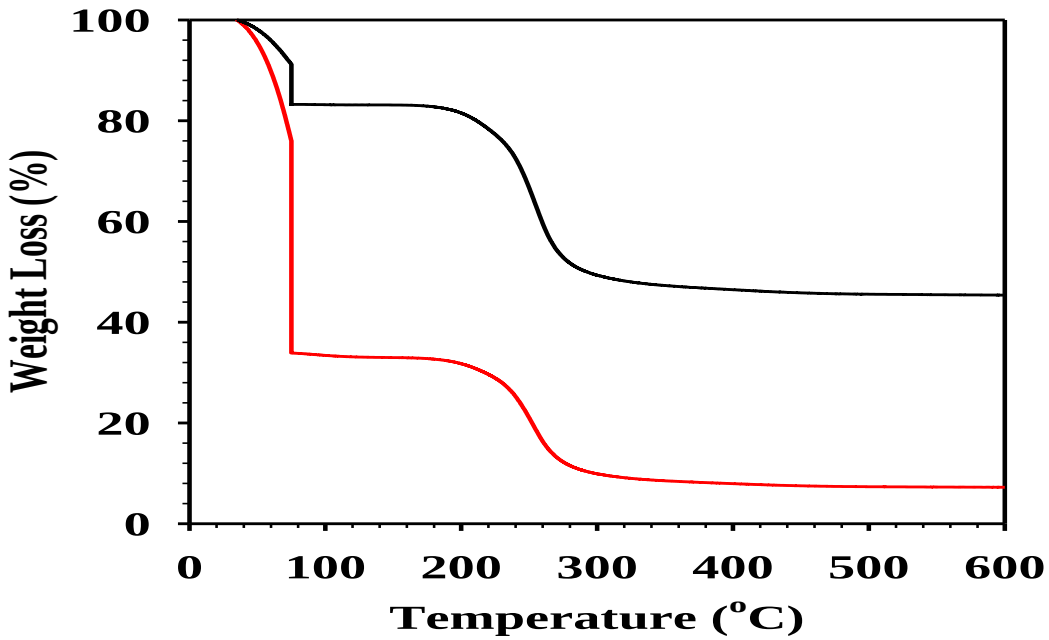

Figure 6. TGA curves regenerated cellulose from final pulp in [Emim][OAc]/ DMSO mixture (black curve) and [Emim][OAc]/DMF mixture (red curve).

The initial drops occurring near 100 ˚C are quite significant in all cases which are probably due to the evaporation of retained moisture (Lan et al., 2011). The native cellulose as shown in literature (Liu et al., 2011) is reported to decompose at 228 ˚C, whereas the regenerated cellulose from raw and final pulps dissolved in [Emim][OAc]/DMSO or DMF mixtures as

shown in Figures 6, begin to decompose at around 200 ˚C, which clearly indicates that native cellulose has a higher thermal stability compared to the regenerated cellulose. In Figure 6, the retained weight was 50 % for the regenerated cellulose from IL/DMSO mixture and 10 % for regenerated cellulose from IL/ DMF mixture, as compared to the original cellulose which retained 8 % weight while pulp dissolved in pure [Emim][OAc] gave a retained weight of 15 % (Kilulya et al. , 2011). This can be attributed to DMSO reported to increase the speed of dissolution and remained in solution, decreasing its viscosity which makes it less efficient for dissolving the pulp in IL, and pulp material still contains large amount of water even after drying.

CONCLUSIONS

Cellulose was regenerated successfully from Southern African raw and final pulp [Emim][OAc]/ co-solvent systems with the cellulose yield recovery being greatest in cellulose regenerated from bleached pulp in [Emim][OAc]/ DMF mixture due to the less amount of hemicelluloses and lignin present in the bleached pulp, which then makes it more easier for the solvents to break the hydrogen bonds in the pulp samples.
The pXRD results indicate that the crystal structure of cellulose was transformed from cellulose 1 to cellulose II. The SEM images show that the surface of the regenerated cellulose became homogeneous after dissolving in IL/co-solvent mixtures.

ACKNOWLEDGEMENTS

The authors are grateful for the support of the National Research Foundation, CSIR Forestry and Forest Products Research Centre, Durban University of Technology and Centre for Green Manufacturing and Department of Chemistry, The University of Alabama.

REFERENCES

Ang, T.N., Yoon, L.W., Lee, K.M., Ngoh, G.C., Chua, A.S.M. and Lee, M.G., 2011. Efficiency of ionic liquids in the dissolution of rice husk. *BioResources*, **6**(4), pp. 4790.

Biemann, C.J., 1993. *Essentials of pulping and papermaking.* 72-100. new york: academic press.

Cao, Y., Wu, J., Zhang, J., Li, H., Zhang, Y. and He, J., 2009. Room temperature ionic liquids (RTILs): A new and versatile platform for cellulose processing and derivatization. *Chemical Engineering Journal*, **147**(1), pp. 13-21.

Casas, A., Alonso, M.V., Oliet, M., Rojo, E. and Rodrĭguez, F., 2012a. FTIR analysis of lignin regenerated from Pinus radiata and Eucalyptus globulus woods dissolved in imidazolium-based ionic liquids. *Journal of Chemical Technology and Biotechnology*, **87**(4), pp. 472-480.

Casas, A., Oliet, M., Alonso, M.V. and Rodrĭguez, F., 2012b. Dissolution of Pinus radiata and Eucalyptus globulus woods in ionic liquids under microwave radiation: Lignin

regeneration and characterization. *Separation and Purification Technology,* **97**(0), pp. 115-122.

Dafchachi, M.N. and Resalati, N., 2012. Evaluation of pre-hydrolyzed soda-AQ dissolving pulp from Populus Deltoides using an ODED bleaching sequence. *BioResources,* **7**(3), pp. 3283.

Ding, Z., Chi, Z., Gu, W., Gu, S., Liu, J. and Wang, H., 2012. Theoretical and experimental investigation on dissolution and regeneration of cellulose in ionic liquid. *Carbohydrate Polymers,* **89**(1), pp. 7-16.

Duan, X., Xu, J., He, B., Li, J. and Sun, Y., 2011. Preparation and rheological properties of cellulose / chitosan homogeneous solution in ILs. *BioResources,* **6**(4), pp. 4640.

Hazarika, S., Dutta, N.N. and Rao, P.G., 2012. Dissolution of lignocellulose in ionic liquids and its recovery by nanofiltration. *Separation and Purification Technology,* , pp. 1.

Hermanutz, F., Gähr, F., Uerdingen, E., Meister, F. and Kosan, B., 2008. New developments in dissolving and processing of cellulose in ionic liquids, *Macromolecular Symposia,* 2008, Wiley Online Library pp23-27.

Karatzos, K.S., Edye, L.A. and Doherty, W.O.S., 2012. Sugarcane baggase pretreatment using three imidazolium-based ionic liquids; mass balances and enzyme kinetics. *Biotechnology for Biofuels,* **62**(5), pp. 2.

Kilpeläinen, I., Xie, H., King, A., Granstom, M., Heikkinen, S. and Argyropoulos, D.S., 2007. Dissolution of wood in ionic liquids. *Journal of Agricultural and Food Chemistry,* **55**(22), pp. 9142-9148.

Kilulya, K.F., Msagati, T.A.M., Mamba, B.B., Ngila, J.C. and Bush, T., 2011. Imidazolium ionic liquids as dissolving solvents for chemical grade cellulose in the determination of fatty acids using gas chromatography-mass spectrometry. *BioResources,* **6**(3), pp. 3272.

Kosan, B., Michels, C. and Meister, F., 2008. Dissolution and forming of cellulose with ionic liquids. *Cellulose,* **15**(1), pp. 59-66.

Kuzmina, O. 2012. *Research of Dissolution Ability of Ionic Liquids for Polysaccharides such as Cellulose.* Msc edn. Leningrad (Sankt Petersburg), Russland: Rat der Chemisch-Geowissenschaftlichen Fakultät der Friedrich-Schiller-Universität Jena.

Kuzmina, O., Heinze, T. and Wawro, D., 2012. Blending of Cellulose and Chitosan in Alkyl Imidazolium Ionic Liquids. *ISRN Polymer Science,* **2012**.

Lan, W., Liu, C., Yue, F., Sun, R. and Kennedy, J.F., 2011. Ultrasound-assisted dissolution of cellulose in ionic liquid. *Carbohydrate Polymers,* **86**(2), pp. 672-677.

Lateef, H., Grimes, S., Kewcharoenwong, P. and Feinberg, B., 2009. Separation and recovery of cellulose and lignin using ionic liquids: a process for recovery from paper-based waste. *Journal of Chemical Technology and Biotechnology,* **84**(12), pp. 1818-1827.

Liebert, T. and Heinze, T., 2008. Interaction of ionic liquids with polysaccharides 5. Solvents and reaction media for the modification of cellulose. *BioResources,* **3**(2), pp. 576-601.

Lindman, B., Karlström, G. and Stigsson, L., 2010. On the mechanism of dissolution of cellulose. *Journal of Molecular Liquids,* **156**(1), pp. 76.

Liu, H., Sale, K.L., Holmes, B.M., Simmons, B.A. and Singh, S., 2010. Understanding the interactions of cellulose with ionic liquids: a molecular dynamics study. *The Journal of Physical Chemistry B,* **114**(12), pp. 4293-4301.

Liu, D., Xia, K., Cai, W., Yang, R., Wang, L. and Wang, B., 2012. Investigations about dissolution of cellulose in the 1-allyl-3-alkylimidazolium chloride ionic liquids. *Carbohydrate Polymers,* **87**(2), pp. 1058-1064.

Liu, Z., Wang, H., Li, Z., Lu, X., Zhang, X., Zhang, S. and Zhou, K., 2011. Characterization of the regenerated cellulose films in ionic liquids and rheological properties of the solutions. *Materials Chemistry and Physics,* **128**(1–2), pp. 220-227.

Lv, Y., Wu, J., Zhang, J., Niu, Y., Liu, C., He, J. and Zhang, J., 2012. Rheological properties of cellulose/ionic liquid/dimethylsulfoxide (DMSO) solutions. *Polymer,* **53**(12), pp. 2524-2531.

Mahadeva, S.K. and Kim, J., 2012. Influence of residual ionic liquid on the thermal stability and electromechanical behaviour of cellulose regenerated from 1-ethyl-3-methylimidazolium acetate. *Fibers and Polymers,* **13**(3),.

Mäki-Arvela, P., Anugwom, I., Virtanen, P., Sjöholm, R. and Mikkola, J.P., 2010. Dissolution of lignocellulosic materials and its constituents using ionic liquids—A review. *Industrial Crops and Products,* **32**(3), pp. 175-201.

Mikkola, J.P., Kirilin, A., Tuuf, J.C., Pranovich, A., Holmbom, B., Kustov, L.M., Murzin, D.Y. and Salmi, T., 2007. Ultrasound enhancement of cellulose processing in ionic liquids: from dissolution towards functionalization. *Green Chemistry,* **9**(11), pp. 1229-1237.

Phillips, D.M., Drummy, L.F., Conrady, D.G., Fox, D.M., Naik, R.R., Stone, M.O., Trulove, P.C., Hugh, C. and Mantz, R.A., 2004. Dissolution and regeneration of Bombyx mori silk fibroin using ionic liquids. *Journal of the American Chemical Society,* **126**(44), pp. 14350-14351.

Pinkert, A., Marsh, K.N., Pang, S. and Staiger, M.P., 2009. Ionic liquids and their interaction with cellulose. *Chem.Soc.Rev.,* **109**, pp. 6712.

Qiu, Z., Aita, G.M. and Walker, M.S., 2012. Effect of ionic liquid pretreatment on the chemical composition, structure and enzymatic hydrolysis of energy cane bagasse. *Bioresource technology,* , pp. 1.

Sjöstrom, E., 1981. Wood chemistry: fundamentals and applications. pp. 169-189.

Sun, N., 2010.
Dissolution and processing of cellulosic materials with ionic liquids: fundamentals and applications , University of Alabama.

Sun, N., Rahman, M., Qin, Y., Maxim, M.L., Rodrĭgues, H. and Rogers, R.D., 2009. Complete dissolution and partial delignification of wood in the ionic liquid 1-ethyl-imidazolium acetate. *Green Chem.*, **11**, pp. 646.

Swatloski, R.P., Spear, S.K., Holbrey, J.D. and Rogers, R.D., 2002. Dissolution of cellose with ionic liquids. *Journal of the American Chemical Society*, **124**(18), pp. 4974-4975.

Wu, R., Wang, X., Li, F., Li, H. and Wang, Y., 2009. Green composite films prepared from cellulose, starch and lignin in room-temperature ionic liquid. *Bioresource technology*, **100**(9), pp. 2569-2574.

Xu, A., Zhang, Y., Zhao, Y. and Wang, J., 2013. Cellulose dissolution at ambient temperature: Role of preferential solvation of cations of ionic liquids by a cosolvent. *Carbohydrate Polymers*, **92**(1), pp. 540-544.

Xu, F., Shi, Y. and Wang, D., 2012. Enhanced production of glucose and xylose with partial dissolution of corn stover in ionic liquid, 1-Ethyl-3-methylimidazolium acetate. *Bioresource technology*, **114**(0), pp. 720-724.

Zhang, H., Wu, J., Zhang, J. and He, J., 2005. 1-Allyl-3-methylimidazolium chloride room temperature ionic liquid: A new and powerful nonderivatizing solvent for cellulose. *Macromolecules*, **38**(20), pp. 8272-8277.

Zhao, H., Xia, S. and Ma, P., 2005. Use of ionic liquids as 'green'solvents for extractions. *Journal of chemical technology and biotechnology*, **80**(10), pp. 1089-1096.

Zhao, Y. (1,2), Wang, J.(.1.)., Liu, X.(.2.). and Zhang, S.(.2.)., 2012. Effects of cationic structure on cellulose dissolution in ionic liquids: A molecular dynamics study. *ChemPhysChem*, **13**(13), pp. 3126-3133.

Zhao, Y., Liu, X., Wang, J. and Zhang, S., 2013. Insight into co-solvent effect of cellulose dissolution in imidazolium-based ionic liquid systems. *Phys.Chem.B*, **DOI: 10.1021/jp4038039**.

Zhao, D.(.1.)., Fu, L.(.1.)., Ren, P. (1,2), Li, J.(.1.). and Li, H.(.1.)., 2012a. The dissolution of cellulose in N-allylpyridinium chloride ionic liquid/organic solvent. *Gaofenzi Cailiao Kexue Yu Gongcheng/Polymeric Materials Science and Engineering*, **28**(7), pp. 31-34.

Zhao, D.S. et al. 2012b. *Study on the Dissolution of Cellulose in N-Allylpyridinium Chloride Ionic Liquid and Co-Solvent Composites.*

Dissolution of South African *Eucalyptus* Sawdust Wood in [Emim][OAc]/ Co-solvent Mixtures

Zikhona Tywabi[1], Nirmala Deenadayalu[1]and Bruce Sithole[2]

[1] ***Department of Chemistry, Faculty of Applied Sciences, Durban University of Technology, KwaZulu Natal, Durban, South Africa, 4001.***

[2] ***Council for Scientific and Industrial Research, Natural Resources and Environment, Forestry and Forest Products Research Centre, KwaZulu Natal, Durban, South Africa, 4013.***

To whom correspondence should be addressed: **Email ztywabi@gmail.com**

Keywords: Ionic Liquids, Wood Biomass, Cellulose, Lignin and Co-solvents.

ABSTRACT

Due to several advantageous properties ionic liquid (IL), 1-ethyl-3-methylimidazolium acetate [Emim][OAc] was used in this study together with organic solvents; dimethylformamide (DMF) and dimethylsulfoxide (DMSO) as co-solvents. The addition of co-solvents decreased the viscosity of the IL and facilitated the dissolution of sawdust. Sawdust after dissolution in IL/co-solvent mixture was regenerated with reconstituents solvents 1:1 (v/v) acetone/water mixture followed by filtration. The results showed that the [Emim][OAc]/DMF gave a higher percent cellulose yield of 32.50 % while the [Emim][OAc]/DMSO mixture gave a percent cellulose yield of 17.83 % for the sawdust wood sample, while the neat [Emim][OAc] gave gave a percent cellulose yield of 7.21 %. The regenerated cellulose materials were characterized by FTIR, pXRD, SEM and TGA, and compared with microcrystalline standard of cellulose (MCC) standard, and it was found that the crystalline structure of cellulose was converted to cellulose II from cellulose I. It was also found that the regenerated cellulose had a good thermal stability with [Emim][OAc]/co-solvent mixtures.

1. INTRODUCTION

The efficient utilization of biomass is increasingly important due to diminishing resources of fossil fuels as well as global heating warnings caused by green gas emissions. Wood is mainly used for the production of paper from cellulose and most of the other components of wood are burnt to produce energy (Kilpeläinen et al., 2007). Biomass is one of the biorenewable resources (Muhammad et al., 2011) with an estimated global production of around 1.0×10^{11} tons per year. The major constituents of lignocellulose biomass include cellulose 45-50 %, hemicellulose 15-25 %, lignin 23-33 % and extractives (Kilpeläinen et al., 2007; Muhammad et al., 2011; Zhang and Zhao, 2010) . Dissolution of biomass in common solvents is practically difficult due to the three dimensional network structures of lignin which binds the plant cells together providing mechanical strength to the biomass structure (Muhammad et al., 2011). Various types of solvents have been used for processing the cellulose but the traditional solvents suffer from some drawbacks related to volatility, generation of toxic gas and difficulty in recovery for recycling (Ohno and Fukaya, 2009).

Ionic liquids are a group of new organic salts that exist as liquids at a relative low temperature. The ILs are known as green solvents because of their several attractive properties, such as negligible vapour pressure, chemical and thermal stability, non-flammability and ease of recycling (Cao et al., 2009; Holbrey et al., 2003). In 2002, the use of ILs for cellulose dissolution was discovered by Rogers and his group who carried out comprehensive studies on cellulose dissolution and regeneration (Swatloski et al., 2002). Recently, attention has been drawn towards the application of ILs in lignocellulose processing (Kilpeläinen et al., 2007; Erdmenger et al., 2007; Luo, Cai and Gu, 2013; Sun et al., 2009) studied the biomass dissolution in different ILs. A range of ionic liquids based on the imidazolium cation have been shown to be effective cellulose solvents (Zhang and Zhao, 2010; Swatloski et al., 2002; Fukaya et al., 2008; Kohler et al., 2007), yielding viscous solutions of cellulose. Generally, hydrophilic ILs are able to completely solubilize wood over 100 ˚C and cellulose rich materials can be precipitated by adding water or protic organic solvents such as ethanol (Swatloski et al., 2002). It is recognized that ILs are potential "green" recyclable alternative to environmentally harmful organic solvents, have been increasingly exploited as solvents and/or co-solvents and/or reagents in a wide range of applications including pretreatment of lingo-cellulosic (Kilpeläinen et al., 2007; Sun et al., 2009). However, the production of high strength biomaterials and biocomposites requires structurally strong cellulose fibers. To date, a number of pretreatment approaches including physical (e.g., phyrolysis and mechanical disruption), physic-chemical (e.g., steam explosion and ammonia fiber explosion), chemical (e.g. hydrolysis, alkaline hydrolysis and oxidative delignification), and biological methods have been investigated to delignify wood biomass for extraction of cellulose. Many of these methods require high temperatures and pressures as well as highly concentrated chemicals
In this present paper, changes in the structure of the cellulose regenerated from sawdust wood previously dissolved in 1-ethyl-3-methylimidazolium acetate [Emim][OAc]/dimethylsulfoxide [DMSO] and dimethylformamide [DMF] mixtures. To confirm the dissolution effect of ILs on the biomass, the regenerated cellulosic material from IL/co-solvent mixtures has been characterized by TGA, FTIR, XRD and SEM and compared to MCC standard of cellulose.

2. EXPERIMENTAL

2.1 Materials

The sample used in this study was the South African *Eucalyptus* ED5CW sawdust wood sample that was supplied by SAPPI Saiccor mill from the South Coast of Durban, South Africa. The sawdust wood samples were dried in the vacuum at 50 °C for 12 hours to remove the water, and then ground into small particles using a mortar and pestle before use. The IL [Emim][OAc], with a purity of > 95 %, was purchased from IOLITEC USA. Prior to using, the ionic liquid was dried at 50 °C using a vacuum pump for 12 hours; and its water content was determined by Coulometric Karl Fischer and found to be 1035 ppm. Dimethylsulfoxide (DMSO) and dimethylformamide (DMF) with a purity of 99.9 % were purchased from Sigma Aldrich and were used as received. Nylon membrane filter paper, 10 and 0.8 µm, was purchased from Sterlitech Corporation, USA. Microcystalline cellulose (MCC) standard, with depolymerization degree of 270 and purity of 99.9 %, was purchased from Sigma Aldrich.

2.2 Dissolution and regeneration of biomass

Approximately 5 wt% of the previously dried and ground sawdust wood sample was dissolved in [Emim][OAc]/DMSO and [Emim][OAc]/DMF mixtures, the concentration of co-solvents used in the mixtures was 25 %, with stirring at 120 °C for 10 hours in an oil bath. Once dissolution was completed, the samples were cooled to room temperature. The cooled solutions were then washed 3 times with 50 mL mixture of water/acetone (1:1, v/v). The solution was then centrifuged in a Clays Adams centrifuge at 700 rpm for 10 minutes. It was observed that a white cellulosic material settled at the bottom of the centrifuge tube. The top liquid phase was taken out and the cellulosic material was further washed with 50 mL of the mixture of water/acetone twice more. The cellulosic material was finally obtained by filtration using a Nylon membrane filter paper with pore size of 10 µm, then dried in an oven at 80 °C for one hour. The dried weight of the precipitate was recorded and the percentage recovery of the cellulose was calculated by using the Equation taken from literature (Brown, 2012):

$$\text{Cellulosic material recovery (\%)} = \frac{\text{mass of regenerated cellulosic material (g)}}{\text{mass of pulp for dissolution (g)}} \times 100\% \quad (1)$$

Lignin was recovered by stirring the filtrate which consists of acetone, water and IL in open air for 3 hours, while evaporating the acetone and precipitating the lignin. A few small black particles were observed at the bottom of the beaker. The small lignin precipitate was then analysed by FTIR and compared to the lignin standard Indulin.

2.3 Recycling of ionic liquid

The ionic liquid liquor (filtrate) obtained after washing was transferred into a round bottom flask attached to a rotary evaporator and distilled to remove any water and acetone remaining in the mixture. The [Emim][OAc] recovered was then dried under vacuum at 50 °C for 12 hours, characterized by FTIR and compared with the IL spectrum before the dissolution process.

2.4 Characterization

Infrared spectra of MCC standard and regenerated cellulose samples from sawdust wood previously dissolved in [Emim][OAc]/DMF or DMSO mixtures were collected using Bruker Alpha FTIR spectrometer, and spectra were obtained in the range of ν_{max} = 400–4000 cm^{-1}. The cellulose samples for sawdust wood regenerated from IL/DMSO and IL/DMF mixtures were cut and ground into very small particles and characterized by FTIR.

SEM images of the regenerated cellulose samples were taken at 300 x magnification using a Jeol 6310 Electron Probe analyser SEM instrument which was operated at 5-10 Kv accelerating voltage. Prior to imaging, the samples were sputter-coated with gold to make the fibres electrically conductive, avoiding degradation and build -up of charge on them.

The diffraction patterns of the regenerated cellulose samples and MCC standard were obtained using a Bruke D2 Phaser Powder XRD instrument. The patterns were recorded using a Cu-Ka radiation at 40kV and the range for angle of diffraction was 2θ =5-40º.

Thermal analysis was recorded with a Perklin Elmer TGA analyser. Approximately 10 mg of the regenerated cellulose samples were carried out by the Thermo Analyzer at a heating rate of 5 °C /min under continuous nitrogen flow in a temperature range from 25 °C to 600 °C, with an isotherm process at 75 °C for 30 min to remove any absorbed water.

3. RESULTS AND DISCUSSIONS

3.1 Dissolution and regeneration of biomass

The dissolution of the sawdust in [Emim][OAc]/DMSO and [Emim][OAc]/DMF mixtures at 120 °C was studied and the cellulose was regenerated by adding the mixture of water/acetone (1:1, v/v), and separated from the liquid phase by centrifugation followed by filtration, which was further dried in the oven. The cellulose yield was calculated and is shown in Table 1.

Dissolution of biomass in ionic liquid depends on the initial sample load, particle size, high hydrogen bond basicity of IL (Sun et al., 2009). It has also been reported that ionic liquids that can incorporate anions with strong hydrogen bonding acceptors such as acetate, are the most effective solvents for cellulose due to their ability to disrupt the extensive hydrogen bonding network of cellulose and lead to its dissolution (Swatloski et al., 2002; Feng & Chen , 2008; Kilulya et al., 2011). The viscosity of the ILs also plays a crucial role in the dissolution of biomass in ILs (Kilpeläinen et al., 2007). The viscosity of the IL plays an important role in the dissolution speed (Fukaya et al., 2006). Addition of co-solvents results in a reduction of the viscosity of the mixture, and thus leads to an acceleration of the dissolution process due to facilitated diffusion, thereby enhancing further processing of the polymer solution (Liu et.al., 2008; Froschauer et.al., 2013).

Dissolution of cellulose in ILs is attributed to their ability to break the extensive network of hydrogen bonds existing in the cellulose. [Emim][OAc] disrupts the hydrogen bonding interactions present in the cellulose allowing it to diffuse into the interior of the cellulose, which then results in the complete dissolution of cellulose (Kilpeläinen et al., 2007).

The acetate-based IL was reported to show better dissolution of wood (Sun *et. al.* 2009) and cellulose (Ang *et. al.* 2011). One possible reason for this is that the acetate anion seems to favour dissolution because acetate has higher hydrogen bond basicity (a property of the anion that is influenced primarily by the size and charge localization on the anion) than other anions (Brandt *et.al.* 2010; Karatoz *et.al.* 2012a). Thus it has the ability to disrupt hydrogen bonds in cellulose and thereby have a potential to dissolve cellulose is higher. This positive correlation between the hydrogen bond basicity of the IL anion and the IL's ability to dissolve cellulose or lignocellulose is discussed more in literature (Brandt *et.al.* 2010). However, Swatolski *et.al.* (2002) claimed that [Bmim][Cl] is the most effective IL in dissolving pure cellulose, such as cellulose-dissolving pulps, fibrous cellulose, and Whatman cellulose filter papers. This indicates that IL dissolution is selective on the type of substrate, and the selectivity of ILs could be attributed to their ionic functional groups.

The sawdust previously dissolved in [Emim][OAc]/DMF mixture gave higher regenerated cellulose yields than cellulose regenerated from sawdust previously dissolved in [Emim][OAc]/DMSO mixture and pure [Emim][OAc]. This can be attributed to the fact that DMSO has a higher dielectric constant of 44 than DMF that has a dielectric constant of 38, which makes DMSO more polar than DMF, and this has some effect on the dissolution process because, DMSO has a stronger ion-dipole interaction which results in the force of attraction becoming stronger between ions in a solution and the dipole-dipole interaction (hydrogen bonding) between solvent molecules.

This effect results in the reduce in cellulose solubility because DMSO forms competing hydrogen bond to the macromolecular chains of cellulose (Swatolski 2002; Cao et al., 2009). This has been found to be consistent with the literature reports showing that solvents with higher dielectric constants provide stronger ion-solvent interactions with ILs, which can strongly affect or extremely reduce the viscosity of ILs solutions (Lv et al., 2012). The lignin content after dissolution of sawdust wood in [Emim][OAc]/DMF and DMSO mixtures could not be weighed because only a few precipitated black particles were observed, so the lignin contents are not in agreement with literature that reported lignin content to be approximately 20 % in hardwoods (Casas et al., 2012). In the regenerated cellulose according to (Dadi et al., 2006), it was reported that the dissolving maple wood powder by [Emim][OAc], the crystalline structure of cellulose in wood powder was disrupted when the experiment was performed at higher temperatures i.e. about 130 ˚C.

For the regenerated cellulose, Dadi *et.al.* (2006) reported that in dissolving the maple wood powder by [Emim][OAc], the crystalline structure of cellulose in wood powder was disrupted when the experiment was performed at higher temperatures, i.e., about 130 ˚C. At the same time, lignin extraction also took place.

The dissolution rate of wood is highly dependent on the particle size of the wood sample. This is because the complex and compact structure of wood cell walls would inhibit the diffusion of the ionic liquid into its interior, resulting in only a partial dissolution of wood (Kilpeläinen *et.al.* 2007).

Kilpeläinen *et.al.* (2007) discovered that the solubilisation efficiency of lignocellulose materials in ILs is in the order of: ball-milled wood powder > sawdust > thermo mechanical pulp fibres > wood chips.

The water content of a wood sample plays a key role in determining its solubility in ILs.

3.2 FTIR Spectroscopy of the regenerated cellulose fibers

Figure 1, illustrates the spectra of cellulose regenerated from sawdust wood sample previously dissolved in [Emim][OAc]/DMSO (**1**) and [Emim][OAc]/DMF (**2**) mixtures compared to the MCC standard of cellulose (**3**) while Figure 2 illustrates the spectra of lignin regenerated from sawdust wood dissolved in [Emim][OAc]/DMF (**1**), lignin sample obtained after Kraft pulping supplied by Sappi (**2**) compared to Indulin AT standard of lignin (**3**).

From Fig. 1, it can be seen that the structure of MCC standard and regenerated cellulose material from [Emim][OAc]/DMF and DMSO mixtures, showed the same basic structure, which was similar to the results reported by previously (Zhang et al., 2005).

There was a broad O-H stretching absorption around ~3400 cm^{-1} and a prominent C-H stretching absorption around ~2900 cm^{-1} in all the spectra. The absorbance at ~1600 cm^{-1} is because of the bending mode of the absorbed water (Kilulya et al., 2011) From the FTIR spectra as shown in Fig.1, in the fingerprint region between 800 and 1800 cm^{-1}, many well defined peaks were observed which provided abundant information on various functional groups present in the sawdust wood and the regenerated cellulose material from IL/DMF and DMSO. The C-O stretching absorption around ~1500 cm^{-1} (in hemicellulose) which had a greater intensity in the MCC standard spectra than both the regenerated cellulose spectra which was lower in intensity due to the loss of hemicellulose during dissolution and regeneration from IL/co-solvent mixtures (Sun et al., 2009). The peaks around ~1300 $cm^{-1,}$ ~1100 cm^{-1},~1000 cm^{-1} and ~900 cm^{-1} were mainly related to the carbohydrates in all the spectra (Muhammad et al., 2011). From the spectra of the regenerated cellulose it has been observed that IL/co-solvent treatment removed the lignin as it can be seen that the peaks of the lignin were absent.

It was observed that there is a close similarity of Lignin standard (**3**) to the lignin recovered after Kraft pulping (**2**) where the typical peaks of lignin were observed and the spectrum of lignin precipitate (**1**) shows large differences of absorbance's in the spectrum.

The absorption from O-H stretching was observed at ~3200-3400 cm^{-1} indicating the content of free hydroxyl group. The FTIR spectra shown in (Figure 2 spectrum (**1**)) shows the characteristic vibration of lignin, at ~1510 cm^{-1} which appears as the aromatic skeletal vibration of lignin and is similar to Indulin standard of lignin (Figure 2 spectrum (**3**)), and similar results have been reported in literature (Casas et.al. 2012a; Casas et.al. 2012b). A decrease in the aromatic skeletal vibrations may be due to the transformation of the aromatic ring into the quinonoid structures during the dissolution and regeneration process (Casas et.al. 2012a).

The band at ~1200 cm^{-1} corresponds to the vibration of the guaicyl ring in lignin and the characteristic vibration of the syringly ring appears at ~1300 cm^{-1} (Casas et.al. 2012b).

All the spectra have intense absorbance at the hemicellulose characteristic bands between ~1200 cm^{-1} and 1000 cm^{-1} and are more intense in the Indulin spectra than in the recovered lignin and lignin sample from Sappi. The low intensity of these bands may be due to the oxidation of the secondary and primary alcohols to form carbonyl groups, as consequence of dissolution and regeneration process (Casas et.al. 2012a). This indicates that the majority of the non-lignin components are comprised of hemicellulose and this is in agreement with results reported in literature (Karatzos et.al. 2012a).

The spectra of lignin recovered after evaporation of acetone (Figure 2 spectra (**1**)) did not compare very well with the lignin standard (shown in Figure 2 spectra (**3**)), but small peaks can be seen around the 600-1300 cm^{-1} which compare with the lignin standard, so one can conclude that indeed the spectra refers to a lignin. The precipitated lignin after dissolution also shows a strong absorbance ~980 cm^{-1} indicative of arabinosyl groups. This is in agreement with a previous discussion supporting preservation of covalent bonds to arabinosyl groups during [Emim][OAc] dissolution (Karatzos et al. 2012a).

The bands at ~ 800 cm^{-1} corresponds to the C-H out of plane vibrations in guaiacyl rings in lignin (Casas et.al. 2012a) and the vibration of the glucose ring in cellulose.

Therefore, according to these results, lignin mixed with cellulose, could not be regenerated from solutions of *eucalyptus* sawdust wood in [Emim][OAc]/co-solvent mixtures, and this may be probably due to the limitations in the operating conditions (higher temperature leads to IL decomposition) (Casas et al., 2012).
Similar results were reported by Lan et.al. (2011) where they revealed that the cellulose isolated from bagasse in [Bmim][Cl] was found to be free of residual lignin and Casas et.al. (2012b) also concluded that lignin could not be precipitated from solutions of Eucalyptus woods in ILs with acetate anions because acetate based ILs are able to establish hydrogen bonds with wood and probably dissolve it. The unaccounted losses maybe a result of fragmentation of lignin and changed solubilities in the washing steps (Sun et.al, 2011).

To achieve environmentally friendly biomass processing, the recovery and reuse of ILs is one of the main challenges. The [Emim][OAc] was recovered in excellent yield, > 99 % by using the rotary evaporator by evaporation and drying from aqueous solution obtained after regeneration. Hermanutz et.al. (2008) reported that ILs used as solvents for manufacturing cellulose fibres were almost entirely recovered (99.5 %).The colorless [Emim][OAc] became reddish brown after recycling, this may be due to exposure to elevated temperatures and contaminants present in [Emim][OAc], which could be degradation from [Emim][OAc] and biomass as well as carbohydrate (Sun et.al. 2011; Wu et.al. 2012).
From Fig. 3, it can be seen that FTIR spectrum of the recovered IL (spectrum **2**) is not in good agreement with the dried IL before dissolution (reference FTIR spectra **1**), with the only difference being an increase in the OH absorption, which reflects both the use of water in the process chemistry and the hygroscopic nature of the IL. Generally the hydrogen bonding will greatly increase the intensity of the band and move to lower frequencies and if the hydrogen bonding is especially strong, the band becomes quite broad.

3.3 Powder X-Ray diffraction

P'XRD analysis was conducted to further examine the crystallinity of the regenerated cellulose. The crystallinity index (CrI) gives a quantitative measure of the crystallinity in powders, and can relate to the strength and stiffness of fibres (Azubuike et.al., 2012).
CrI of MCC and regenerated cellulose was calculated by using equation 2, proposed by Segal et.al (1962):

$$\mathbf{CrI} = I_{TOT}\text{-}I_{AM}/\ I_{TOT} \times 100\ \% \qquad (2)$$

Where I_{TOT} is the maximum intensity of the principal peak (002) lattice diffraction at ($2\theta = 22.7°$ for cellulose I and $2\theta = 21.7°$ for cellulose II) and I_{AM} is the intensity diffraction attributed to the amorphous cellulose at $2\theta = 18°$ for cellulose I and $2\theta = 16°$ for cellulose II (Azubuike et.al. 2012).
The X-ray diffraction patterns of MCC standard native cellulose (diffractogram **A**) and regenerated cellulose fibres from sawdust wood that was previously dissolved in [Emim][OAc]/DMSO (diffractogram **B**) and [Emim][OAc]/DMF mixture (diffractogram **C)** are shown in Fig. 4.
The diffraction patterns of MCC as shown in Fig. 4, showed typical cellulose I structure, with a sharp peak at 22.5° and a wide peak between 12° and 18° (Liu et.al. 2011; Sun et.al. 2009) and a weak band peak at

35°. After dissolution and regeneration, the regenerated cellulose samples from sawdust previously dissolved in [Emim][OAc]/DMSO or DMF mixtures showed typical cellulose II structure with peaks at 12° and 20°, the results illustrates that after the dissolution and regeneration processes, the crystal structure of the sawdust wood was transformed from cellulose I to cellulose II. It also shows that the crystallinity of the regenerated cellulose decreased significantly, which indicated that the [Emim][OAc]/DMF or DMSO mixtures broke the intermolecular hydrogen bonds of the original cellulose during the dissolving process (Liu et. al. 2011). In their work, Wei et.al. (2012) investigated the structural differences between cellulose regenerated from [Bmim][Cl] and untreated cellulose, using FTIR, XRD and TGA. Their data showed that the crystalline form of wood pulp cellulose was transformed completely from cellulose I to cellulose II after regeneration from [Bmim][Cl] solution which was not the case in this study because the cellulose regenerated from the sawdust wood still had some crystallinity.

Results from both FTIR and pXRD suggests that dissolving the sawdust wood samples in [Emim][OAc]/ DMF or DMSO mixture can reduce the cellulose crystallinity in the regenerated cellulosic samples.

The pXRD analysis indicated that the MCC is more crystalline than the regenerated cellulosic material. The changes in diffractograms were analysed in order to determine the crystallinity index (CrI) of MCC and regenerated cellulose from sawdust wood previously dissolved in [Emim][OAc]/DMSO or DMF mixtures and the values are reported in Table 2.

From the CI results presented in Table 2, it can be seen that MCC had the highest crystallinity index of 90.4 % as compared to the regenerated cellulose samples, which then confirms the presence of the strong crystalline peak at $2\theta = 23°$. There is a controversy as to which baseline should be used for the measurement of the intensity values in equation 2, of which this was also found to be a challenge in literature as well (Karatoz et.al., 2012b).

The straight baseline used in this study was drawn by hand. This approach may lead to overestimation of crystallinity (since there is no account for background scattering). However, this overestimation will be of similar magnitude for all the samples and thus should not affect the overall reliability and consistency of the conclusions.

The values of CI are in the range 39-40 % and are not in agreement with those reported by Andersson et.al. (2004) who found the crystallinity of wood to be varying from 24 % to 31% for Scots pine wood. The increase of CrI can be attributed to the degradation caused by weathering, which causes the amorphous fractions of wood, consequently, enriches the relative crystalline content, taking into account that less than one third of the wood polysaccharides are crystalline and the remaining wood constituents are hemicelluloses, amorphous and para-crystalline regions of cellulose fibrils. If the amorphous polysaccharides are degraded more than the crystalline cellulose, the overall crystallinity content is then expected to increase (Lionetto et.al. 2012). Compared to the MCC, the crystallinity of the regenerated cellulose was lower than that of MCC (results shown in Table 2). These results means that the inter- and intramolecular hydrogen bonds between cellulose molecule were rapidly broken during the dissolution process, thus destroying the original crystalline form (Pang et.al. 2014)

For XRD methods, one important factor to consider is the preferred orientation of crystallites (also known as texture). Often the manner in which samples are synthesized, the nature of crystallites and the method of

sample preparation for XRD causes the development of texture in the sample. It is well known that this will drastically influence the relative intensities of the diffraction peaks (Park et.al. 2010).

3.4 Morphology of regenerated cellulose

The SEM images of the morphology of the regenerated cellulose from sawdust wood and [Emim][OAc]/DMSO and DMF mixtures are shown in Fig.5 images **A**-**B**, respectively compared to the SEM images of MCC shown in Fig. 5 image **C**. SEM has been useful in order to monitor the altered structure of pretreated lignocellulosic biomass via various ILs (Swatloski et.al. 2002)

As shown in Fig. 5, the compact framework exhibited by the MCC standard of cellulose (image **C**) was highly disrupted after dissolution of sawdust wood in [Emim][OAc]/DMSO and DMF mixtures. The regenerated cellulose-rich material (Fig. 5 images **A**-**B**) shows a different morphology compared to the MCC (Fig. 5 image **C**), with a conglomerate texture in wood fibres that is fused into a relatively more homogeneous macrostructure and similar results were reported in literature (Muhammad et.al. 2011; Sun et.al. 2009; Swatloski et.al. 2002). The results indicate that the decrease in cellulose concentration resulted in the formation of a rough surface because of lower polymer chain entanglement and larger free chain mobility (Liu et al., 2011). Regenerated cellulose samples show a structure that is rather loose, disordered and curly, and this was probably due to the removal of lignin and decrease of cellulose crystallinity which have already been confirmed by FTIR (Qiu *et.al.*, 2012) Upon dissolution and regeneration, the DMF and DMSO were removed by evaporation

3.5 Thermal analysis

Thus the regenerated samples gave a higher char yield (non-volatile carbonaceous materials) on pyrolysis (Swatloski et al., 2002), which was exhibited by the higher mass residual after decomposition compared to the original cellulose. These results are in agreement with that reported previously (Swatloski et al., 2002; Fort et al., 2007).

The TGA curves of the native cellulose (MCC standard) shown in Fig.6, was taken from literature (Su 2012) while the TGA curves of cellulose regenerated from sawdust previously dissolved in [Emim][OAc]/DMSO(curve **A**) and [Emim][OAc]/DMF (curve **B**) mixtures are shown in Fig.7.

The cellulose regenerated from sawdust wood previously dissolved in [Emim][OAc]/DMSO mixture (curve **A**) and [Emim][OAc]/DMF mixture (curve **A**) regenerated cellulose has a lower decomposition temperature of 200 ˚C than the MCC which is reported in literature to have a decomposition of 250 ˚C (Kilulya et.al. 2011). A decrease in the crystallinity and the decrease in depolymerization of the regenerated cellulose explain this finding (Li et.al. 2012; Liu et.al. 2011). It was also noted that the thermal stabilities of the regenerated cellulose samples were lower than that of MCC, which was probably caused by the lower crystallinity of the regenerated cellulose as the previous work has shown that lower crystallinity and lower cellulose crystallite size can accelerate the degradation process and reduce wood thermal stability (Pang et.al. 2014).

TGA curves of regenerated cellulose from sawdust wood shown in Fig.7, that was previously dissolved in [Emim][OAc]/DMF retained 10 wt. %, while the cellulose regenerated from sawdust previously dissolved in [Emim][OAc]/DMSO retained 48 wt.%, whereas the MCC retained 8 wt.% . These regenerated cellulose samples shows higher char yields (non-volatile carbonaceous materials) which is exhibited by the higher mass residual after decomposition compared to the original cellulose (TGA diffractogram shown in Fig. 6) where MCC retained 8 wt.%, this may probably happen because of IL that remained in the regenerated cellulose (Li et.al. 2012) and may also be attributed to the incomplete pyrolysis of the non-volatile carbonaceous materials, which are characteristics of regenerated cellulose (Swatloski et.al. 2002) . Similar kind of TGA results has been observed by (Mikkola et.al. 2007; Swatloski et.al. 2002), indicating a good accordance with our results.

4. CONCLUSIONS

The present work has reported the successful use of ionic liquids/ co-solvent mixtures as solvents in the dissolution of biomass. It was observed that ILs possess the ability to dissolve biomass and reconstitute the cellulose upon addition of any precipitating solvents, as has been previously reported.

The dissolution of cellulose in [Emim][OAc]/DMSO or DMF mixtures effectively stimulated the escalating of active research towards the better utilization of cellulose and biomass.

Cellulose was regenerated successfully from South African *Eucalyptus* sawdust wood sample in [Emim][OAc]/DMSO or DMF mixtures with the cellulose yield recovery being greatest in cellulose regenerated from sawdust wood previously dissolved in [Emim][OAc]/DMF mixture.

The pXRD results indicate that the crystal structure of cellulose was transformed from cellulose 1 to cellulose II. The SEM images show that the surface of the regenerated cellulose became homogeneous after dissolving in IL/co-solvent mixtures.

The regenerated cellulosic material seems to be more amorphous, and therefore might be easier for the solvent penetration.

From this study it can be concluded that the employed procedures can be useful for the processing of biomass in ionic liquid/ co-solvent mixtures, and furthermore the use of ILs in such analytical procedures as solvent promotes the reduction of environmental pollution and avoids use large amounts of volatile organic solvents in such analyses.

For large-scale application of ILs the development of energy-efficient recycling methods for ILs is a prerequisite and should be investigated in detail in further studies.

5. ACKNOWLEDGEMENTS

The authors are grateful to Council for Scientific and Industrial Research (CSIR), University of Alabama Centre for Green Manufacturing for research facilities.

National Research Foundation, Department of Agriculture Fisheries and Forestry and Durban University of Technology for funding.

6. REFERENCES

Andersson, S., Wikberg, H., Pesonen, E., Maunu, S.L., and Serimaa, R. (2004). Studies of crystallinity of Scots pine and Norway spruce cellulose. *Trees struct. Fund.*, **18**: 346-353.

Ang, T.N., Yoon, L.W., Lee, K.M., Ngoh, G.C., Chua, A.S.M. and Lee, M.G. (2011). Efficiency of ionic liquids in the dissolution of rice husk. *BioResources*, **6**(4): 4790-4800.

Azubulke, P.C., and Okhamafe, O.A. (2012). Physiochemical, spectroscopic and thermal properties of MCC derived from corn cobs. *International Journal of Recycling of organic waste in Agriculture*, **1**(9): 1-9.

Brandt, A., Gräsvik, J., Halletta, J.P. and Welton, T. (2013). Deconstruction of lignocellulosic biomass with ionic liquids. *Green Chem.*, 15: 550-583.

Brown, EK (2012). Cellulose dissolution in ionic liquids and their mixtures with solvents: linking ion/ solvent structure and efficacy of biomass pretreatment.

Cao, Y, Wu, J, Zhang, J, Li, H, Zhang, Y, He, J (2009) Room temperature ionic liquids (RTILs): A new and versatile platform for cellulose processing and derivatization. *Chem. Eng. J.* 147:13-21.

Casas, A., Alonso, M.V., Oliet, M., Rojo, E. and Rodríguez, F. (2012a). FTIR analysis of lignin regenerated from *Pinus radiata* and *Eucalyptus globulus* woods dissolved in imidazolium-based ionic liquids. *Journal of Chemical Technology and Biotechnology*, **87**(4): 472-480.

Casas, A., Oliet, M., Alonso, M.V. and Rodríguez, F. (2012b). Dissolution of *Pinus radiata* and *Eucalyptus globulus* woods in ionic liquids under microwave radiation: Lignin regeneration and characterization. *Separation and Purification Technology*, **97**(0):115-122.

Erdmenger, T, Haensch, C, Hoogenboom, R, Schubert, US (2007) Homogeneous Tritylation of Cellulose in 1-Butyl-3-methylimidazolium Chloride. Macromolecular bioscience. 7: 440-445.

Fort, DA, Remsing, RC, Swatloski, RP, Moyna, P, Moyna, G, Rogers, R.D (2007) Can ionic liquids dissolve wood? Processing and analysis of lignocellulosic materials with 1-n-butyl-3-methylimidazolium chloride. Green Chem. 9: 63-69.

Fukaya, Y, Hayashi, K, Wada, M, Ohno, H (2008) Cellulose dissolution with polar Ionic Liquids under mild conditions: required factors for anions. Green Chem. 10: 44.

Hermanutz, F., Gähr, F., Ueringen, E., Meister, F. and Kosan, B. (2008). New developments in dissolving and processing of cellulose in ionic liquids. *Macromolecular Symposia*, 2008, **262**:pp23-27.

Holbrey, JD, Reichert, WM, Reddy, R, Rogers, R (2003) Ionic liquids as green solvents: progress and prospects. 856: 121-133.

Karatzos, K.S., Allan, L. and Mark, R. (2012a). The Undesirable Acetylation of Cellulose by the Acetate Ion of 1-ethyl-3-methylimidazolium acetate. *Cellulose,* **19**(1): 307.

Karatzos, K.S., Edye, L.A. and Doherty, W.O.S. (2012b). Sugarcane baggase pretreatment using three imidazolium-based ionic liquids; mass balances and enzyme kinetics. *Biotechnology for Biofuels,* **62**(5): 2.

Kilpeläinen, I, Xie, H, King, A, Granstrom, M, Heikkinen, S, Argyropoulos, DS (2007) Dissolution of wood in ionic liquids. J. Agric. Food Chem. 55: 9142-9148.

Kilulya, KF, Msagati, TAM, Mamba, BB, Ngila, JC, Bush, T (2011) Imidazolium ionic liquids as dissolving solvents for chemical grade cellulose in the determination of fatty acids using gas chromatography-mass spectrometry. BioResources. 6: 3272.

Kohler, S, Liebert, T, Schobitz, M, Schaller, J, Meister, F, Gunther, W, Heinze, T (2007) Interactions of ionic liquids with polysaccharides: unexpected acetylation of cellulose with 1-ethyl-3-methylimidazolium acetate. Macromol. Rapid. Commun. 28: 2311.

Lan, W., Liu, C., Yue, F., Sun, R. and Kennedy, J.F. (2011). Ultrasound-assisted dissolution of cellulose in ionic liquid. *Carbohydrate Polymers,* **86**(2): 672-677.

Li, D., Sevastyanova, O. and E, M. (2012). Pretreatment of softwood dissolving pulp with ionic liquids. *Holzforschung,* **66**(8): 935-943.

Liu, Z, Wang, H, Li, Z, Lu, X, Zhang, X, Zhang, S, Zhou, K (2011) Characterization of the regenerated cellulose films in ionic liquids and rheological properties of the solutions. Mater. Chem. Phys. 128: 220-227.

Luo, J, Cai, M, Gu, T (2013) Pretreatment of Lignocellulosic Biomass Using Green Ionic Liquids, Anonymous Green Biomass Pretreatment for Biofuels Production. Springer: 127-153.

Lv, Y, Wu, J, Zhang, J, Niu, Y, Liu, C, He, J, Zhang, J (2012) Rheological properties of cellulose/ionic liquid/dimethylsulfoxide (DMSO) solutions. Polymer. 53: 2524-2531.

Mikkola, J.P., Kirilin, A., Tuuf, J.C., Pranovich, A., Holmbom, B., Kustov, L.M., Murzin, D.Y. and Salmi, T. (2007). Ultrasound enhancement of cellulose processing in ionic liquids: from dissolution towards functionalization. *Green Chemistry,* **9**(11): 1229-1237.

Muhammad, N, Man, Z, Bustam, MA, Mutalib, MIA, Wilfred, CD, Rafiq, S (2011) Dissolution and delignification of bamboo biomass using amino acid-based ionic liquid. Appl. Biochem. Biotechnol. 165: 998.

Ohno, H, Fukaya, Y (2009) Task specific ionic liquids for cellulose technology. Chem. Lett. 38: 2-7.

Pang, J., Liu, X., Zhang, X., Wu, Y. and Sun, R. (2014). Fabrication of cellulose film with enhanced mechanical properties in ionic liquid 1-Allyl-3-methyjiimidazolium chloride (AmimCl). *Materials,* **6**(4): 1270-1284.

Park, S., Baker, J.O., Himmel, M.E., Parilla, P.A. and Johnson, D.K. (2010). Cellulose crystallinity index: measurement techniques and their impact on interpreting cellulase performance. *Biotechnology for Biofuels,* **3**(10):1-10.

Qiu, Z, Aita, GM, Walker, MS (2012) Effect of ionic liquid pretreatment on the chemical composition, structure and enzymatic hydrolysis of energy cane bagasse. Bioresource technology. 1.

Segal, L, Creely, J.J., Martin, A.E., Conrad, C.M. (1962). An empirical method for estimating the fdegree of crystallinity of native cellulose using x-ray diffractometer. Tex Res. 29: 786-794.

Su, W. 2012. A study of cellulose dissolution in ionic liquid-water brines, PhD thesis, Umea University.

Sun, N (2010) Dissolution and processing of cellulosic materials with ionic liquids: fundamentals and applications. University of Alabama.

Sun, N, Rahman, M, Qin, Y, Maxim, ML, Rodriguez, H, Rogers, RD (2009) Complete dissolution and partial delignification of wood in the ionic liquid 1-ethyl-imidazolium acetate. Green Chem. 11: 646.

Sun, N, Rahman, M, , Rodriguez, H, Rogers, RD (2011) Where are ionic liquid strategies most suited in the pursuit of chemicals and energy from lignocellulosic biomass? Chem. Commun. 47: 1405-1421.

Swatloski, RP, Spear, SK, Holbrey, JD, Rogers, RD (2002) Dissolution of cellulose with ionic liquids. J. Am. Chem. Soc. 124: 4974-4975.

Wei, L., Li, K., Ma, Y. and Hou, X. (2012). Dissolving lignocellulosic biomass in a 1-butyl-3-methylimidazolium chloride–water mixture. *Industrial Crops and Products*, **37**(1): 227-234.

Zhang, Z, Zhao, ZK (2010) Microwave-assisted conversion of lignocellulosic biomass into furans in ionic liquids. Bioresource technology. 101: 1111.

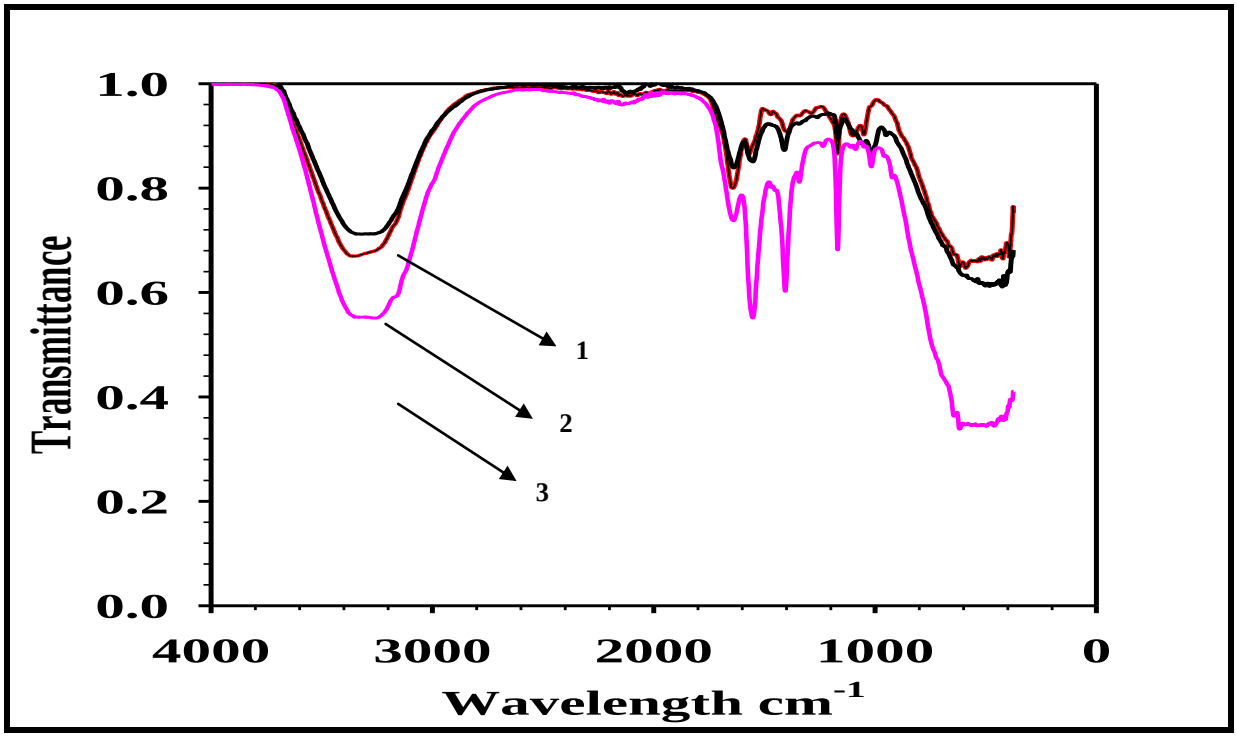

Figure 1 FTIR spectra of cellulose regenerated from the sawdust wood previously dissolved in [Emim][OAc]/DMSO (**1**) and [Emim][OAc]/DMF (**2**) mixtures compared to the MCC standard of cellulose (**3**)

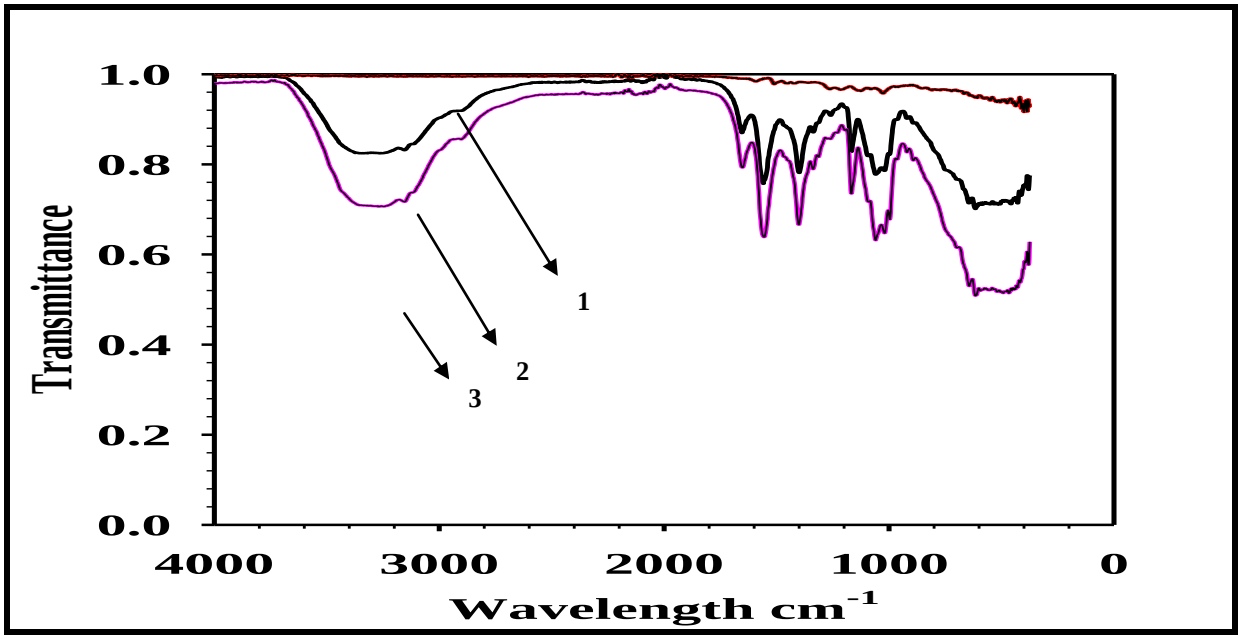

Figure 2 FTIR spectra of lignin precipitate regenerated from the sawdust wood previously dissolved in [Emim][OAc]/DMF (**1**) mixtures, lignin sample obtained after Kraft pulping supplied by Sappi (**2**) compared to the Indulin AT standard of lignin (**3**)

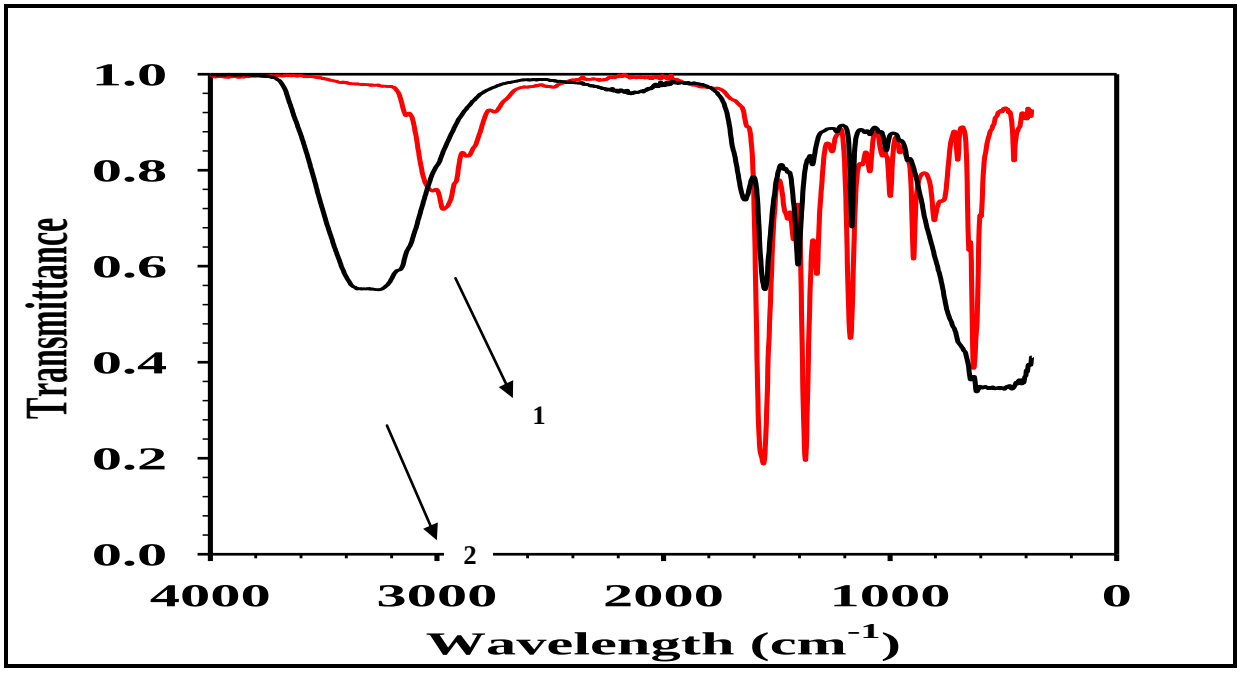

Figure 3 FTIR spectra of pure [Emim][OAc] after drying (**1**) with the recovered [Emim][OAc] after dissolution of pulp (**2**)

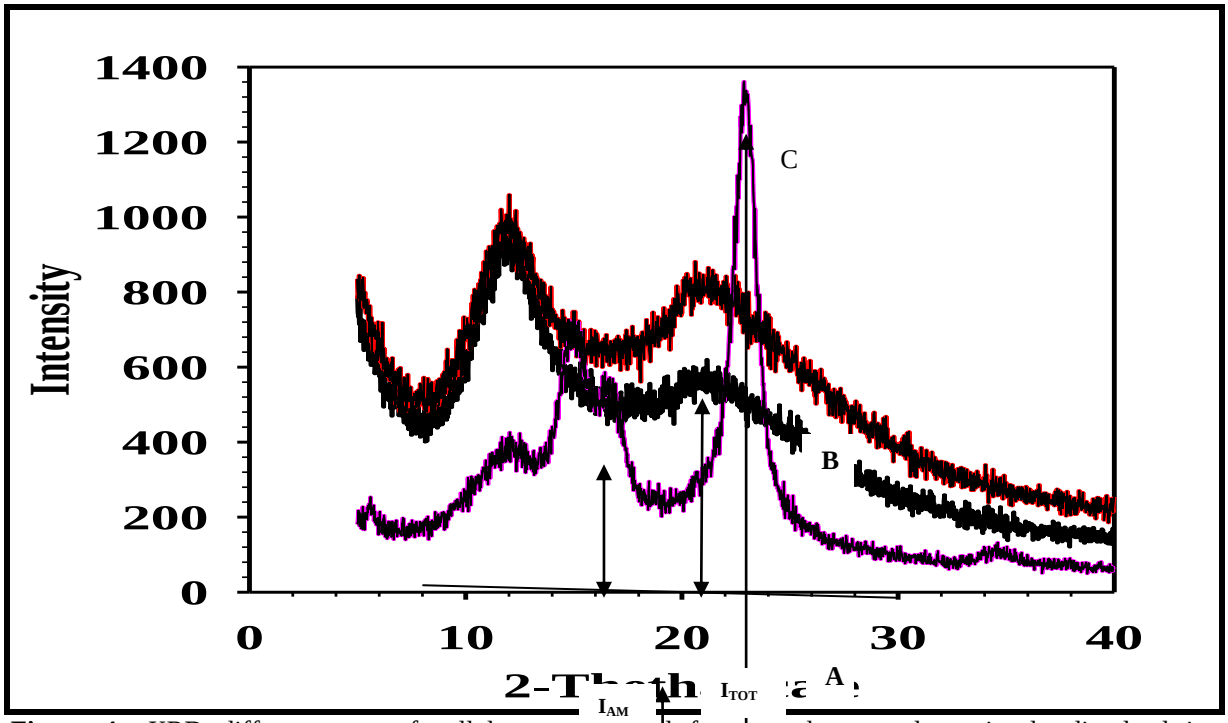

Figure 4 pXRD diffractograms of cellulose reg[illegible] from sawdust wood previously dissolved in [Emim][OAc]/DMF and DMSO mixtures compared to MCC standard of cellulose

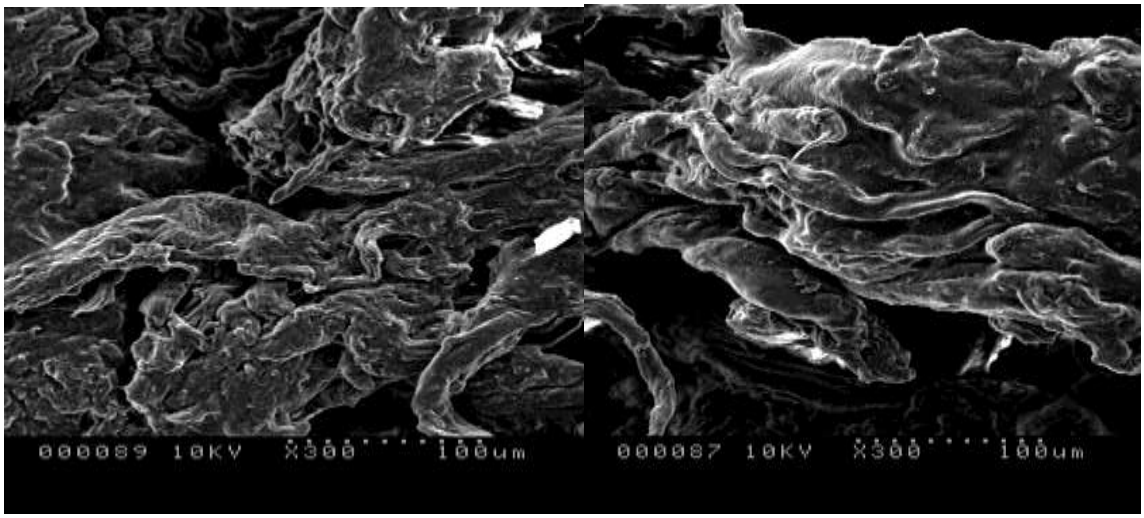

A **B**

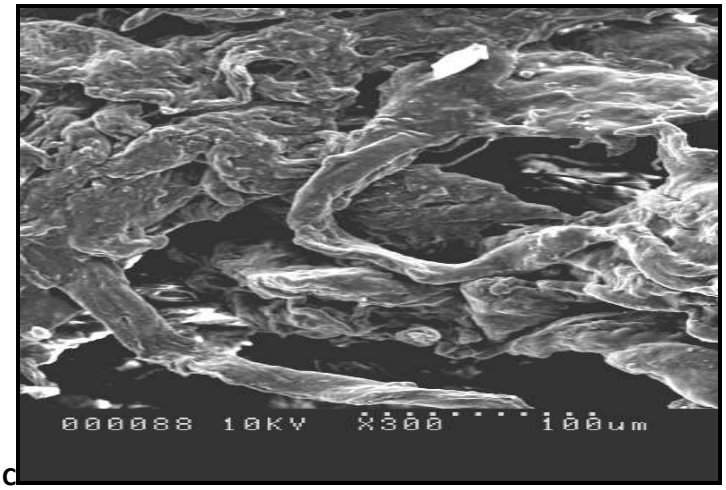

C

Figure 5 SEM photographs of the cellulose regenerated from sawdust wood in **A**) [Emim][OAc]/DMSO mixture, **B**) [Emim][OAc]/DMF mixture compared to pure cellulose sample **C**

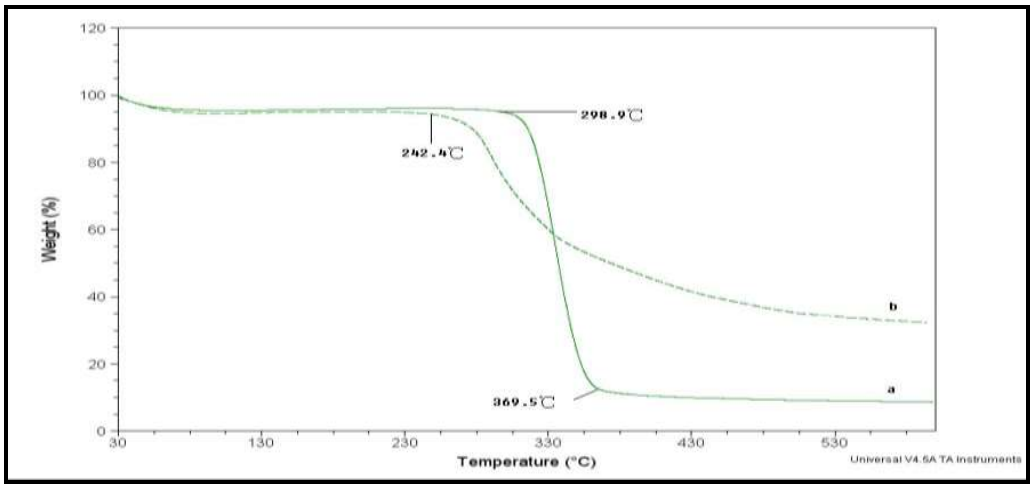

Figure 6 Thermal decomposition profiles of different cellulose **a**) MCC standard, **b**) regenerated cellulose (Su 2012)

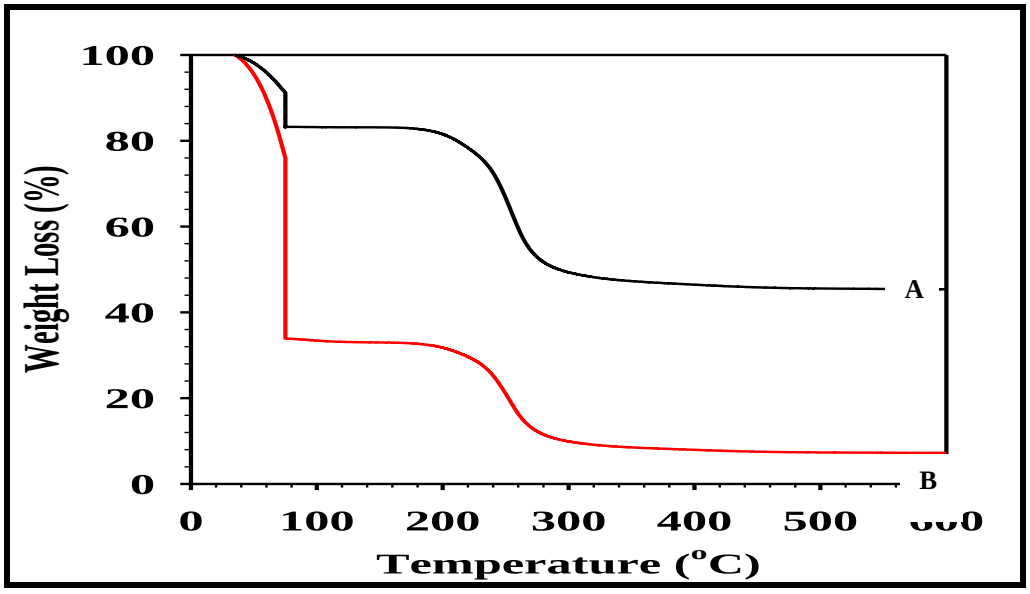

Figure 7 TGA curves of regenerated cellulose from sawdust wood in [Emim][OAc]/ DMSO mixture (curve **A**) and [Emim][OAc]/DMF mixture (curve **B**)